

RECOVERY OF IONIC LIQUIDS FROM AQUEOUS SOLUTION BY NANOFILTRATION

Vom Fachbereich Produktionstechnik

der

UNIVERSITÄT BREMEN

zur Erlangung des Grades
Doktor-Ingenieur
genehmigte

Dissertation

von

M.Sc. José Francisco Fernández Dámaso

Gutachter:

Prof. Dr.-Ing. Jorg Thöming

Prof. Dr.-Ing. Lucio Colombi Ciacchi

Tag der mündlichen Prüfung: 02. September 2011

Diese Arbeit wurde in der Zeit von April 2007 bis Februar 2011 im
Fachbereich 04 (Produktionstechnik) der Universität Bremen angefertigt.

Eingereicht am: 15. März 2011

Verteidigt am: 02. September 2011

Prüfungskommission:

Gutachter: Prof. Dr.-Ing. Jorg Thöming
Prof. Dr.-Ing. Lucio Colombi Ciacchi

Prüfer: Prof. Dr.-Ing. Kurosch Rezwan
Prof. Dr. Dr. h.c. mult. Bernd Jastorff

Mitarbeiter: Dr. rer. nat. Stefan Stolte

Studentin: Wiebke Schildt

*“A theory is something nobody believes,
except the person who made it.
An experiment is something everybody believes,
except the person who made it”
Albert Einstein*

*To Max and Jule:
my soulfulness*

SUMMARY

Ionic liquids are regarded as a promising substance class; because they are potential substituents for volatile solvents as well as they allow the design of new processes. However, up to the present, there are only few industrial processes using them. One of the reasons is related with handling wastes containing contamination of possibly toxic and not easily biodegradable ionic liquids. As a direct consequence, an application of ionic liquids should minimize waste generation and allow the recovery of the ionic liquids, especially from wastewaters.

Nanofiltration seems to be a versatile method for this task, because membranes can be selected properly according to the required purpose: either to retain the ionic liquid or to allow it to pass through the membrane. However, in the field of membrane technology, the scientific base for the rational and task-specific design of membranes is very limited. This is especially true for nanofiltration membranes, in which their performance is based on several solute-membrane interaction mechanisms. Therefore, any deeper understanding of these mechanisms will improve the predictability of the separation behaviour of nanofiltration membranes.

“Thinking in terms of Structure-Activity-Relationships” (T-SAR) is a methodology developed at the University of Bremen in 2003. It permits to describe properties and effects of different substance classes on biological systems, like ionic liquids, biocides or chitosan. This methodology applies a systematic analysis of a chemical entity based on its structural formula. Admittedly with increasing size of the molecule, as in the case of polymeric membranes, the SAR analysis becomes more complex.

In the first part of this work, the T-SAR methodology was combined with classical membrane characterization methods, deriving in a new methodology which allowed not only to explain membrane characteristics, but also to evidence the importance of the chemical structure for separation performance. An application of the combined approach and its potential to discover stereochemistry, molecular interaction potentials, and reactivity of two commercial FilmTec nanofiltration membranes (NF-90 and NF-270) was demonstrated. Based on these results, it was possible to

successfully predict the performance of both membranes for the recovery of hydrophobic and hydrophilic ionic liquids from aqueous solution.

In the second part of this work, the relationships already developed were used to establish the fundament for the recovery of ionic liquids from aqueous solution. They were also applied in two case studies by testing the possibility to recover hydrophobic and hydrophilic ionic liquids from their respective industrial wastewater.

Using model solutions of 1-hexyl-1-methylpyrrolidinium bis(trifluoromethylsulfonyl)-amide, Pyr16 (CF₃SO₂)₂N, it could be evidenced that the formation of a new phase of ionic liquid during the concentration process follows a nucleation-growth mechanism. In this case, 66% of the ionic liquid originally present in the feed was separated. Additionally, the effective recovery rate was duplicated up to 30% by using a coalescence filter. Some suggestions to increase both theoretical and effective recovery rates were also discussed. Furthermore, the hydrophobic ionic liquids from wastewaters produced in biotransformations of 2-octanone to 2-octanol, could be recovered as a separate phase by concentrating them beyond the solubility limit.

Contrary to the hydrophobic ionic liquids, hydrophilic ionic liquids which are used for the dissolution of cellulose and its subsequent regeneration could be recovered as an aqueous solution. It could be done in a way that the recovered solution is similar to the originally used process solution but it is also almost free of undesired by-products. Finally, some recommendations for the systematic recovery of ionic liquids from industrial wastewaters were also introduced.

ZUSAMMENFASSUNG

Ionische Flüssigkeiten werden als eine vielversprechende Substanzklasse angesehen, weil sie potentielle Substituenten für leichtflüchtige Lösemittel sind und die Entwicklung neuer Prozesse ermöglichen. Trotzdem gibt es bis heute nur wenige industrielle Prozesse, bei denen ionische Flüssigkeiten verwendet werden. Als einer der Gründe dafür wird die Entsorgung von Abfällen mit Kontaminationen von möglicherweise toxischen und schwer biologisch abbaubaren ionischen Flüssigkeiten angesehen. In direkter Konsequenz ist die Produktion von derartigen Abfällen zu minimieren und die Rückgewinnung der ionischen Flüssigkeiten zu ermöglichen, insbesondere aus Abwässern.

Nanofiltration scheint eine vielseitig einsetzbare Methode für diese Aufgabe zu sein, weil die Membranen ihrem Verwendungszweck entsprechend gewählt werden können: entweder, um die ionische Flüssigkeit zurückzubehalten, oder um sie durch die Membrane fließen zu lassen. Im Gebiet der Membrantechnologie sind jedoch die wissenschaftlichen Grundlagen für die theoretische und aufgabenspezifische Entwicklung der Membranen sehr begrenzt. Dies gilt insbesondere für Nanofiltrationsmembranen, deren Funktion auf mehreren Stoff-Membran-Wechselwirkungsmechanismen basiert. Folglich verbessert jedes tiefere Verständnis dieser Mechanismen die Voraussagbarkeit des Trennverhaltens der Nanofiltrationsmembranen.

„Struktur-Wirkungs-Denken in der Chemie“ (T-SAR) ist eine Methode, die im Jahr 2003 an der Universität Bremen entwickelt wurde. Sie erlaubt es, die Eigenschaften von verschiedenen Substanzklassen und ihre Effekte auf biologische Systeme anschaulich zu beschreiben, beispielsweise bei ionischen Flüssigkeiten, Bioziden oder Chitosan. Diese Methode basiert auf der systematischen Analyse einer chemischen Einheit mit Hilfe der Betrachtung seiner Strukturformel. Allerdings wird bei Zunahme der Molekülgröße, wie im Fall von Polymermembranen, die SAR-Analyse recht aufwändig.

Im ersten Teil dieser Arbeit wurde T-SAR mit den klassischen Charakterisierungsmethoden für Membranen zu einer neuen Methode kombiniert, die nicht nur Membraneigenschaften erklärt, sondern auch

Anhaltspunkte für die Bedeutung der chemischen Struktur für die Trennungsleistung der Membran geben kann. Eine Anwendung dieses kombinierten Ansatzes und seines Potenzials, die Stereochemie, die molekularen Wechselwirkungspotenziale und die Reaktivität von zwei kommerziellen FilmTec Nanofiltrationsmembranen (NF-90 und NF-270) zu ergründen, wurde hier gezeigt. Aufgrund dieser Resultate war es möglich, die Leistung der Membranen für die Rückgewinnung von hydrophoben und hydrophilen ionischen Flüssigkeiten von wässrigen Lösungen erfolgreich vorauszusagen.

Im zweiten Teil dieser Arbeit wurden die zuvor erarbeiteten Zusammenhänge angewendet, um Grundlagen für die Rückgewinnung von ionischen Flüssigkeiten aus wässrigen Lösungen zu schaffen und in zwei Fallstudien anzuwenden. Dabei wurde die Möglichkeit geprüft, hydrophobe und hydrophile ionische Flüssigkeiten aus ihrem jeweiligen industriellen Abwasser zurückzugewinnen.

Unter Verwendung von Pyr16 (CF₃SO₂)₂N Modelllösungen (1-Hexyl-1-methylpyrrolidinium bis-(trifluoromethylsulfonyl)amid) konnte gezeigt werden, dass die Entstehung einer neuen Phase der ionischen Flüssigkeit während des Konzentrationsprozesses einem Keimbildungs- und Wachstumsmechanismus folgt. In diesem Fall konnten 66% der eingesetzten ionischen Flüssigkeit zurückgewonnen werden. Zusätzlich konnte die effektive Wiederfindungsrate dadurch auf 30% dupliziert werden, dass man einen Koaleszenzfilter verwendete. Einige Vorschläge, um die theoretischen und effektive Wiederfindungsrate zu erhöhen, wurden auch diskutiert. Außerdem konnten die hydrophoben ionischen Flüssigkeiten, die in der Biotransformation von 2-Octanone zu 2-Oktanol verwendet wurden, als zweite Phase von den Abwässern zurückgewonnen werden, indem man sie über die Löslichkeitsgrenze hinaus konzentrierte.

Im Gegensatz zu den hydrophoben ionischen Flüssigkeiten konnten die hydrophilen ionischen Flüssigkeiten, die für die Auflösung von Zellulose und seine darauffolgende Regeneration benutzt wurden, als wässrige Lösung zurückgewonnen werden. Dies konnte so erfolgen, dass sie der ursprünglich benutzten Lösung ähnlich und von unerwünschten Nebenprodukten fast frei sind. Schließlich wurden einige Empfehlungen für die systematische Rückgewinnung ionischer Flüssigkeiten von industriellen Abwässern eingeführt.

ACKNOWLEDGEMENTS

It is very difficult to establish the right and faithful order inside the list of institutions and/or persons that supported me during these years of work; but I will try regardless their contributions...

...Two universities have played an important role in my professional career: the Central University of Venezuela and the University of Bremen. Thanks for let me grow as engineer and person and for show where my ideal workplace is!

...Prof. Jorg Thöming: you gave me the opportunity to work in your group, you offered me a fascinating theme, and you kept challenging me to go beyond my limits and to be more and more self-confident. If I see back in the last five years, now I could only be proud of your work.

... Prof. Lucio Colombi Ciacci and Prof. Kuroschi Rezwan: thanks for accepting to be part of the evaluation committee and I am sure you will contribute to an enriching discussion!

...Prof. Bernd Jastorff: you are a source of pure inspiration. It is incredible the way you talk about your career and your experience, and your enthusiasm is very contagious. Ten years ago, a chemistry teacher had a big influence on my decision to study Chemical Engineering, and after our recently discussions, you confirmed me that I took the right decision!

...The "Dream-Team" of Doctors: Marianne Matzke, Stefan Stolte, Jürgen Arning, Jan Köser and Michael Baune... Thanks for the support, for the nice conversations, social evenings and discussions, for your acceptance and your friendship!

...All the students that worked with me during this time: Katja Springsguth, Shaza Elmenshawy, Christoph Hillebrand, Joseph Kiprotich, Justyna Grzelak, and specially, Robert Bartel, which helped me to solve a lot of problems with the filtration equipment.

...All the personal of the University of Bremen, who helped me during the construction and operation of the filtration equipment: Michael Birkner,

Dieter Stadtlander, Dieter Brüns and his team, Frank Lubish, Roswitta Krebs-Goldbecker and the team from ZVES (Uni-Bremen).

...The technical and administrative team: Ruth Krumrey-Rosch, Antje Mathews, Anne Nienstedt, Detlef Bobenhausen, Dietmar Grotheer, Andrea Böschen, Brunhilde Hans, for your support with some of the daily tasks, and particularly, Ulrike Bottin-Weber for carrying out most of the chromatographic analysis that made this work possible.

...The actual and former PhD students of AG Thöming and the actual and former members of AG Jastorff, my adoptive work-group: thanks for the nice time, and especially Jenny, for our musical hours at the office!!!!

...Our partners from Praktibiokat Project: William-Robert Pitner (Merck KGaA), Jeffrey Lutje-Spelberg (Jülich Chiral Solutions) and Prof. Dirk Weuster-Botz, Stefan Bräutigam and Danielle Dennewald (Institute of Biochemical Engineering, Technische Universität München). Thanks for the nice cooperation and the experience related to work in such a project.

...All the persons who carried out some specific analyses for me: Andreas Schaefer, Jan Hendrik Bredehöft, Kelly Briceño, Alexandra Ewers, Thomas Luxbacher, Juliane Lehmann, Ralf Donau, Heike Anders, Petra Witte and Jolanta Kumirska. Thanks to Birgit Kosan (TITK) for provide some wastewater samples.

...All the persons of the team of “Ionic Liquids” for the interesting presentations and the fruitful discussions, especially to Prof. Juliane Filser and Prof. Detlef Gabel. Thanks to Reinhold Störmann and Chul-Woong Cho for supporting me with some MOPAC/COSMO calculations.

...The German Academic Exchange Service (DAAD), the Federal Ministry of Education and Research (BMBF) and the Senator of Environment, Civil Engineering, Transportation and Europe of the City of Bremen, for supporting either my stay in Bremen or part of my research work.

...Of course, my family and friends for giving me support and for always encouraging me to reach this goal!

... And finally, thanks to all the people I have known in Germany, thanks for your support and especially, for your patience with my German!

TABLE OF CONTENTS

List of Tables	xiii
List of Figures	xv
List of Symbols and Abbreviations	xix
1 INTRODUCTION	1
1.1 Problem definition.....	1
1.2 State of technology.....	7
1.3 Scope and key questions.....	10
1.4 Outline.....	12
References.....	13
2 UNDERSTANDING MEMBRANE CHEMISTRY	19
2.1 Background.....	19
2.1.1 <i>Preparation of composite nanofiltration membranes</i>	21
2.1.2 <i>Thinking in terms of Structure-Activity-Relationships</i>	23
2.2 Experimental.....	25
2.2.1 <i>Materials</i>	25
2.2.2 <i>Infrared spectroscopy</i>	25
2.2.3 <i>Membrane characterization methods</i>	26
2.2.4 <i>Analytical methods</i>	28
2.3 Applying the T-SAR algorithm to NF-membranes.....	28
2.3.1 <i>Chemical structure determination</i>	29
2.3.2 <i>Stereochemistry</i>	34
2.3.3 <i>Molecular interaction potentials</i>	37
2.3.4 <i>Reactivity</i>	40
2.3.5 <i>A picture of both nanofiltration membranes</i>	45
2.4 Understanding membrane characteristics.....	62
2.4.1 <i>Morphology parameters</i>	64
2.4.2 <i>Charge parameters</i>	69
2.4.3 <i>Stability parameters</i>	71
2.4.4 <i>Performance parameters</i>	72
2.5 Understanding the separation of ionic liquids.....	74
References.....	78

3 ACHIEVING IONIC LIQUID RECOVERY.....	85
3.1 Background.....	85
3.1.1 <i>Components of a membrane process</i>	86
3.1.2 <i>Performance of membrane separations</i>	89
3.1.3 <i>Second phase formation by concentration</i>	92
3.2 Experimental.....	96
3.2.1 <i>Materials</i>	96
3.2.2 <i>Dead-end nanofiltration experiments</i>	98
3.2.3 <i>Cross-flow nanofiltration experiments</i>	98
3.2.4 <i>Adsorption experiments</i>	101
3.2.5 <i>Analytical methods</i>	101
3.3 Membrane screening and IL-selection.....	102
3.4 Concentration of Pyr16 (CF ₃ SO ₂) ₂ N.....	105
3.5 Recovery of Pyr16 (CF ₃ SO ₂) ₂ N.....	112
3.6 Approaches to improve IL-recovery.....	117
3.7 Two cases studies with real wastewaters.....	119
3.7.1 <i>Biocatalytic production of chiral alcohols</i>	120
3.7.2 <i>Dissolution and regeneration of cellulose</i>	128
3.8 Facing problems and prospect.....	135
References.....	137
4 CONCLUSIONS & OUTLOOK.....	143
4.1 Conclusions.....	143
4.2 Suggestions for further research.....	144
References.....	147
Appendixes.....	149
Appendix A: Dead-End Module.....	149
List of Publications.....	151
Curriculum Vitae.....	153
Erklärung.....	154

LIST OF TABLES

Table	Title	Page
1.1	Selection of cations commonly used.....	1
1.2	Selection of anions commonly used.....	2
1.3	Current prices for selected ionic liquids	4
1.4	Qualitative estimation of persistence, bioaccumulation potential and toxicity of selected ionic liquids.....	7
2.1	Classification of membranes for liquid pressure-driven separations.....	19
2.2	Algorithm for the T-SAR analysis of a chemical compound.....	25
2.3	Characteristics of selected nanofiltration membranes.....	26
2.4	Characteristic infrared bands of polysulfone.....	31
2.5	Characteristic infrared bands for polyamide in NF-membranes....	33
2.6	Chemical structure of FilmTec NF-membranes constituting units.	35
2.7	Atom hybridisation and expected geometry.....	36
2.8	Stereochemistry of FilmTec NF-membranes constituting units....	38
2.9	Molecular interaction potentials of FilmTec NF-membranes constituting units, according to the colour code from Figure 2.4...	39
2.10	Molecular interaction potentials for charged groups of FilmTec NF-membranes, according to the colour code from Figure 2.4.....	41
2.11	pKa values for the compounds involved on the membrane chemistry.....	42
2.12	pKa values for compounds with a chemical structure similar than that found in the membrane chemistry.....	43
2.13	Reactivity of functional groups present in polyamide membranes.	44
2.14	Atomic concentrations for NF-membranes and constituting units..	46
2.15	Basic information needed to assemble the membranes patterns..	48
2.16	Theoretical determination of the isoelectric point for the pattern presented in Figures 2.8 (NF-90 membrane).....	53
2.17	Theoretical determination of the isoelectric point for the pattern presented in Figures 2.9 (NF-270 membrane).....	54
2.18	Determination of the number of charged groups for the NF-90 membrane based on the experimental IEP value (pH = 4.0).....	55

Table	Title	Page
2.19	Determination of the number of charged groups for the NF-270 membrane based on the experimental IEP value (pH = 2.5).....	56
2.20	Surface atomic concentrations for NF-membranes and the membranes patterns developed in this work.....	57
2.21	Nano-openings resulting from the polyamide structure of NF-membranes.....	61
2.22	Membrane surface roughness derived from AFM measurements at different scan sizes.....	66
2.23	Pore sizes of nanofiltration membranes.....	67
2.24	Different representations of the membrane openings.....	68
2.25	Contact angles as a measure of membrane hydrophobicity.....	69
2.26	Isoelectric points of nanofiltration membranes.....	70
2.27	Amount of membrane charged groups obtained by titration.....	70
2.28	Pure water permeability values of nanofiltration membranes.....	74
2.29	Ionic volumes and radii for selected cations and anions.....	75
2.30	Molecular radii and diameter for selected ionic liquids.....	76
2.31	Molecular interaction potentials for three hydrophobic ionic liquids: Py6 (CF ₃ SO ₂) ₂ N, IM16 (CF ₃ SO ₂) ₂ N and Pyr16 (CF ₃ SO ₂) ₂ N.....	77
3.1	Ionic liquids selected for membrane screening.....	97
3.2	Comparison of analytical results by the determination of Pyr16 (CF ₃ SO ₂) ₂ N for different samples.....	104
3.3	Estimation of the viscosity for a mixture water – ionic liquid at different concentrations.....	110
3.4	Performance parameters associated to the concentration experiments with Pyr16 (CF ₃ SO ₂) ₂ N.....	111
3.5	Performance parameters associated to the recovery experiments with Pyr16 (CF ₃ SO ₂) ₂ N.....	116
3.6	Performance of nanofiltration with hydrophobic ionic liquids in terms of permeate flux.....	123
3.7	Performance of nanofiltration with hydrophobic ionic liquids in terms of retention and recovery of ionic liquid.....	124

LIST OF FIGURES

Figure	Title	Page
1.1	Approaches used for handling wastes containing ionic liquids: a) Traditional approach, b) Nanofiltration-based process for ionic liquid recovery.....	11
1.2	Structure and organization of the present study.....	12
2.1	Schematic representation of a composite nanofiltration membrane.....	20
2.2	Membrane production process by phase separation.....	21
2.3	Membrane production process by interfacial polycondensation...	22
2.4	The T-SAR Triangle.....	24
2.5	Whole ATR-FTIR spectra for three NF-membranes with zoom into the fingerprint region.....	29
2.6	Chemical structure of polysulfone.....	30
2.7	ATR-FTIR spectra for three NF-membranes over 1400-1700 cm ⁻¹	32
2.8	Pattern developed for the NF-90 membrane (9 cross-linked and 5 linear units), coloured according to Figure 2.4. Black points are “open” bonds.....	49
2.9	Pattern developed for the NF-270 membrane (6 cross-linked and 8 linear units), coloured according to Figure 2.4. Black points are “open” bonds.....	50
2.10	Distribution of charged groups according to the pH of the feed solution: a) NF-90, b) NF-270.....	52
2.11	pH dependence of Z-potential for the NF-membranes under study.....	54
2.12	Z-potential and theoretical net charge for both NF-membranes...	56
2.13	Modified pattern for the NF-90 membrane to assure expected IEP, coloured according to Figure 2.4. Black points are “open” bonds.....	58
2.14	Modified pattern for the NF-270 membrane to assure expected IEP, coloured according to Figure 2.4. Black points are “open” bonds.....	59

Figure	Title	Page
2.15	Most important characteristics of nanofiltration membranes.....	63
2.16	The new approach uses T-SAR to understand membrane characteristics.....	64
2.17	Microscopy views (left: ESEM, right: SEM) of nanofiltration membranes top layer surface: a) NF-90, b) NF-270.....	65
2.18	Determination of the pure water permeability of nanofiltration membranes considering the effect of membrane compaction.....	73
3.1	Separation characteristics of different membrane processes.....	85
3.2	Main components of a pressure-driven membrane process.....	86
3.3	Laboratory set up: (a) dead-end stirred cell, (b) cross-flow tester.....	87
3.4	The three stages of batch operation for producing a concentrate.....	88
3.5	Main variables related to membrane performance.....	89
3.6	Graphical expression of the material balance for the solute.....	92
3.7	Concentration polarization phenomenon.....	92
3.8	(a) Temperature-composition diagram for ionic liquid and water at constant pressure. (b) The same diagram showing stability zones and limits.....	94
3.9	Phase diagram showing phase separation obtained by quenching into the metastable or unstable regions.....	95
3.10	Phase diagram showing phase separation obtained by isothermal concentration into the metastable region.....	95
3.11	Schematic diagram of the cross-flow module used in this work.	98
3.12	Membrane module and its components.....	99
3.13	Cross-flow module used in this work.....	100
3.14	Permeate fluxes for each ionic liquid – membrane combination..	102
3.15	Performance of NF-270 membrane with respect to the ionic liquid employed ($V_P/V_F = 80\%$, 35 bar, IL-saturated feed solutions).....	103
3.16	Concentration process at 25°C for an aqueous solution of Pyr16 (CF ₃ SO ₂) ₂ N with 27% initial undersaturation.....	105

Figure	Title	Page
3.17	Changes observed in the feed tank during the concentration process: (a) $V_P/V_F = 0\%$, (b) $V_P/V_F = 40\%$, (c) $V_P/V_F = 50\%$, (d) $V_P/V_F = 60\%$, (e) second phase formed after sedimentation of collected retentate.....	107
3.18	Concentration process at 25°C for aqueous solutions of Pyr16 (CF ₃ SO ₂) ₂ N with different initial undersaturation degrees.....	108
3.19	Coalescence filter employed.....	112
3.20	Second phase observed at the surface of the retentate at the end of the experiment.....	113
3.21	Comparison of the changes observed in the feed tank during the concentration process when a coalescence filter is used.....	114
3.22	Comparison of the concentration process at 25°C for aqueous solutions of Pyr16 (CF ₃ SO ₂) ₂ N when a coalescence filter is used.....	115
3.23	Reduction of ketone catalyzed by alcohol dehydrogenase with enzymatic cofactor regeneration.....	121
3.24	Recovery schema for hydrophobic ionic liquids.....	122
3.25	Variation of the normalized permeate flux with increasing recovery rate for several hydrophobic ionic liquids.....	123
3.26	Adsorption of IM16 (CF ₃ SO ₂) ₂ N from wastewater on active carbon.....	125
3.27	Process flow diagram for the recovery of IM16 (CF ₃ SO ₂) ₂ N.....	126
3.28	Cost-effectiveness analysis for the recovery of IM16 (CF ₃ SO ₂) ₂ N from wastewater.....	128
3.29	The arrangement of cellulose in plant cell walls.....	129
3.30	Recovery schema for hydrophilic ionic liquids.....	131
3.31	Recovery of IM14 Cl and IM14 1COO from wastewater in a single NF-stage: (a) Visual differences between feed and products, (b) Performance in terms of ionic liquid (IL) and cellulose degradation by-products (CD) separation.....	132
3.32	Variation of the normalized permeate flux with increasing recovery rate for a three-stage nanofiltration process.....	133
3.33	Recovery of IM14 Cl and IM14 1COO from wastewater in three NF-stages.....	134

Figure	Title	Page
3.34	Process flow diagram for the recovery of IM14 Cl and IM14 1COO.....	134
3.35	Strategic approach for the recovery of ionic liquids from waste...	135
4.1	Approaches used to extend the lifetime of ionic liquids.....	144
A.1	Schematic diagram of the dead-end module used in this work...	149
A.2	Components of the dead-end module used in this work.....	150

LIST OF SYMBOLS AND ABBREVIATIONS

LATIN AND GREEK SYMBOLS

A	%	Normalised absorbance
A_M	m^2	Membrane area
A_{MS}	nm^2	Membrane surface exposed to solution
C	g/L	Concentration of ionic liquid
C_0	mmol/L	IL-Concentration for samples without active carbon
CD	mg/L	Concentration of cellulose degradation by-products
C_{eq}	mmol/L	Equilibrium IL-concentration for samples with active carbon
CF	-	Concentration factor
C_F	g/L, %v/v	Concentration of ionic liquid in feed
C_{F0}	g/L	Initial concentration of ionic liquid in feed
C_F^{Sat}	g/L	Concentration of ionic liquid in feed at saturation point
$C_{F,local}$	g/L, %v/v	Local concentration in feed
C_{ION}	mol/L	Concentration of cesium or fluoride ions
C_{INV}	€/year	Nanofiltration capital cost
$C_{M,local}$	g/L, %v/v	Local concentration at the membrane surface
C_{NF-IL}	€/kg	Nanofiltration recovery cost
$C_{O\&M}$	€/year	Nanofiltration operation and maintenance cost
C_P	g/L, %v/v	Concentration of ionic liquid in permeate
$C_{P,local}$	g/L, %v/v	Local concentration in permeate
C_R	g/L, %v/v	Concentration of ionic liquid in retentate
C_{RW}	g/L	Concentration of ionic liquid in rinsing water
C_R/C_F	-	Concentration factor
C_R/C_{F0}	-	Retentate to original feed concentration ratio
C_{TOTAL}	€/year	Nanofiltration total cost
d_m	nm	Molecular diameter
J_P	L/m^2h	Permeate flux
J_{P0}	L/m^2h	Initial permeate flux

J_{Pm}	L/m ² h	Mean permeate flux
J_P^{Sat}	L/m ² h	Permeate flux at saturation point
J_P/J_{P0}	-	Normalised permeate flux (with respect to J_{P0})
J_P^{Sat}/J_{P0}	-	Normalised permeate flux at saturation point (with respect to J_{P0})
J_P/J_P^{Sat}	-	Normalised permeate flux (with respect to J_P^{Sat})
J_W	L/m ² h	Pure water flux
K_{ow}	-	Octanol-water partition coefficient
$\log k_0$	-	Chromatographic parameter describing cation hydrophobicity
L_P	L/m ² hbar	Pure water permeability
m	-	Number of linear constituting units
M_{AC}	g	Mass of active carbon added
n	-	Number of cross-linked constituting units
n/m	-	Cross-linked to linear units ratio
N_A	-	Avogadro constant
N_C	-	Number of carbon atoms
N_{COO^-}	-	Number of deprotonated carboxylic acid groups
N_N	-	Number of nitrogen atoms
N_{NHx^+}	-	Number of protonated amino groups
N_O	-	Number of oxygen atoms
O/N	-	Oxygen to nitrogen ratio
pH	-	pH of the solution
pKa	-	pKa value for the charged group under consideration
q	mmol/g	Amount of ionic liquid adsorbed in active carbon
Q	L/day	Amount of wastewater produced
Q_F	L	Volume of feed
Q_P	L	Volume of permeate
Q_R	L	Volume of retentate
Q_{RW}	L	Volume of rinsing water
r_{ION}^+	nm	Ionic radius
r_{ION}^-	nm	Anionic radius
r_{ION}^+	nm	Cationic radius

r_m	nm	Molecular radius
R	-	(Mean) Retention, rejection
Rec	-	Recovery of ionic liquid (total)
Rec-eff-lab	-	Effective recovery of ionic liquid at lab scale
t	h	Time
t_{END}	h	Finish time for concentration
t_{START}	h	Start time for concentration
T_f	°C,K	Final temperature
T_g	°C,K	Glass-transition temperature
T_o	°C,K	Initial temperature
T_s	°C,K	Temperature at saturation point
V	L	Volume of solution
V_{ION}^{\pm}	nm^3	Ionic volume
V_{SOL}	L	Volume of $MgCl_2$ or Na_2SO_4 solution
V_P/V_F	-	(Process) recovery
$(V_P/V_F)_{Sat}$	-	(Process) recovery at saturation point
W_{IL}	kg/year	Amount of ionic liquid loss in wastewater
x_F	mol/mol	Concentration of ionic liquid in feed as molar fraction
δ	nm	Membrane top layer thickness
ΔP	bar	Pressure difference
λ^{-1}	cm^{-1}	Wavenumber
μ	mPa.s	Viscosity of the mixture ionic liquid – water
θ	°	Contact angle
ρ	groups/ nm^3	Density of membrane charged groups
ζ	mV	Z-potential
%Acid	%	Amount of protonated amino groups already formed
%Conjugate_base	%	Amount of carboxylate anions already formed
%C	%	Carbon composition
%COO ⁻	%	Amount of deprotonated carboxylic acid groups already formed at pH=IEP
%N	%	Nitrogen composition
%NHx ⁺	%	Amount of protonated amino groups already formed at pH=IEP

%O	%	Oxygen composition
%X _{CL}	%	Element X composition for the cross-linked constituting unit
%X _L	%	Element X composition for the linear constituting unit
%X _{TL}	%	Element X composition for the top layer
$\frac{[\text{conjugate base}]}{[\text{acid}]}$	-	Concentration ratio of conjugate base to acid

ABBREVIATIONS AND SPECIAL TERMS

1COO	Acetate anion
AA	Arithmetic average
ADH	Alcohol dehydrogenase (enzyme)
AFM	Atomic Force Microscopy
ATR	Attenuated Total Reflection
BF ₄	Tetrafluoroborate anion
Br	Bromide anion
CAS	Chemical Abstracts Service (registry number)
CB-FDH	<i>Candida boidinii</i> formate dehydrogenase (enzyme)
(CF ₃ SO ₂) ₂ N	Bis(trifluoromethylsulfonyl)amide anion
Cl	Chloride anion
DCDPS	4,4'-dichlorophenyl sulfone
DMSO	Dimethyl sulfoxide
ESEM	Environmental Scanning Electron Microscopy
FDH	Formate dehydrogenase (enzyme)
FTIR	Fourier-Transform Infrared
GDH	Glucose dehydrogenase (enzyme)
HPLC	High-Pressure (performance) Liquid Chromatography
IC	Ion Chromatography
ICP-MS	Inductively Coupled Plasma – Mass Spectrometry
ID	Internal diameter
IEP	Isoelectric point
IL(s)	Ionic liquid(s)
IM12	1-ethyl-3-methylimidazolium cation

IM14	1-butyl-3-methylimidazolium cation
IM16	1-hexyl-3-methylimidazolium cation
JCS	Julich Chiral Solutions GmbH
LB-ADH	<i>Lactobacillus brevis</i> alcohol dehydrogenase (enzyme)
MF	Microfiltration
NAD	Nicotinamide adenine dinucleotide
NADH	Reduced form of nicotinamide adenine dinucleotide
NADP	Nicotinamide adenine dinucleotide phosphate
NADPH	Reduced form of nicotinamide adenine dinucleotide phosphate
NF	Nanofiltration
NMMO	N-methylmorpholine-N-oxide
OECD	Organisation for Economic Co-operation and Development
PEEK	Polyether ether ketone
PF6	Hexafluorophosphate anion
Py6	1-hexylpyridinium cation
Pyr14	1-butyl-1-methylpyrrolidinium cation
Pyr16	1-hexyl-1-methylpyrrolidinium cation
PV	Pervaporation
RMS	Root-Mean-Square
RO	Reverse osmosis
SAR	Structure-Activity-Relationships
SEC	Size-Exclusion Chromatography
SEM	Scanning Electron Microscopy
SO4	Sulphate anion
TFC	Thin Film Composite
TITK	Thüringisches Institut für Textil- und Kunststoff-Forschung e.V.
TUM	Technischen Universität München
T-SAR	Thinking in terms of Structure-Activity-Relationships
UCST	Upper critical solute temperature
UF	Ultrafiltration
UFT	Zentrum für Umweltforschung und nachhaltige Technologien
UV	Ultraviolet
XPS	X-ray Photoelectron Spectroscopy

1 INTRODUCTION

1.1 PROBLEM DEFINITION

Ionic liquids (ILs) are compounds that consist exclusively of ions, and have melting points below 100°C [1]. Because ionic liquids consist of cations (head group and side chains) and anions, they have dual functionality. Tables 1.1 and 1.2 summarize several cations and anions commercially available [2].

Table 1.1: Selection of cations commonly used.

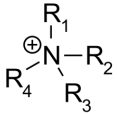
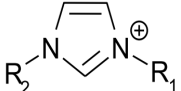
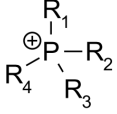
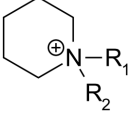
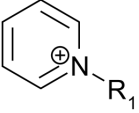
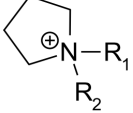
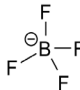
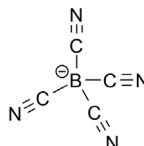
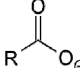
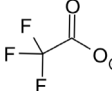
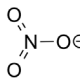
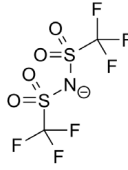
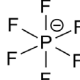
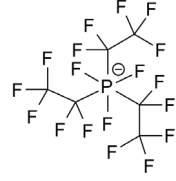
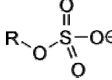
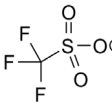
Head group		Side chains
Name	Structure	
Ammonium		R ₁₋₄ : -H, -C _n H _{2n+1}
Imidazolium		R ₁ : -H, -CH ₃ , -C ₂ H ₅ R ₂ : -C _n H _{2n+1}
Phosphonium		R ₁₋₄ : -H, -C _n H _{2n+1}
Piperidinium		R ₁ : -CH ₃ R ₂ : -C _n H _{2n+1}
Pyridinium		R ₁ : -C _n H _{2n+1}
Pyrrolidinium		R ₁ : -CH ₃ , -C ₂ H ₅ R ₂ : -C _n H _{2n+1}

Table 1.2: Selection of anions commonly used.

Central element	Chemical name	Structure
Boron	Tetrafluoroborate	
	Tetracyanoborate	
Carbon	Alkylcarboxylate (R: -H, -C _n H _{2n+1})	
	Trifluoroacetate	
Halides	Bromide	Br [⊖]
	Chloride	Cl [⊖]
Nitrogen	Nitrate	
	Bis(trifluoromethylsulfonyl)amide	
Phosphorus	Hexafluorophosphate	
	Tri(pentafluoroethyl)trifluorophosphate	
Sulphur	Alkylsulphate (R: -H, -C _n H _{2n+1})	
	Trifluoromethanesulphonate	

Ionic liquids are regarded as a promising substance class, because they can potentially replace more hazardous solvents in industrial processes, but also can be used as new materials in a wide field of applications. Potential uses of ionic liquids have been reported in the fields of synthesis and catalysis, biocatalysis, electrochemistry, analytical chemistry, liquid and gas separations, and polymer science [3-12].

However, their impact in industrial processes is still marginal. In 2001 it was pointed out that processes and technologies based on ionic liquids could not reach large-scale commercial applications quickly, and that certain time is needed between invention and implementation of ionic liquids in full-scale commercial programs [13]. Ten years later, the situation has not changed significantly. However, an important growth of the ionic liquids market worldwide is expected, reaching 3.4 billion US \$ by 2020 from 300 million US \$ today [14].

Actually, there are only about twenty applications known to public that use ionic liquids, which are commercialized and/or used in chemical industries [1,15,16]. Within all the reported industrial applications using ionic liquids, a common denominator for those which are commercially relevant is the following: all of them reuse the ionic liquid regularly and seem to be waste-free. No references have been found for industrial applications that include recovery and removal of ionic liquids from wastewater [17].

This situation could indicate that there are still some unsolved problems related with handling wastes containing ionic liquids. Additionally, economical and environmental factors play the most decisive role. The major cost associated with adopting ionic liquids in many industrial processes is not necessarily the capital associated with the concerned technology, but the cost of the ionic liquid itself [18]. If the process generates wastes containing ionic liquids, the operating costs for the make-up of lost ionic liquids should be considered, as well as the environmental acceptability of the waste in terms of (eco)toxicity and biodegradability. However, these and other issues of importance for the lifecycle of ionic liquids have been commonly neglected [19], and the majority of ionic liquids actually used are considered to be low or not environmental compatible [20].

Despite this discouraging scenario, it could be possible to make more use of the advantages of the ionic liquids if they are part of a closed system, where their recovery can be carefully controlled [21]. Then, the research focus for industrial applications of ionic liquids must be either finding new

ionic liquids which reduce waste generation and/or developing processes to recover ionic liquids from wastes. This last point constitutes the central idea of this study.

Additionally, if the performance of an ionic liquid is much better than the performance of the conventional material it aims to replace, less amounts of ionic liquid may be needed for a specific process [22]. In this case, the economical and environmental issues could be totally or partially overruled. However, this situation is not true for the ionic liquid lost in wastewater, in which an economic impact in the overall performance of the application, as well as potential environmental effects, have to be considered.

Ionic liquids are more expensive than common organic solvents, because they are manufactured mainly in kilogram quantities and therefore are offered at high prices. On the one hand, industrial users will not show real interest in ionic liquids while the price remains so high and the supply remains uncertain. On the other hand, manufacturers of ionic liquids have to bear huge research and development costs as well as product and market development costs [23]. The prices of one kilogram product of several hydrophilic and hydrophobic ionic liquids, commonly used in the case studies considered later in this work are presented in Table 1.3, with values ranging from 300 €/kg to 1100 €/kg approximately [24,25].

Table 1.3: Current prices for selected ionic liquids.

Ionic liquids ¹		Price (€/kg) [Reference]
Hydrophilic character	IM12 Cl	495 [24]
	IM14 Cl	290 [24]
	IM12 1COO	617 [25]
	IM14 1COO	562 [25]
Hydrophobic character	Pyr14 (CF ₃ SO ₂) ₂ N	725 [24]
	Pyr16 (CF ₃ SO ₂) ₂ N	Not found
	IM14 (CF ₃ SO ₂) ₂ N	795 [24]
	IM16 (CF ₃ SO ₂) ₂ N	1075 [24]

¹ IM12: 1-ethyl-3-methylimidazolium cation, Cl: chloride anion, IM14: 1-butyl-3-methylimidazolium cation, 1COO: acetate anion, Pyr14: 1-butyl-1-methylpyrrolidinium cation, (CF₃SO₂)₂N: bis(trifluoromethylsulfonyl)amide anion, Pyr16: 1-hexyl-1-methylpyrrolidinium cation, IM16: 1-hexyl-3-methylimidazolium cation

Accurate information regarding pricing of bulk quantities of ionic liquids is not currently available, because the processes are not well established, the market price does not exist and there are not any analogous products on the market [26]. However, based on its data about first production runs on a ton scale, the company BASF expects to see prices for standard quality ionic liquids with growing demands in tons quantities below 30 €/kg [27].

The environmental issues concerning the entrance of ionic liquids into the environment are persistence, bioaccumulation potential and toxicity, and this data which should be considered together during the hazard assessment of ionic liquids:

- Persistence is the ability of a chemical substance to remain in an environment in an unchanged form. The longer a chemical persists, the higher the potential exposure to it [28]. The most important process minimizing this hazard potential in water and soil is biodegradation [29]. Biodegradation studies determine if an ionic liquid persists in the environment. When an ionic liquid passes a biodegradation test, it is unlikely to bioaccumulate. On the contrary, an ionic liquid which does not pass biodegradation tests has greater potential to bioaccumulate [30].
- Bioaccumulation is the process by which the chemical concentration in an aquatic organism achieves a level that exceeds that in the water, as a net result of the uptake, distribution and elimination of the chemical through all possible routes of exposure, i.e. exposure to air, water, soil/sediment and food [28,31]. The octanol-water partition coefficient (K_{OW}) describes the hydrophobicity or hydrophilicity of a compound and is the basis of correlations to calculate bioaccumulation [32,33]. However, it exhibits some important limitations in the case of ionic substances [34,35]. In the case of ionic liquids, it has been shown that chromatographic parameters are even better descriptors than octanol-water partition coefficients. Furthermore, the same chromatographic parameters describing cation and anion hydrophobicity can be used to estimate toxicity and water solubility of ionic liquids [36,37].
- Toxicity is defined as the inherent potential or capacity of a substance to cause adverse effects on a living organism, seriously damaging structure or function, or producing death. Because persistent and bioaccumulative chemicals are long-lasting substances that can build up in the food chain to high levels, they have a higher potential to express toxicity and be harmful to humans and the ecosystem [28,31].

Different ionic liquids have been investigated at the UFT (University of Bremen) in screening toxicity assays, and some of them have been characterised in detail using an (eco)toxicological test battery comprising different levels of biological complexity - from enzymes, cells, microorganisms up to organisms and multi-species-systems [38].

The (eco)toxicity of ionic liquids seems to be predominantly determined by the side chains connected to the cationic head group, while the cationic head group itself has a minor relevance for the (eco)toxicity [39,40]. Most of the tested anions do not exhibit significant (eco)toxicological effects in nearly so far investigated systems, but hydrophobic and mostly fluorinated anions, like $(CF_3SO_2)_2N$, do it in some of the tested systems [38,41].

Furthermore, several biodegradation tests and the determination of hydrophobicity chromatographic parameters have been also performed to determine the biodegradability and bioaccumulation potential of ionic liquids. Imidazolium cations with short side chains are not biodegradable, while no biodegradability data is known for ionic liquids based on pyrrolidinium head groups [30].

In general, for anionic moieties like chloride or acetate, the shorter the alkyl side chain, the safer the chemical is with respect to (eco)toxicity issues due to reduced hydrophobicity, but the higher the risk of persistency due to the missing of biodegradability [42]. Furthermore, anions like $(CF_3SO_2)_2N$ can lead to decrease the biodegradability of the cation due reduced water solubility and to increase the bioaccumulation potential due to higher hydrophobicity, accumulating in tissues of living organisms and thus exhibiting strong (eco)toxicological effects [43].

All results from these systematic studies, completed with data from literature, were collected in the UFT / Merck Ionic Liquids Biological Effects Database [44]. Using the information available in this database, it is possible to estimate qualitatively the importance of the environmental issues concerning the ionic liquids used in the applications considered later in this study. Table 1.4 comprises the results of this qualitative evaluation.

According to these economical and environmental issues, the recovery of hydrophobic ionic liquids should receive more and primary attention compared to the recovery of hydrophilic ionic liquids.

Table 1.4: Qualitative estimation of persistence, bioaccumulation potential and toxicity of selected ionic liquids.

Ionic liquids		Persistence (biodegradability)	Bioaccumulation potential	Mammalian toxicity (1)	Aquatic toxicity (2)
Hydrophilic	IM12 Cl	Moderate (non biodegradable cation, anion not relevant)	Very low	Low to moderate	
	IM14 Cl		Low	Moderate to high	Moderate
	IM12 1COO		Very low	Low	Unknown
	IM14 1COO		Low	Unknown	
Hydrophobic	Pyr14 (CF ₃ SO ₂) ₂ N	Unknown (anion no biodegradable)	Moderate	Moderate	
	Pyr16 (CF ₃ SO ₂) ₂ N		High	Moderate	Moderate to high
	IM14 (CF ₃ SO ₂) ₂ N	High (cation and anion no biodegradable)	Moderate	Moderate to high	
	IM16 (CF ₃ SO ₂) ₂ N		High	Moderate	Moderate to high

(1) Enzyme inhibition assay with acetylcholine esterase and cytotoxicity assay with the IPC-81 cell line (rat leukemia cells).

(2) Luminisence inhibiton assay with the marine bacterium *Vibrio fischeri* and reproduction inhibition assay with the unicellular limnic green algae *Scenedesmus vacuolatus*.

1.2 STATE OF TECHNOLOGY

Due to the negligibly low vapour pressure of ionic liquids under normal operational conditions, it is clear that they do not contribute to air pollution, except by forming aerosols. However, they can cause soil and water pollution [45]. If an aqueous mixture containing an ionic liquid is not reusable anymore, it finally becomes wastewater. According to the OECD-Eurostat Joint Questionnaire on Waste, waste recovery is defined as any operation that diverts a waste material (in our case, ionic liquid) from the waste stream (in our case, wastewater) and which results in a certain product with a potential economic or ecological benefit [46].

In the case of aqueous dispersions of a hydrophobic ionic liquid the separation can be achieved by gravity settling, but can also be improved by using a centrifugal contactor [47]. However, even though hydrophobic ionic liquids have low water solubility, some ionic liquid remains dissolved and its amount in water could be still relative high. The simplest method to remove water from an ionic liquid would be evaporation, due to the non-volatility of ionic liquids. However, the high energy costs associated with

evaporating the water from a solution of ionic liquid makes this method impractical [48].

As alternative separation method, simple salting-out processes have been investigated [49-53]. In this case, the mixture of ionic liquid and water has to be brought into contact with an electrolyte (as solid or as saturated aqueous solution), which has the power to withdraw some of the present water to form a second phase that can be removed by decantation. Despite the formation of such aqueous biphasic systems open new areas of research and development, the introduction of inorganic ions hinders the recovery of the ionic liquid in its original form, due to additional ions related to ion exchange reactions and possible mixed salts. To avoid this situation, one option is to replace inorganic structuring salts with molecular kosmotropes, like sugars, which can be removed more easily in comparison to inorganic ions by crystallization [54-56].

A different form of salting-out is observed when aqueous solutions of ionic liquids in presence of carbon dioxide (gaseous or liquid), form three phases. One liquid phase is enriched with ionic liquid; a second one is enriched with water and the third phase (vapour) contains mostly carbon dioxide with a small amount of dissolved water [57,58]. It is believed that carbon dioxide generates carbonic acid and its dissociation products in aqueous solution, thus lowering the pH, changing the solution equilibrium between the ionic liquid and water, and finally, leading to phase separation [57].

Another method for the separation of ionic liquids from water is membrane filtration. Membranes can be designed to pass water and retain ionic liquids selectively. Membrane-based processes offer clear advantages over the aforementioned techniques because separation is achieved without phase change and little or no chemical addition is required [59].

Dissolved ionic liquids ions are preferably retained by nanofiltration (NF) membranes, which are known to interact more strongly with ions compared to neutral compounds. Since nanofiltration membranes are negatively charged, it is the anion repulsion which mainly determines solute rejection [60]. In addition, cations will be rejected simultaneously due to the macroscopically need of maintaining electroneutrality [61]. However, due to the organic nature of ionic liquids cations, their size and affinity to the membrane chemistry also play a role during the separation.

At a fundamental level, nanofiltration is a very complex process. The events leading to rejection are taking place on a length scale of the order of one nanometre (not much greater than atomic dimensions), at which macroscopic descriptions of hydrodynamics and interactions are beginning to break down [62]. As a consequence, the modelling of nanofiltration processes for design purposes is often performed by applying black-box models or short-cut methods which can lead to unreliable results, because the complexity of the molecular interactions on and inside the membrane [63]. Insofar, the scientific base for the rational design of membranes for specific applications (like the recovery of ionic liquids) is very limited, and hence there is an immense frontier to be conquered [64].

To the best of our knowledge, there are no earlier references about the use of nanofiltration for the concentration of aqueous solutions of hydrophobic ionic liquids. Some preliminary results for membrane screening with three commercial nanofiltration membranes (FilmTec NF-90 and NF-270, and GE Osmonics Desal DK) and four different hydrophobic ionic liquids (IM14 PF6², IM14 (CF3SO2)2N, IM16 PF6 and IM14 (CF3SO2)2N) were presented by us in 2008 during the 10th World Filtration Congress. Tendencies for permeate flux (NF-270 > Desal DK > NF-90) and retention (NF-90 > Desal DK > NF-270) were reported for each ionic liquid, and high retention values (>99%) were achieved with the NF-90 membrane. In this study, the concentration of each ionic liquid in feed was around 50% of solubility level at 25°C (ranging from 1 to 10 g/L) and HPLC-analysis was used to determine the concentration of imidazolium cations [65].

On the other hand, the first reference about the application of nanofiltration to separate aqueous solutions containing hydrophilic ionic liquids was published in 2003. Two preliminary experiments were conducted using 10 mM aqueous solutions of IM14 BF4³ and (IM14)₂ SO4⁴ and two commercial nanofiltration membranes (GE Osmonics Desal DVA 032 for IM14 BF4 and GE Osmonics Desal DVA00 for (IM14)₂ SO4). Retentions of 82% and 95% were found respectively, concluding that such retention can be high enough for concentration of the ionic liquids from various solutions in order to clean or recover the ionic liquid. In this study, the concentrations of ionic liquid in permeate and retentate were measured by conductivity [66].

² PF6: hexafluorophosphate anion,

³ BF4: tetrafluoroborate anion

⁴ SO4: sulphate anion

Other experiences with aqueous solutions of hydrophilic ionic liquids (IM14 BF4 and IM14 Br) were published in 2009. The aim of this work was to demonstrate the potential of nanofiltration to concentrating ionic liquids, but the maximum retentions obtained with a feed concentration of 45 mM were low: 60% for IM14 BF4 und 67% for IM14 Br⁵, using a Koch TFC-SR3 commercial membrane. In this case, concentrations of ionic liquids in permeate and retentate were determined by UV-spectrophotometry. Despite these results, the authors consider that nanofiltration remain as a promising way to concentrate aqueous solutions of ionic liquids if the operational conditions can be improved [67].

The third and last reference known about the use of nanofiltration for the concentration of aqueous solutions of hydrophilic ionic liquids was published in 2010. In this case, three commercial nanofiltration membranes (Microdyn-Nadir N30F, FilmTec NF45 and GE Osmonics Desal DK) were used to concentrate a solution containing 0.1% wt. of IM12 Cl and 0.1% wt. of AlCl₃. In this study, an analytical method using ion chromatography (IC) was developed for the determination of Al⁺³ and IM12 cation concentrations. The N30F membrane was reported as inadequate for a practical application (retention values around 20% for IM12 cation and no retention for Al⁺³); while a two step membrane separation process with the remaining membranes was proposed. In the first step, the membrane NF45 is used for solution concentration due to high retention values for both IM12 cation (>99%) and Al⁺³ (>95%). In the second step, the Desal DK membrane separates selectively both cations, because it exhibits retention values of >98% for IM12 cation and around 40% for Al⁺³ [68].

1.3 SCOPE AND KEY QUESTIONS

According to the information already presented, is desirable (or even imperative) to avoid the entrance of ionic liquids into the environment as wastewater, with respect to environmental as well as economical issues. Contrary to the traditional approach considering the complete removal of ionic liquids (Figure 1.1a), a recovery process using nanofiltration membranes is the approach selected for this study (Figure 1.1b).

The removal of ionic liquids from wastewater can transfer the pollution into a solid, if adsorption techniques are used [48,69]; or destroy completely the ionic liquid by using advanced oxidation processes [70,71]. In both

⁵ Br: bromide anion

cases, the losses of ionic liquid and the cost of the removal treatment should be considered into the global process economical analysis. By using nanofiltration, it would be possible to separate selectively the ionic liquid from the wastewater and recycling it into the process, but also a less- or even non-polluting wastewater could reach the environment, requiring or not further treatment.

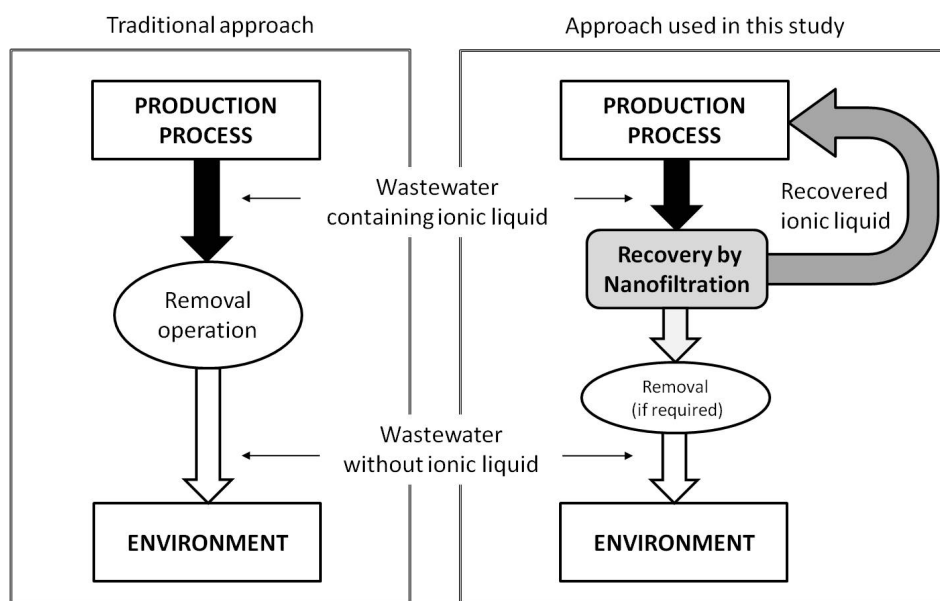


Figure 1.1: Approaches used for handling wastes containing ionic liquids: a) Traditional approach, b) Nanofiltration-based process for ionic liquid recovery.

This study has been carried out under an interdisciplinary atmosphere at the Centre for Environmental Research and Sustainable Technology (UFT) of the University of Bremen. The topic here developed combines two main UFT research fields (Sustainable Chemicals and Selective Separation Technology), in order to find a solution for the recovery of ionic liquids from wastewater, but also to understand their selective separation by nanofiltration by conducting an exemplarily study of Structure-Activity-Relationships (SAR) of nanofiltration membranes and ionic liquids, and their interplay.

In this context, the key questions of this study are:

1. Considering that the interactions between the chemical structure of the ionic liquid and the membrane are responsible for the separation, is the methodology "Thinking in Terms of Structure-Activity-Relationships" (T-SAR) able to provide a better picture of a nanofiltration membrane? Can such a model be used to understand membrane properties and also predict the performance of nanofiltration membranes for the

recovery of ionic liquids? Are these predictions in agreement with experimental data?

2. Considering that the recovery of hydrophobic ionic liquids is physically limited by the water solubility of the ionic liquid, it is possible to use nanofiltration to promote the formation of a second phase of ionic liquid by continuously concentrating an ionic liquid aqueous solution? On what parameters is the efficiency of the recovery depending on? How is the recovery influenced by the presence of additional compounds present in real wastewaters?
3. Considering that hydrophilic ionic liquids could not be recovered in the same way as hydrophobic ionic liquids, due to higher water solubility values, can be nanofiltration also used for their recovery from industrial wastewaters? Due to the lack of information about many topics related with ionic liquids, how could the development of ionic liquids recovery conducted in a systematic way?

1.4 OUTLINE

Consequently, this study is divided into four chapters (Figure 1.2). The definition of the current problem together with the available range of solutions, followed by the approach description and the establishment of the key questions of this study, comprises the current Chapter 1.

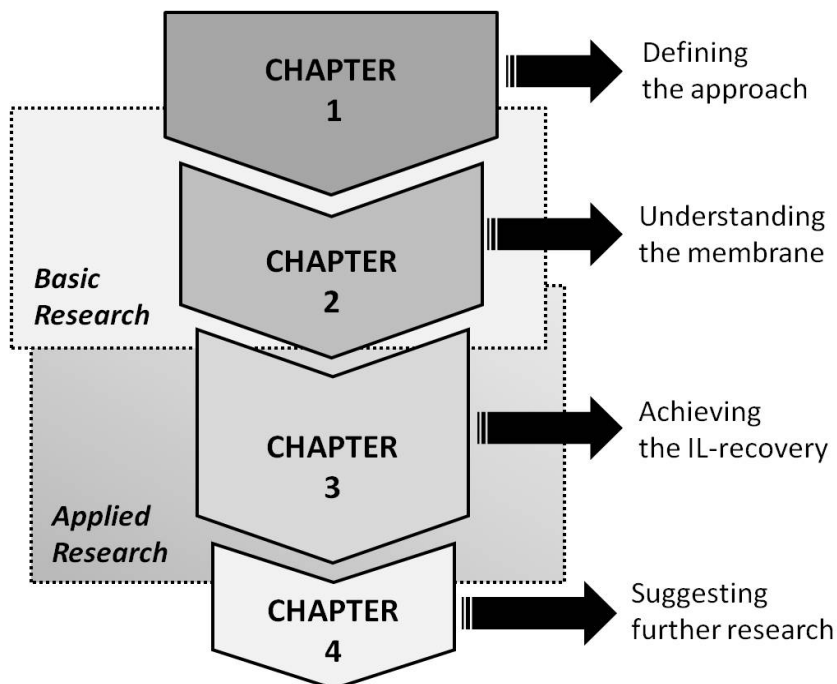


Figure 1.2: Structure and organization of the present study.

In order to facilitate comprehension, Chapters 2 and 3 were conceived as independent entities. That means, each of these chapters contain not only the corresponding results and their discussion, but also the theoretical background and the experimental issues involved. However, these chapters do not remain unconnected. The level of knowledge achieved in Chapter 2 is used later in Chapter 3, covering aspects which ranging from basic to applied research.

Due to the nanofiltration membrane is responsible for the selective separation of the ionic liquid; the research interest was focused at the beginning on the separation agent and its acting separation mechanisms. In Chapter 2, an analysis tool based on Structure-Activity-Relationships is used to produce a better picture of two commercial nanofiltration membranes. Then, this picture can be used not only to explain membrane properties derived from the application of well-established membrane characterization methods, but also to predict performance based on the interactions between ionic liquids and the membrane chemical structure.

Chapter 3 begins with the recovery of hydrophobic ionic liquids by nanofiltration. In consequence, the complexity of the wastewater is reduced in order to investigate how the recovery of ionic liquid is achieved and how it could be improved. After studying two different case studies for the recovery of ionic liquids from wastewaters derived from potential industrial applications, Chapter 3 concludes with some issues about the systematic development of solutions for the recovery of ionic liquids from real wastewaters.

Finally, Chapter 4 summarizes the main conclusions of this study and the research contributions already done, with special emphasis on suggesting fields for further research in this area.

REFERENCES

- [01] FREEMANTLE, M. *An introduction to ionic liquids*, Royal Society of Chemistry: Cambridge (UK), **2010**.
- [02] JASTORFF, B.; Mölter, K.; Behrend, P.; Bottin-Weber, U.; Filser, J.; Heimers, A.; Ondruschka, B.; Ranke, J.; Schaefer, M.; Schröder, H.; Stark, A.; Stepnowski, P.; Stock, F.; Störmann, R.; Stolte, S.; Welz-Biermann, U.; Ziegert, S.; Thöming, J. Progress in evaluation of risk potential of ionic liquids – basis for an eco-design of sustainable products. *Green Chemistry*, **2005**, *7*, 362-372.
- [03] ROGERS, R.D.; Seddon, K.R. *Ionic liquids: industrial applications for green chemistry*, American Chemical Society: Washington DC (USA), **2002**.
- [04] ROGERS, R.D.; Seddon, K.R.; Volkov, S. *Green industrial applications of ionic liquids*, Kluwer Academic Publishers: Dordrecht (The Netherlands), **2002**.

- [05] ROGERS, R.D.; Seddon, K.R. *Ionic liquids as green solvents: progress and prospects*, American Chemical Society: Washington DC (USA), **2003**.
- [06] BRAZEL, C.S.; Rogers, R.D. *Ionic liquids in polymer systems: solvents, additives, and novel applications*, American Chemical Society: Washington DC (USA), **2005**.
- [07] DYSON, P.J.; Geldbach, T.J. *Metal catalysed reactions in ionic liquids*, Springer: Dordrecht (The Netherlands), **2005**.
- [08] ROGERS, R.D.; Seddon, K.R. *Ionic liquids IIIB: fundamentals, progress, challenges, and opportunities. Transformation and Processes*, American Chemical Society: Washington DC (USA), **2005**.
- [09] BRENNECKE, J.F.; Rogers, R.D.; Seddon, K.R. *Ionic liquids IV: not just solvents anymore*, Oxford University Press: New York (USA), **2007**.
- [10] WASSERSCHIED, P.; Welton, T. *Ionic liquids in synthesis*, Wiley-VCH: Weinheim (Germany), **2007**.
- [11] ENDRES, F.; MacFarlane, D.; Abbott, A. *Electrodeposition from ionic liquids*, Wiley-VCH: Weinheim (Germany), **2008**.
- [12] KOEL, M. *Ionic liquids in chemical analysis*, CRC Press: Boca Raton (USA), **2008**.
- [13] HOLBREY, J.D.; Rogers, R.D. Green industrial applications of ionic liquids: Technology review. In: *Ionic liquids: industrial applications for green chemistry*; K.R. Seddon and R.D. Rogers, Eds.; Oxford University Press: Washington DC (USA), **2002**; Vol. 818, pp. 446-458.
- [14] AAILS - All Around Ionic Liquids. Newsletter 03/2010. <http://98.131.55.98/newsletter/newsletter201006.pdf> (Accessed July 16, **2010**).
- [15] MEINDERSMA, G.W.; Maase, M.; de Haan, A.B. *Ullmann's Encyclopedia of Industrial Chemistry*, Wiley-VCH: Weinheim (Germany), **2007**.
- [16] PLECHKOVA, N.V.; Seddon, K.R. Applications of ionic liquids in the chemical industry. *Chemical Society Reviews*, **2008**, 37, 123-150.
- [17] FERNÁNDEZ, J.F.; Neumann, J.; Thöming, J. Regeneration, recovery and removal of ionic liquids. *Current Organic Chemistry*, **2011**, 15, 1992-2014.
- [18] BRENNECKE, J.F.; Maginn, E.J. Ionic liquids: innovative fluids for chemical processing. *AIChE Journal*, **2001**, 47, 2384-2389.
- [19] SCAMMELLS, P.J.; Scott, J.L.; Singer, R.D. Ionic liquids: the neglected issues. *Australian Journal of Chemistry*, **2005**, 58, 155-169.
- [20] ZHAO, D.B.; Liao, Y.C.; Zhang, Z.D. Toxicity of ionic liquids. *Clean - Soil Air Water*, **2007**, 35, 42-48.
- [21] MCFARLANE, J.; Ridenour, W.B.; Luo, H.; Hunt, R.D.; DePaoli, D.W. Room temperature ionic liquids for separating organics from produced water. *Separation Science and Technology*, **2005**, 40, 1245-1265.
- [22] SHORT, P.L. Out of the ivory tower. *Chemical and Engineering News*, **2006**, 84, 15-21.
- [23] JOGLEKAR, H.G.; Rahman, I.; Kulkarni, B.D. The path ahead for ionic liquids. *Chemical Engineering and Technology*, **2007**, 30, 819-828.
- [24] IOLITEC – Ionic Liquid Technologies. *Ionic Liquids – Price Catalogue*. **2009**.
- [25] SIGMA-ALDRICH. Ionic Liquids. <http://www.sigmaaldrich.com/technical-service-home/product-catalog.html> (Accessed July 22, **2010**)
- [26] PITNER, W.R. *Ionic liquids' price*. Personal Communication. **2008**.
- [27] BASF. Basonics / Ionic liquids: Frequently asked questions. What prices can be expected for ionic liquids? <http://www.basionics.com/en/ionic-liquids/faq.htm> (Accessed July 20, **2010**).

- [28] PBT PROFILER. Persistent, Bioaccumulative, and Toxic Profiles Estimated for Organic Chemicals On-Line. Definitions. <http://www.pbtprofiler.net/Details.asp> (Accessed July 15, 2010)
- [29] BEEK, B.; Böhling, S.; Franke, C.; Jöhncke, U.; Studinger, G.; Thumm, E. The assessment of biodegradation and persistence. In: *The Handbook of Environmental Chemistry*; B. Beek, Ed.; Springer-Verlag: Berlin (Germany), 2001, Vol. 2, Part K, pp. 291-320.
- [30] COLEMAN, D.; Gathergood, N. Biodegradation studies of ionic liquids. *Chemical Society Reviews*, 2010, 39, 600-637.
- [31] VAN LEEUWEN, C.J.; Hermens, J.L.M. *Risk Assessment of chemicals: An introduction*, Kluwer Academic Publishers: Dordrecht (Netherlands), 1995.
- [32] ROPEL, L.; Belveze, L.S.; Aki, S.N.V.K.; Stadtherr, M.A.; Brennecke, J.F. Octanol-water partition coefficients of imidazolium-based ionic liquids. *Green Chemistry*, 2005, 7, 83-90.
- [33] MEYLAN, W.M.; Howard, P.H.; Boethling, R.S.; Aronson, D.; Printup, H.; Gouchie, S. Improved method for estimating bioconcentration/bioaccumulation factor from octanol/water partition coefficient. *Environmental Toxicology and Chemistry*, 1999, 18, 664-672.
- [34] BEEK, B.; Böhling, S.; Bruckmann, U.; Franke, C.; Jöhncke, U.; Studinger, G. The assessment of bioaccumulation. In: *The Handbook of Environmental Chemistry*; B. Beek, Ed.; Springer-Verlag: Berlin (Germany), 2000, Vol. 2, Part J, pp. 235-276.
- [35] JASTORFF, B.; Störmann, R.; Ranke, J. Thinking in Structure-Activity-Relationships – A way forward towards sustainable chemistry. *Clean – Soil, Air, Water*, 2007, 35, 399-405.
- [36] RANKE, J.; Müller, A.; Bottin-Weber, U.; Stock, F.; Stolte, S.; Arning, J.; Störmann, R.; Jastorff, B. Lipophilicity parameters for ionic liquid cations and their correlation to in vitro cytotoxicity. *Ecotoxicology and Environmental Safety*, 2007, 67, 430-438.
- [37] RANKE, J.; Othman, A.; Fan, P.; Müller, A. Explaining ionic liquid water solubility in terms of cation and anion hydrophobicity. *International Journal of Molecular Sciences*, 2009, 10, 1271-1289.
- [38] MATZKE, M.; Stolte, S.; Thiele, K.; Juffernholz, T.; Arning, J.; Ranke, J.; Welz-Biermann, U.; Jastorff, B. The influence of anion species on the toxicity of 1-alkyl-3-methylimidazolium ionic liquids observed in an (eco)toxicological test battery. *Green Chemistry*, 2007, 9, 1198-1207.
- [39] STOLTE, S.; Arning, J.; Bottin-Weber, U.; Müller, A.; Pitner, W.R.; Welz-Biermann, U.; Jastorff, B.; Ranke, J. Effects of different head groups and functionalised side chains on the cytotoxicity of ionic liquids. *Green Chemistry*, 2007, 9, 760-767.
- [40] STOLTE, S.; Matzke, M.; Arning, J.; Bösch, A.; Pitner, W.R.; Welz-Biermann, U.; Jastorff, B.; Ranke, J. Effects of different head groups and functionalised side chains on aquatic toxicity of ionic liquids. *Green Chemistry*, 2007, 9, 1170-1179.
- [41] STOLTE, S.; Arning, J.; Bottin-Weber, U.; Matzke, M.; Stock, F.; Thiele, K.; Uerdingen, M.; Welz-Biermann, U.; Jastorff, B.; Ranke, J. Anion effects on the cytotoxicity of ionic liquids. *Green Chemistry*, 2006, 8, 621-629.
- [42] STOLTE, S.; Abdulkarim, S.; Arning, J.; Blomeyer-Nienstedt, A.K.; Bottin-Weber, U.; Matzke, M.; Ranke, J.; Jastorff, B.; Thöming, J. Primary biodegradation of ionic liquids cations, identification of degradation products of 1-methyl-3-octylimidazolium chloride and electrochemical wastewater treatment of poorly biodegradable compounds. *Green Chemistry*, 2008, 10, 214-224.
- [43] MATZKE, M.; Arning, J.; Ranke, J.; Jastorff, B.; Stolte, S. Design of inherently safer ionic liquids: Toxicology and biodegradation. In: *Handbook of Green Chemistry*; W.

- Leitner, P.G Jessop, C. Li, P. Wasserscheid, A. Stark, Eds.; Wiley-VCH: Weinheim (Germany), **2010**.
- [44] UFT – Universität Bremen. The UFT / Merck Ionic Liquids Biological Effects Database. <http://www.il-eco.uft.uni-bremen.de> (Accessed July 21, **2010**).
- [45] ZHU, S.; Chen, R.; Wu, Y.; Chen, Q.; Zhang, X.; Yu, Z. A mini-review on greenness of ionic liquids. *Chemical and Biochemical Engineering Quarterly*, **2009**, 23, 207-211.
- [46] EIONET. European Environment Information and Observation Network. Definitions and Glossary. <http://scp.eionet.europa.eu/definitions/recovery> (Accessed July 14, **2010**).
- [47] BIRDWELL, J.F.; McFarlane, J.; Hunt, R.D.; Luo, H.; DePaoli, D.W.; Schuh, D.L.; Dai, S. Separation of ionic liquid dispersions in centrifugal solvent extraction contactors. *Separation Science and Technology*, **2006**, 41, 2205-2223.
- [48] ANTHONY, J.L.; Maginn, E.J.; Brennecke, J.F. Solution thermodynamics of imidazolium-based ionic liquids and water. *Journal of Physical Chemistry B*, **2001**, 105, 10942-10949.
- [49] GUTOWSKI, K.E.; Broker, G.A.; Willauer, H.D.; Huddleston, J.G.; Swatloski, R.P.; Holbrey, J.D.; Rogers, R.D. Controlling the aqueous miscibility of ionic liquids: aqueous biphasic systems of water-miscible ionic liquids and water-structuring salts for recycle, metathesis, and separations. *Journal of the American Chemical Society*, **2003**, 125, 6632-6633.
- [50] BRIDGES, N.J.; Gutowski, K.E.; Rogers, R.D. Investigation of aqueous biphasic systems formed from solutions of chaotropic salts with kosmotropic salts (salt-salt ABS). *Green Chemistry*, **2007**, 9, 177-183.
- [51] TRINDADE, J.R.; Visak, Z.P.; Blesic, M.; Marrucho, I.M.; Coutinho, J.A.P.; Canongia Lopes, J.N.; Rebelo, L.P.N. Salting-out effects in aqueous ionic liquid solutions: cloud-point temperature shifts. *Journal of Physical Chemistry B*, **2007**, 111, 4737-4741.
- [52] NAJDANOVIC-VISAK, V.; Canongia Lopes, J.N.; Visak, Z.P.; Trindade, J.; Rebelo, L.P.N. Salting-out in aqueous solutions of ionic liquids and K₃PO₄: aqueous biphasic systems and salt precipitation. *International Journal of Molecular Sciences*, **2007**, 8, 736-748.
- [53] DENG, Y.; Chen, J.; Zhang, D. Phase diagram data for several salt + salt aqueous biphasic systems at 298.15 K. *Journal of Chemical and Engineering Data*, **2007**, 52, 1332-1335.
- [54] WU, B.; Zhang, Y.; Wang, H.; Yang, L. Aqueous biphasic systems of hydrophilic ionic liquids + sucrose for separation. *Journal of Chemical and Engineering Data*, **2008**, 53, 983-985.
- [55] WU, B.; Zhang, Y.; Wang, H.; Yang, L. Phase behavior for ternary systems composed of ionic liquid + saccharides + water. *Journal of Physical Chemistry B*, **2008**, 112, 6426-6429.
- [56] WU, B.; Zhang, Y.; Wang, H.; Yang, L. Temperature dependence of phase behavior for ternary systems composed of ionic liquid + sucrose + water. *Journal of Physical Chemistry B*, **2008**, 112, 13163-13165.
- [57] SCURTO, A.M.; Aki, S.N.V.K.; Brennecke, J.F. Carbon dioxide induced separation of ionic liquids in water. *Chemical Communications*, **2003**, 5, 572-573.
- [58] ZHANG, Z.; Wu, W.; Gao, H.; Han, B.; Wang, B.; Huang, Y. Tri-phase behavior of ionic liquid-water-CO₂ system at elevated pressures. *Physical Chemistry Chemical Physics*, **2004**, 6, 5051-5055.
- [59] JUDD, S.; Jefferson, B. *Membranes for Industrial Wastewater Recovery and Re-use*, Elsevier Science Ltd: Oxford (UK), **2003**.

- [60] ERIKSON, P. Nanofiltration extends the range of membrane filtration. *Environmental Progress*, **1988**, 7, 58-62.
- [61] WAITE, T.D. Chemical speciation effects in nanofiltration separation. In: *Nanofiltration. Principles and Applications*; A.I. Schäfer, A.G. Fane and T.D. Waite, Eds.; Elsevier Advanced Technology: Oxford (UK), **2005**.
- [62] BOWEN, W.R.; Welfoot, J.S. Modelling the performance of nanofiltration membranes. In: *Nanofiltration. Principles and Applications*; A.I. Schäfer, A.G. Fane and T.D. Waite, Eds.; Elsevier Advanced Technology: Oxford (UK), **2005**.
- [63] NORONHA, M.; Mavrov, V.; Chmiel, H. Computer-aided simulation and design of nanofiltration processes. *Annals of the New York Academy of Sciences*, **2003**, 984, 142-158.
- [64] NATIONAL RESEARCH COUNCIL. Committee on Chemical Engineering Frontiers. *Frontiers in Chemical Engineering: research needs and opportunities*; The National Academies Press: Washington (USA), **1988**.
- [65] FERNÁNDEZ, J.F.; Chilyumova, E.; Waterkamp, D.; Thöming, J. Ionic liquid recovery from aqueous solutions by cross-flow nanofiltration. *Proceedings of the 10th World Filtration Congress* (Leipzig, Germany), **2008**, Volume II, 528-532.
- [66] KRÖCKEL, J.; Kragl, U. Nanofiltration for the separation of non-volatile products from solutions containing ionic liquids. *Chemical Engineering and Technology*, **2003**, 26, 1166-1168.
- [67] WU, B.; Zhang, Y.M.; Wang, H.P. Non-equilibrium thermodynamic analysis of transport properties in the nanofiltration of ionic liquid-water solutions. *Molecules*, **2009**, 14, 1781-1788.
- [68] SOLÁ CERVERA, J.L. Crystallization behaviour in the system EMIM[Tf₂N]-AlCl₃. PhD Thesis, Universität Erlangen-Nürnberg (Germany), **2010**.
- [69] PALOMAR, J.; Lemus, J.; Gilarranz, M.A.; Rodríguez, J.J. Adsorption of ionic liquids from aqueous effluents by activated carbon. *Carbon*, **2009**, 47, 1846-1856.
- [70] STEPNOWSKI, P.; Zaleska, A. Comparison of different advanced oxidation processes for the degradation of room temperature ionic liquids. *Journal of Photochemistry and Photobiology A: Chemistry*, **2005**, 170, 45-50.
- [71] CZERWICKA, M.; Stolte, S.; Müller, A.; Siedlecka, E.M.; Golebiowski, M.; Kumirska, J.; Stepnowski, P. Identification of ionic liquid breakdown products in an advanced oxidation system. *Journal of Hazardous Materials*, **2009**, 171, 478-483.

2 UNDERSTANDING MEMBRANE CHEMISTRY

2.1 BACKGROUND

An ideal membrane material should have a reasonable mechanical strength, maintain a high throughput and be selective for the desired permeate constituent [1]. Synthetic membranes for molecular liquid pressure-driven separations can be classified according to their cross-section structure, the membrane material and their selective barrier, as is summarized in Table 2.1 [2-7].

Table 2.1: Classification of membranes for liquid pressure-driven separations.

Criterion for classification	Types of membrane	Description
Cross-section structure	Anisotropic	Exhibit two or more planes of different morphologies but same composition
	Isotropic	Exhibit an uniform composition and morphology throughout
	Composite	Consist of layers of dissimilar materials joined together into a single membrane
Membrane material	Inorganic	Made from metals, glass, silica or ceramic
	Organic	Made from synthetic polymeric compounds
Selective barrier	Charged	Can exhibit fixed electric charges or can acquire electric charge in water
	Dense	Have no detectable pores and the material itself determines performance
	Porous	Exhibit discrete pores which vary in size and distribution

Although nanofiltration is used to characterize the process in between reverse osmosis and ultrafiltration, there is still confusion whether a membrane is called a reverse osmosis membrane or a nanofiltration membrane. Moreover, nanofiltration membranes are often considered to be loose reverse osmosis membranes or tight ultrafiltration membranes, despite the last membranes do not retain any salts [8]. In general, commercially available nanofiltration membranes are typically composite and organic membranes, as is shown schematically in Figure 2.1.

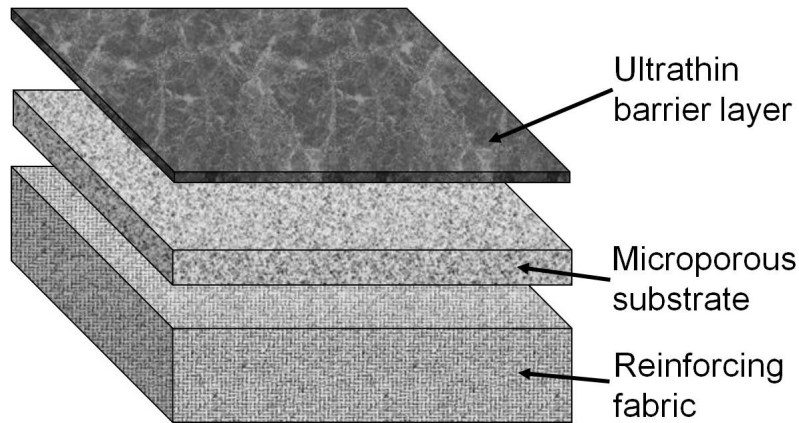


Figure 2.1: Schematic representation of a composite nanofiltration membrane.

Such a composite membrane consists of a base layer of a woven or a non-woven fabric (typically a polyester web) for handling strength. This base layer is over-coated with a layer of an anisotropic porous polymer, usually polysulfone. Then, the surface of this substrate is coated with an ultrathin veneer of a polymeric composition, which provides the controlling properties.

The composite approach is applied to form on the top a selective layer that is both thin and sufficiently hydrophilic to give high water flux, but at the same time cross-linked enough to the extent required for nanofiltration selectivity [9]. Furthermore, each individual layer can be optimized for its particular function: the ultrathin barrier layer can be optimized for the desired combination of solvent flux and solute rejection, while the porous substrate can be optimized for maximum strength and compression resistance, but also minimum resistance to permeate flow [10].

Nanofiltration membranes are charged membranes, but also exhibit characteristics of dense and porous membranes. Separation by dense membranes implies physicochemical interactions between the permeating components and the membrane material, by a solution-diffusion process. Porous membranes, on the other hand, achieve material separation mechanically by size exclusion (sieving), depending on material size relative to that of the pores. Thus, nanofiltration membranes use a combination of charge retention, solution-diffusion and sieving through pores smaller than 2 nm to separate materials [1,11].

Basically, the preparation of composite membranes involves first the preparation of the porous substrate and afterwards the deposition of a selective barrier layer on this porous support. Several methods can be

employed for the formation of either the ultrathin barrier layer [10] or the porous substrate [12]. However, the most important processes actually used to prepare composite nanofiltration membranes (phase separation and interfacial polymerization) are going to be described in detail in the next section.

2.1.1 Preparation of composite nanofiltration membranes

The majority of porous substrates are prepared by controlled phase separation. This process, sometimes also called phase inversion or polymer precipitation, describes the process changing a one-phase casting solution into two separate phases. That means, a liquid polymer solution is precipitated into two phases: one with a high polymer concentration, and a second one with a low polymer concentration. The concentrated phase solidifies shortly after phase separation and forms the matrix of the membrane, while the diluted phase forms the pores [3].

The polysulfone family of polymers (polysulfone, polyphenylsulfone and polyethersulfone) is of practical interest for making porous supports for nanofiltration and reverse osmosis membranes, due to their chemical, mechanical, thermal and hydrolytic stability [13]. A common way to produce the formation of a second phase is to immerse the cast polymer solution in a non-solvent bath (typically water). Precipitation can occur because the good solvent in the polymer solution is exchanged for non-solvent [14]. A diagram of a small casting machine is shown in Figure 2.2.

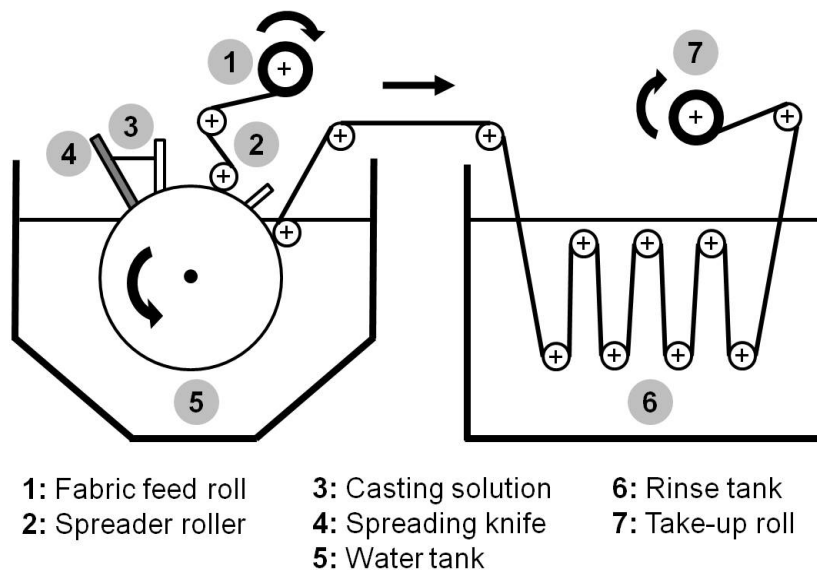


Figure 2.2: Membrane production process by phase separation. Adapted from [3].

The polymer solution is cast onto a moving non-woven web. The cast film is then precipitated by immersion in a water bath. The water precipitates the top surface of the cast film rapidly, forming a finely microporous skin. This skin forms a barrier that slows further entry of water into the underlying polymer solution, which precipitates much more slowly and forms a more porous substructure [3]. The membrane structure is dependent on which type of phase transition (crystallisation, gelation or liquid-liquid demixing) takes place first. The kinetics competition of these three different types of phase transitions is a dominant factor in determining the configuration of the membrane, the thickness and density of the skin, and the porosity of the sub-layer [14].

Once the porous substrate is obtained, interfacial polymerization based on condensation reactions, can occur in order to produce the ultrathin barrier layer. Interfacial polycondensation is a rapid, irreversible polymerization at the interface between water containing a difunctional intermediate and an inert immiscible organic solvent containing a complementary di- or trifunctional reactant. It is based on the Schotten-Baumann reaction in which acid chlorides react with compounds containing active hydrogen atoms (-OH, -NH and -SH) and a large number of polymers can be prepared using it [15]. Polyamides clearly dominate the field of thin film composites (TFC) by interfacial polycondensation and they can be prepared under very mild conditions starting from a solution of a diamine in water and a di- or triacyl chloride dissolved in an organic solvent [10,16]. The term “thin film” describes the manner in which these membranes are fabricated, as it is shown in Figure 2.3.

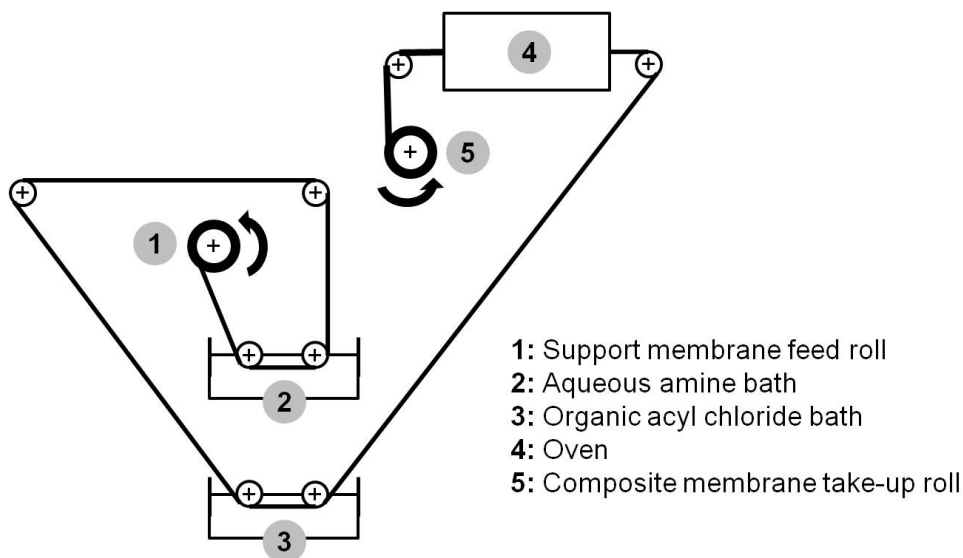


Figure 2.3: Membrane production process by interfacial polycondensation. Adapted from [3].

The polysulfone used as the support film is first immersed in an aqueous diamine bath. On leaving this bath the membrane passes to a second organic di- or triacyl chloride bath. Immediately after the two components are brought together a polymer film is formed at the interface. With increasing thickness of the polymer film the reaction stops after some time. On leaving the oven, the membrane is already formed [3,17]. It has been generally believed that polymerization occurs in a thin region of the organic phase close to the interface and that the interface has no specific effect other than permitting a controlled diffusion of the water soluble monomers into the organic phase and removing acid by-product from the polymerization zone [18,19].

The choice of the organic solvent is most important since it will affect several other polymerization factors such as the partition potential of the reactants between the two phases, the diffusion of reactants, reaction rate, and the solubility, swelling, or permeability of the growing polymer. Additionally, for many polycondensation reactions it has been found that there is an optimum ratio of concentration of reactant in the organic phase to the concentration of reactant in the water phase. The optimum ratio is affected by the properties of the reactants, the organic solvent, agitation, additives in the aqueous phase such a salt or alkali, and the overall concentration of reactants in both phases [15,16].

2.1.2 Thinking in terms of Structure-Activity Relationships

The methodology denominated “Thinking in terms of Structure-Activity Relationships” (T-SAR) was introduced by Jastorff, Störmann and Wölcke at the University of Bremen in 2003 [20]. T-SAR applies a systematic analysis of a chemical entity based on its structural formula and it allows the formulation of working hypotheses about properties and effects of chemicals that have not yet been experimentally verified [21]. Indeed, it has been applied with success to determine the properties and the effects on biological systems of different substance classes, like ionic liquids [22-24], biocides [25,26] and chitosan [27].

The T-SAR approach can be represented as a triangle, like in Figure 2.4. From the chemical structure it is necessary to identify systematically several aspects related with the stereochemistry, the molecular interaction potentials and the reactivity of the desired compound; these three parameters constitute the cornerstones of the T-SAR analysis.

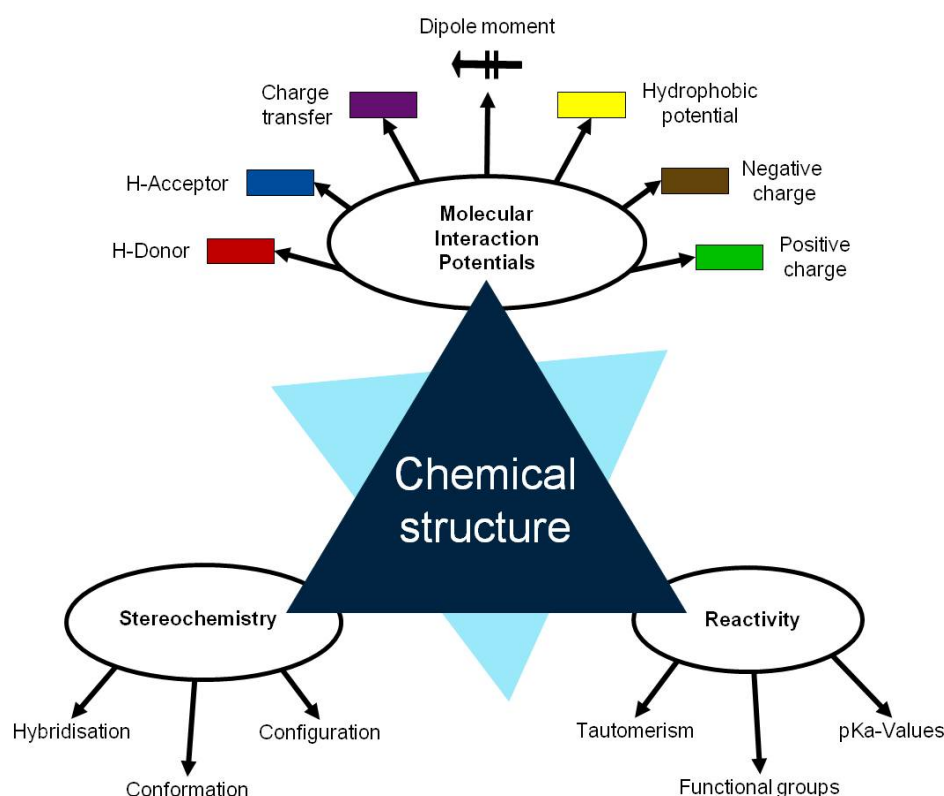


Figure 2.4: The T-SAR Triangle. Adapted from [21].

The chemical structure should ideally be represented by the corresponding three-dimensional formula, which is the graphical representation of the molecular structure, showing how the atoms are arranged.

The stereochemistry describes the shape of the molecule on the one hand and its flexibility on the other. Thus it also describes directionality and spatial organization of molecular interaction potentials, which are identified by using a colour code (Figure 2.4). These interaction potentials describe the possible attractions and repulsions within a molecule, between different molecules or molecular superstructures. Finally, the reactivity indicates the potential of the molecule for further transformation and it is related with the presence of functional groups, tautomerism and pKa-values [20,21].

A practically oriented algorithm for the T-SAR approach implies the observance of seventeen steps [21], organized in Table 2.2. By following these steps it is possible to analyse every compound using only its three-dimensional chemical structure, but the analysis becomes more complex as the size of the molecule increases.

Table 2.2: Algorithm for the T-SAR analysis of a chemical compound.

Chemical structure	<ol style="list-style-type: none">1. Identify the atoms from the structural formula2. Identify the types of bond that are present3. Localize free electron pairs
Stereo-chemistry	<ol style="list-style-type: none">4. Identify the hybridization of all the atoms5. Identify ring systems and their stereochemical features6. Identify steric hindrance and conformational freedom7. Identify possible geometric isomerism8. Determine the presence of chiral centres
Molecular Interaction Potentials	<ol style="list-style-type: none">9. Identify hydrogen bond donor potential10. Identify hydrogen bond acceptor potential11. Identify charge transfer (π-π) interaction potential12. Identify groups with local dipole moments13. Identify groups with hydrophobic interaction potential14. Identify permanently charged groups (ionic potential)
Reactivity	<ol style="list-style-type: none">15. Identify possibilities for prototropic shifts (tautomerism)16. Estimate pKa values for groups able to accept or donate protons17. Identify remaining functional groups and their reactivity

2.2 EXPERIMENTAL

2.2.1 Materials

Three nanofiltration membranes: FilmTec NF-90 and NF-270 (Dow Chemical), and Desal DK (GE Osmonics) were employed. The main characteristics of the membrane were obtained from the manufacturers [28-30] and they are summarized in Table 2.3.

2.2.2 Infrared spectroscopy

Attenuated total reflection (ATR) Fourier-transform infrared (FTIR) spectroscopy is a technique used to determine the chemical composition of membrane samples. ATR-FTIR spectra were obtained using a Thermo Nicolet Avatar 370 FTIR spectrometer (Thermo Electron Corporation) equipped with an ATR element (zinc selenide crystal) and Omnic software (Thermo Electron Corporation) at the University of Bremen (AG Swiderek).

Table 2.3: Characteristics of selected nanofiltration membranes.

	Membrane		
	FilmTec NF-90	FilmTec NF-270	Desal-DK
Manufacturer	Dow Chemical	Dow Chemical	GE Osmonics
Membrane type*	Polyamide TFC	Polyamide TFC	TFC
Max. operating pressure (bar)	41	41	41 (T < 35°C) 30 (T > 35°C)
Max. operating temperature (°C)	45	45	50
pH range: operation and cleaning	3 – 10	2 – 11	3 – 9
	1 – 13	1 – 12	2 – 10.5
Free chlorine tolerance	< 0.1 ppm	< 0.1 ppm	500 ppm-hours

* TFC = Thin-Film Composite. Exact compositions are not available.

An instrument blank was taken to account for differences in instrument response and atmospheric environment (i.e. H₂O and CO₂). The membrane active layers were pressed tightly against the crystal plate. At least four or five replicates were obtained for every membrane type, with each spectrum averaged from 200 scans collected from 650 to 4000 cm⁻¹ at 4 cm⁻¹ resolution, and rationed to the appropriate background spectra. No baseline or further ATR corrections were applied. The absorbance intensities were normalised for further comparison between the spectra.

2.2.3 Membrane characterization methods

The streaming potential measurements were performed by Anton Paar GmbH (Graz, Austria) with the SurPASS Adjustable Gap Cell in presence of a 5 mM solution of KCl as background electrolyte at different pH values, which was adjusted with 0.1 M HCl or 0.1 M NaOH solutions. For each measurement a pair of membrane (cross section of 20 x 10 mm²) was used. The electrolyte pH was first decreased by adding 0.1 M HCl. After that, the same membranes samples were rinsed with deionised water and fresh 5 mM KCl solution and titration continues towards the alkaline range using 0.1 M NaOH.

The surface morphology of the top layer of each membrane was visualized by Environmental Scanning Electron Microscopy, ESEM (FEI, Quanta 600) at the Rovira i Virgili University (Tarragona, Spain) and Scanning Electron Microscopy, SEM (Carl Zeiss AG, SUPRA 40) at the University of Bremen (AG Willems). Samples were examined without previous metallization.

A titration was carried out to determine the amount of charged groups on the membrane. Three pieces of membrane (each 2 x 2 cm²) were immersed for 15 minutes into 50 mL of a 0.1 M CsCl or NaF solution. After rinsing with demineralised water, the membrane pieces were immersed for 15 minutes into 50 mL of a 0.01 M MgCl₂ or Na₂SO₄ solution and these solutions were taken for later analysis.

Considering that the number of cesium ions measured is equal to the number of negatively charged groups, while the number of fluoride ions measured is equal to the number of positively charged groups [31] and using top layer thickness values from already published results [32,33], the following equation was used to determine the density of charged groups:

$$\rho = \frac{C_{ION} \cdot V_{SOL} \cdot N_A}{A_{MS} \cdot \delta} \quad (\text{Eq. 2.1})$$

where:

ρ : density of membrane charged groups (groups/nm³)

C_{ION} : concentration of cesium or fluoride ions (mol/L)

V_{SOL} : volume of MgCl₂ or Na₂SO₄ solution (0.05 L)

N_A : Avogadro constant (6.022x10²³ ions/mol)

A_{MS} : Membrane surface exposed to solution (24x10¹⁴ nm²)

δ : membrane top layer thickness (nm)

For the determination of pure water permeability, the membranes were placed in deionised water for two days before use to assure complete swelling. For the experiments, a stirred dead-end cell HP4750 (Sterlitech Corporation) was used, with a membrane active area of 13.9 cm² (Appendix A).

The feed pressure was achieved by an inert nitrogen atmosphere and experiments were carried out at ambient temperature. The swollen membrane was conditioned with deionised water by increasing pressure progressively in 10 bar steps until a final pressure of 40 bar was reached. After that, deionised water was filled again in the cell; operating pressure difference was fixed (from 10 to 40 bar, increasing the pressure in 5 bar every time) and the time required to collect 25 mL permeate volume was

measured. Values reported are the averages of at least five measurements using in each case a new membrane piece.

2.2.4 Analytical methods

Cesium ions were determined by Inductively Coupled Plasma - Mass Spectrometry (ICP-MS) at the University of Bremen (AG Bach), while fluoride anions and ionic liquid anions/cations were determined by ion-chromatography (IC).

The ICP-MS measurements were carried out using a Finnigan Element 2 (Thermo Electron Corporation) which contain a PEEK cyclonic spray chamber with a micro-flow nebulizer operating in self-aspirating mode was used for sample introduction (sample flow rate of 100 $\mu\text{L}/\text{min}$). For such analyses the solutions were diluted (1:2000) in a nitric acid solution (2%) and spiked with indium (2.5 $\mu\text{g}/\text{L}$) used as internal standard. The gas flow rates used were 16 L/min (coolant gas), 1.0-1.2 L/min (auxiliary gas) and 0.8-1.2 L/min (sample gas). Standard solutions for the external calibrations (Merck VI, Darmstadt, Germany) were prepared in 2-3% nitric acid and also spiked with indium.

The ion-chromatography (IC) measurements were carried out using a Metrohm 881 Compact IC system with Metrohm accessories and software (Metrohm, Herisau, Switzerland). It is equipped with an online eluent degasser, a 20 μL injection loop and a conductometric detector (maintained at 30 ± 0.1 °C). All chromatographic data were recorded by the MagICNet 1.1 compact software. All measurements were done as duplicate and several dilutions factor were used (1:2). Fluoride chromatographic separations were performed with an A Supp ion exchange column (50 x 4.0 mm ID and 5 μm mean particle size) coupled with A Supp 4/5 Guard and RP Guard. A flow rate of 0.7 mL/min of eluent (3.2mM Na_2CO_3 , 1mM NaHCO_3 , 0% CH_3CN) was applied. Additionally, a self-regenerating Suppressor Module and a CO_2 -Suppressor were used.

2.3 APPLYING THE T-SAR ALGORITHM TO NF-MEMBRANES

The separation process in nanofiltration membranes is a surface phenomenon mainly controlled by the chemistry of the ultrathin barrier layer. The micro-porous support can provide some hydraulic resistance to permeate flow [10], while the reinforcing fabric located at the bottom provides mechanical strength without playing any role during the

separation. Consequently, the main effort is related to follow the seventeen steps of the T-SAR algorithm only for the top layer.

2.3.1 Chemical structure determination

The membranes were analysed by ATR-FTIR spectroscopy in order to obtain indications about their chemical composition. The corresponding spectra are shown in Figure 2.5.

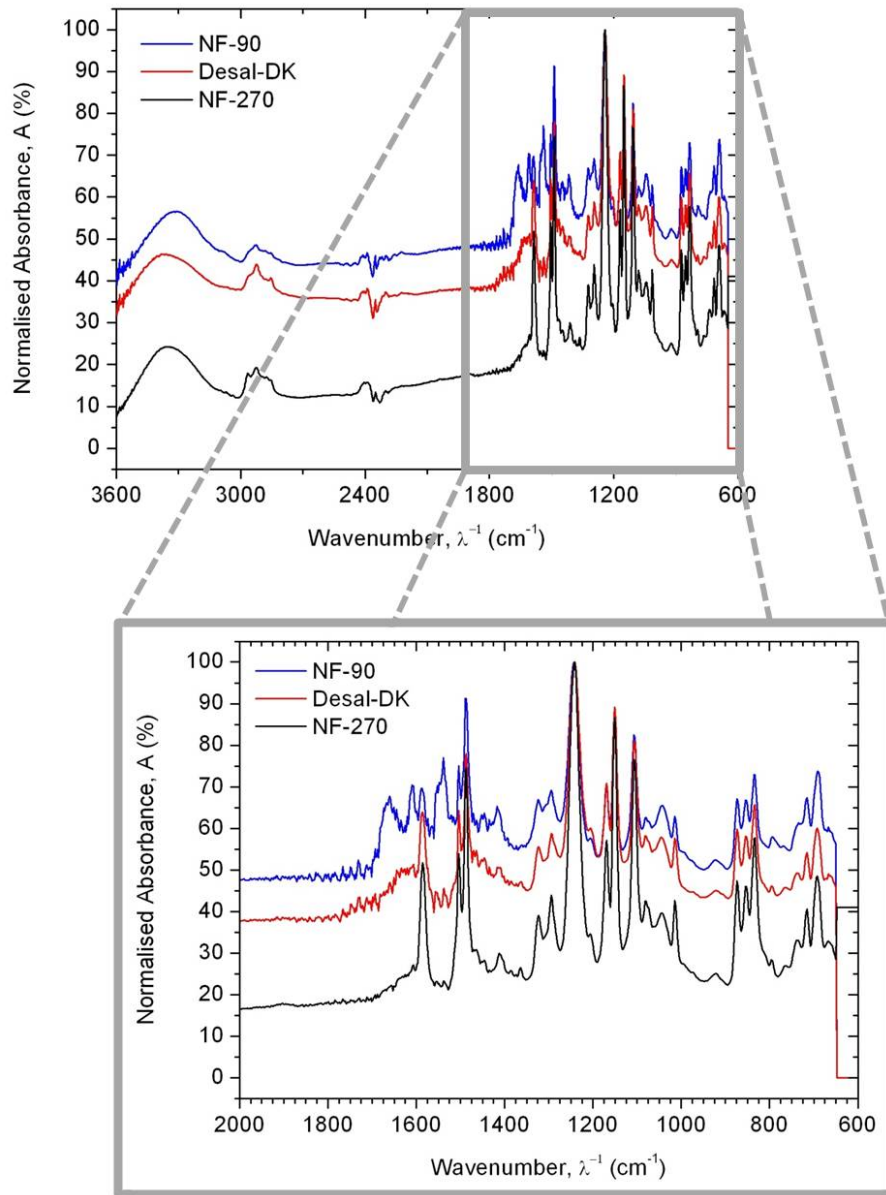


Figure 2.5: Whole ATR-FTIR spectra for three NF-membranes with zoom into the fingerprint region.

At first sight, the three spectra look very similar and the explanation should be found in the characteristics of the infrared spectroscopy method used. The analysis depth varies between 1 and 10 μm when ATR is used [34]. Considering that the top layer in a thin-film composite has a thickness around 0.3 and 3 μm [10], the ATR-FTIR spectra are showing information of both, the top layer and the micro-porous support.

UDEL® polysulfone is one of the preferred materials for the micro-porous support and it is synthesized by nucleophilic substitution of 4,4'-dichlorophenyl sulfone (DCDPS) by 2,2-bis-(4-hydroxyphenyl)-propane (Bisphenol A) in a dipolar aprotic solvent, such as dimethyl sulfoxide (DMSO) [35]. The solvent promotes very rapid reaction rates and the molecular mass of the polymer is controlled by the addition of methyl chloride, dealing with a methoxy end-group [36].

The chemical structure of the repeating unit of this kind of polysulfone is represented in Figure 2.6, while the identification and assignment of the corresponding polysulfone bands, according to the characteristics group frequencies [37-39], is condensed in Table 2.4.

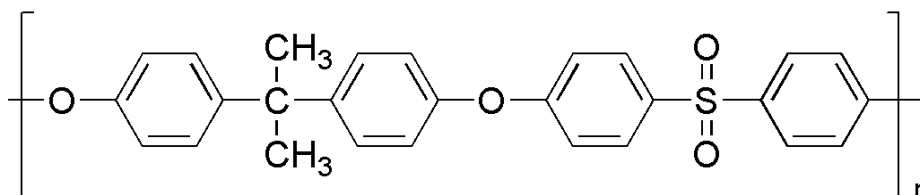


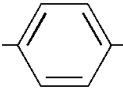
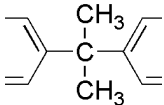
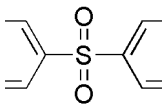
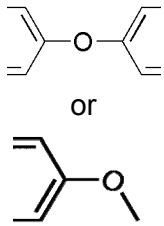
Figure 2.6: Chemical structure of polysulfone.

These values are in good agreement with those found in polysulfone UF-membranes [40] and some other commercial NF- and RO-membranes supported on micro-porous polysulfone [41,42]; but also in compounds like 2,2-diphenylpropane [43], diphenyl ether [44] and diphenylsulfone [45].

To determine the chemical composition of the top layer, it is necessary to concentrate the attention on the differences between the spectra already shown. Having again a look at Figure 2.5 it is possible to determine obvious differences in the range $1700\text{-}1500\text{ cm}^{-1}$, and they can be better appreciated in Figure 2.7.

From a superficial analysis it can be concluded that the NF-90 membrane clearly possesses a chemical composition which differs from those of Desal-DK and NF-270 membranes.

Table 2.4: Characteristic infrared bands of polysulfone.

Functional group	Peak assignment	Wavenumber, λ (cm ⁻¹)	
		Expected	Observed
	Ring C–C stretching	1625-1590 1590-1575 1525-1480 1420-1400	1610 1586 1504,1488 1416-1411
	C–H in-plane deformation (p-disubstituted ring)	1185-1165 1130-1110 1025-1005 995-975	1169 1106 1014 Very weak
	C–H out-of-plane deformation (p-disubstituted ring)	860-780 710-680	853,833,795 691
	C-H stretching	2990-2850	2925,2875
	>C(CH ₃) ₂ deformation	1385-1335	1385 1365
	>C(CH ₃) ₂ skeletal vibrations	1060-1040 955-900	1044 921
	SO ₂ asymmetric stretching	1350-1270	1323 1294
	SO ₂ symmetric stretching	1180-1145	1151
	C-H stretching	3005-2935 2860-2815	2970 2850
	C-H deformation	1485-1435 1460-1420 1235-1155	1470-1464 1452-1446 1205
	C-O-C asymmetric stretching	1310-1210	1242
	C-O-C symmetric stretching	1120-1020	1044

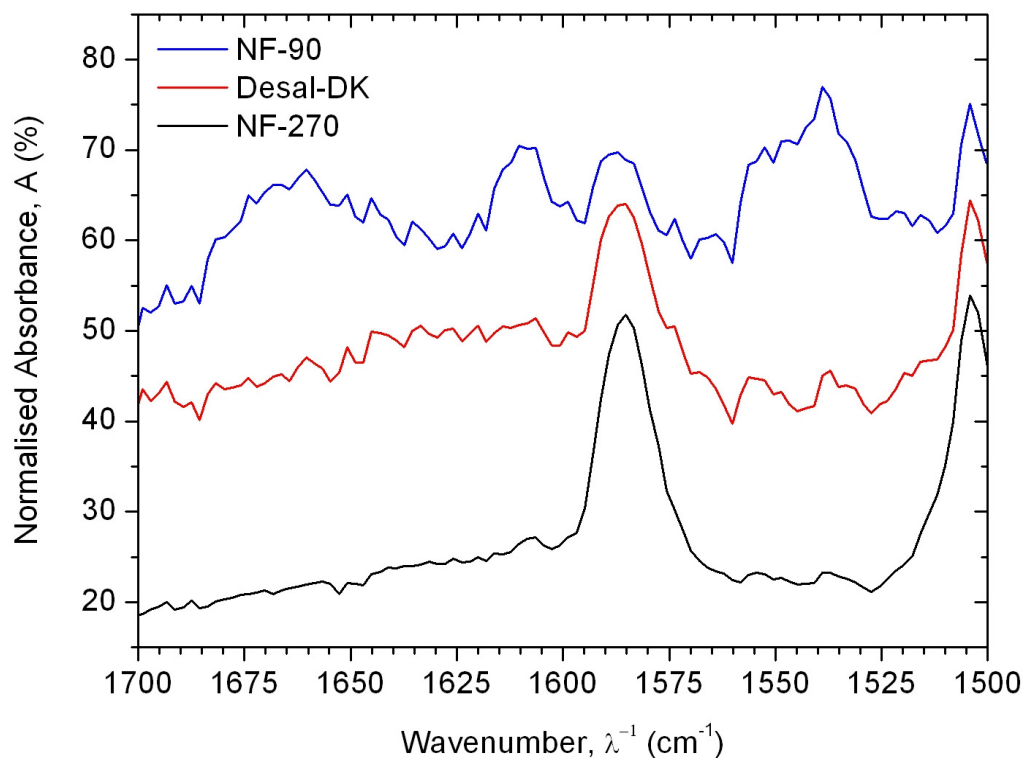


Figure 2.7: ATR-FTIR spectra for three NF-membranes over 1400-1700 cm^{-1} .

FilmTec produces two different types of polyamide membranes based on the early membranes developed and patented by Cadotte [46]: the first type is an aromatic polyamide and the second type is a mixed aromatic-aliphatic polyamide (polypiperazine).

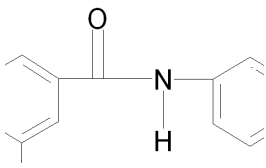
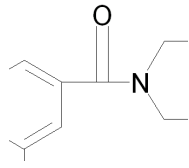
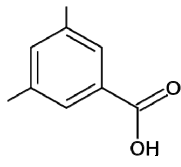
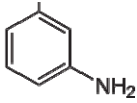
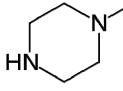
Both types of membranes are produced from the reaction of aromatic trimesoyl chloride (benzene-1,3,5-tricarboxyl chloride) with the corresponding amine: m-phenylene diamine (aromatic) or piperazine (aliphatic). As consequence, the differences observed in the spectra are due to the polyamide formed during the interfacial polymerization reaction.

Additionally, the polymeric chains could finish either with an unreacted amino group or with a carboxylic acid group, product of the hydrolysis of the acyl chloride group. In Table 2.5 are summarized the bands expected for the polyamides and their end-groups from both types of FilmTec membranes, which are in good agreement with those already published for both kinds of polyamide membranes [47-50] and similar amide compounds [51].

In the case of the Desal-DK membrane, its spectrum is very similar to that obtained for the NF-270 membranes, and it could be concluded that the

membrane is also based on a piperazine polyamide. However, due to the differences between the characteristics for both membranes already shown in Table 2.3, it is believed that the membrane suffered some modification, like blending with unreactive polymers (e.g. polyvinyl alcohol) to change hydrophobicity and density of the top layer [52,53].

Table 2.5: Characteristic infrared bands for polyamide in NF-membranes.

Functional group	Peak assignment	Wavenumber, λ (cm ⁻¹)	
		Expected	Observed
	Amide I (C=O stretching)	1680-1630	1670-1655
	Amide II (N-H deformation and C-N stretching)	1570-1515	1560-1530
	Amide I (C=O stretching)	1670-1630	Very weak peaks
	Amide II (C-N-C stretching)	750-700	735
	C=O stretching	1755-1735 1715-1660	Several peaks
	C-H deformation (1,3,5-trisubstituted ring)	890-810 730-660	873 715, 670
	N-H deformation	1615-1580	1610
	N-H deformation	1580-1490 750-700	1556, 1537 735

In a publication appeared during the accomplishment of this work, similar conclusions were obtained with respect to the chemistry of the FilmTec membranes, while the authors consider that Desal-DK membrane contains a modifying agent containing only carbon, oxygen and hydrogen [54].

In another publication, it was pointed out that Desal-DK membrane has a proprietary active layer based on polypiperazine amide and that it consists of three sub-layers [55]. Further information in this direction was found in a brochure of Osmonics Inc. (acquired by General Electric), which highlights

the advantages of the Osmonics 3-layer NF-membranes containing a proprietary layer between the polyamide top layer and the polysulfone layer [56]. It is believed that the middle layer consists of a discrete layer of insolubilized polyvinyl alcohol resting upon a polysulfone microporous support, and a polypiperazine amide barrier layer resting upon the polyvinyl alcohol layer, similar to those developed by Nitto-Denko [10,57].

From now on, the Desal-DK membrane will be excluded during the T-SAR analysis, due to the additional complexity and uncertainty associated with the eventual presence of a polyvinyl alcohol intermediate layer.

On the contrary, both FilmTec membranes exhibit clear advantages for further T-SAR analysis: trimesoyl chloride takes part in both structures, meaning that the origin of the differences should be associated with the difunctional amine used in each case. Furthermore, both kinds of amines were confirmed without any doubt by infrared analysis.

Because the acyl chloride groups (-COCl) can react either with the amino groups or with water, there are two possible main constituting units for the polyamide chains: the linear one, in which only two of the three acyl chloride groups are forming amide bonds and the third one reacts with water to form a carboxylic acid group; and the cross-linked unit, in which every acyl chloride group is forming amide bonds [58,59].

All these mentioned structures are represented in Table 2.6, with the lone pairs of electrons being explicitly marked. For simplification purposes, the hydrogen atoms bounded to the carbon atoms are not represented.

With these constituting units conclude the application of the three first steps of the algorithm for T-SAR analysis. Now it is necessary to concentrate the attention on the stereochemistry of each of these constituting units.

2.3.2 Stereochemistry

The analysis of the stereochemistry begins by determining the hybridisation of each atom. For such a task, four components of the constituting units are going to be considered, three of them regardless the membrane type: the aromatic ring, the amide bond and the carboxylic acid end group; while the amino end group is related to the type of the amine used in each case. The information corresponding to the atoms hybridisation of each component is summarized in Table 2.7.

Table 2.6: Chemical structure of FilmTec NF-membranes constituting units.

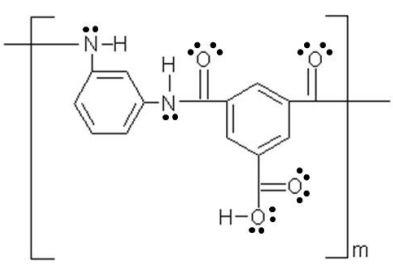
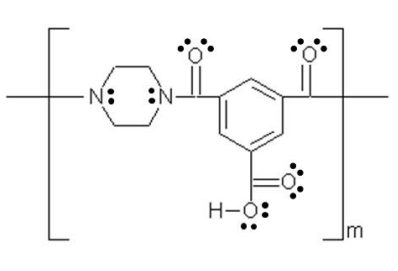
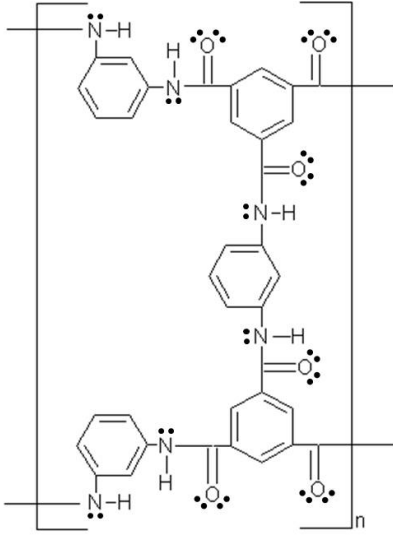
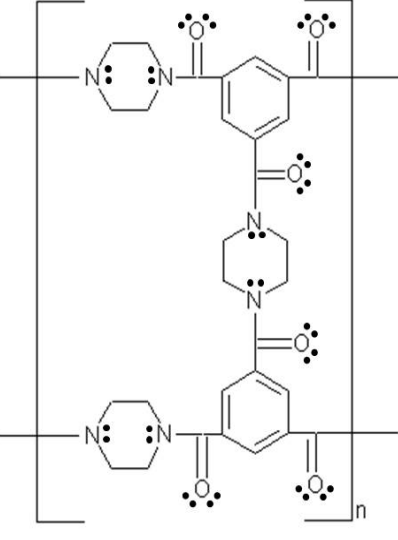
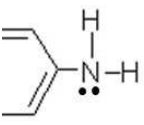
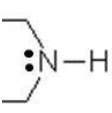
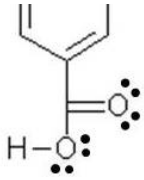

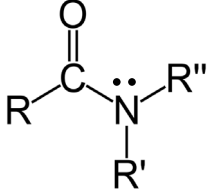
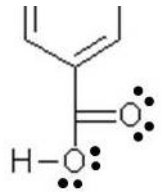
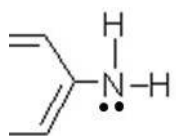
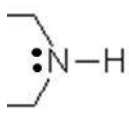
Constituting unit	Membrane	
	NF-90	NF-270
Linear		
Cross-linked		
Amino end-group		
Carboxylic acid end-group		

Table 2.7: Atom hybridisation and expected geometry.

Component		Atom hybridisation	Expected atom geometry
Benzene ring		C: sp^2 H: s	Trigonal planar geometry. π -molecular orbitals delocalized above and below the ring plane [60].
Amide bond		C: sp^2 O: sp^2 N: sp^2	Trigonal planar geometry. A second resonance structure exists with a C=N bond, and charged O ⁻ and N ⁺ atoms [61].
Carboxylic acid end group		C: sp^2 O: sp^2 H: s	Trigonal planar geometry. There are two resonance structures, both with negative charge on the carbonyl oxygen when deprotonated [62,63].
Amine end-group		C: sp^2 N: sp^2 H: s	Trigonal planar geometry. Overlap of the electron lone pair with the π -molecular orbitals in the ring [62,64].
		C: sp^3 N: sp^3 H: s	Pseudo tetrahedral geometry, preferring a chair conformation. N-H bonds favour the equatorial position [65,66].

Furthermore, two kinds of ring systems can be observed: planar aromatic rings from trimesoyl chloride and m-phenylene diamine, and spatial heterocyclic rings from piperazine.

As it is pointed out in Table 2.7, there is a second resonance structure for the amide bond, which restricts rotation occurring around the partial double C-N bond, making possible the existence of isomeric species if the two groups bonded to the nitrogen atom are different ($R' \neq R''$). That is only true in the case of the membrane NF-90, because $R' = H$ and $R'' = C_6H_4-$.

For such amide bonds, the trans-isomer (or Z-configuration) is the most preferred configuration due to steric factors and charge interactions [67]. Some evidence in this direction is observed in the chemical structure of N,N'-(p-phenylene)-dibenzamide, which contains planar phenyl rings which are rotated with respect to the plane of the amide group owing to steric hindrance [68]. Moreover, in the poly(p-phenylene terephthalamide) it was also found that the phenylene rings are twisted in opposite senses with respect to the amide plane [69].

In the case of the NF-270 membrane, the piperazine ring introduces another possibility for different conformations: chair or boat, like every cyclohexane derivative. The chair conformation is more energetically favoured than the boat conformation. The free activation enthalpy of ring inversion for piperazine is 43.1 KJ/mol [65]. In the case of N,N'-dibenzoylpiperazine, the piperazine ring adopts a chair conformation and the two phenyl rings are in parallel [70]. Furthermore, in a related polypiperazine amide (product of the reaction of piperazine with a diacyl chloride) it was remarked that hindered rotation exists, because the rotation around the amide bond or by inversion of the piperazine ring involves relatively high activation energy, around 54.4 KJ/mol [71].

From these results, the geometry of each membrane can be established: the constituting units of the fully aromatic chemistry of NF-90 membrane exhibit planar geometry (but it does not mean that the whole polyamide structure lies in the same plane), while the constituting units of the mixed aliphatic-aromatic chemistry of NF-270 membrane combines both, planar and spatial geometries.

In Table 2.8 are represented the same constituting units of Table 2.6, but this time they were drawn under the considerations described above with respect to bond angles and the spatial distribution of the atoms. However, in these structures the lone pairs of electrons were not represented.

Finally, there is no evidence of chiral centres in all the analyzed constituting units and they are even unlikely, due to the absence of sp^3 hybridised carbon atoms with four different substituents.

2.3.3 Molecular interaction potentials

Using the colour code developed to identify molecular interaction potentials [20], it is possible to obtain a map of inherent interaction

potentials for the membrane constituent units under consideration (Table 2.9).

Table 2.8: Stereochemistry of FilmTec NF-membranes constituting units.

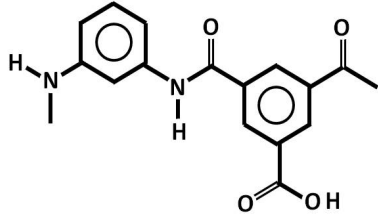
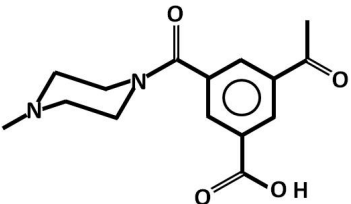
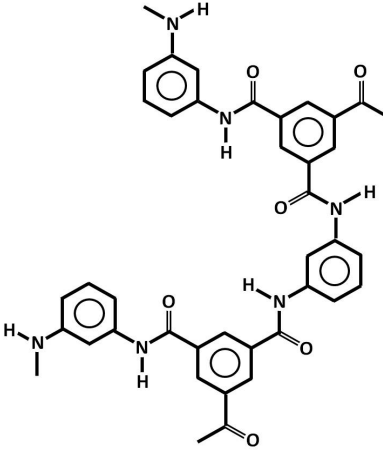
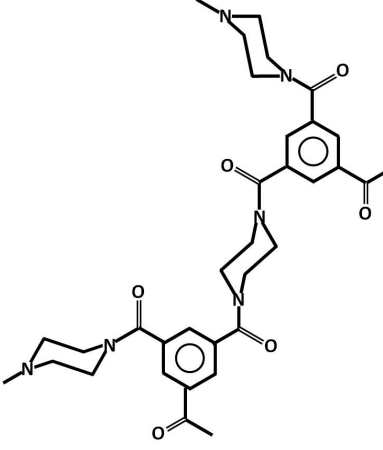
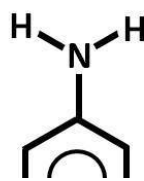

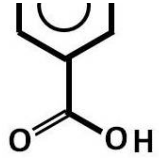
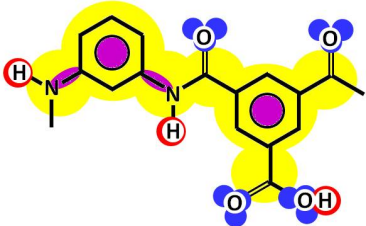
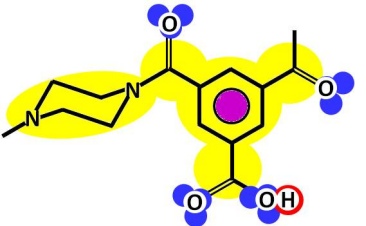
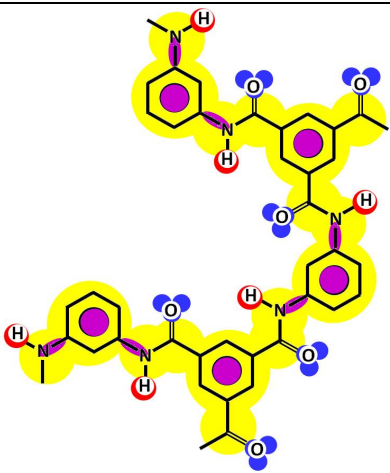
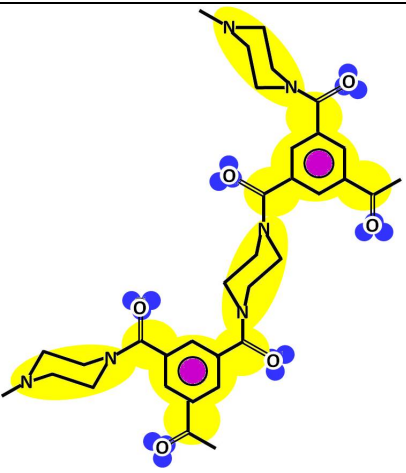
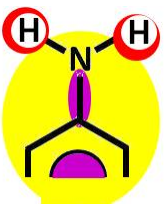
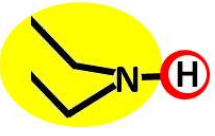
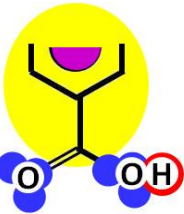
Constituting unit	Membrane	
	NF-90	NF-270
Linear		
Cross-linked		
Amino end-group		
Carboxylic acid end-group		

Table 2.9: Molecular interaction potentials of FilmTec NF-membranes constituting units, according to the colour code from Figure 2.4.

Constituting unit	Membrane	
	NF-90	NF-270
Linear		
Cross-linked		
Amino end-group		
Carboxylic acid end-group		

As it can be observed in Table 2.9, the membranes in the dry state do not possess permanently charged groups. However, both amino and carboxylic acid end groups are responsible for the electrical charge that nanofiltration membranes acquire in contact with water. Then, water introduces changes in the interaction potential map of both membranes

(and also in the stereochemistry of the end groups) which are going to be discussed together with the reactivity aspects later in Section 2.3.4.

The molecular interaction potentials for the NF-90 membrane constituting units can be described as follows. It is evident that strong H-donor (hydrogen atom of amide/amine groups and hydrogen atoms of carboxylic acid groups) and H-acceptor (oxygen atom of carbonyl/carboxylic acid groups) potentials are represented by red and blue colours. Additionally, strong charge transfer potentials are found in both types of aromatic rings, identified with violet colour; while a permanent dipole exists in the aromatic ring due to the 1,3-disubstitution of both amino groups. The carbon skeleton and also the nitrogen atoms (due to conjugation with an aromatic ring and with an aliphatic double bond) exhibit hydrophobic potential and thus are coloured yellow.

Contrarily, in the case of the NF-270 membrane constituting units the H-donor potentials (red colour) are limited to the hydrogen atoms derived from carboxylic acid groups and in a minor scale to hydrogen atoms from amino end groups, because during the amide bond formation the single hydrogen atoms available were removed from piperazine. Then, mainly strong H-acceptor potentials (blue coloured) dominate the interaction potential map for this membrane. Moreover, the charge transfer interaction potential is limited only to the aromatic rings derived from trimesoyl chloride and no dipole moments can be identified due to symmetric geometry. Finally, the strong hydrophobic interaction potential is located along the whole chemical structure, as it is determined by the yellow colour.

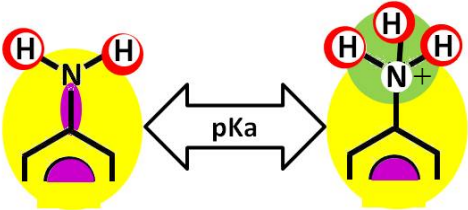
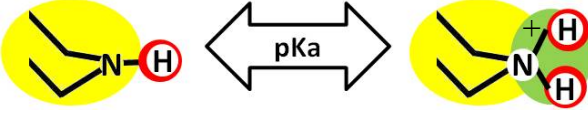
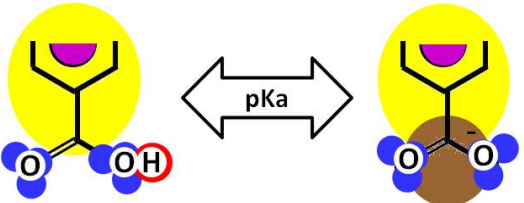
2.3.4 Reactivity

The analysis of the membrane reactivity begins with the identification of possibilities for prototropic shifts, the most common form of tautomerism referring to the relocation of protons [72]. In the membranes considered, the only possibility for such a shift is related to the presence of hydrogen in the amide group. However, that is only true for the NF-90 membrane (secondary amide), because the NF-270 membrane is formed by tertiary amides, which do not have available hydrogen atoms.

In the case of aromatic polyamides, similar to that forming the NF-90 membrane, it was found that the amide form (NHC=O) is more profitable than the imidol form (NC-OH) on account of both greater bond energies and greater resonance energies [73]. Then, tautomerism is not possible.

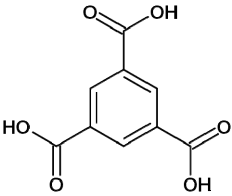
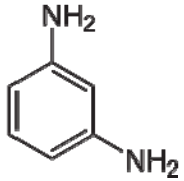
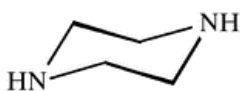
Both membranes possess amino and carboxylic acid groups which, in contact with water, can accept and donate a proton respectively; changing their interaction potentials and thus acquiring electrical charge (Table 2.10). The existence and the amount of the protonated form of carboxylic acid and amino groups is pH-dependent and can be determined using the acid-base equilibrium and the Henderson-Hasselbalch equation [74]. A stereochemical change also occurs (from sp^2 to sp^3 hybridization), when the nitrogen atoms of the NF-90 membrane amino groups are protonated.

Table 2.10: Molecular interaction potentials for charged groups of FilmTec NF-membranes, according to the colour code from Figure 2.4.

Constituting unit	Membrane	Corresponding reaction
Amino end-group	NF-90	
	NF-270	
Carboxylic acid group (linear unit or end-group)	Both membranes	

Following the T-SAR algorithm, it is necessary to identify the pKa values for the functional groups with H-acceptor or H-donor potential. A first approach to the pKa values is to identify the pKa values of the monomer structures: trimesic acid (product of the hydrolysis of trimesoyl chloride), m-phenylene diamine und piperazine (Table 2.11).

Table 2.11: pKa values for the compounds involved on the membrane chemistry.

Compound	Chemical structure	pKa values [Reference]		
Trimesic acid		3.12 [75,76] 3.17 [77]	3.89 [75] 4.10 [76] 3.96 [77]	4.70 [75,77] 5.18 [76]
m-phenylene diamine		4.88 [75,78] 4.92 [78]	2.65 [75,78] 2.48 [78]	---
Piperazine		9.82 [75] 9.73 [79]	5.68 [75] 5.35 [79]	---

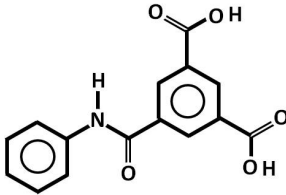
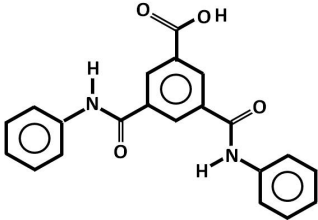
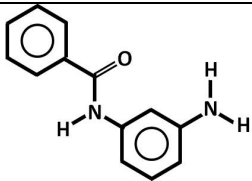
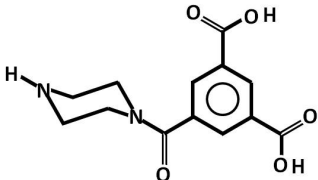
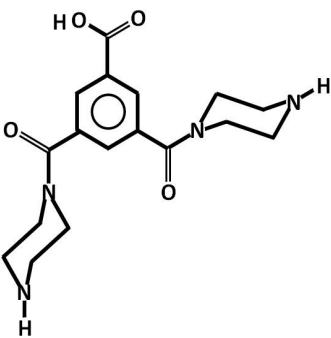
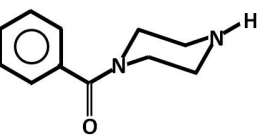
The last pKa value for trimesic acid and amines does not play any role in the case of the membrane constituting units, because the carboxylic acid or amine group was already substituted by the amide bond. In the case of pendant carboxylic groups (in the linear constituting units) the second pKa value loses its physical sense too. However, the remaining values from Table 2.11 must be considered only as a first approximation to the real ones, which are conditioned by the ring substitutions and/or the effects of polymerization [80].

Insofar, there are some existing chemical compounds which are similar to some parts of the membrane structures, and the pKa values of these compounds can be used as a refined approximation with respect to the pKa values of the monomers involved in polymerization. These chemical structures are summarized in Table 2.12 with their respective pKa values, which were calculated using MOPAC2009TM calculation tools for pKa determination [81] or were found in the CAS-databases [82].

By comparison of these values with those presented in Table 2.11, it can be concluded that further (aromatic or aliphatic) rings decrease the pKa values found for the original monomers. Then, values from Tables 2.12 are later used in this study, despite every carboxyl group of the linear units should not be described by the same pKa value. However, better values

are not available due to the difficulty related to their calculation in more complex structures.

Table 2.12: pKa values for compounds with a chemical structure similar than that found in the membrane chemistry.

	Compound	Chemical structure	pKa value [Reference]
Similar to NF-90 membrane chemistry	5-[(phenylamino)carbonyl]-1,3-benzenedicarboxylic acid		2.66 2.92 (both calculated)
	3,5-bis[(phenylamino)carbonyl]-benzoic acid		2.52 (calculated)
	N-(3-aminophenyl)-benzamide		4.23 [82]
Similar to NF-270 membrane chemistry	5-(1-piperazinylcarbonyl)-1,3-benzenedicarboxylic acid		2.81 2.91 (both calculated)
	3,5-bis(1-piperazinylcarbonyl)-benzoic acid		2.56 (calculated)
	1-benzoyl-piperazine		8.48 [82]

The last step of the T-SAR algorithm is to indicate the reactivity of each functional group. From all possible reactions [83,84] which could take

place from the chemical point of view, only those which have a certain probability to occur in aqueous applications of nanofiltration membranes are summarized in Table 2.13.

Table 2.13: Reactivity of functional groups present in polyamide membranes.

Functional group	Reaction	Observations
Aromatic ring	Electrophilic substitution	<ul style="list-style-type: none"> • Substitution of a hydrogen atom by an electrophile. • The position of the substituted hydrogen is decided by the actual substituents in the ring (activating or deactivating). • The compound obtained depends on the electrophile used.
Amide group	Hydrolysis	<ul style="list-style-type: none"> • Takes place under both acidic and alkaline conditions. • Vigorous conditions (heating or concentrated solutions) are needed. • In both cases the corresponding carboxylic acid is obtained
Amino end group	Oxidation	<ul style="list-style-type: none"> • Takes place in aqueous solution of hydrogen peroxide. • From primary and secondary amines a complex mixture of products is obtained.
	Salt formation	In presence of acids, related with the dissociation behaviour in aqueous media.
Carboxylic acid end group	Oxidation	Produce the removal of the carboxylic carbon as carbon dioxide.
	Salt formation	In presence of bases, related with the dissociation behaviour in aqueous media.

In the case of very complexes structures the different structural elements should be first analyzed as before, and subsequently, the gained knowledge should be used to understand the whole chemical structure, like in a puzzle [20]. However, despite the amount of worthy knowledge gained until now, there is still a lack of information about how the polyamide layer of both membranes looks and this matter is subject of attention in the next section.

2.3.5 A picture of both nanofiltration membranes

According to the last point discussed in the previous section, in order to obtain a picture of the nanofiltration membrane, it is necessary first to visualize how the top layer is built. If it is supposed that the membrane begins to grow in the plane of polymerization (corresponding to the interface between both solvents), then additional diamine monomers which are able to diffuse through the first formed polymer sheet, begin the process again in a subsequent membrane sheet. All the sheets which constitute the top layer are kept together either by cross-linking reactions or by attractions derived from molecular interaction potentials.

In this context, the chemical structure of each membrane sheet is a consequence of a given combination between linear and cross-linked constituting units, as well as both kinds of end-groups. At this point, experimental information derived from X-ray photoelectron spectroscopy (XPS) characterization analysis can be helpful to reveal how such combination of constituting units looks. XPS is a technique which allows the detection of all the elements (except hydrogen) which are present in the sample under analysis. Additionally, the analysis depth is located typically between 1 and 3 nm [34], which means that the obtained data should correspond to the chemical composition of the last sheet forming the top layer in a thin-film composite membrane.

In Table 2.14 are summarized the XPS experimental data corresponding to the FilmTec membranes, which were recently published [85], together with the element compositions for the linear and cross-linked constituting units, directly determined from their chemical structures (Table 2.7) as follows:

$$\%C = \frac{N_C}{N_C + N_N + N_O} \cdot 100 \quad (\text{Eq. 2.2})$$

where:

%C = carbon composition (%)

N_C : number of carbon atoms (-)

N_N : number of nitrogen atoms (-)

N_O : number of oxygen atoms (-)

$$\%N = \frac{N_N}{N_C + N_N + N_O} \cdot 100 \quad (\text{Eq. 2.3})$$

where:

%N = nitrogen composition (%)

$$\%O = \frac{N_O}{N_C + N_N + N_O} \cdot 100 \quad (\text{Eq. 2.4})$$

where:

%O = oxygen composition (%)

$$\frac{O}{N} = \frac{N_O}{N_N} \quad (\text{Eq. 2.5})$$

where:

O/N = oxygen to nitrogen ratio (-)

Table 2.14: Atomic concentrations for NF-membranes and constituting units.

Membrane	Constituting unit	Element composition (%)			O/N ratio
		Carbon	Nitrogen	Oxygen	
NF-90	Top layer [85]	73.9 ± 1.4	12.1 ± 1.0	14.0 ± 1.5	1.16 ± 0.16
	Linear C ₁₅ N ₂ O ₄	71.5	9.5	19.0	2.0
	Cross-linked C ₃₆ N ₆ O ₆	75.0	12.5	12.5	1.0
NF-270	Top layer [85]	71.1 ± 1.1	12.5 ± 0.4	16.4 ± 1.0	1.31 ± 0.09
	Linear C ₁₃ N ₂ O ₄	68.5	10.5	21.0	2.0
	Cross-linked C ₃₀ N ₆ O ₆	71.4	14.3	14.3	1.0

The experimentally determined element composition can be approximately considered as a weighted mean of the element composition of each constituting unit, with the amount of each constituting unit as weights, as follows:

$$\%X_{TL} = \left(\frac{m}{m+n} \right) \cdot \%X_L + \left(\frac{n}{m+n} \right) \cdot \%X_{CL} \quad (\text{Eq. 2.6})$$

where:

%X_{TL} = element X composition for the top layer (%)

m: Number of linear constituting units (-)

n: Number of cross-linked constituting units (-)

%X_L = element X composition for the linear constituting unit (%)

%X_{CL} = element X composition for the cross-linked constituting unit (%)

As it was pointed out, this last equation must be seen as an approximation that considers that linear and cross-linked units have very much higher weights than both types of end-groups. Indeed, amino groups do not contribute with any atom to this calculation (hydrogen atoms are excluded during XPS analysis), while carboxylic acid end-groups contribute only with an additional oxygen atom.

In this context, the ratio oxygen-nitrogen is a measure for the membrane cross-linking degree [54]. An O/N ratio of 2 represents a fully linear polyamide structure ($n = 0$), while an O/N ratio of 1 represents a fully cross-linked polyamide structure ($m = 0$). Considering that each membrane comprises “m” linear units and “n” cross-linked units, it is possible to relate this amount of constituting units with the O/N ratio as follows:

$$\frac{O}{N} = \frac{4 \cdot m + 6 \cdot n}{2 \cdot m + 6 \cdot n} \quad (\text{Eq. 2.7})$$

Furthermore, if the O/N ratio is known (i.e. from XPS data), then it is possible to determine the ratio between cross-linked and linear units, as follows:

$$\frac{n}{m} = \frac{2 - \frac{O}{N}}{3 \cdot \left(\frac{O}{N} - 1\right)} \quad (\text{Eq. 2.8})$$

where:

n/m : Cross-linked to linear units ratio (-)

Applying this equation to the experimental O/N ratios shown in Table 2.14, an n/m ratio can be obtained for the NF-90 membrane, which can be represented as a fractional number by 9/5. In a similar way, an n/m ratio for the NF-270 membrane can be also obtained, which can be represented as a fractional number by 3/4. However, an equivalent value of 6/8 (instead of 3/4) was selected in this study for the NF-270 membrane.

That means that the smallest pattern representing the chemistry of the NF-90 top layer comprises 9 cross-linked constituting units and 5 linear constituting units, while the equivalent pattern representing the chemistry of the NF-270 membrane top layer comprises 6 cross-linked constituting units and 8 linear constituting units. In both cases is the total number of constituting units the same (14 in total). Then, by direct comparison of the numbers of cross-linked units in each case, it is possible to confirm that the NF-90 membrane has a higher cross-linking degree (9/14) than the NF-270 membrane (6/14).

However, the actual challenge consists of finding an arrangement containing 14 constituting units for each membrane. According to Table 2.15, the number of linear and cross-linked constituting units defines how many trifunctional and difunctional monomers are involved. Trimesoyl chloride can build three covalent bonds, while both amines can build only two covalent bonds. As consequence, some covalent bonds remain “open” for further growth of the polymeric structure.

Table 2.15: Basic information needed to assemble the membranes patterns.

Number of	Membrane	
	NF-90	NF-270
Linear units (m)	5	8
Cross-linked units (n)	9	6
Trifunctional monomers	23 ($5 \cdot 1 + 9 \cdot 2$)	20 ($8 \cdot 1 + 6 \cdot 2$)
Difunctional monomers	32 ($5 \cdot 1 + 9 \cdot 3$)	26 ($8 \cdot 1 + 6 \cdot 3$)
Remaining bonds	5 ($23 \cdot 3 - 32 \cdot 2$)	8 ($20 \cdot 3 - 26 \cdot 2$)

With all these assumptions in mind, the constituting units should be randomly arranged to form the polyamide structure. A first approach to possible arrangements for the chemical structure of both FilmTec NF-membranes is represented in Figures 2.8 (NF-90) and 2.9 (NF-270), considering also the presence of charged groups and the molecular interaction potentials for the whole arrangement.

In the first case, a dense structure was obtained in agreement with a higher cross-linking degree; while in the second case a loose structure was found. In both cases, the existence of openings is evident: the NF-90 membrane exhibit two kinds of such openings, while the NF-270 membrane exhibits only one opening type.

However, an obvious criticism for such patterns is related to the question: are only these arrangements possible? And the answer should be no.

In order to consider an arrangement as reliable, it should be coherent with the properties exhibited by the membrane and able to describe them in an adequate way.

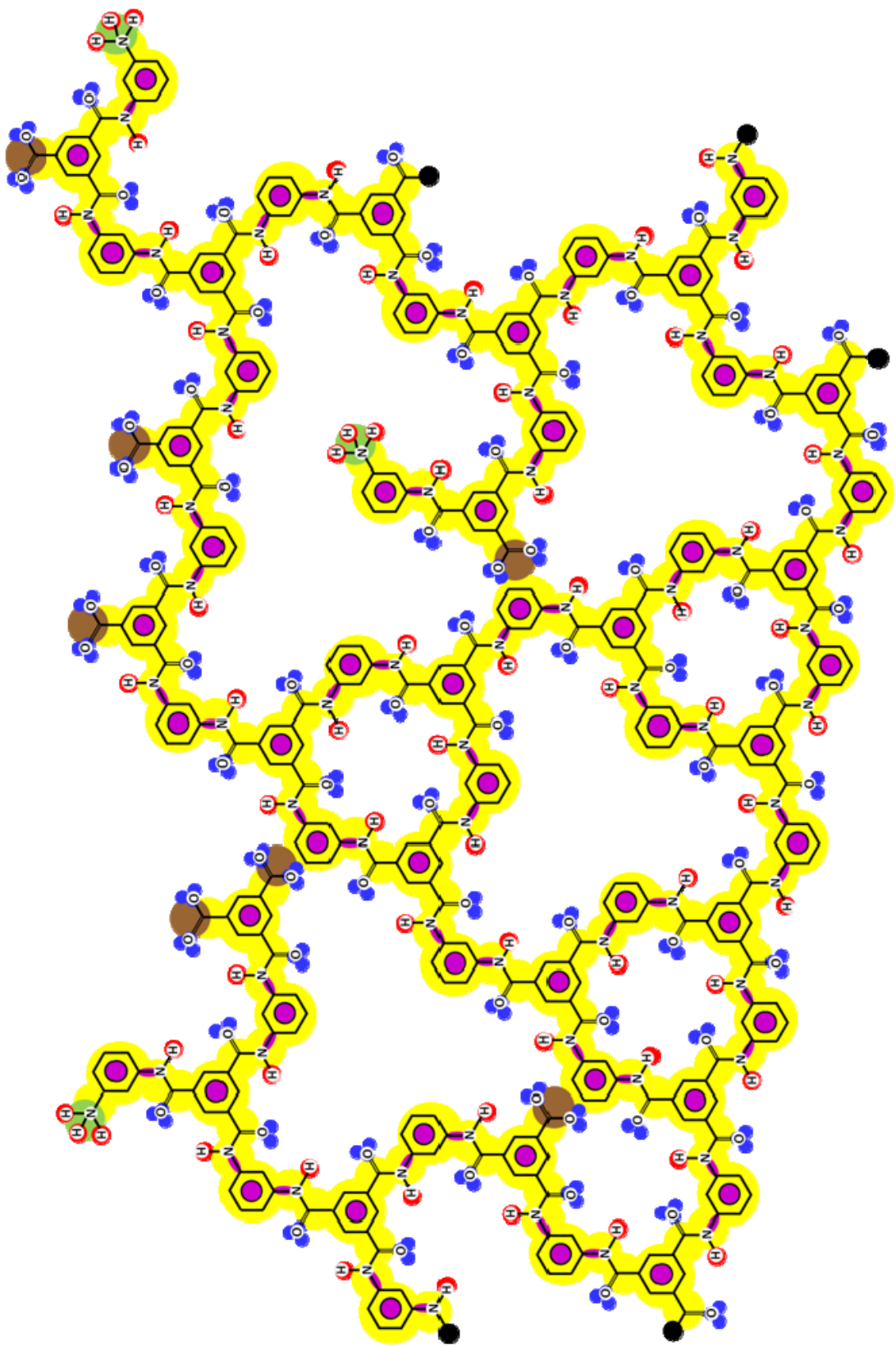


Figure 2.8: Pattern developed for the NF-90 membrane (9 cross-linked and 5 linear units), coloured according to Figure 2.4. Black points are “open” bonds.

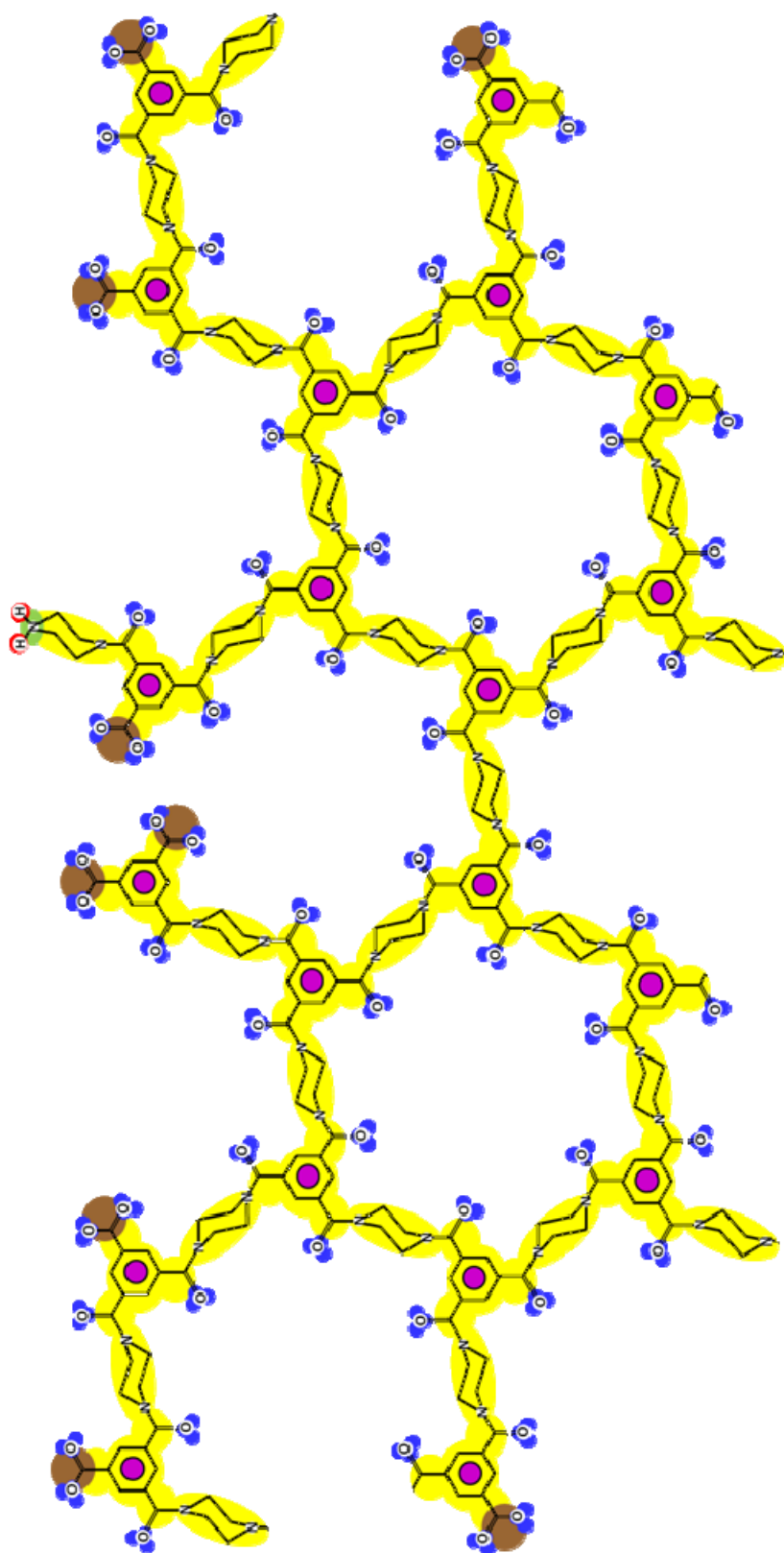


Figure 2.9: Pattern developed for the NF-270 membrane (6 cross-linked and 8 linear units), coloured according to Figure 2.4. Black points are “open” bonds.

Because several arrangements may differ in the number and nature of end-groups, the determination of the theoretical isoelectric point (IEP) in the wet state can be a useful way to check such coherence, considering that the IEP is the pH at which a particular molecule carries not net electrical charge [83].

In this case, the chemical structures for both membranes as well as the pKa values of their charged groups are needed. Based on the following dissociation reaction:



for carboxylic groups (acting in this case as acid, -COOH), the conjugate base is the carboxylate anion (COO⁻), while for amino groups (acting in this case as conjugate base, -NH₂ or -NH), the corresponding acid is the protonated amino group (H₂N⁺ or H₃N⁺).

If the pH of the solution is given and the pKa value for each involved group is known, it is possible to calculate the amount of charged groups already formed, using the following equations:

$$pH = pKa + \log \frac{[conjugate_base]}{[acid]} \quad (\text{Eq. 2.9})$$

where:

pH: pH of the solution (-)

pKa: pKa value for the charged group under consideration (-)

[conjugate_base]/[acid]: concentration ratio of conjugate base to acid (-)

$$\%Conjugate_base = \frac{[conjugate_base]/[acid]}{1 + [conjugate_base]/[acid]} * 100 \quad (\text{Eq. 2.10})$$

where:

%Conjugate_base: amount of carboxylate anions already formed (-)

$$\%Acid = 100 - \%Conjugate_base \quad (\text{Eq. 2.11})$$

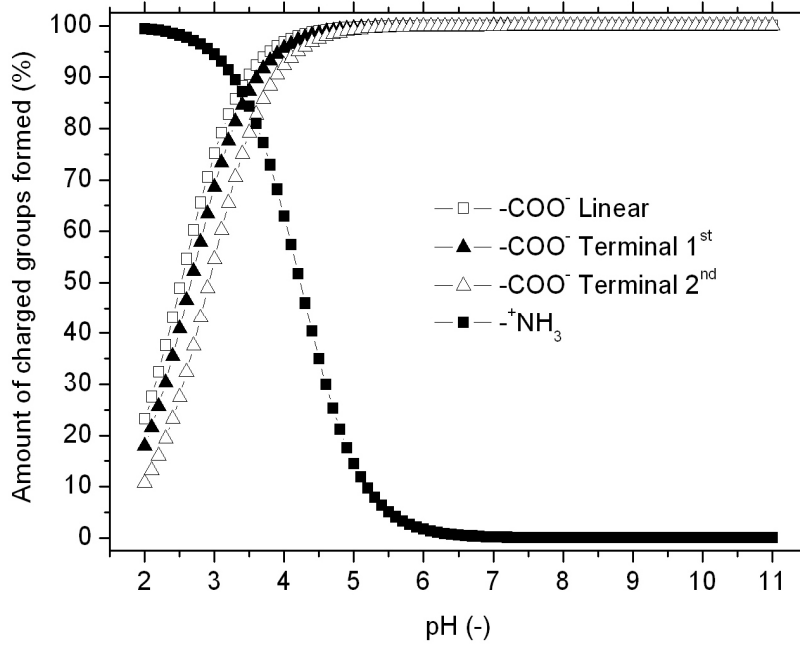
where:

%Acid: amount of protonated amino groups already formed (%)

When the pH of the solution is equal to the pKa value of the group under consideration, the concentration quotient of conjugate base to acid is equal to unity, meaning that 50% of the compound exists in the acid form, and 50% exist in the conjugate base form.

Then, using the pKa values from Table 2.12, it is possible to calculate the pH-dependence of the amount of charged groups for both membranes, as it is shown in Figures 2.10a (NF-90) and 2.10b (NF-270).

a)



b)

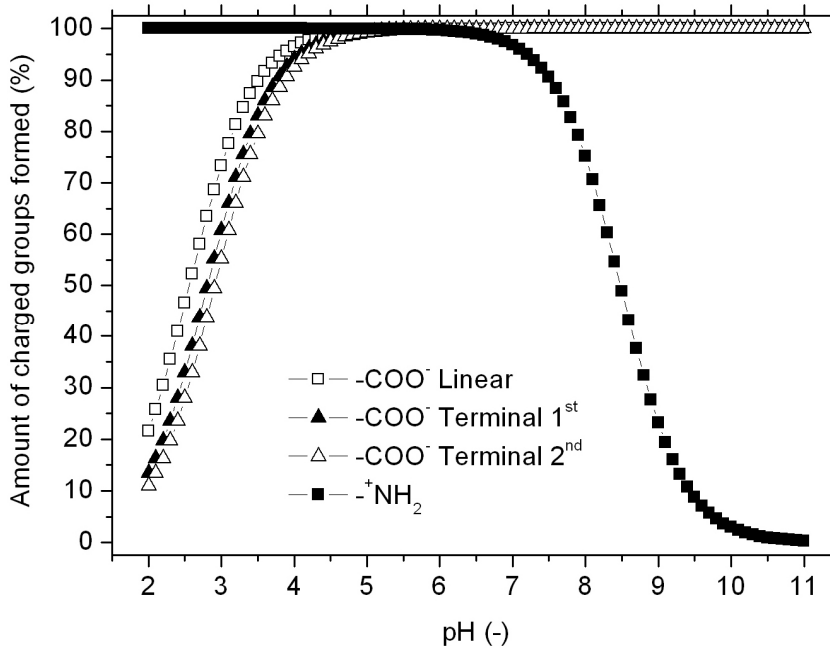


Figure 2.10: Distribution of charged groups according to the pH of the feed solution: a) NF-90, b) NF-270.

Regardless the type of carboxyl end-group, 90% or more of the carboxylate anions are already formed at pH above 5; while the same amount of protonated amino groups are already formed when the pH is below 3.5 for the NF-270 membrane or below 8 for the NF-90 membrane.

To calculate the theoretical IEP it is necessary to combine the information about the relative amount of charged groups (Figure 2.10, Equations 2.9 to 2.11), with the number of positive and negative groups for each membrane pattern, which can be directly obtained from Figures 2.8 and 2.9. Then, the theoretical IEP corresponds to the pH in which the net charge obtained is zero, as follows:

$$-\sum N_{\text{COO}^-} \cdot \left(\frac{\% \text{COO}^-}{100} \right)_{\text{pH=IEP}} + N_{\text{NH}_x^+} \cdot \left(\frac{\% \text{NH}_x^+}{100} \right)_{\text{pH=IEP}} = 0 \quad (\text{Eq. 2.12})$$

where:

N_{COO^-} : number of deprotonated carboxylic acid groups (-)

$\% \text{COO}^-$: amount of deprotonated carboxylic acid groups already formed at pH = IEP (%)

$N_{\text{NH}_x^+}$: number of protonated amino groups (-)

$\% \text{NH}_x^+$: amount of protonated amino groups already formed at pH = IEP (%)

These calculations are summarized in Table 2.16 (NF-90 membrane) and Table 2.17 (NF-270 membrane).

Table 2.16: Theoretical determination of the isoelectric point for the pattern presented in Figures 2.8 (NF-90 membrane).

NF-90 membrane	Charged group			
	COO ⁻ Linear	COO ⁻ Terminal		H ₃ N ⁺
Number of groups (from Figure 2.8)	5	1	1	3
pKa value (from Table 2.12)	2.52	2.66	2.92	4.23
Amount formed at pH = 2.45 (Eq. 2.9-2.11)	46.23%	38.38%	25.50%	98.35%
Contribution to charge (Eq. 2.12)	-2.31	-0.38	-0.26	+2.95
	-2.95			+2.95

Table 2.17: Theoretical determination of the isoelectric point for the pattern presented in Figures 2.9 (NF-270 membrane).

NF-270 membrane	Charged group			
	COO ⁻ Linear	COO ⁻ Terminal		H ₂ N ⁺
Number of groups (from Figure 2.9)	7	1	1	1
pKa value (from Table 2.13)	2.56	2.81	2.91	8.48
Amount formed at pH = 1.71 (Eq. 2.9-2.11)	12.39%	7.36%	5.94%	100.00%
Contribution to charge (Eq. 2.12)	-0.87	-0.07	-0.06	+1.00
	-1.00			+1.00

The theoretical IEP is equal to pH = 2.45 and pH = 1.71 for the NF-90 and NF-270 membranes, respectively. However, both IEP values are lower than the experimental ones determined by zeta potential measurements, as it is shown in Figure 2.11.

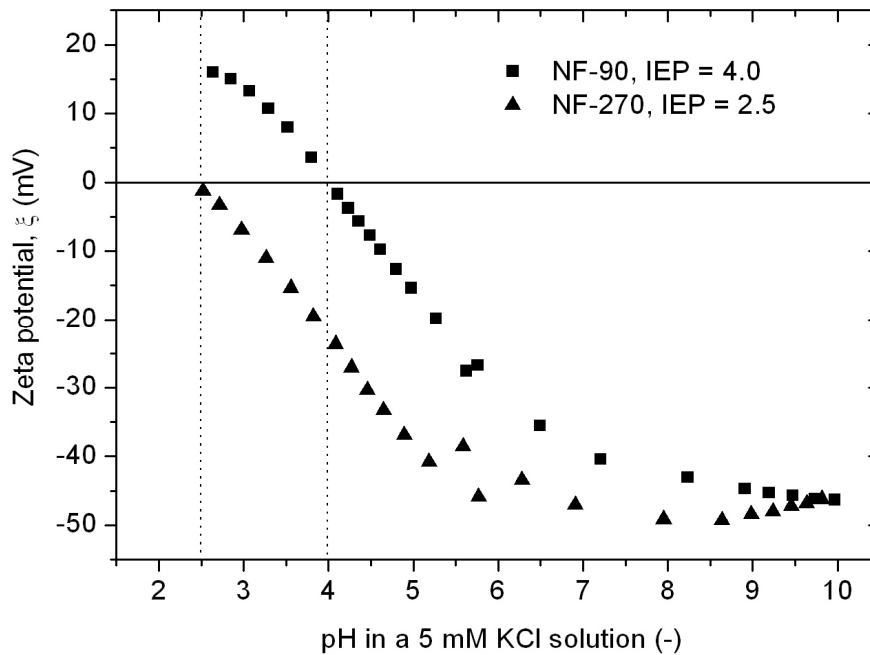


Figure 2.11: pH dependence of Z-potential for the NF-membranes under study.

Considering that in this case, the IEP is the pH for which the zeta potential is zero, values of 4.0 and 2.5 were determined for the NF-90 and the NF-270 membranes, respectively. Furthermore, in a pH range between 2.5 and 10, the NF-270 membrane exhibit always a net negative charge, while the NF-90 membrane can exhibit either positive (below the IEP) or negative (above the IEP) net charge depending of the pH of the solution.

Based on these results, it can be concluded that the patterns proposed in Figures 2.8 and 2.9 are not representing the real arrangements, despite there are using all the constituting units involved and respecting the open bonds condition (Table 2.15). However, from the experimental IEP values it could be possible to find a new arrangement for both membranes, but a new challenge has to be solved: how many charged groups are needed in each pattern to obtain theoretical IEP values equal or very similar to the IEP experimental values?

Considering that at least one terminal group (carboxylic acid or amine) should be present and the number of carboxylic acid groups should be at least equal to the number of linear constituting units, the results of such iterative procedures are summarized in Table 2.18 (NF-90 membrane) and Table 2.19 (NF-270 membrane). From this information, it can be concluded that the number of protonated amino groups is decisive for the IEP location: now 6 (instead of 3) and 4 (instead of 1) protonated amino groups are required for the NF-90 and NF-270 membranes, respectively.

Table 2.18: Determination of the number of charged groups for the NF-90 membrane based on the experimental IEP value (pH = 4.0).

NF-90 membrane	Charged group			
	COO ⁻ Linear	COO ⁻ Terminal		H ₃ N ⁺
Amount formed at pH = 3.43 (Eq. 3-5)	89.04%	85.47%	76.37%	86.33%
pKa value (from Table 2.12)	2.52	2.66	2.92	4.23
Number of groups needed	4	1	1	6
Contribution to charge	-3.56	0.86	0.76	+5.18
	-5.18			+5.18

Table 2.19: Determination of the number of charged groups for the NF-270 membrane based on the experimental IEP value (pH = 2.5).

NF-270 membrane	Charged group			
	COO ⁻ Linear	COO ⁻ Terminal		H ₂ N ⁺
Amount formed at pH = 2.56 (Eq. 3-5)	50.00%	35.99%	30.88%	100.00%
pKa value (from Table 2.12)	2.56	2.81	2.91	8.48
Number of groups (from Figure 2.9)	8	0	0	4
Contribution to charge	-4.00	0	0	+4.00
	-4.00			+4.00

After this calculations IEP values equal to pH = 3.43 and pH = 2.56 were obtained for the NF-90 and the NF-270 membranes, respectively, being the last value in good agreement with the experimental one (pH = 2.5). Furthermore, if the net charge is calculated for different pH values, very different tendencies to those expected are obtained (Figure 2.12).

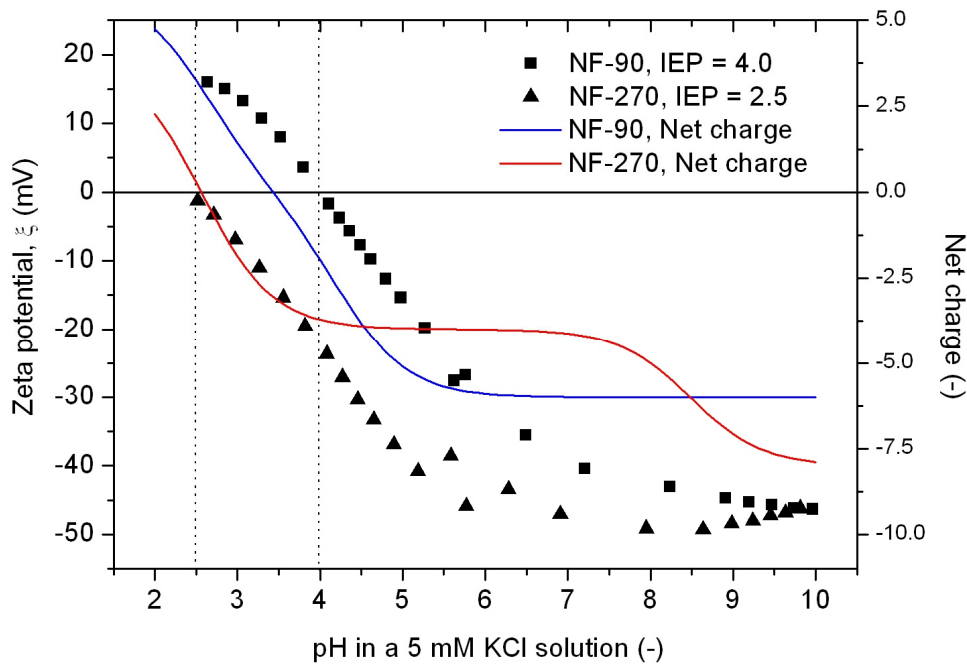


Figure 2.12: Z-potential and theoretical net charge for both NF-membranes.

The curves exhibit a similar tendency around the IEP (despite the displacement in the case of NF-90 membrane), but exhibiting completely different behaviours at higher pH values. These tendencies are suggesting that each charged group possesses definitively an own pKa value, determined by the influence of the surrounding chemical structure. However, they can also indicate that charged groups in the sheet underneath the surface sheet have also an influence in the determination of both theoretical and experimental IEP values.

However, the aim of this work is to propose a better picture for both nanofiltration membranes and not to discover their real structures. Then, it should be necessary to modify the patterns already presented in Figures 2.8 and 2.9, in order to satisfy the new conditions with respect to the number of charged groups. Both modified patterns are represented in Figures 2.13 (NF-90 membrane) and 2.14 (NF-270 membrane). By direct comparison of the original and new patterns, it is clear than to achieve the new condition of more amino end-groups, a looser structure is achieved in both cases. Additionally, the big opening initially found disappears from the NF-90 structure.

The atomic concentrations and the O/N ratio for all the pattern structures are summarized in Table 2.20. All values are in good agreement with the experimental ones, even after loose the original patterns.

Table 2.20: Surface atomic concentrations for NF-membranes and the membranes patterns developed in this work.

Membrane	Constituting unit	Element composition (%)			O/N ratio
		Carbon	Nitrogen	Oxygen	
NF-90	Top layer [85]	73.9 ± 1.4	12.1 ± 1.0	14.0 ± 1.5	1.16 ± 0.16
	Pattern Figure 2.8	74.03	11.87	14.10	1.188
	Pattern Figure 2.13	74.16	11.90	13.94	1.171
NF-270	Top layer [85]	71.1 ± 1.1	12.5 ± 0.4	16.4 ± 1.0	1.31 ± 0.09
	Pattern Figure 2.9	70.12	12.84	17.04	1.327
	Pattern Figure 2.14	70.30	12.87	16.83	1.308

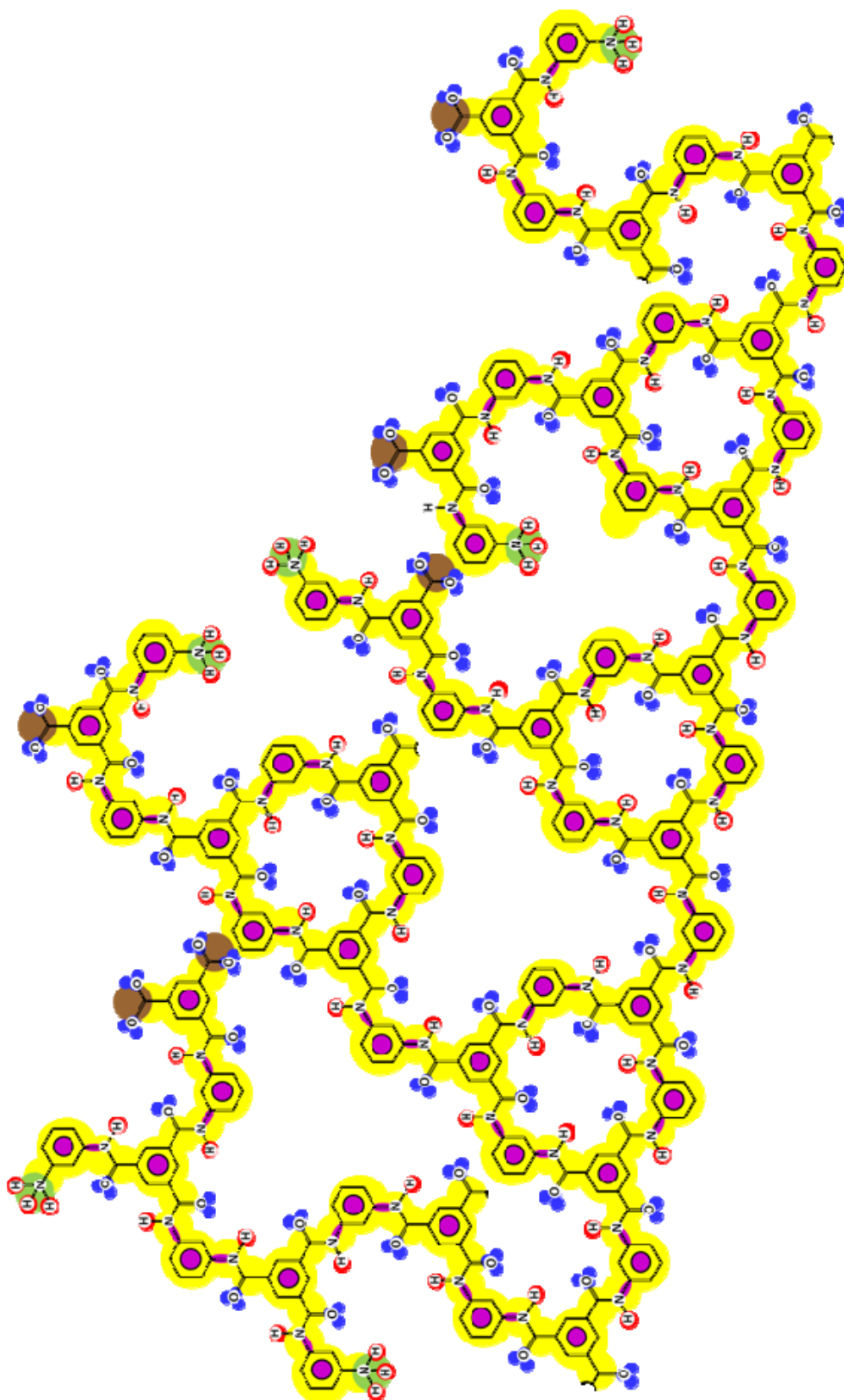


Figure 2.13: Modified pattern for the NF-90 membrane to assure expected IEP, coloured according to Figure 2.4. Black points are “open” bonds.

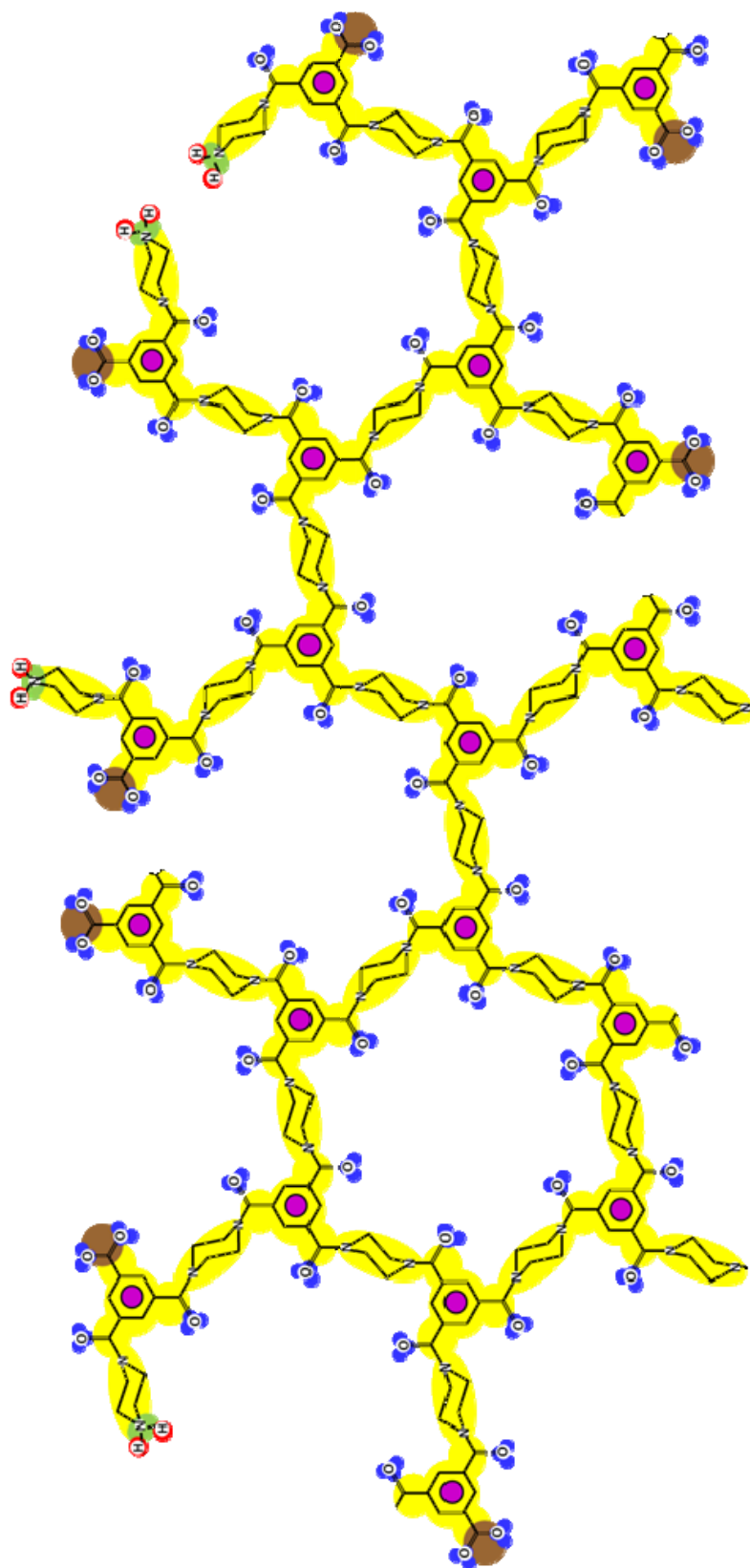


Figure 2.14: Modified pattern for the NF-270 membrane to assure expected IEP, coloured according to Figure 2.4. Black points are “open” bonds.

In this context, the molecular structures for the three kinds of openings identified in Figures 2.8 and 2.9 (but also in Figures 2.13 and 2.14) were drawn using ISISTM/Draw 2.4 (MDL Information Systems, Inc.), with every open bond being represented as a carboxylic acid end-group.

Then the structures were optimized using HyperChemTM 7.5 (Hypercube, Inc.) or MOPAC2009TM (Stewart Computational Chemistry) and the results are summarized in Table 2.21. Finally, optimized structures were processed with Jmol 11.8.7 (an open-source Java viewer for chemical structures in 3D) in order to determine opening size as the distance between two opposite atoms.

The NF-270 membrane has a mean opening size of 1.60 nanometres. This kind of opening was already described for polypiperazine amides, but no details about how such a structure was established were given [86]. However, the opening size reported (1.5 nanometres) is in good agreement with our measurements.

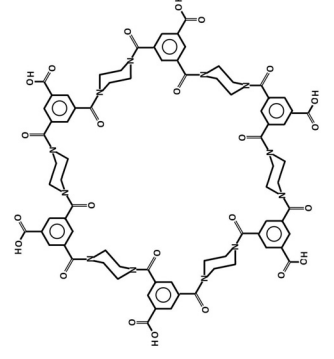
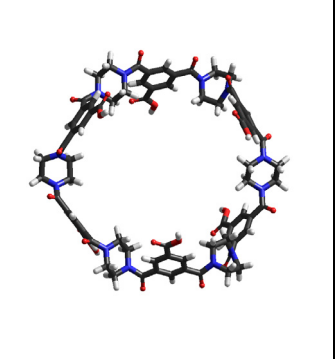
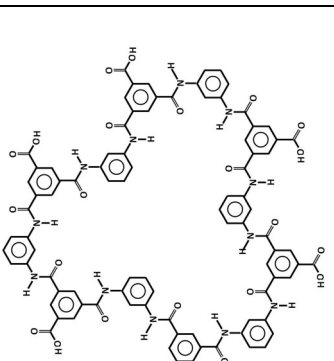
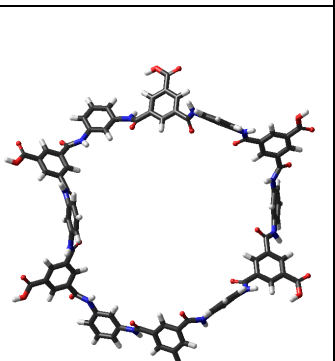
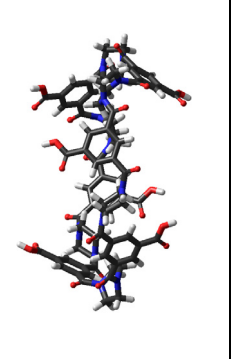
On the other hand, the openings found in the NF-90 membrane structure exhibit two different mean sizes: 1.20 and 2.05 nanometres, for the small and big openings, respectively. In this case, no previous references were found for these openings.

However, it is known that trimesic acid (derived from trimesoyl chloride by hydrolysis) forms a two-dimensional network of six-molecule rings which is kept together by internal hydrogen bonds. This network exhibits a similar structure than the smallest opening of NF-90, and its size was estimated to be 1.4 nanometres [87].

Similar structures to those presented in Table 2.21, which have opening sizes below 1 nanometre and exhibit also separating properties already used in chromatographic and chemical analysis, are found in cyclodextrins [88] and crown ethers [89].

Additionally, considering the aforementioned picture that the top layer is formed by several sheets and also considering that every sheet contains such openings, then the existence of pores in nanofiltration membranes can be thus explained as the connection between openings located in adjacent sheets.

Table 2.21: Nano-openings resulting from the polyamide structure of NF-membranes.

	NF-270		NF-90		
Chemical structure					
Front view					
Side view					
Opening size (nm)					1.52 – 1.72
					2.04 – 2.06
					1.06 – 1.34

Furthermore, if the current classification of pore size for catalysis recommended by the IUPAC is used [90], these pores are micropores, as

the pore width (smallest dimension) is smaller than 2 nanometres. However, a new proposal for the classification of pore sizes indicates that these pores can be considered as inter-nanopores (pore size between 1 and 10 nanometres) [91].

By using the structures from Table 2.21 it is also possible to identify the spatial distribution of the molecular interaction potentials. H-acceptor and H-donor potentials are operating within the NF-90 membrane openings; while H-acceptor potential and hydrophobic potentials are operating within the NF-270 membrane openings. For both membranes, charge transfer and hydrophobic potentials are also operating above and below the plane in which the openings are located.

Finally, the gained knowledge allows to conclude that the separation by charge and solution-diffusion mechanisms could be explained using the molecular interaction potentials of each membrane; while the separation by sieving could be explained through the stereochemistry aspects, especially those concerning to the arrangement of the constituting structures and the existence of nano-openings in the membrane structure.

2.4 UNDERSTANDING MEMBRANE CHARACTERISTICS

Up to now, the traditional approach to characterize membranes focus on the determination (by using several well-established methods) of four groups of parameters in order to explain membrane properties or the performance obtained in a specific application. These parameters are summarized in Figure 2.15 and can be described as follows:

- *Morphology parameters* intend to characterize the membrane in terms of its surface roughness and porous structure, as well as its hydrophobicity.
- *Charge parameters* describe the characteristics of the membrane when it acquires electrical charge in contact with water.
- *Performance parameters* are related to the retention measurements of both charged and uncharged solutes, which give an idea about surface charge and pore size; as well as permeability measurements to determine the resistance offered by the membrane to solvent flow.
- *Stability parameters* are not normally considered as part of the classical membrane characterization [92], but they comprise thermal, mechanical and chemical resistance (especially against extreme acid or basic environments and chlorine attack), but also low tendency to fouling.

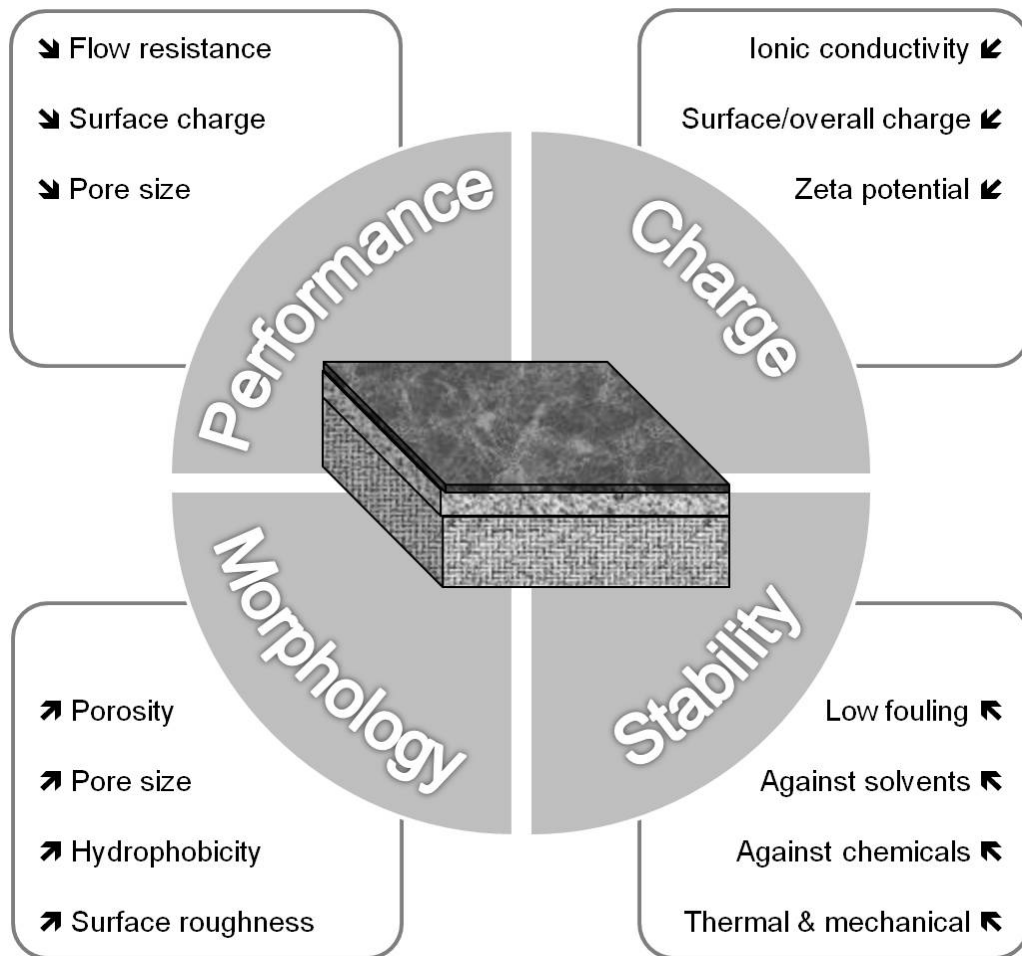


Figure 2.15: Most important characteristics of nanofiltration membranes.

However, by following this traditional approach it is only possible to establish few and dispersed connections between chemical structure, properties and performance.

In this work, a new approach based on the T-SAR analysis is developed to understand membrane characteristics from its chemical structure. In Figure 2.16 the T-SAR triangle is combined with a second triangle comprising the four groups of parameters from Figure 2.15.

Once that the T-SAR algorithm is successfully applied as in Section 2.3, a detailed analysis of the membrane characteristics can be conducted, either by direct determination of membrane characteristics or simply by using data already published about the membranes. As it can be observed in Figure 2.15, the data derived from at least two corners of the T-SAR triangle is required to explain each group of membrane characteristics:

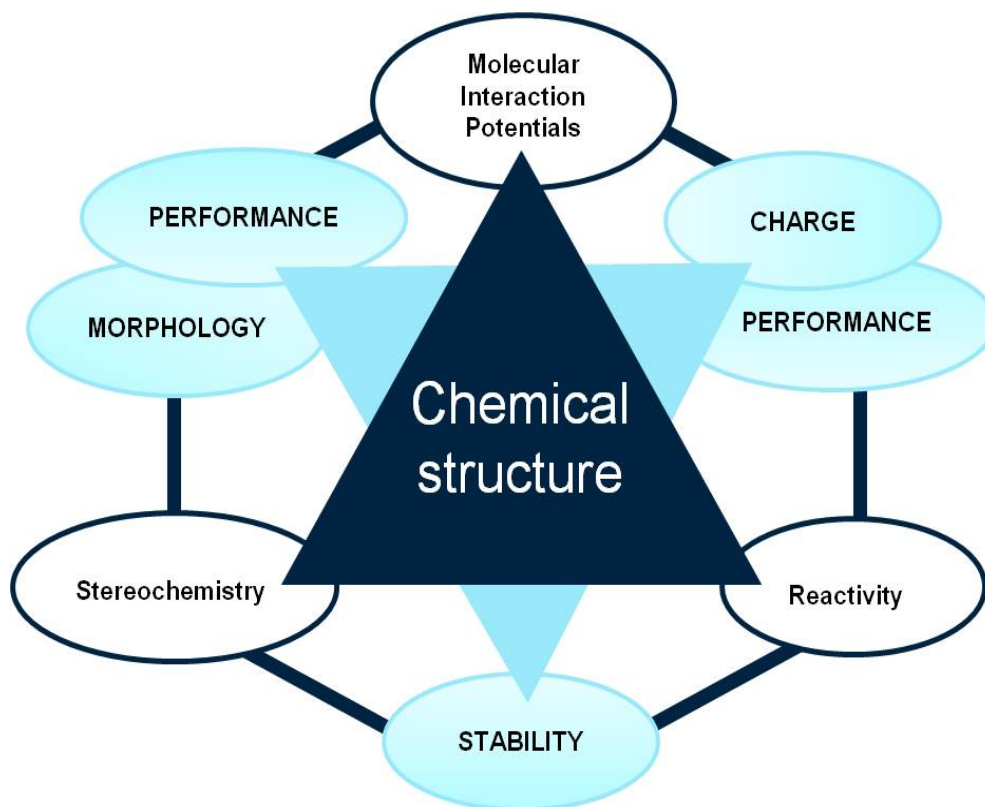


Figure 2.16: The new approach uses T-SAR to understand membrane characteristics.

- By combining stereochemistry data and the corresponding molecular interaction potentials, both morphology and performance (permeability) parameters can be discussed.
- The analysis of charge and performance (retention) parameters requires molecular interaction potentials together with reactivity data.
- The information related to stereochemistry and reactivity gives evidence to support the stability behaviour of the membrane against thermal, mechanical and chemical agents.

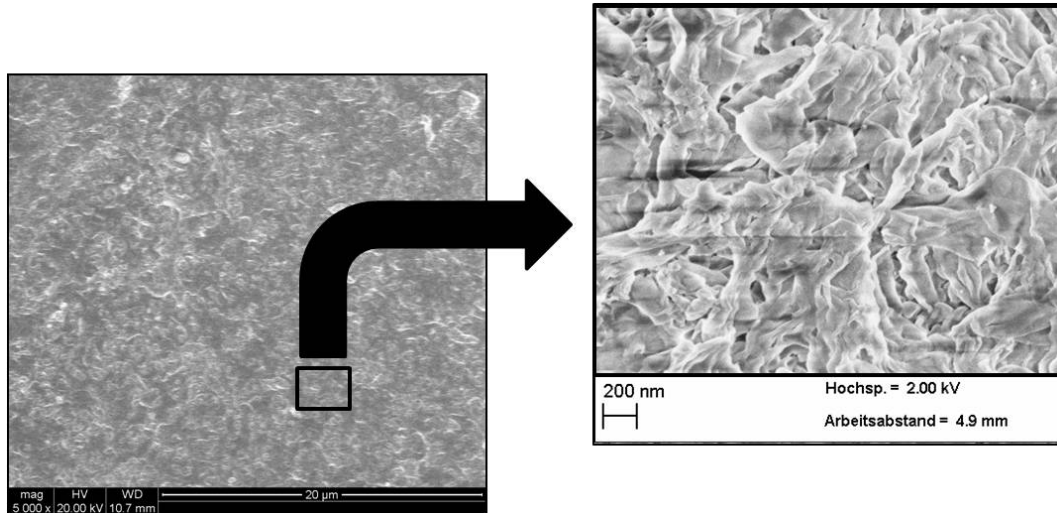
In order to illustrate the use of the new approach and aiming to ascertain its advantages in comparison to the classical one, it will be employed for the analysis of the NF-90 and NF-270 FilmTec membranes.

2.4.1 Morphology parameters

A first approach to learn more about the morphology of the membranes is to visualize it by scanning electron microscopy. The NF-90 membrane (Figure 2.17a) exhibits a rougher surface than the NF-270 membrane (Figure 2.17b). The structure of NF-90 showed the typical ridge-and-valley

structure, which is characteristic of those membranes where aromatic amines reacted with trimesoyl chloride [8].

a)



b)

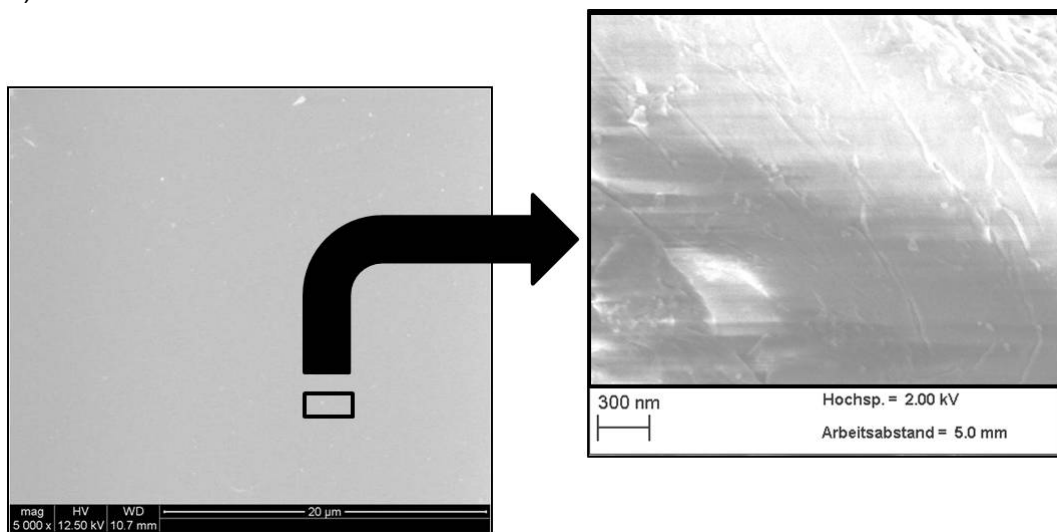


Figure 2.17: Microscopy views (left: ESEM, right: SEM) of nanofiltration membranes top layer surface: a) NF-90, b) NF-270

Despite the role of the polysulfone layer on the surface morphology of polyamides has been recently discussed [93], it is believed that the characteristics of the surface are more related with the cross-linking degree of each membrane. For example, comparing the chemical structure of both membranes, it can be observed that the NF-90 membrane pattern (Figure 2.13) contain less open bonds, which allows certain flexibility on the resulting surface. Then, those constituting units

nearby the open bonds constitute deep regions in the surface, while the units which are not suffering the strain derived from the open bonds, lead to produce high regions in the surface. On the contrary, the NF-270 membrane pattern (Figure 2.14) has more open bonds by the same number of constituting units, which tend to strain the structure and thus, to smooth down the resulting surface.

The surface roughness can be derived from Atomic Force Microscopy (AFM) measurements, in which a three-dimensional picture from the membrane surface can be obtained [92]. Surface roughness values already published for both FilmTec membranes are summarized in Table 2.22. Arithmetic Average (AA) and Root-Mean-Square (RMS) are alternative methods by which the roughness mean value is computed. The AA method uses the absolute values of the deviations from the mean line, while the RMS method uses the squared values of the same deviations [94].

Table 2.22: Membrane surface roughness derived from AFM measurements at different scan sizes.

Type of roughness	Scan size (μm^2)	Surface roughness (nm)		Reference
		NF-90	NF-270	
Arithmetic Average, AA	1 x 1	31.3	3.0	[95]
	2 x 2	22.8	3.4	[94]
	5 x 5	84.5	10.2	[95]
Root mean square, RMS	1 x 1	21.9	2.8	[96]
	2 x 2	27.8	4.4	[94]
	5 x 5	38.8	4.6	[96]

The differences between the values are due to the heterogeneity of the membrane surface and the scan sizes used. However, a tendency is clear: the surface roughness for the NF-90 membrane is manifestly higher than the surface roughness for the NF-270 membrane. These results support the qualitative conclusions derived from microscopy analyses and are a consequence of the chemical structure and the cross-linking degree of the studied membranes.

From AFM measurements, and also by using retention data of uncharged solutes (like sugar, polyethylene glycol and glycerol), it is possible to estimate the pore size of membranes (Table 2.23).

Table 2.23: Pore sizes of nanofiltration membranes.

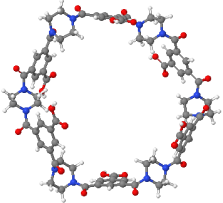
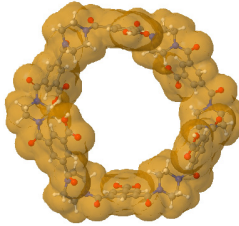
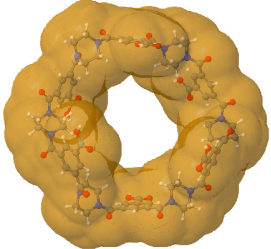
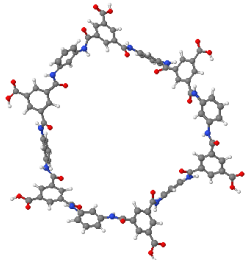
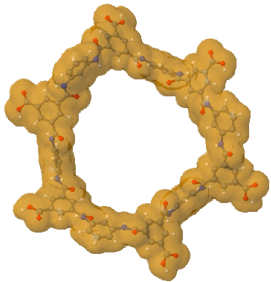
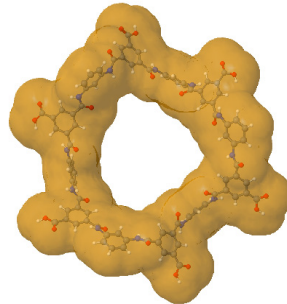
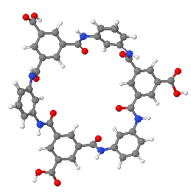
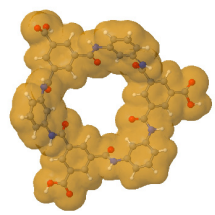
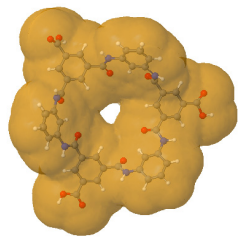
Parameter	Membrane		Derived from	Reference
	NF-90	NF-270		
Pore size (nm)	0.51	0.68	AFM data	[94]
	0.399	0.395	Retention data	[95]
	0.34	0.42	Retention data	[97]

Apart the results for reference [95], which were not expected and were argued due to experimental errors; the pore size for the NF-270 membrane is slightly higher than the pore size for the NF-90 membrane. However, all values are considerably smaller than those values showed in Table 2.21. On the one hand, it is known that pore sizes derived from AFM measurements can be underestimated due to the tip can not probe into the depth of the pore and that pore sizes derived from retention data are subject to the limitations of the available models to describe separation performance [98].

On the other hand, real pore sizes should be smaller than the values shown in Table 2.21, because the latter values represent the distance between two opposite atoms of the opening structure and they are, in consequence, the biggest size possible. It can be demonstrated when the surface area surrounding the opening structure is considered. The membrane openings are represented again in Table 2.24, but now including the Van der Waals surface area and the solvent accessible surface area, if the solvent is water. The reduction in the opening size as a measurement of free space to permeation results evident and can reach up to 76% of the original size for the NF-90 membrane smallest pore.

Hydrophobicity can be also described using the T-SAR approach. Theoretically and according to the identified molecular interaction potentials for each membrane (Figures 2.13 and 2.14), the NF-90 membrane exhibit both H-donor and H-acceptor potentials, the same potentials exhibited by the water molecule. That means that the NF-90 membrane must interact easily with water. On the contrary, interactions between the NF-270 membrane and water molecules are less favourable because H-donor potentials are absent in its structure, leaving more parts of the membrane which exhibit hydrophobic interaction potential in contact with water.

Table 2.24: Different representations of the membrane openings.

		Representation used		
		Only chemical structure	Van der Waals surface area	Solvent accessible surface area
NF-270	 <p>Mean size \approx 1.60 nm</p>	 <p>Mean size \approx 1.26 nm</p>	 <p>Mean size \approx 0.86 nm</p>	
	 <p>Mean size \approx 2.05 nm</p>	 <p>Mean size \approx 1.91 nm</p>	 <p>Mean size \approx 1.46 nm</p>	
NF-90	 <p>Mean size \approx 1.20 nm</p>	 <p>Mean size \approx 0.83 nm</p>	 <p>Mean size \approx 0.29 nm</p>	

The contact angle (θ) is a measure of wettability of the membrane i.e., the capacity of water to be adsorbed, which can be interpreted as the hydrophobicity of the membrane. Furthermore, measurements in wet state are beneficial, because they are less influenced by swelling and presence

of pores [92]. In Table 2.25 contact angle values are summarized from literature for both membranes, either determined by the captive bubble method or the sessile drop method, but the contact angle being always measured in the fluid phase with a higher density [99]. In both cases, contact angles lower than 90° indicate a hydrophilic surface, being 0° the contact angle for perfect wetting.

Table 2.25: Contact angles as a measure of membrane hydrophobicity.

Method	Contact angle, θ (°)		Membrane state	Reference
	NF-90	NF-270		
Sessile drop	44.7	32.6	Vacuum dried	[85]
	54	27	Wet	[96]
	45.4	28.8	Air dried	[100]
Captive bubble	38.7	51.4	Wet	[101]
	42.5	55.0	Wet	[102]

Those values determined by using the captive bubble method are in good agreement with the behaviour expected derived from the analysis of molecular interaction potentials, indicating that the NF-90 membrane is more hydrophilic than the NF-270 membrane. However, the results obtained by the sessile drop method (regardless the membrane state) are contradictory to those expected from the chemical structure, and in consequence can be hardly considered as reliable. Finally, no matter the method used, well swollen membranes should be used and the time evolution of the contact angle has to be considered in order to provide equilibrium values rather than instantaneous values; but also the membrane roughness and surface texture effects should be considered during the analysis of experimental data [103].

2.4.2 Charge parameters

The isoelectric points obtained in this work and those values from literature are presented in Table 2.26. Values reported for the NF-90 membrane exhibit more consistency than those reported for the NF-270 membrane, which can be related with the difficulty of the swelling process for this membrane, due to its higher hydrophobicity. In our measurements, it was found that after 90 minutes and 3 days exposure to aqueous solution, the zeta potential for the NF-270 membrane varied 30% and 70%

respectively, when compared to the zeta potential measured after instantaneous exposure to aqueous solution.

Table 2.26: Isoelectric points of nanofiltration membranes.

Isoelectric point, IEP (pH units)		Electrolyte used	Reference
NF-90	NF-270		
4.0	2.5	5 mM KCl	This work
4.2	2.8	5 mM KCl	[95]
3.5	3.5	10 mM KCl	[96]
4.0	Not reported	10 mM KCl	[101]
4.0	3.5	20 mM NaCl 1 mM NaHCO ₃	[104]

By means of a two steps titration already described in Section 2.2.3, the amount of positively and negatively charged groups for each membrane were determined, using top layer thickness already published in the literature (Table 2.27).

Table 2.27: Amount of membrane charged groups obtained by titration.

Membrane NF-90	Density of charged groups, ρ (groups/nm ³), according to the membrane thickness (δ)		
	$\delta = 134$ nm From Ref. [32]	$\delta = 180$ nm From Ref. [33]	$\delta = 214$ nm From Ref. [32]
Positively charged	9 ± 1	7 ± 1	6 ± 1
Negatively charged	9 ± 1	7 ± 1	6 ± 1
Membrane NF-270	Density of charged groups (groups/nm ³), according to the membrane thickness (δ)		
	$\delta = 27$ nm From Ref. [32]	$\delta = 80$ nm From Ref. [32]	$\delta = 170$ nm From Ref. [33]
Positively charged	43 ± 9	14 ± 3	7 ± 1
Negatively charged	46 ± 11	15 ± 4	7 ± 2

For a given thickness, it can be observed that the amount of positively and negatively charged groups is almost the same. Despite this result can be considered at a first sight as unforeseen, it should be expected, because titration determines not only the charge at the exterior surface, the contribution of the total membrane charge is taken also into account [31]. Furthermore, it is known that the reaction mechanisms involved in interfacial polymerization lead to an asymmetric distribution of end-groups. The surface exposed to the water phase during reaction contains only amino end-groups, while the opposite surface is rich in carboxyl end-groups. In between, density and kind of end-groups change continuously [17].

The second aspect to be discussed from Table 2.27 is related to the real thickness of the top layer for each membrane. For the NF-90 membrane, both references found are in good agreement and in consequence, the densities of charged groups obtained are very similar. However, in the case of the NF-270 membrane all values reported are very different, leading to a big variation in the density of charged groups. In both cases, charge density real values should be lower than calculated values, because the membrane thicknesses used were determined for membranes in dry state. Moreover, in a previous reference which uses the same method to determine membrane thickness, an increase up to 26% of thickness for swollen membranes was reported [105].

2.4.3 Stability parameters

Both membrane top layers are formed by cross-linked polymers, which can be considered as amorphous materials. With increasing temperature, they should exhibit a reversible transition from a hard state (chain motion is limited) into a rubber-like state (chains are able to rotate or slip), generally characterized by the glass-transition temperature (T_g) [5].

In a recent publication, the glass-transition temperatures for the NF-90 and NF-270 membranes were reported as 43°C and 41°C, respectively [33], values which are in good agreement with the maximal operating temperature (45°C) derived from the manufacturer information (Table 2.3). Despite the glass transition should be a reversible process; increasing the operating temperature can produce irreversible changes in the original membrane morphology (thickness and pore size) due to further compaction above the glass-transition temperature.

Additionally, membranes exposed to chlorine lose their properties to structural changes, as result from chlorine attack on amide nitrogen and aromatic rings [106].

In the case of the NF-90 membrane, both mechanisms are possible due to the presence of a secondary amide with fully aromatic chemistry. Furthermore, the patented procedure related to the synthesis of fully aromatic polyamides indicate that a post-treatment with chlorine or with a chlorine-releasing agent in order to reduce the possibilities for further chlorine attack was employed. Moreover, the tan colour of the NF-90 membrane is a direct consequence of this post-treatment, which reduced the flux but slightly improved the salt rejection [59]. According to the structure presented in Figures 2.8 and 2.12, it is believed that the chlorine atoms can find place inside the biggest pores leading to a reduction of this size, which can also explain the reduction in flux and the increase in rejection.

On the contrary, the NF-270 membrane should exhibit stronger resistance against chlorine, due to the absence of a hydrogen atom linked to the amide nitrogen, but also due to the aliphatic nature of the diamine ring. Some evidence in this direction is already known [107].

2.4.4 Performance parameters

Finally, an analysis of separation performance parameters following the T-SAR approach is presented. The simplest membrane characterization experiment is the determination of the pure water permeability. In Figure 2.18 water flux values for compacted membranes are represented as a function of the transmembrane pressure differences (full dots), but also the effect of membrane compaction can be also observed (open dots).

Linear regressions give, as a slope, the pure water permeabilities, resulting in a higher value for the NF-270 membrane (11.7 L/m²hbar) compared with the NF-90 membrane (4.6 L/m²hbar). These results are in qualitative agreement with the results derived from the stereochemistry and the molecular interaction potentials for both membranes. In the one hand, the NF-90 membrane possesses smaller pores and higher roughness than the NF-270 membrane. Additionally, the NF-90 top layer is thicker than the NF-270 top layer, a factor which is also contributing to the reduction in the water permeability

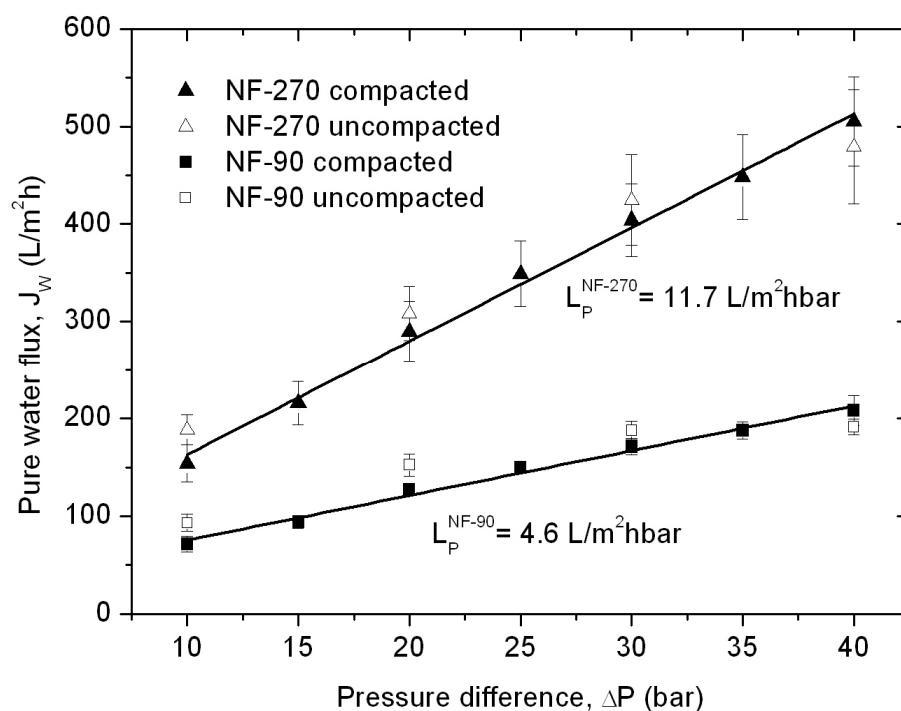


Figure 2.18: Determination of the pure water permeability of nanofiltration membranes considering the effect of membrane compaction.

On the other hand, the NF-90 membrane exhibit stronger interactions with the water molecules due to the formation of hydrogen bonds. While these interactions are weaker within the NF-270 membrane pores. All of these effects complicate the flow of water through the membrane, leading to a smaller water flux for a given pressure difference.

Water fluxes obtained during the compaction process are slightly higher than those obtained for the same membrane after compaction, except for those water fluxes obtained at the highest pressure difference used, which are slightly lower and indicate the status of compaction.

For comparison purposes, Table 2.28 contains the pure water permeability values reported by other studies for the membranes under consideration. In all cases it was obtained that the NF-270 membrane possesses higher water permeability than the NF-90 membrane. However, except the results derived from this work, all the measurements were carried out at low pressures, at which the compaction process can not proceed completely. Then, higher values than those reported here can be expected. Additionally, in some studies the water permeability is calculated based on a single point and thus the reported value is missing reliability.

Table 2.28: Pure water permeability values of nanofiltration membranes.

Pure water permeability, L_P (L/m ² hbar)		Applied pressure (bar)	Experimental conditions	Reference
NF-90	NF-270			
4.6	11.7	10 – 40	Deionised water 13.9 cm ² membrane	This work
11.2	14.5	13.8	MilliQ water 140 cm ² membrane	[85]
13.0	17.6	3 – 13	Deionised water 274 cm ² membrane	[95]
5.2	8.5	8	No details are given 59 cm ² membrane	[96]
6.4	13.5	12	Deionised water 46 cm ² membrane	[102]
9.6	26.3	6 – 9	No details are given 30 cm ² membrane	[108]

Until now, it has been evidenced by discussing several membrane characteristics that not only the surface heterogeneity must be considered (or its influence must be minimized by increasing either the area under study or the number of repetitions), but also the experimental conditions and the analysis methods used have an influence on the results. Then, absolute values do not exist and discussions must be carried out with carefulness and more desirably, together with the membrane chemical structure, according to the approach proposed in this work.

In this context, the complexity related to the variety of solutes tested, feed concentrations and pH values, analytical methods, pressure differences, type of filtration and so on; makes it almost impossible to use already published experimental data for the retention of charged and uncharged solutes. In this work, the analysis of retention values will be only considered for the case of ionic liquids, as follows in the next and last section.

2.5 UNDERSTANDING THE SEPARATION OF IONIC LIQUIDS

As a final part of the discussion, the developed model for nanofiltration membranes will be used to understand the separation of ionic liquids later used in this work. In general, membranes derived from aromatic diamines (NF-90) show lower water fluxes, but higher retentions than those derived from aliphatic diamines (NF-270) [12].

The first aspect to be considered is the size of the ionic liquid ions. Ionic volumes were determined by using BP86/TZVP + COSMO calculations [109], while the ionic radius was calculated from the ionic volume assuming ideally spherical behaviour [110], as follows:

$$r_{ION}^{\pm} = \sqrt[3]{\frac{3 \cdot V_{ION}^{\pm}}{4\pi}} \quad (\text{Eq. 2.13})$$

where:

r_{ION}^{\pm} : ionic radius (nm)

V_{ION}^{\pm} : ionic volume (nm³)

In Table 2.29 are summarized the corresponding ionic radii for selected anions and cations, ordered by increasing size.

Table 2.29: Ionic volumes and radii for selected cations and anions.

Ionic liquid entity ⁶		Ionic volume, V_{ION}^{\pm} (nm ³)	Ionic radius, r_{ION}^{\pm} (nm)
Anions	Cl	0.03577	0.204
	1COO	0.07797	0.265
	(CF ₃ SO ₂) ₂ N	0.2178	0.373
Cations	IM14	0.1966	0.361
	Py6	0.2387	0.385
	IM16	0.2438	0.388
	Pyr16	0.2589	0.395

Chloride and acetate anions are considerably smaller than the (CF₃SO₂)₂N anion, while this last anion has a size located between both imidazolium cations (IM14 and IM16 respectively). Moreover, all cations containing a hexyl side chain exhibit a similar size.

In this context, the molecular radius for an ionic liquid can be calculated as the sum of anionic and cationic radius [110], as follows:

$$r_m = r_{ION}^{-} + r_{ION}^{+} \quad (\text{Eq. 2.14})$$

where:

r_m : molecular radius (nm)

⁶ Py6: 1-hexylpyridinium cation

r_{ION}^- : anionic radius (nm)
 r_{ION}^+ : anionic radius (nm)

The molecular diameter can be calculated as follows:

$$d_m = 2 \cdot r_m \quad (\text{Eq. 2.15})$$

where:

d_m : molecular diameter (nm)

Both molecular radius and molecular diameter for each ionic liquid considered later in this study were calculated and summarized in Table 2.30. Because the molecular diameter does not consider hydration effects, these values should be only compared with the sizes of the membrane openings obtained when the Van der Waals surface is considered (second column in Table 2.24).

Table 2.30: Molecular radii and diameter for selected ionic liquids.

Ionic liquid		Molecular radius, r_m (nm)	Molecular diameter, d_m (nm)
Hydrophilic character	IM14 Cl	0.565	1.130
	IM14 1COO	0.626	1.252
Hydrophobic character	Py6 (CF ₃ SO ₂) ₂ N	0.758	1.516
	IM16 (CF ₃ SO ₂) ₂ N	0.761	1.522
	Pyr16 (CF ₃ SO ₂) ₂ N	0.768	1.536

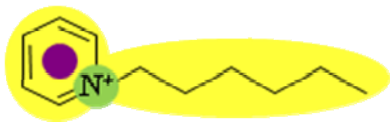
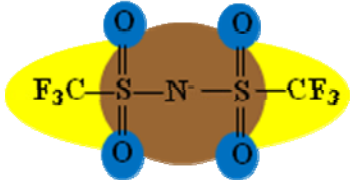

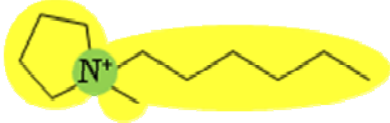
According to this, hydrophilic ionic liquids can permeate through the openings of the NF-270 membrane (opening size around 1.26 nm), while hydrophobic ionic liquids should be retained at a great extent due their whole size. However, it has to be taken into account that the molecular diameter consider that anion and cation are together due to charge interactions, but their permeation through the openings must not occurs simultaneously.

In the case of the NF-90 membrane, all cations may be retained by the smaller openings (0.83 nm), but all ions could permeate through the bigger openings (1.91 nm). However, in the NF-90 membrane structure smaller openings are in higher amount than bigger openings, which also could posses a reduced opening size due to the presence of chlorine atoms or it

simply does not exist, as it was pointed out in Section 2.4.3. Then, it is expected that the NF-90 membrane retains preferably all ionic liquids considered in this study mainly by a sieving mechanism.

On the contrary, in order to explain the differences in retention by the NF-270 membrane, molecular interactions potentials of the hydrophobic ionic liquids selected are required. They are quite different, due to the differences in the cations, as it is represented in Table 2.31.

Table 2.31: Molecular interaction potentials for three hydrophobic ionic liquids: Py6 ($(CF_3SO_2)_2N$), IM16 ($(CF_3SO_2)_2N$) and Pyr16 ($(CF_3SO_2)_2N$).

Ionic liquid	Cation	Anion
Py6 ($(CF_3SO_2)_2N$)		
IM16 ($(CF_3SO_2)_2N$)		
Pyr16 ($(CF_3SO_2)_2N$)		

The interaction potentials associated to the $(CF_3SO_2)_2N$ anion are a hydrophobic potential at the fluorinated carbon atoms, a delocalized negative charge due to resonance effects and an H-acceptor potential at the oxygen atoms. In the case of the NF-270 membrane, repulsions occur between the $(CF_3SO_2)_2N$ anion and the membrane due to both negative charge (at pH values > 2.5) and H-bonding acceptors in both chemical structures. Then, these repulsions lead mainly to high retentions for such ionic liquids, but also some influence is related to the cation employed.

Both Py6 and IM16 cations exhibit hydrophobic potential and charge transfer potentials, but with an important difference: in case of Py6 the positive charge is localized at the nitrogen atom, while in the case of IM16 there is a delocalized positive charge between both nitrogen atoms. Pyr16 cation exhibits hydrophobic potential but no charge transfer due to an aliphatic ring, with a localized positive charge which can be partially

sheltered because both methyl and hexyl side chains are bounded to the same nitrogen atom. From $\log k_0$ values derived from reversed phase gradient HPLC retention times and used as an approximate measure of cation lipophilicity, the following values were determined: 1.04 for Py6, 1.24 for IM16 and 1.17 for Pyr16 [111,112].

Pyr16 cation exhibits interactions mainly due to the hydrophobic attractions with the NF-270 membrane structure. Both IM16 and Py6 cations experience also charge transfer, which is not present in the Pyr16 cation. Furthermore, the charge delocalization in the IM16 cation leads to weaker attractions with the negatively charged groups of the membrane.

In this context, the following tendencies can be summarized in order of importance:

- Cation size: Pyr16 > IM16 > Py6
- Hydrophobicity: IM16 \geq Pyr16 > Py6
- Charge transfer potential: Py6 > IM16
- Cation positive charge: Py6 > Pyr16 \geq IM16

Then, considering that cation size and hydrophobicity are playing the most important roles in the separation, the retention should decrease as follows: Pyr16 > IM16 > Py6. Finally, the higher the retention (due to lower interactions with the membrane structure) the higher the permeate flux. Then, the tendency Pyr16 > IM16 > Py6 is also valid for permeate fluxes.

REFERENCES

- [01] JUDD, S. Membrane Technology. In: *Membranes for Industrial Wastewater Recovery and Re-use*. Judd, S. and Jefferson, B., Ed.; Elsevier Science Ltd: Oxford (UK), **2003**, pp.13-74
- [02] SUSANTO, H.; Ulbricht, M. Polymeric membranes for molecular separations. In: *Membrane operations – Innovative separations and transformations*. Drioli, E. and Giorno, L., Ed.; Wiley-VCH: Weinheim (Germany), **2009**, pp. 19-43.
- [03] BAKER, R.W. *Membrane technology and applications*, 2nd ed.; John Wiley & Sons: Chichester (UK), **2004**.
- [04] KOROS, W.J.; Ma, Y.H.; Shimidzu, D. Terminology for membranes and membrane processes. *Pure and Applied Chemistry*, **1996**, 68, 1479-1489.
- [05] MELIN, T.; Rautenbach, R. *Membranverfahren*, 2nd ed.; Springer Verlag: Berlin (Germany), **2004**.
- [06] MULDER, M. *Basic principles of membrane technology*. Kluwer Academic Publishers: Dordrecht (Netherlands), **1991**.
- [07] SEADER, J.D.; Henley, E.J. *Separation process principles*, John Wiley & Sons: New York (USA), **1998**.

- [08] MULDER, M.H.V.; van Voorthuizen, E.M.; Peeters, J.M.M. Membrane characterization. In: *Nanofiltration: principles and applications*; Schäfer, A.I., Fane, A.G. and Walte, T.D., Ed.; Elsevier Ltd.: Oxford (UK), **2005**, pp. 89-117.
- [09] LINDER, C.; Kedem, O. History of nanofiltration membranes 1960 to 1990. In: *Nanofiltration: principles and applications*; Schäfer, A.I., Fane, A.G. and Walte, T.D., Ed.; Elsevier Ltd.: Oxford (UK), **2005**, pp. 5-31.
- [10] PETERSEN, R.J. Composite reverse osmosis and nanofiltration membranes. *Journal of Membrane Science*, **1993**, 83, 81-150.
- [11] HILAL, N.; Al-Zoubi, H.; Darwish, N.A.; Mohammad, A.W.; Abu Arabi, M. A comprehensive review of nanofiltration membranes: treatment, pretreatment, modelling, and atomic force microscopy. *Desalination*, **2004**, 170, 281-308.
- [12] VANKELECOM, I.F.J.; De Smet, K.; Gevers, L.E.M.; Jacobs, P.A. Nanofiltration membranes materials and preparation. In: *Nanofiltration: principles and applications*; Schäfer, A.I., Fane, A.G. and Walte, T.D., Ed.; Elsevier Ltd.: Oxford (UK), **2005**, pp. 33-65.
- [13] TWEDDLE, T.A.; Kutory, O.; Thayer, W.L.; Sourirajan, S. Polysulfone ultrafiltration membranes. *Industrial and Engineering Chemistry - Product Research and Development*, **1983**, 22, 320-326.
- [14] VAN DE WITTE, P.; Dijkstra, P.J.; van den Berg, J.W.A.; Feijen, J. Phase separation processes in polymer solutions in relation to membrane formation. *Journal of Membrane Science*, **1996**, 117, 1-31.
- [15] WITTBECKER, E.L.; Morgan, P.W. Interfacial polycondensation. I. *Journal of Polymer Science*, **1959**, 40, 289-297.
- [16] MORGAN, P.W.; Kwolek, S.L. Interfacial polycondensation. II. Fundamentals of polymer formation at liquid interfaces. *Journal of Polymer Science*, **1959**, 40, 299-327.
- [17] ENKELMANN, V.; Wegner, G. Mechanism of interfacial polycondensation and the direct synthesis of stable polyamide membranes. *Makromolekulare Chemie*, **1976**, 177, 3177-3189.
- [18] MORGAN, P.W. *Condensation polymers: by interfacial and solution methods*, Interscience Publishers: New York (USA), **1965**.
- [19] MACRITCHIE, F. Mechanism of interfacial polymerization. *Transactions of the Faraday Society*, **1969**, 65, 2503-2507.
- [20] JASTORFF, B.; Störmann, R.; Wölcke, U. *Struktur-Wirkungs-Denken in der Chemie – eine Chance für mehr Nachhaltigkeit*. Universitätsverlag Aschenbeck und Isensee: Oldenburg (Germany), **2003**.
- [21] JASTORFF, B.; Störmann, R.; Ranke, J. Thinking in Structure-Activity Relationships – A way forward towards sustainable chemistry. *Clean – Soil, Air, Water*, **2007**, 35, 399-405.
- [22] JASTORFF, B.; Störmann, R.; Ranke, J.; Mölter, K.; Stock, F.; Oberheitmann, B.; Hoffmann, W.; Hoffmann, J.; Nüchter, M.; Ondruschka, B.; Filser, J. How hazardous are ionic liquids? Structure-activity relationships and biological testing as important elements for sustainability evaluation. *Green Chemistry*, **2003**, 5, 136-142.
- [23] STOLTE, S.; Arning, J.; Bottin-Weber, U.; Matzke, M.; Stock, F.; Thiele, K.; Uerdingen, M.; Welz-Biermann, U.; Jastorff, B.; Ranke, J. Anion effects on the cytotoxicity of ionic liquids. *Green Chemistry*, **2006**, 8, 621-629.
- [24] ARNING, J.; Stolte, S.; Bösch, A.; Stock, F.; Pitner, W.R.; Welz-Biermann, U.; Jastorff, B.; Ranke, J. Qualitative and quantitative structure-activity relationships for the inhibitory effects of cationic head groups, functionalised side chains and anions of ionic liquids on acetylcholinesterase. *Green Chemistry*, **2008**, 10, 47-58.

- [25] DOOSE, C.A.; Ranke, J.; Stock, F.; Bottin-Weber, U.; Jastorff, B. Structure-activity relationships of pyrithiones – IPC-81 toxicity tests with the antifouling biocide zinc pyrithione and structural analogs. *Green Chemistry*, **2004**, 6, 259-266.
- [26] ARNING, J.; Dringen, R.; Schmidt, M.; Thiessen, A.; Stolte, S.; Matzke, M.; Bottin-Weber, U.; Caesar-Geertz, B.; Jastorff, B.; Ranke, J. Structure-activity relationships for the impact of selected isothiazol-3-one biocides on glutathione metabolism and glutathione reductase of the human liver cell line Hep G2. *Toxicology*, **2008**, 246, 203-212.
- [27] WEINHOLD, M.X.; Sauvageau, J.C.M.; Keddig, N.; Matzke, M.; Tartsch, B.; Grunwald, I.; Kübel, C.; Jastorff, B.; Thöming, J. Strategy to improve the characterization of chitosan for sustainable biomedical applications: SAR guided multi-dimensional analysis. *Green Chemistry*, **2009**, 11, 498-509.
- [28] DOW FILMTEC NANOFILTRATION ELEMENTS. *Membrane NF-90-400*. Product datasheet. http://www.dowwaterandprocess.com/products/membranes/nf90_400.htm (Accessed October 6, **2010**).
- [29] DOW FILMTEC NANOFILTRATION ELEMENTS. *Membrane NF-270-400*. Product datasheet. http://www.dowwaterandprocess.com/products/membranes/nf270_400.htm (Accessed October 6, **2010**).
- [30] SHAHBAZIAN, K. *Datasheet Desal-DK*. Personal Communication. **2009**.
- [31] SCHAEF, J.; Vandecasteele, C. Evaluating the charge of nanofiltration membranes. *Journal of Membrane Science*, **2001**, 188, 129-136.
- [32] NGHIEM, L.D. *Removal of emerging trace organic contaminants by nanofiltration and reverse osmosis*. PhD Thesis, University of Wollongong (Australia), **2005**.
- [33] SAIDANI, H.; Ben Amar, N.; Palmeri, J.; Deratani, A. Interplay between the transport of solutes across nanofiltration membranes and the thermal properties of the thin active layer. *Langmuir*, **2010**, 26, 2574-2583.
- [34] KALLIOINEN, M.; Nystrom, M. Membrane surface characterization. In: *Advanced membrane technology and applications*; Li, N.N.; Fane, A.G.; Winston, W.S. and Matsuura, T., Ed.; John Wiley & Sons, Ltd.: New Jersey (USA), **2008**, pp. 841-877.
- [35] VAN WEYNSBERGHE, C. Polysulfone. In: *Hochleistungs-Kunststoffe: Polyarylate, Thermotrope-Polyester, Polyimide, Polymetherimide, Polyamidimide, Polyarylen-sulfide, Polysulfone, Polyetheretherketone*. Bottenbruch, L., Ed.; Carl Hanser Verlag: Munich (Germany), **1994**, pp.141-218.
- [36] JOHNSON, R.N.; Farnham, A.G.; Clendinning, R.A.; Hale, W.F.; Merriam, C.N. Poly(aryl ethers) by nucleophilic aromatic substitution. I. Synthesis and properties. *Journal of Polymer Science, Part A-1: Polymer Chemistry*, **1967**, 5, 2375-2398.
- [37] SOCRATES, G. *Infrared and Raman characteristic group frequencies: Tables and charts*, John Wiley & Sons, Ltd.: Chichester (UK), **2004**.
- [38] HESSE, M.; Meier, H.; Zeeh, B. *Spektroskopische Methoden in der organischen Chemie*, Georg Thieme Verlag: Stuttgart (Germany), **1991**.
- [39] STUART, B. *Infrared spectroscopy: fundamentals and applications*, John Wiley & Sons, Ltd.: Chichester (UK), **2004**.
- [40] FONTYN, M.; Bijsterbosch, B.H.; van't Riet, K. Chemical characterization of ultrafiltration membranes by spectroscopic techniques. *Journal of Membrane Science*, **1987**, 36, 141-145.
- [41] PURO, L.; Mänttari, M.; Pihlajamäki, A.; Nyström, M. Characterization of modified nanofiltration membranes by octanoic acid permeation and FTIR analysis. *Chemical Engineering Research and Design*, **2006**, 84, 87-96.
- [42] SINGH, P.S.; Joshi, S.V.; Trivedi, J.J.; Devmurari, C.V.; Prakash Rao, A.; Ghosh, P.K. Probing the structural variations of thin film composite RO membranes obtained by

- coating polyamide over polysulfone membranes of different pore dimensions. *Journal of Membrane Science*, **2006**, 278, 19-25.
- [43] KAMALOVA, D.I.; Kolyadko, I.M.; Remizov, A.B.; Galimullin, D.Z.; Salakhov, M.K. The local dynamics of polyetherimides: conformational probes, IR Fourier transform spectra, and quantum-chemical calculations. *Russian Journal of Physical Chemistry A*, **2008**, 82, 2085-2091.
- [44] KATON, J.E.; Fairheller, W.R. The vibrational spectra and molecular configuration of diphenyl ether. *Journal of Molecular Spectroscopy*, **1964**, 13, 72-86.
- [45] SCHREIBER, K.C. Infrared spectra of sulfones and related compounds. *Analytical Chemistry*, **1949**, 21, 1168-1172.
- [46] DOW FILMTEC MEMBRANES. *Basics of RO and NF: Membrane description*. http://www.dow.com/PublishedLiterature/dh_0042/0901b80380042dd8.pdf (Accessed October 20, **2010**).
- [47] FREGER, V.; Gilron, J.; Belfer, S. TFC polyamide membranes modified by grafting of hydrophilic polymers: an FT-IR/AFM/TEM study. *Journal of Membrane Science*, **2002**, 209, 283-292.
- [48] PRAKASH RAO, A.; Joshi, S.V.; Trivedi, J.J.; Devmurari, C.V.; Shah, V.J. Structure-performance correlation of polyamide thin film composite membranes: effect of coating conditions on film formation. *Journal of Membrane Science*, **2003**, 211, 13-24.
- [49] SONG, Y.; Liu, F.; Benhui, S. Preparation, characterization, and application of thin film composite nanofiltration membranes. *Journal of Applied Polymer Science*, **2005**, 95, 1251-1261.
- [50] SAHA, N.K.; Joshi, S.V. Performance evaluation of thin film composite polyamide nanofiltration membrane with variation in monomer type. *Journal of Membrane Science*, **2009**, 342, 60-69.
- [51] GEIGER, W. Infrarotspektroskopische Untersuchungen substituierter N-phenylbenzamide. *Spectrochimica Acta*, **1966**, 22, 495-499.
- [52] VANKELECOM, I.F.J.; De Smet, K.; Gevers, L.E.M.; Jacobs, P.A. Nanofiltration membrane materials and preparation. In: *Nanofiltration: principles and applications*; Schäfer, A.I., Fane, A.G. and Walte, T.D., Ed.; Elsevier Ltd.: Oxford (UK), **2005**, pp. 33-65.
- [53] BOLTO, B.; Tran, T.; Hoang, M.; Xie, Z. Crosslinked poly(vinyl alcohol) membranes. *Progress in Polymer Science*, **2009**, 34, 969-981.
- [54] TANG, C.Y.; Kwon, Y.N.; Leckie, J.O. Effect of membrane chemistry and coating layer on physicochemical properties of thin film composite polyamide RO and NF membranes. I. FTIR and XPS characterization of polyamide and coating layer chemistry. *Desalination*, **2009**, 242, 149-167.
- [55] AL-AMOUDI, A.; Williams, P.; Mandale, S.; Lovitt, R.W. Cleaning results of new and fouled nanofiltration membrane characterized by zeta potential and permeability. *Separation and Purification Technology*, **2007**, 54, 234-240.
- [56] OSMONICS. *NF-Desalination. Nanofiltration technology for seawater desalination*. <http://www.gewater.com/pdf/1233502-%20Lit-%20Desal%20NF%20Desalination%20Brochure.pdf> (Accessed October 22, **2010**).
- [57] KAMIYAMA, Y.; Yoshioka, N.; Nakagome, K. Composite semipermeable membrane. *US Patent 4619767*, October 28, **1986**.
- [58] CADOTTE, J.E. Reverse osmosis membrane. *US Patent 4259183*, March 31, **1981**.
- [59] CADOTTE, J.E. Interfacially synthesized reverse osmosis membrane. *US Patent 4277344*, March 31, **1981**.

- [60] JOULE, J.A.; Mills, K. *Heterocyclic chemistry*, 5th ed.; John Wiley & Sons: Chichester (UK), **2010**.
- [61] KOTZ, J.C.; Treichel, P.; Townsend, J.R. *Chemistry and chemical reactivity*, 7th ed.; Thomson Brook/Cole: Belmont (USA), **2009**.
- [62] FOX, M.A.; Whitesell, J.K. *Organic chemistry*, 3rd ed.; Jones & Barlett Learning: Sudbury (USA), **2004**.
- [63] FAN, Z.; Li, X.; Wang, G. Trimesic acid dihydrate. *Acta Crystallographica*, **2005**, E61, o1607-o1608.
- [64] BETZ, R.; Klüfers, P.; Mayer, P. m-phenylenediamine. *Acta Crystallographica*, **2008**, E64, o2501.
- [65] EICHER, T.; Hauptmann, S. *The chemistry of heterocycles: structure, reactions, syntheses, and applications*, 2nd ed.; Wiley-VCH: Weinheim (Germany), **2003**.
- [66] PARKIN, A.; Oswald, I.D.H.; Parsons, S. Structures of piperazine, piperidine and morpholine. *Acta Crystallographica*, **2004**, B60, 219-227.
- [67] ELIEL, E.L.; Wilen, S.H. *Organische Stereochemie*, Wiley-VCH: Weinheim (Germany), **1998**.
- [68] HARKEMA, S.; Gaymans, R.J. N,N'-(p-Phenylene)dibenzamide. *Acta Crystallographica*, **1977**, B33, 3609-3611.
- [69] MOTHERWELL, W.D.S.; Shields, G.P.; Allen, F.H. Graph-set and packing analysis of hydrogen-bonded networks in polyamide structures in the Cambridge Structural Database. *Acta Crystallographica*, **2000**, B56, 857-871.
- [70] ZHENG, P.; Wang, W.; Duan, X. N,N'-Dibenzoylpiperazine. *Acta Crystallographica*, **2005**, E61, o2513-o2514.
- [71] MIRON, Y.; McGarvey, B.R.; Morawetz, H. Rates of conformational transitions in solutions of randomly coiled polymers. I. Nuclear magnetic resonance study of transitions in the backbone of polyamides. *Macromolecules*, **1969**, 2, 154-161.
- [72] BEYER, H.; Walter, W.; Francke, W. *Lehrbuch der Organischen Chemie*, 23rd Ed., S. Hirzel Verlag: Stuttgart (Germany), **1998**.
- [73] KOSOBUTSKII, V.A.; Kagan, G.I.; Belyakov, V.K.; Tarakanov, O.G. Amide-Imidol tautomerism in aromatic polyamides. *Journal of Structural Chemistry*, **1972**, 12, 753-760.
- [74] HÖLL, K.; Grohmann, A. *Wasser: Nutzung im Kreislauf, Hygiene, Analyse und Bewertung*, 8th Ed., Gruyter: Berlin (Germany), **2002**.
- [75] WILLIAMS, R. *pKa Data*. http://research.chem.psu.edu/brpgroup/pKa_compilation.pdf (Accessed November 16, **2010**).
- [76] PURDIE, N.; Tomson, M.B.; Riemann, N. The thermodynamics of ionization of polycarboxylic acids. *Journal of Solution Chemistry*, **1972**, 1, 465-476.
- [77] APELBLAT, A. Dissociation constants and limiting conductances of organic acids in water. *Journal of Molecular Liquids*, **2002**, 95, 99-145.
- [78] LIN, C.; Chen, Y.; Wang, T. Separation of benzenediamines, benzenediols and aminophenols in oxidative hair dyes by micellar electrokinetic chromatography using cationic surfactants. *Journal of Chromatography A*, **1999**, 837, 241-252.
- [79] KHALILI, F.; Henni, A.; East, A.L.L. pKa values of some piperazines at (298, 303, 313, and 323) K. *Journal of Chemical and Engineering Data*, **2009**, 54, 2914-2917.
- [80] DONG, H.; Du, H.; Wickramasinghe, S.R.; Qian, X. The effects of chemical substitution and polymerization on the pKa values of sulfonic acids. *Journal of Physical Chemistry B*, **2009**, 113, 14094-14101.
- [81] Rayne, S.; Forest, K.; Friesen, K. Examining the PM6 semiempirical method for pKa prediction across a wide range of oxyacids. *Nature Precedings*, **2009** <http://hdl.handle.net/10101/npre.2009.2981.1> (Accessed November 26, **2010**).

- [82] CAS. *SciFinder*. <https://scifinder.cas.org/scifinder/login> (Accessed November 26, 2010).
- [83] VOLLHARDT, K.P.C. *Organische Chemie*, 1st Ed., VCH: Weinheim (Germany), 1988.
- [84] LATSCHA, H.P.; Klein, H.A. *Organische Chemie*, 2nd Ed., Springer: Heidelberg (Germany), 1990.
- [85] TANG, C.Y.; Kwon, Y.N.; Leckie, J.O. Effect of membrane chemistry and coating layer on physicochemical properties of thin film composite polyamide RO and NF membranes. II. Membrane physicochemical properties and their dependence on polyamide and coating layers. *Desalination*, 2009, 242, 168-182.
- [86] ZHANG, Y.; Xiao, C.; Liu, E.; Du, Q.; Wang, X.; Yu, H. Investigations on the structures and performances of a polypiperazine amide/polysulfone composite membrane. *Desalination*, 2006, 191, 291-295.
- [87] HERBSTEIN, F.H. Structural parsimony and structural variety among inclusion complexes (with particular reference to the inclusion compounds of trimesic acid, N-(p-tolyl)-tetrachlorophthalimide, and the Heilbron "complexes"). *Topics in Current Chemistry*, 1987, 140, 107-139.
- [88] CRAMER, F.; Hettler, H. Inclusion compounds of cyclodextrins. *Die Naturwissenschaften*, 1967, 54, 625-632.
- [89] PEDERSEN, C.J. Cyclic polyethers and their complexes with metal salts. *Journal of the American Chemical Society*, 1967, 89, 7017-7036.
- [90] IUPAC. *Compendium of Chemical Terminology*. <http://goldbook.iupac.org> (Accessed November 8, 2010).
- [91] MAYS, T.J. A new classification of pore sizes. *Studies in Surface Science and Catalysis*, 2007, 160, 57-62.
- [92] MULDER, M.H.V.; van Voorthuizen, E.M.; Peeters, J.M.M. Membrane characterization. In: *Nanofiltration: principles and applications*; Schäfer, A.I., Fane, A.G. and Walte, T.D., Ed.; Elsevier Ltd.: Oxford (UK), 2005, pp. 89-117.
- [93] GHOSH, A.K.; Hoek, E.M.V. Impacts of support membrane structure and chemistry on polyamide-polysulfone interfacial composite membranes. *Journal of Membrane Science*, 2009, 336, 140-148.
- [94] HILAL, N.; Al-Zoubi, H.; Darwish, N.A.; Mohammad, A.W. Characterisation of nanofiltration membranes using atomic force microscopy. *Desalination*, 2005, 177, 187-199.
- [95] ARTUG, G.; Roosmasari, I.; Richau, K.; Hapke, J. A comprehensive characterization of commercial nanofiltration membranes. *Separation Science and Technology*, 2007, 42, 2947-2986.
- [96] BOUSSU, K.; Zhang, Y.; Cocquyt, J.; Van der Meeren, P.; Volodin, A.; Van Haesendonck, C.; Martens, J.A.; Van der Bruggen, B. Characterization of polymeric nanofiltration membranes for systematic analysis performance. *Journal of Membrane Science*, 2006, 278, 418-427.
- [97] NGHIEM, L.D.; Schäfer, A.I.; Elimelech, M. Removal of natural hormones by nanofiltration membranes: measurement, modelling, and mechanisms. *Environmental Science and Technology*, 2004, 38, 1888-1896.
- [98] BOWEN, W.R.; Mohammad, A.W.; Hilal, N. Characterisation of nanofiltration membranes for predictive purposes – use of salts, uncharged solutes and atomic force microscopy. *Journal of Membrane Science*, 1997, 126, 91-105.
- [99] BOTT, R.; Langeloh, T. *BOKELA Solid/Liquid Separation Lexicon*. GIT Verlag: Darmstadt (Germany), 2010.
- [100] SIMON, A.; Nghiem, L.D.; Le-Clech, P.; Khan, S.J.; Drewes, J.E. Effects of membrane degradation on the removal of pharmaceutically active compounds

- (PhACs) by NF/RO filtration processes. *Journal of Membrane Science*, **2009**, 340, 16-25.
- [101] NORBERG, D.; Hong, S.; Taylor, J.; Zhao, Y. Surface characterization and performance evaluation of commercial fouling resistant low-pressure RO membranes. *Desalination*, **2007**, 202, 45-52.
- [102] NGHIEM, L.D.; Schäfer, A.I.; Elimelech, M. Nanofiltration of hormone mimicking trace organic contaminants. *Separation Science and Technology*, **2005**, 40, 2633-2649.
- [103] MCHALE, G.; Newton, M.I.; Shirtcliffe, N.J. Water-repellent soil and its relationship to granularity, surface roughness and hydrophobicity: a materials science view. *European Journal of Soil Science*, **2005**, 56, 445-452.
- [104] NGHIEM, L.D.; Schäfer, A.I.; Elimelech, M. Pharmaceutical retention mechanisms by nanofiltration membranes. *Environmental Science and Technology*, **2005**, 39, 7698-7705.
- [105] FREGER, V. Swelling and morphology of the skin layer of polyamide composite membranes: an Atomic Force Microscopy study. *Environmental Science and Technology*, **2004**, 38, 3168-3175.
- [106] GLATER, J.; Hong, S.; Elimelech, M. The search for a chlorine-resistant reverse osmosis membrane. *Desalination*, **1994**, 95, 325-345.
- [107] KONAGAYA, S.; Watanabe, O. Influence of chemical structure of isophthaloyl dichloride and aliphatic, cycloaliphatic, and aromatic diamine compound polyamides on their chloride resistance. *Journal of Applied Polymer Science*, 2000, 76, 201-207.
- [108] HILAL, N.; Al-Abri, M.; Al-Hinai, H.; Abu-Arabi, M. Characterization and retention of NF membranes using PEG, HS and polyelectrolytes. *Desalination*, **2008**, 221, 284-293.
- [109] PREISS, U.P.R.M.; Slattery, J.M.; Krossing, I. In silico prediction of molecular volumes, heat capacities, and temperature-dependent densities of ionic liquids. *Industrial & Engineering Chemistry Research*, **2009**, 48, 2290-2296.
- [110] PREISS, U.; Emel'yanenko, V.N.; Verevkin, S.P.; Himmel, D.; Paulechka, Y.U.; Krossing, I. Temperature-dependent prediction of the liquid entropy of ionic liquids. *European Journal of Chemical Physics and Physical Chemistry*, **2010**, 11, 3425-3431.
- [111] RANKE, J.; Müller, A.; Bottin-Weber, U.; Stock, F.; Stolte, S.; Arning, J.; Störmann, R.; Jastorff, B. Lipophilicity parameters for ionic liquid cations and their correlation to in vitro cytotoxicity. *Ecotoxicology and Environmental Safety*, **2007**, 67, 430-438.
- [112] CHO, C.W. *Hydrophobicity Py6 cation*. Personal Communication. **2011**.

3 ACHIEVING IONIC LIQUID RECOVERY

3.1 BACKGROUND

Nanofiltration is a membrane process which falls between reverse osmosis and ultrafiltration in its separation characteristics: ultrafiltration membrane processes are not able to discriminate efficiently between low molecular weight species, whereas reverse osmosis membrane processes reject both low molecular weight species and salts. Such a process rejects species which have a size in the order of one nanometer, and then a suitable name for it should be nanofiltration [1].

The most distinctive features of nanofiltration in comparison with other membrane processes are summarized in Figure 3.1.

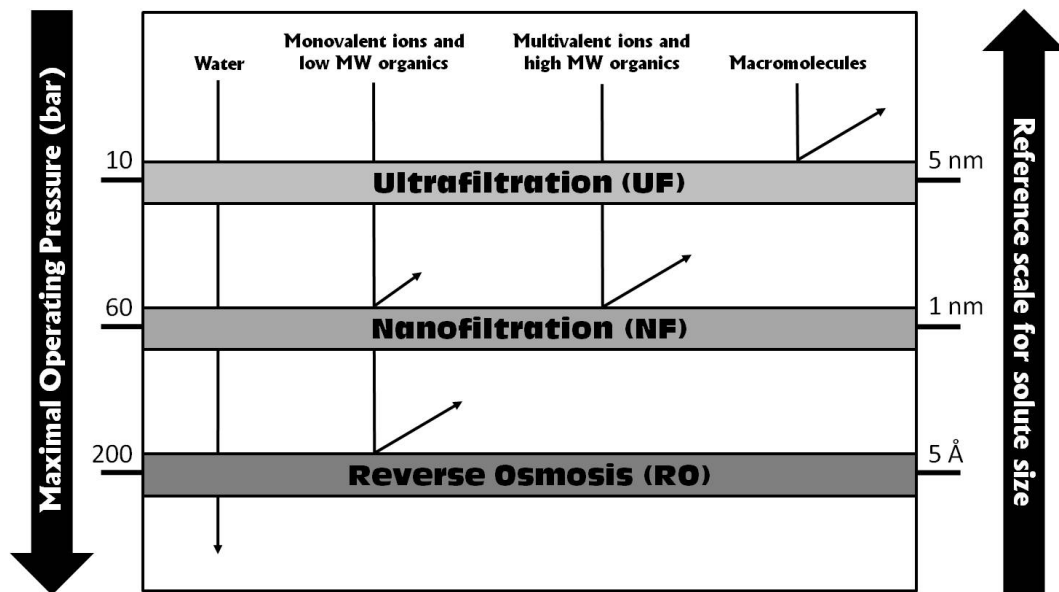


Figure 3.1: Separation characteristics of different membrane processes.

Nanofiltration exhibits low rejection for salts with monovalent anions and non-ionized organics with molecular weight below 150 g/mol, while the rejection is high for salts with di- and multivalent anions and organics with molecular weight above 300 g/mol. As consequence, nanofiltration has introduced a new perspective for applications in the processing of foods, pharmaceuticals, demineralising water, separation processes, for downstream processes and treatment of industrial effluents [1,2].

3.1.1. Components of a membrane process

Nanofiltration, like all the pressure-driven membrane processes, separates a feed stream in two streams: permeate and retentate. The retentate stream contains the material rejected by the membrane, while the permeate stream contains the material that permeated through it, as it is shown in Figure 3.2.

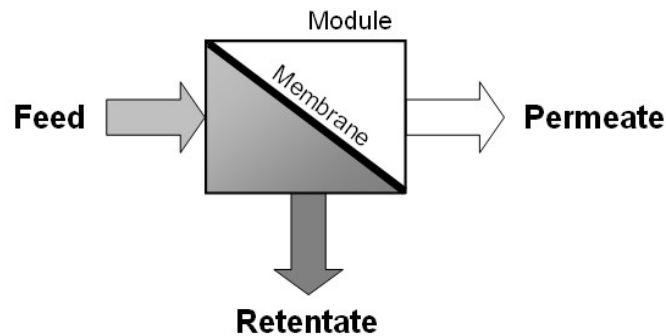


Figure 3.2: Main components of a pressure-driven membrane process.

If the feed is pumped directly towards the membrane and no retentate stream is leaving the module, the process is termed *dead-end*; but if the feed is pumped across or tangentially to the membrane surface and two streams are leaving the module, the process is known as *cross-flow* [3].

The necessary components of a membrane process are the membrane, the module and the operating concept, which are completed with the system comprising the arrangement of modules, pumps, piping, tanks, controls and monitoring, pre-treatment and cleaning facilities [4].

A membrane can be defined as a material through which one type of substance can pass more readily than other types, thus presenting the basis of the separation process. It is only useful if it takes a form which allows some components present in the feed to pass through it [5]. The module supports the membrane and provides effective fluid management. Membranes are produced either as flat sheets or tubes, and most industrial membrane equipment can be divided into three general classes [6]:

- *Plate and frame*, comprising flat membranes in a filter-press type arrangement,
- *Spiral wound*, where flat membranes are bounded together and wound into a spiral arrangement, and
- *Tubular*, where cylindrical membranes are placed in a shell-tube heat exchanger arrangement.

However, for laboratory trials, the dead-end stirred cell and the cross-flow tester are used with flat membranes. Which such set-ups is possible to test new membranes or to evaluate conveniently parameters concerning a specific separation problem; despite they do not provide the highest area per unit volume of equipment [4].

The *dead-end stirred cell* is the simplest test system and has the advantage that relatively small liquid volume and membrane sample are required, as it is schematized in Figure 3.3(a). The solution to be treated is introduced in the upper chamber of the cell and then pressure is applied to force it through the membrane. Stirring is used to reduce concentration polarization and the system does not operate at steady state: samples must be taken for both chambers after several time periods to determine the performance of the separation [6].

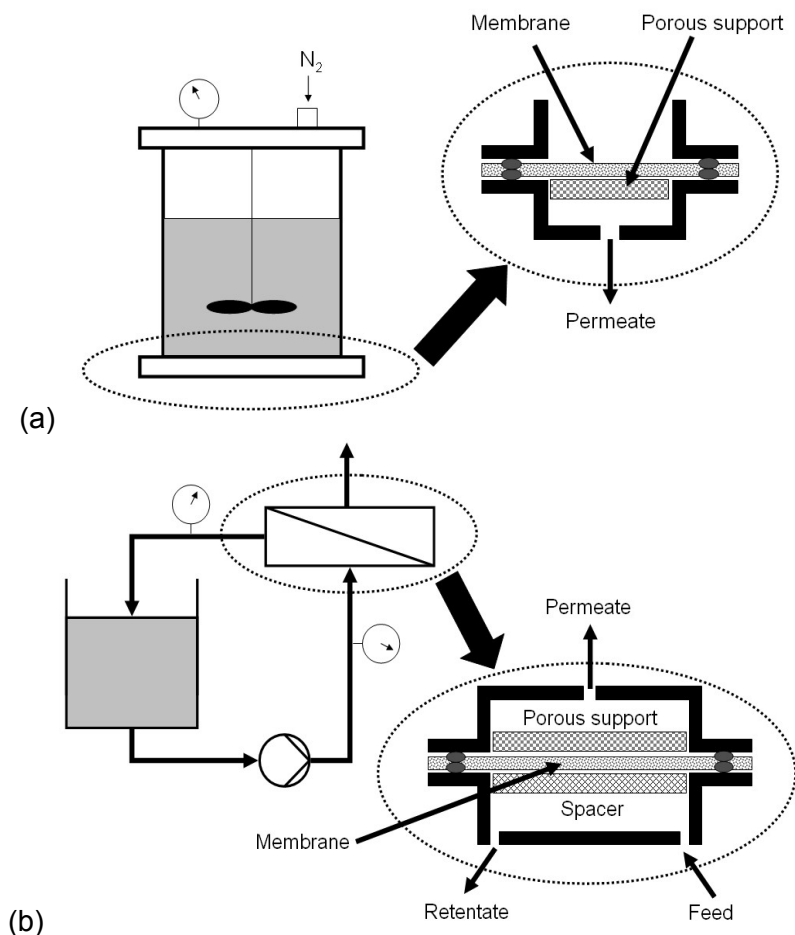


Figure 3.3: Laboratory set up: (a) dead-end stirred cell, (b) cross-flow tester.

The *cross-flow tester* involves a flat membrane, preferably with a feed channel spacer to simulate the spiral wound module, as it is shown in Figure 3.3(b). The feed stream is pumped from the feed tank and flow continues into the membrane cavity. Once there, the solution flows tangentially across the membrane surface. A portion of the solution permeates the membrane and is collected in a permeate tank. The retentate continues sweeping over the membrane and then flows into a separate tank or back into the feed tank [7].

Membrane systems can operate in batch or continuous mode. The selection is based on process objectives and economics. A batch operation is the better option when concentrating ionic liquids, as it is shown in Figure 3.4.

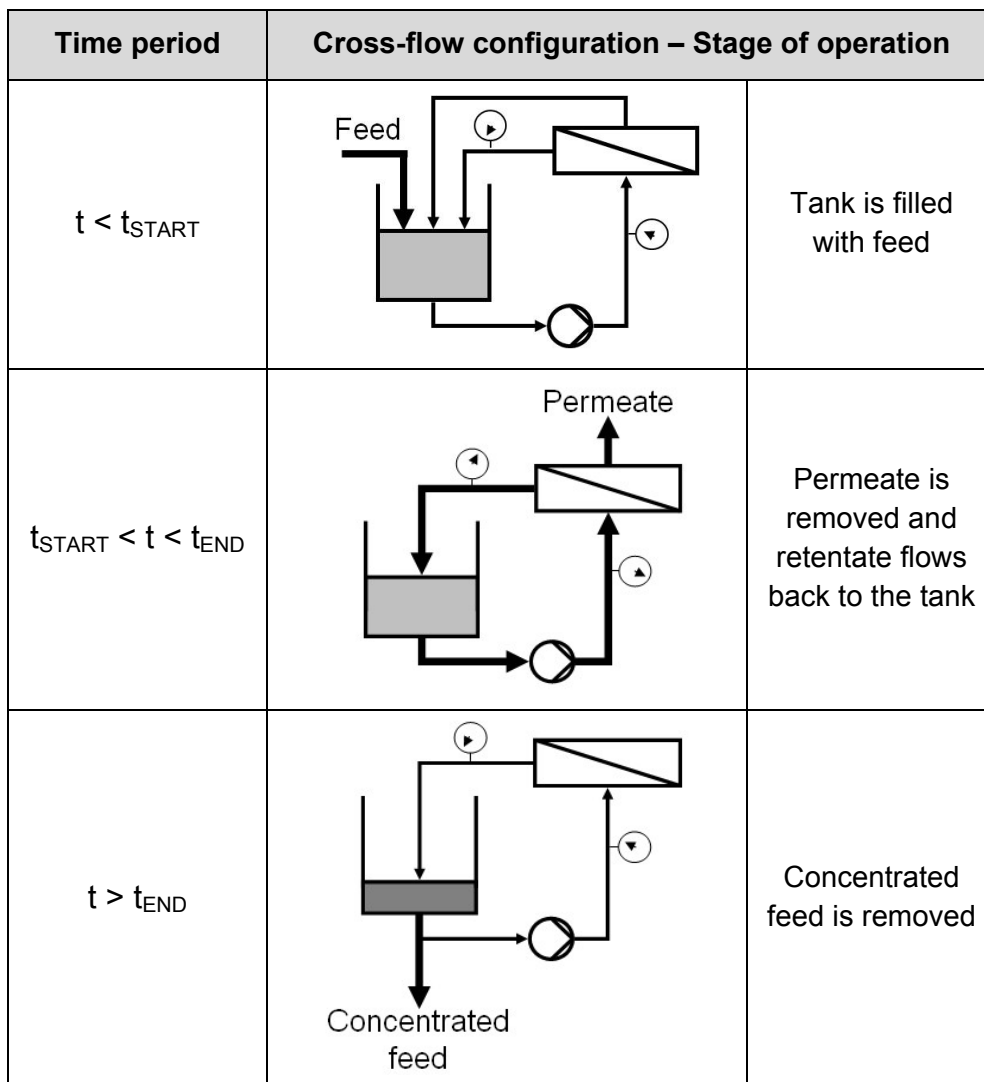


Figure 3.4: The three stages of batch operation for producing a concentrate.

This batch operation mode requires the least membrane area but a larger process tank. The tank is first filled with the entire quantity of feed to be concentrated ($t < t_{\text{START}}$), then, as feed circulates through the membrane ($t_{\text{START}} < t < t_{\text{END}}$), retentate flows back into the tank. The feed is concentrated by small amounts with each pass through the membrane, and the overall concentration in the feed tank increase as water is removed by permeation through the membrane. When the final concentration is reached ($t > t_{\text{END}}$), the concentrated feed is removed. After that, the system is cleaned, the process tank is then refilled with fresh feed and the processing begins again. Such batch systems are mainly used in smaller wastewater treatment applications that typically process less than 4000 L/day [8].

3.1.2 Performance of membrane separations

In a simple membrane separation process, a feed consisting of a mixture of two components (solute and solvent) is partially separated by means of the membrane through which one component (normally the solvent) move faster than another (in this case, the solute). Then, the feed mixture is separated into a retentate stream, enriched in solute, and a permeate stream, depleted in solute.

Applying *material balances* for the overall flow and the solute it is possible to relate the amounts of each stream and their compositions, based on the definitions shown in Figure 3.5, as follows:

$$Q_F = Q_P + Q_R \quad (\text{Eq. 3.1})$$

where:

Q_F : Volume of feed (L)

Q_P : Volume of permeate (L)

Q_R : Volume of retentate (L)

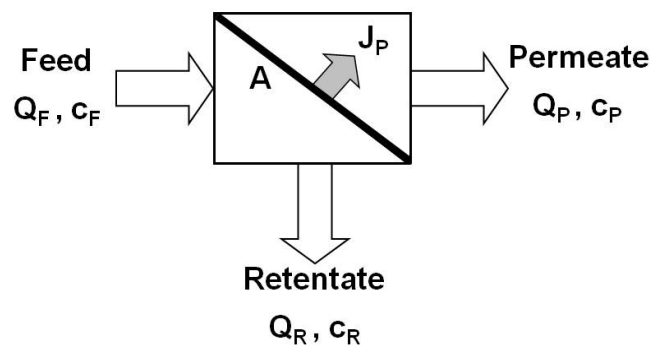


Figure 3.5: Main variables related to membrane performance.

$$Q_F \cdot C_F = Q_P \cdot C_P + Q_R \cdot C_R \quad (\text{Eq. 3.2})$$

where:

C_F : Concentration of ionic liquid in feed (g/L)

C_P : Concentration of ionic liquid in permeate (g/L)

C_R : Concentration of ionic liquid in retentate (g/L)

When more than one solute is present, a material balance for each solute should be applied.

The applied pressure difference, the membrane resistance, the hydrodynamics conditions at the feed-membrane interface and the fouling of the membrane surface determine the *permeate flux*, which is defined as the quantity of material passing through a unit area of membrane per unit time. This means that it takes SI units of $\text{m}^3/\text{m}^2\text{s}$ (or simply m/s), and is occasionally named as the permeate velocity. Other non-SI units used are $\text{L}/\text{m}^2\text{h}$, which tends to give more accessible numbers: membranes generally operate at fluxes between 10 and 1000 $\text{L}/\text{m}^2\text{h}$. Then, it can be determined as follows:

$$J_P = \frac{Q_P}{A_M \cdot t} \quad (\text{Eq. 3.3})$$

where:

J_P : Permeate flux ($\text{L}/\text{m}^2\text{h}$)

A_M : Membrane area (m^2)

t: Time (h)

The permeate flux relates directly to the driving force and the total resistance offered by the membrane and the interfacial region adjacent to it [5].

The combination of the flux and the total membrane area determine the *recovery or conversion* of the process. The recovery, which can be also expressed as percentage, is the amount of the feed that is recovered as permeate:

$$\frac{V_P}{V_F} = \frac{Q_P}{Q_F} \quad (\text{Eq. 3.4})$$

where:

V_P/V_F : (Process) recovery (-)

A high recovery is aimed at in order to minimize the retentate fraction and to maximize the volume of the permeate [9].

The perm-selective property of the membrane to the solute is normally quantified as the *retention or rejection*, where:

$$R = 1 - \frac{C_P}{C_F} \quad (\text{Eq. 3.5})$$

where:

R: Retention, rejection (-)

Retention values are expressed normally as percentage. Furthermore, it is possible to have negative retention values if the membrane is selective for the solute. The retention of a membrane is a function of the permeation rate (thus the pressure drop across the membrane) and the solution composition. There are various models proposed to explain the retention, and the dependence of retention upon permeation rate and solution concentration can be different to each model. The agreement of such models with experimental data provides the principal justification for using them. However, most models can not take into account all the possible phenomena that take place in membrane transport [6].

Finally, the composition of the retentate is qualitatively identical to the feed composition, but for components rejected by the membrane the concentration is higher than in the feed. The concentration factor is defined as the ratio of the concentration of the solute in retentate and feed:

$$CF = \frac{C_R}{C_F} \quad (\text{Eq. 3.6})$$

where:

CF: Concentration factor (-)

Combining the Equations 3.4, 3.5 and 3.6 with the Equation 3.2, it is possible to express the material balance for the solute as a function of three performance parameters: recovery, retention and concentration factor. The resulting equation is:

$$CF = \frac{1 - \frac{V_P}{V_F} \cdot (1 - R)}{1 - \frac{V_P}{V_F}} \quad (\text{Eq. 3.7})$$

This can be also presented in a graphic form, as in Figure 3.6. For low recovery values, the retention has a minor influence on the concentration factor. However, for high recovery values the higher the retention the higher the concentration factor. For every recovery rate, no changes in the retentate concentration (it remains equal to the feed concentration) are observed if the solute is not rejected by the membrane ($R = 0$).

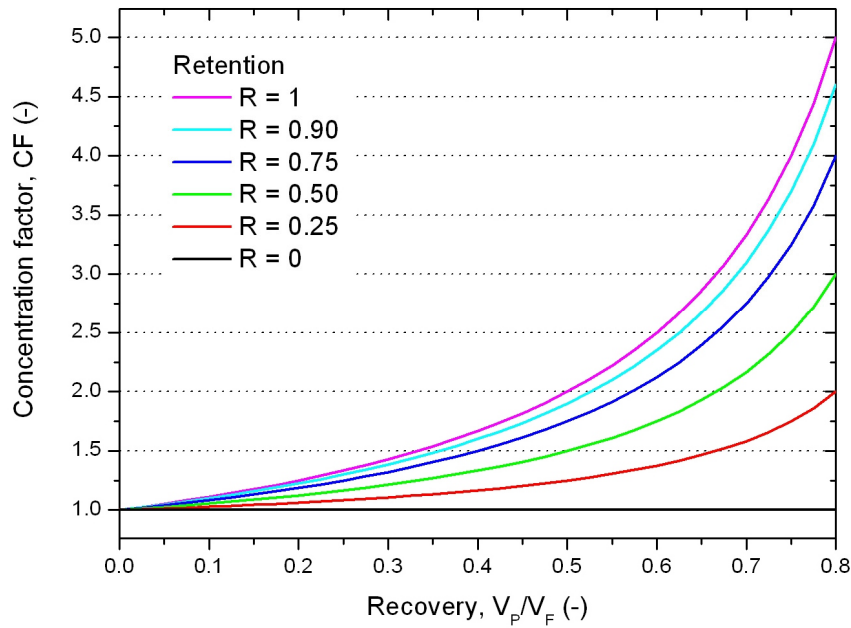


Figure 3.6: Graphical expression of the material balance for the solute.

3.1.3 Second phase formation by concentration

In pressure-driven liquid-phase membrane processes, such as nanofiltration, the accumulation of retained species close to the membrane is known as concentration polarization [4,10], which can be represented by the concentration gradient within a boundary layer adjacent to the membrane (Figure 3.7).

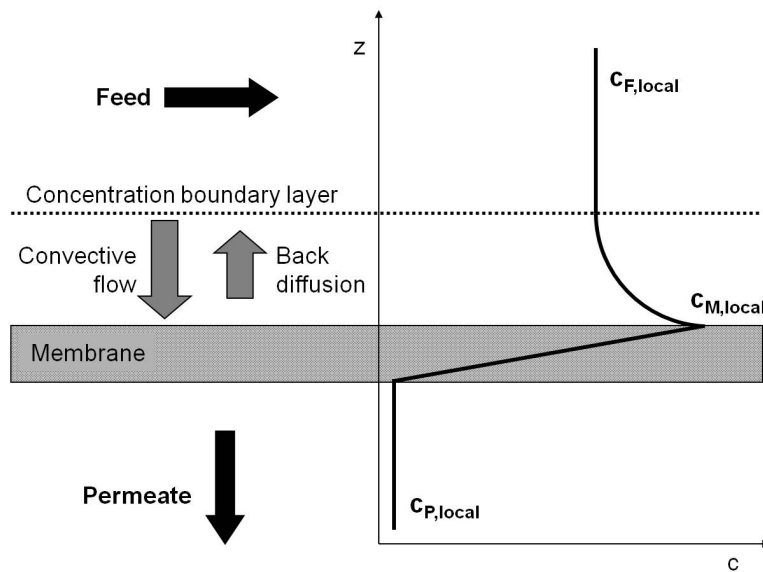


Figure 3.7: Concentration polarization phenomenon. Adapted from [10].

This layer contains near-stagnant liquid, since at the membrane surface itself the liquid velocity must be zero. Thus, rejected materials build up in the region adjacent to the membrane, increasing their concentration over the bulk value. Such a concentration build-up will generate a diffusive flow back to the bulk of the feed. A balance between the forces transporting the water and materials towards, through and away from the membrane occurs and the concentration profile within the boundary layer is established [5,11].

The concentration achieved in this concentration boundary layer adjacent to the membrane and the spatial extend of this layer will be dependent upon a number of intrinsic and operational factors including concentration of the feed stream, the permeate flux and the hydrodynamic conditions at the membrane surface [12]. When the concentration within this boundary layer exceeds the solubility limit for the solute in the mixture, the onset of a second phase could be observed. In the case of dissolved salts, the solubility product is exceeded and the precipitation of the corresponding solid salt occurs. In the case of ionic liquids in aqueous solution such a situation is also expected, if the water solubility of the ionic liquid is exceeded a second phase will appear.

Hydrophobic ionic liquids and water are one of the numerous liquid-liquid systems which show partial miscibility. However, few contributions dealing with liquid-liquid phase equilibrium of ionic liquids and water as a function of temperature have been reported [13,14]. In these binary systems under constant pressure, an increase in temperature will cause an increase in the limits of solubility for both ionic liquid in water and water in ionic liquid.

For some ionic liquids [15], it has been observed that the two solubility curves slope toward one another and merge into each other at a temperature which is termed the upper critical solution temperature (UCST), as it is shown in Figure 3.8(a). Above the solid line representing the phase boundary, both ionic liquid and water are completely miscible and only one phase exists. Below the phase boundary, two phases of different chemical composition are in equilibrium and phase separation is expected [16].

The same diagram can be analyzed in terms of the system stability, as in Figure 3.8(b). The coexistence curve is often called the binodal curve and the area within it is termed miscibility gap, where are two phases coexisting. Below the binodal curve there is a metastable region, in which the system is stable to small fluctuations but is unstable to large

fluctuations. The line representing the stability limit in a miscibility gap is called a spinodal curve and inside the region of the phase diagram bounded by this curve, the system is in unstable equilibrium. The critical point is the only point where the stability limit can be reached by a stable system, because two coexisting states become identical here [17].

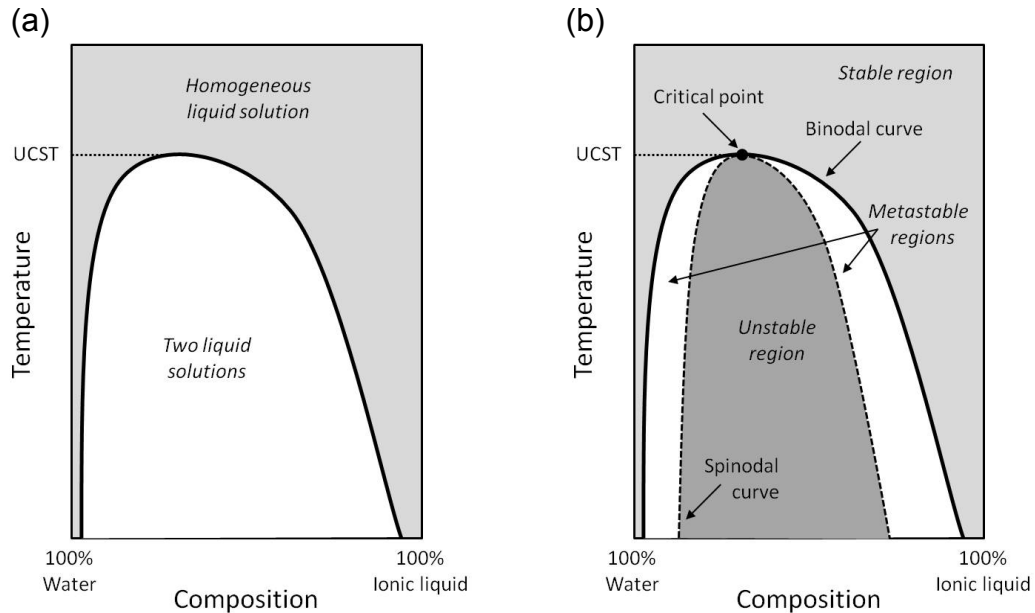


Figure 3.8: (a) Temperature-composition diagram for ionic liquid and water at constant pressure. (b) The same diagram showing stability zones and limits.

When a mixture from the one-phase region is brought inside the two-phase domain by quenching, as it is represented in Figure 3.9, the homogeneous phase abruptly reaches either a non-equilibrium state (inside the spinodal curve) or a metastable equilibrium state (between the spinodal and binodal curves). Then, the system evolves toward a stable equilibrium state, where two phases are formed [18]. In the first case, the phase separation mechanism is called spinodal decomposition which is small in degree and large in extent and would generally produce an interconnected structure, while in the second case it is known as nucleation and growth; which is large in degree and small in extent, generally leading to the droplet morphology [19].

If a concentration process at constant temperature is carried out, the change occurs now from the stable homogeneous phase into the metastable region, as is represented in Figure 3.10. Then, the transformation is initiated within the original phase by the nucleation of clusters of the new phase (containing a few atoms or molecules), which then grow to macroscopic dimensions.

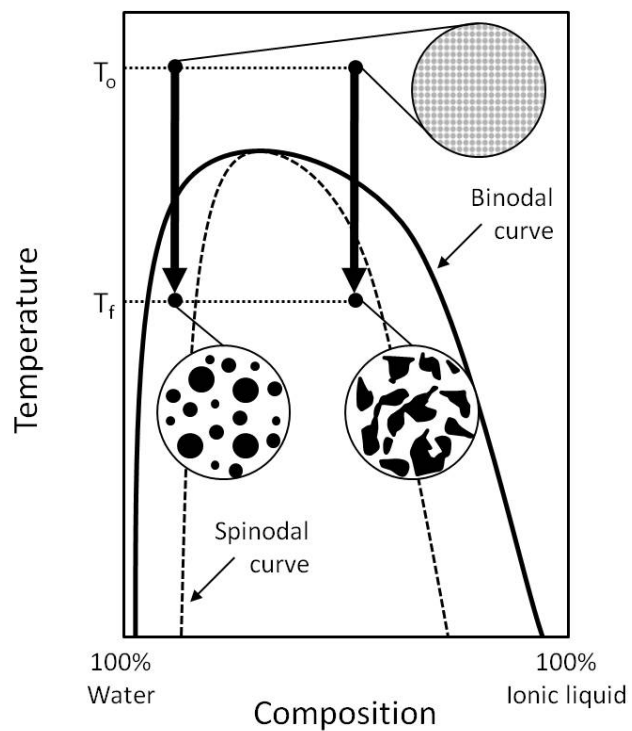


Figure 3.9: Phase diagram showing phase separation obtained by quenching into the metastable or unstable regions. Adapted from [20].

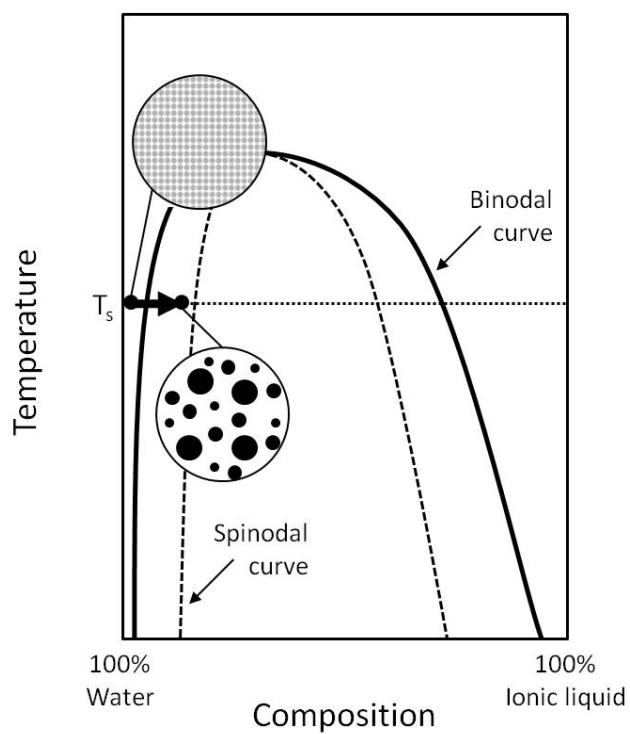


Figure 3.10: Phase diagram showing phase separation obtained by isothermal concentration into the metastable region.

However, there is an energetic barrier to nucleation and a critical cluster size: smaller clusters will on average dissolve, while larger clusters will on average grow to complete the phase transformation. But this critical size is kinetic dependent and it changes as any of the parameters of the system change [20,21].

Furthermore, if a mixture containing droplets of a new minority phase is exposed to shear (like that existing inside the nanofiltration module); two opposite tendencies can occur. At the beginning, shear can enhance the aggregation of droplets, thus speeding up the growth. However, if the shear exceeds a relatively small critical value, then droplets bigger than the critical size can be even broken, leading to complete suppression of the droplet formation [22-25].

3.2 EXPERIMENTAL

3.2.1 Materials

Nanofiltration membranes used are the same already described in Section 2.2.1 (Chapter 2). Three ionic liquids containing the (CF₃SO₂)₂N anion were obtained from Merck KGaA (Darmstadt, Germany) and they were used as received. Their information is summarized in Table 3.1.

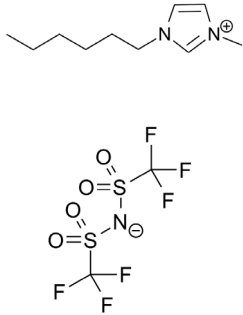
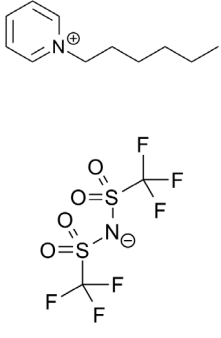
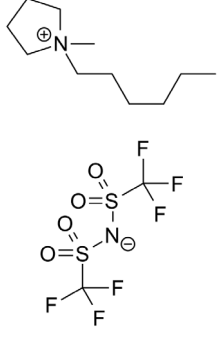
They were selected for model solutions due to their performance during the biotransformation of 2-octanone into (R)-2-octanol in a 200 mL reaction system [26]. They exhibited higher conversion (91% for IM16, 86% for Pyr16 and 78% for Py6) compared with the traditional one-phase system (55% for aqueous buffer) after five hours of reaction. To reduce the influence of additional ions, water for ion chromatography (Fluka Analytical, Sigma-Aldrich) with an electric conductivity lower than 2 μS/cm was used to prepare model solutions.

All wastewaters were used as received, after having stabilized the temperature at 298 K for one day. The wastewater from the dissolution of cellulose comprised an aqueous mixture of IM14 Cl and IM14 1COO (about 85:15), with a content of ionic liquid around 18-20%, and exhibiting a dark gold colour. It was provided by the Thuringian Institute of Textile and Plastic Research (TITK).

Two reaction mixtures from the reduction of 2-octanone catalyzed by the *Lactobacillus brevis* alcohol dehydrogenase (LB-ADH), containing IM16

(CF₃SO₂)₂N and Pyr14 (CF₃SO₂)₂N, were provided by Jülich Chiral Solutions (JCS, Codexis).

Table 3.1: Ionic liquids selected for membrane screening.

Ionic liquid	IM16 (CF ₃ SO ₂) ₂ N	Py6 (CF ₃ SO ₂) ₂ N	Pyr16 (CF ₃ SO ₂) ₂ N
Chemical name IUPAC	1-hexyl-3-methyl-imidazolium	1-hexylpyridinium	1-hexyl-1-methylpyrrolidinium
	bis(trifluoromethylsulfonyl)amide		
Chemical structure			
CAS Number	382150-50-7	460983-97-5	380497-19-8
Mol. weight (g/mol)	447.417	444.413	450.461
Water solubility at 20°C (mol/L)	3.69x10 ⁻³	7.76x10 ⁻³	4.22x10 ⁻³

These mixtures contained initially 30% v/v of ionic liquid, 1 M 2-octanone, 20 U/mL LB-ADH and 1 mM NADP in 0.2 M phosphate buffer (pH = 7.0). Conversion of 2-octanone to 2-octanol was reported around 60% for Pyr14 cation, while more than 90% conversion was reported for IM16 cation. The differences are related with the cofactor regeneration method used: in the first case 2-propanol was oxidized to acetone, while in the second case glucose was oxidized by means of glucose dehydrogenase (GDH). After reaction, the ionic liquid phase was completely separated by sedimentation after 5 hours.

The aqueous phase from whole-cell biotransformation of 2-octanone into 2-octanol, contained initially 20% v/v of Pyr16 (CF₃SO₂)₂N, 0.3 M 2-octanone, 50 g/L dry biomass and 1 M sodium formate in 0.5 M phosphate buffer (pH = 6.5). The biomass contained an *Escherichia coli* strain able to produce the *Lactobacillus brevis* alcohol dehydrogenase (LB-ADH) and

the *Candida boidinii* formate dehydrogenase (CB-FDH) for the cofactor regeneration. After reaction (conversion around 80-90%), the ionic liquid was separated by centrifugation from cells and aqueous phase. This sample was provided by the Institute of Biochemical Engineering (Technische Universität München, TUM)

3.2.2 Dead-end nanofiltration experiments

For the experiments, the same stirred dead-end cell described in Section 2.2.3 (Chapter 2) was used. Membranes were placed in deionised water for two days before use to assure complete swelling. Each swollen membrane was conditioned with deionised water by increasing pressure progressively until a pressure of 40 bar was reached. After that, the desired amount of feed (100-150 mL at 25°C) was filled in the cell, the pressure difference was fixed at 35 bar and permeate was removed continuously until the desired recovery rate was reached. The time required to obtain different volumes was measured, in order to calculate permeate fluxes. Samples of feed, retentate and cumulated permeate were taken for later analysis and used to calculate retentions.

3.2.3 Cross-flow nanofiltration experiments

Experiments were carried out using a laboratory scale-test cell developed and constructed at the University of Bremen (Figure 3.11).

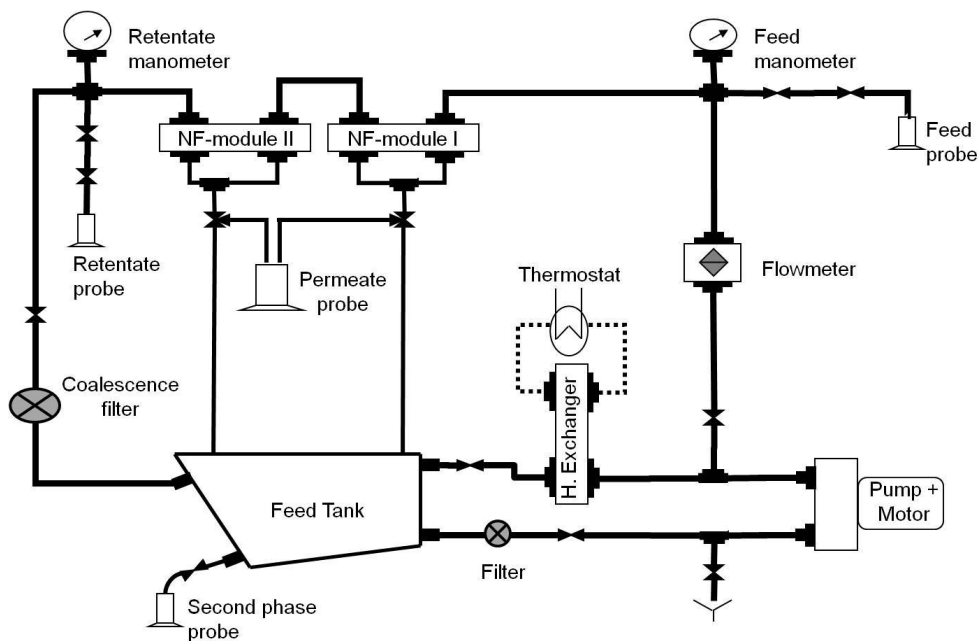


Figure 3.11: Schematic diagram of the Cross-flow module used in this work.

The membrane active area was 270 cm^2 , distributed in two identical modules connected in series. The two filtration modules are identical and were also constructed also at the University of Bremen. Their components are shown in Figure 3.12. The use of a spacer in the feed channel and a high cross flow velocity of 0.5 m/s (45 L/h) should create enough turbulence to reduce concentration polarization effects.

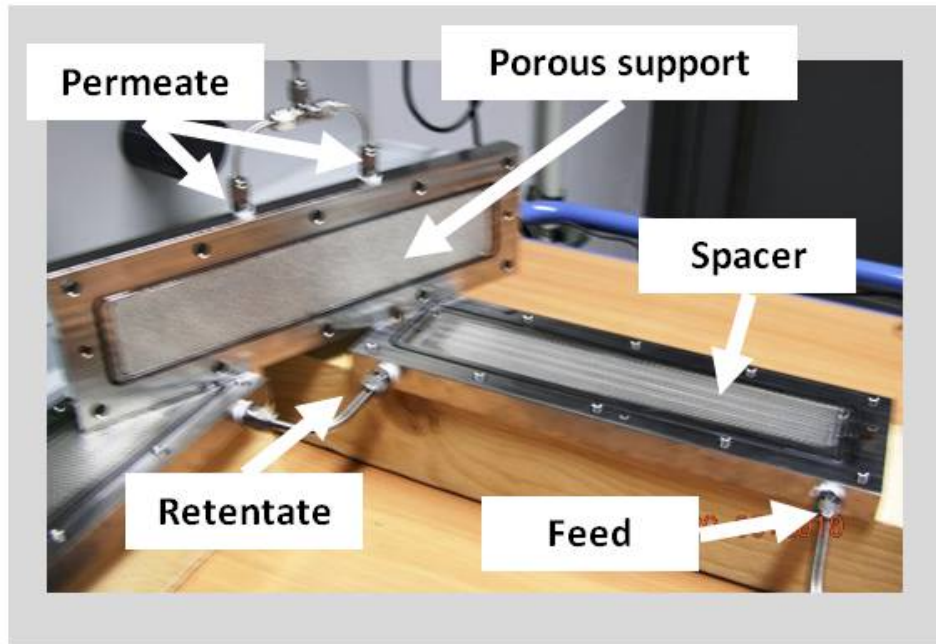


Figure 3.12: Membrane module and its components.

The equipment was designed for batch filtration of 5 L , and the feed tank was made of Plexiglas to observe feed appearance changes. The equipment has a plunger pump (NP10 / 4-140 RE, Speck Triplex) with a maximal pressure of 140 bar , maximal output of 4 L/min and stainless steel valve casings and wetted parts.

The temperature of the solution in the system was maintained at $25 \pm 0.01^\circ\text{C}$, by using a plate heat exchanger (BHM 22 -20 GBH, FeRo) with a maximal operating pressure of 45 bar coupled with a thermostat (ProLine RP 845C, Lauda). The feed pressure and the feed flow rate were adjusted by needle valves. An oval gear-wheel flowmeter (VO-01.VA.80.VI.ST.IM, Profimess) with an operating range of $14\text{-}80 \text{ L/h}$ was used.

The pipelines ($1/4''$ for feed and retentate, and $1/8''$ for permeate), the coalescence filter housing, the particle filter, the manometers ($0\text{-}60 \text{ bar}$), the valves and all the fittings used are Swagelok parts (Best

Fluidsysteme). For the coalescence filter housing a filter element (12-57-01-SS, MTS Filtertechnik) of stainless steel were also used. The main parts of this nanofiltration equipment are also shown in Figure 3.13.

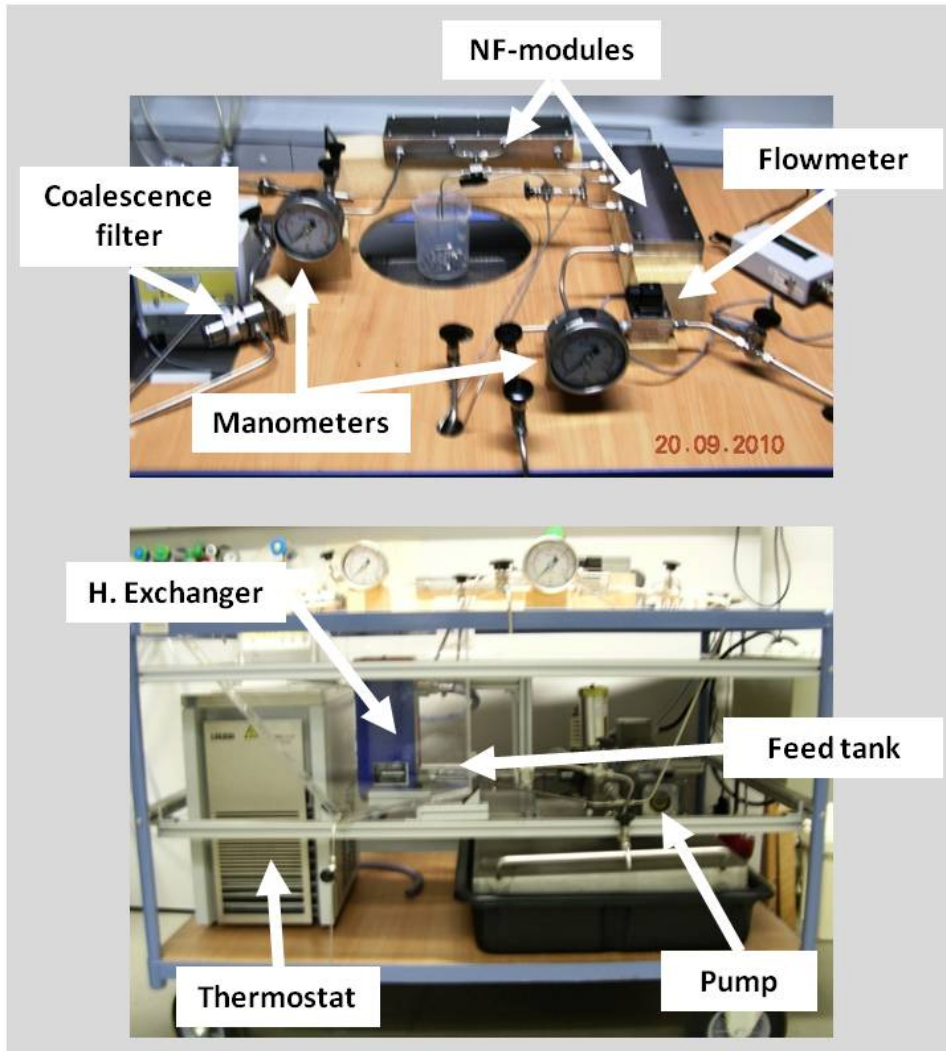


Figure 3.13: Cross-flow module used in this work.

Swollen membrane pieces were placed in the modules and conditioned progressively with deionised water. This conditioning process comprises five different pressure levels (0, 10, 20, 30 and 35 bar), and pressure was kept 30 minutes for each pressure level, except for the last one (45 minutes). After that the deionised water was completely discharged and the solution of ionic liquid was filled in the tank. The system was operated at 35 bar during 30 minutes in the full recirculation mode, while both retentate and permeate were continuously returned to the feed tank.

After membrane conditioning and system stabilization, the concentration process started, remaining the operation parameters: 25°C, 35 bar and 45 L/h. A feed sample for analysis was taken direct from the feed tank before starting to collect permeate, which was collected step-by-step in bottles (250 mL) until a recovery rate around 75% ($V_P/V_F = 0.75$) was reached. Thus a total volume of permeate around 4.0 L was collected and a volume of retentate about 1.0 L remained in the tank. For each permeate sample collecting time was measured and the exact volume was later determined with a graduated cylinder. For each bottle of permeate a sample for analysis was taken. The retentate was collected in a separate bottle and a sample for analysis was also taken.

3.2.4 Adsorption experiments

Active carbon as powder (Merck KGaA) was used. The equilibrium adsorption tests were carried out in stoppered glass bottles (25 mL) placed in a shaking thermostat (Lauda A-120S) at 23°C. Different amounts of active carbon were placed in contact with 10 cm³ samples of wastewater containing IM16 (CF₃SO₂)₂N, to cover a range of concentrations between 0 and 50 g/L. The contact time was 72 hours for all the samples, to assure equilibrium conditions. After that, samples were centrifuged (20 minutes, 4500 rpm) and filtered before analysis to determine initial and equilibrium concentrations. The amount of ionic liquid adsorbed was determined as follows:

$$q = \frac{(C_0 - C_{eq}) \cdot V}{M_{AC}} \quad (\text{Eq. 3.8})$$

where:

q: Amount of ionic liquid adsorbed in active carbon (mmol/g)

C₀: IL-Concentration for samples without active carbon (mmol/L)

C_{eq}: Equilibrium IL-concentration for samples with active carbon (mmol/L)

V: Volume of solution (0.025 L)

M_{AC}: Mass of active carbon added (g)

3.2.5 Analytical methods

The ion-chromatography (IC) measurements were carried out using a Metrohm 881 Compact IC system described in Section 2.2.5 to determine concentrations of ionic liquids cations and anions. For cation separations a C4 ion exchange column (50 x 4.0 mm ID and 5 μm mean particle size) coupled with C4 Guard and RP Guard was used. A flow rate of 0.9 mL/min eluent (2mM HNO₃, 30% CH₃CN) was applied. For the determination of

ionic liquid anions, two different eluents (3.2mM Na₂CO₃, 2mM NaHCO₃, 35% CH₃CN or 1mM NaHCO₃, 3.9mM H₃PO₄, 30% CH₃CN) were used.

Electrical conductivity was measured at 25°C with an inoLab Cond-Level-2-Meter using an epoxy TetraCon® 325 probe (WTW GmbH). The temperature was kept constant with a thermostat. All measurements were done as duplicate. An estimation of the content of cellulose degradation by-products was obtained using the anthrone method, applied for the colorimetric determination of carbohydrates [27]. The concentration of ionic liquids in wastewaters from cellulose dissolution was determined by the supplier using its own calibration curves for refractive index versus ionic liquid content, method already established for such a task [28].

3.3 MEMBRANE SCREENING AND IL-SELECTION

Before starting with the recovery of hydrophobic ionic liquids from model aqueous solutions by nanofiltration in detail, the selection of a properly ionic liquid – membrane pair should be first accomplished.

For an optimal recovery of hydrophobic ionic liquids, it is necessary that both permeate flux and retention exhibit highest values possible. A high retention assures the concentration process of ionic liquid in the retentate stream; while a high permeate flux benefits the concentration process but also reduces the needs of membrane area. In Figure 3.14, results that were obtained after a series of experiments carried out in a dead-end filtration cell at 35 bar are represented.

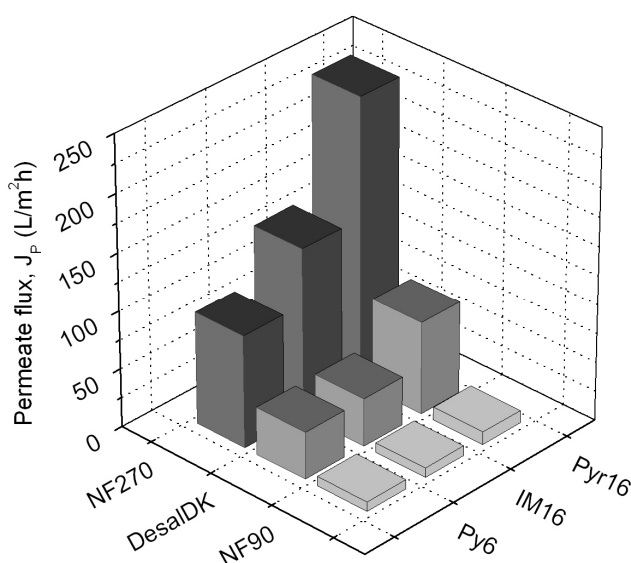


Figure 3.14: Permeate fluxes for each ionic liquid – membrane combination.

In the case of both NF-270 and Desal DK membranes, a process recovery rate (V_P/V_F) of 80% could be achieved within 90 minutes of filtration, while recovery rates between 50 and 65% could be only achieved for the NF-90 membrane, corresponding to 4.5 hours of filtration. That means, than permeate fluxes for the NF-90 membrane at a feed recovery rate of 80% are notable lower than those presented in Figure 3.14.

However, a clear trend can be observed for each membrane: the lowest permeate flux is related to the Py6 cation, while the highest permeate flux belongs to the Pyr16 cation. Furthermore, the NF-270 membrane provides the highest permeate fluxes (more than twice the values obtained for the Desal-DK membrane), no matter the ionic liquid employed.

Based on these results, the membrane NF-270 was selected for further experiments; but more information is needed to select properly the ionic liquid. For this purpose, the results about membrane performance were collected and represented in Figure 3.15.

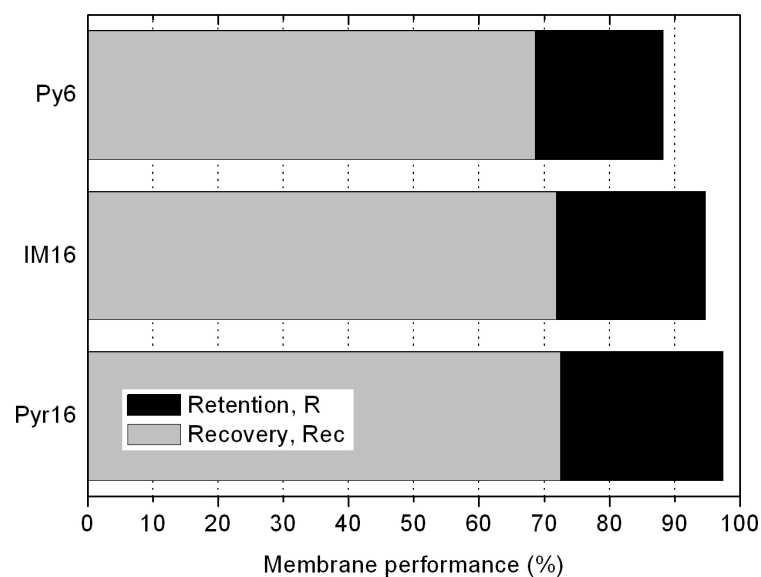


Figure 3.15: Performance of NF-270 membrane with respect to the ionic liquid employed ($V_P/V_F = 80\%$, 35 bar, IL-saturated feed solutions)

Only the ionic liquid based on the Py6 cation exhibits a retention value under 90%. This ionic liquid exhibit also the higher solubility (around 5 g/L) in comparison with the solubilities values for IM16 and Pyr 16 based ionic liquids (around 2.0 g/L). That means that either the IM16 cation or the Pyr16 cation could be selected for further experiments, considering that the differences between both retention values (95 and 97%, respectively)

are not big enough. Additionally, the recovery rate of ionic liquid as second phase exhibit values around 72% for both cases. It was calculated from the ionic liquid material balance as follows:

$$\text{Rec} = \frac{Q_F \cdot C_F - Q_P \cdot C_P - Q_R \cdot C_R}{Q_F \cdot C_F} \quad (\text{Eq. 3.9})$$

where:

Rec: Recovery of ionic liquid (total) (-)

and can be also expressed in terms of the performance parameters:

$$\text{Rec} = R \cdot \frac{V_P}{V_F} - (CF - 1) \cdot \left(1 - \frac{V_P}{V_F}\right) \quad (\text{Eq. 3.10})$$

As it was already mentioned, water solubility values can not be considered to decide which ionic liquid should be used, because of their similarity; but it is known that the ionic liquid containing the IM16 cation exhibits higher toxicity than that containing the Pyr16 cation, for all the toxicity tests comprising the UFT test battery [29].

According to this information, the more suitable pair ionic liquid – membrane corresponds to the combination Pyr16 (CF₃SO₂)₂N and NF-270, which is in good agreement with the tendencies predicted in Section 2.5 (Chapter 2). As a consequence, this pair ionic liquid - membrane was employed to perform concentration experiments in a bigger scale using a cross-flow filtration equipment.

Finally, independent measurements of cation and anion for different samples were also carried out by ion chromatography (Table 3.2).

Table 3.2: Comparison of analytical results by the determination of Pyr16 (CF₃SO₂)₂N for different samples.

Sample	Concentration of ionic liquid, C (g/L)		Relation Anion/Cation
	By measuring anion	By measuring cation	
Feed	2.046 ± 0.001	2.037 ± 0.001	1.004
Permeate 1	0.123 ± 0.001	0.124 ± 0.001	0.991
Permeate 2	0.154 ± 0.001	0.152 ± 0.001	1.013
Permeate 3	0.167 ± 0.001	0.168 ± 0.001	0.994
Retentate	2.239 ± 0.001	2.203 ± 0.001	1.016

No matter which specie was determined, both concentrations are almost the same. With this experience, not only was possible to verify that no ion exchange occurs during the filtration process (the risk was minimized using ultra pure water), but also it was possible to simplify the analytic work (due the time and costs involved), determining the concentrations of only one of the two charged species.

From Table 3.2 and assuming that the concentration of ionic liquid in retentate is equal to the water solubility of ionic liquid, it is also possible to conclude that the solubility value for Pyr16 (CF₃SO₂)₂N is around 2.2 g/L, equivalent to a molar fraction (x_F) of 0.88×10^{-4} . This value could not be compared with values in the literature, but it is in good agreement with those solubility values already published for Pyr13 (CF₃SO₂)₂N and Pyr14 (CF₃SO₂)₂N, which are 4.36×10^{-4} and 2.38×10^{-4} respectively [30].

3.4 CONCENTRATION OF PYR16 (CF₃SO₂)₂N

The progress of the concentration process for a model solution containing the Pyr16 (CF₃SO₂)₂N ionic liquid is shown (Figure 3.16). The curve shows the variation of the concentration factor and the permeate flux with the process recovery rate. The variation of the concentration factor was calculated according to Eq. 3.7 and it represents the theoretical progress of the retentate concentration without phase separation.

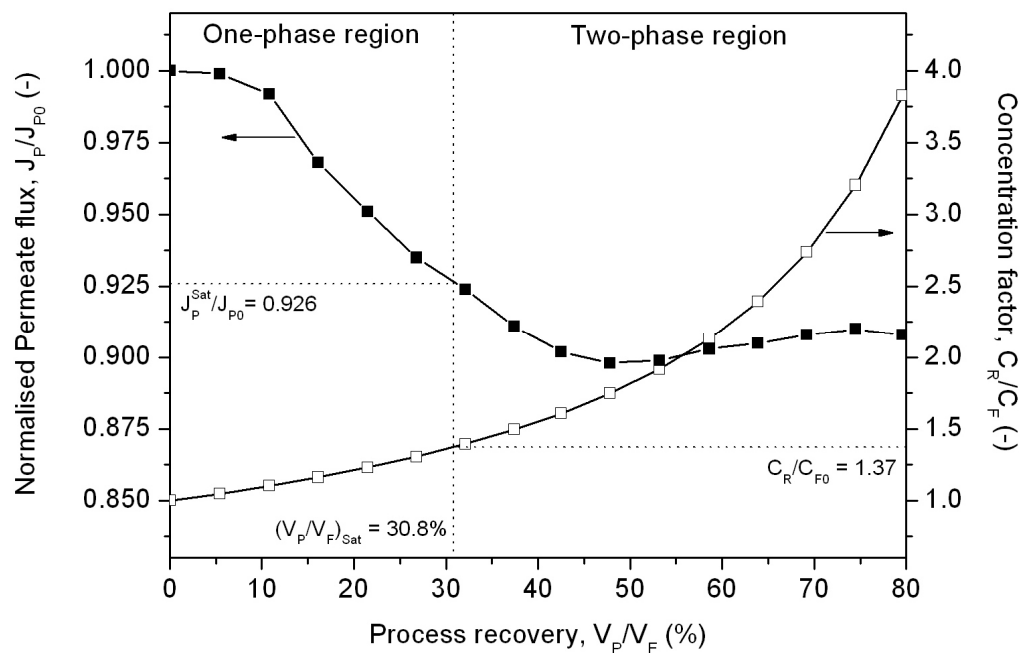


Figure 3.16: Concentration process at 25°C for an aqueous solution of Pyr16 (CF₃SO₂)₂N with 27% initial undersaturation.

The feed solution exhibited 27% of undersaturation, which means that the starting concentration (around 1.60 g/L) represents only the 73% of the saturation concentration for an aqueous solution of this ionic liquid at 25°C (around 2.20 g/L). However, the coexistence of two phases is theoretically possible from the very beginning, but at this point it is important to distinguish between the local and the global formation of a second phase.

The local formation of a second phase occurs at the surface of the membrane due to concentration polarization effects if the concentration near the membrane surface exceeds the solubility limit, but in the presence of flow and undersaturation of the whole solution the dissolution of the ionic liquid should take place again. Only when the whole solution is saturated, the second phase can not dissolve anymore and remains unalterable in the system. In this case, the global formation of a second phase is achieved.

The point where the global formation of a second phase begins, denoted as $(V_P/V_F)_{\text{Sat}}$ in this work, can be identified with the help of the retentate concentration, considering that the retentate stream consists of a solution at the saturation point plus the ionic liquid forming the second phase. Using this information, it is possible to identify in Figure 3.16 that the global formation of a second phase occurs when a process recovery value of 30.8% is achieved. That means that only one phase “exists” below this value (the second phase locally formed has a short existence before diluting again), while two phases may coexist above this value as long as no thermodynamically supersaturation occurs.

While during concentration process in the one-phase region a clear feed solution was observed in the feed collector tank, the liquid becomes cloudier as the concentration process proceeds. This indicates that the second phase formed remains dispersed due to agitation caused by continuous flow. The higher the process recovery, cloudier the liquid in the feed tank becomes (Figure 3.17a-d). After collecting 80% of the original feed as permeate, a very cloudy retentate volume was obtained, that after sedimentation at room temperature (2 days) became clear and many droplets of ionic liquid could be observed at the bottom of the bottle (Figure 3.17e).

Further evidence for the dissolution of the second phase locally formed is the diminution of the permeate flux observed in the one-phase region, as it is shown in Figure 3.16. This behaviour can be associated with the typical reduction of permeate flux with increasing feed concentration.

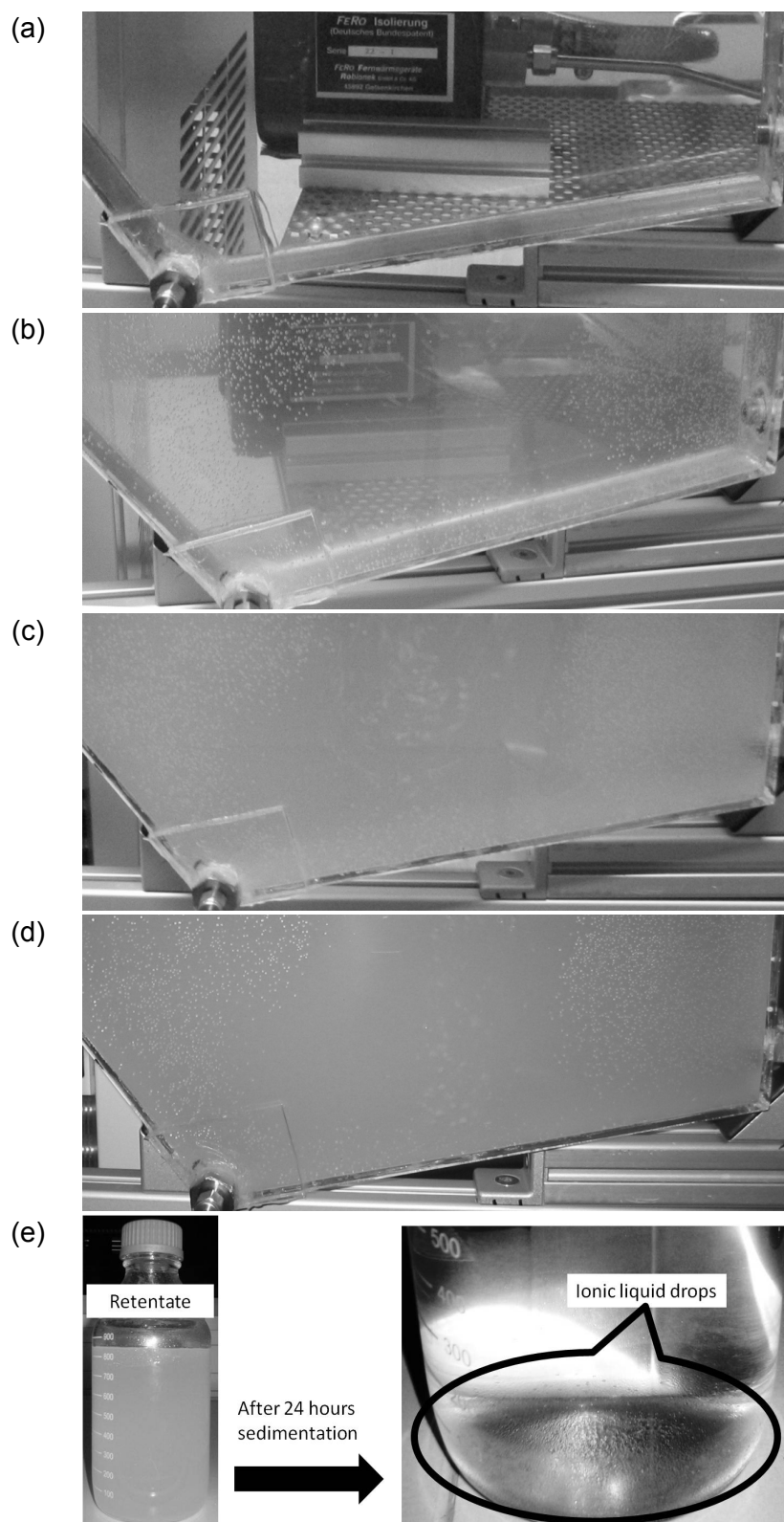


Figure 3.17: Changes observed in the feed tank during the concentration process: (a) $V_P/V_F = 0\%$, (b) $V_P/V_F = 40\%$, (c) $V_P/V_F = 50\%$, (d) $V_P/V_F = 60\%$, (e) second phase formed after sedimentation of collected retentate.

At the frontier between the one-phase and the two-phase regions, it is possible to determine the permeate flux at the saturation point. This value is necessary for a further treatment of the experimental data; because it represents the initial permeate flux for concentration process from a saturated feed solution. In this case, for process recovery values higher than 30.8%, permeate flux behaves differently, which can be associated with a constant feed concentration (equal to the solubility value at 25°C), but also with increasing formation of the second phase. This last point is going to be discussed in detail in the following paragraphs.

As it was mentioned above, the identification of the permeate flux at the saturation point is important, because it represents a common point if different concentration experiments need to be compared (Figure 3.18). In this case, the saturation point represents a process recovery rate of 0%, while negative process recovery values are associated to the concentration process between the starting feed concentration (lower than saturation) and the saturation concentration. Then, to reach such a concentration, permeate should be added to the feed volume at saturation point (instead of removed), explaining the negative values reported.

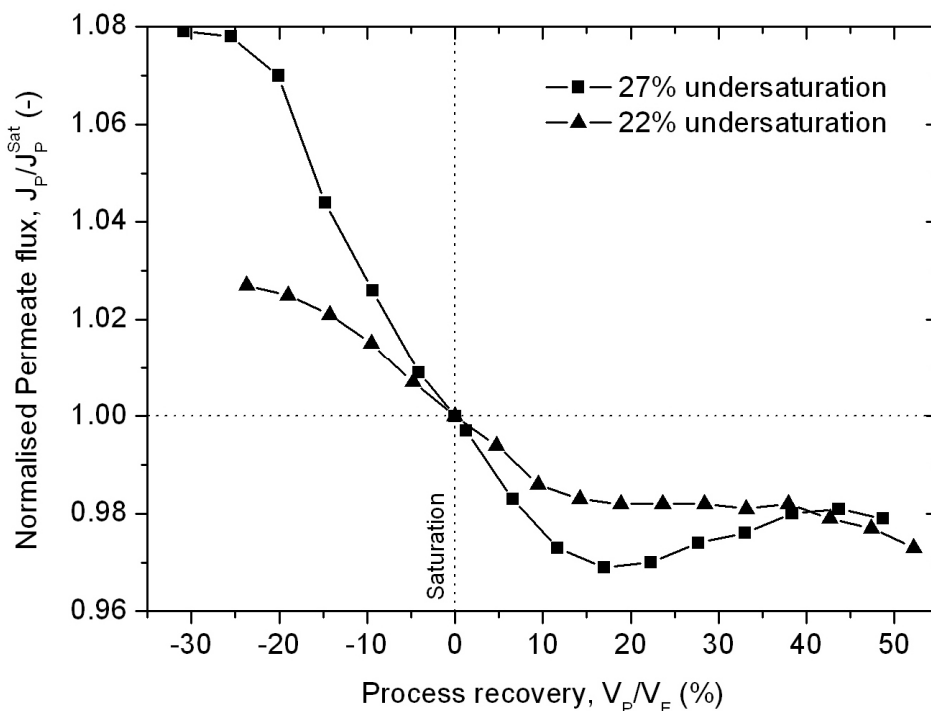


Figure 3.18: Concentration process at 25°C for aqueous solutions of Pyr16 (CF₃SO₂)₂N with different initial undersaturation degrees.

In Figure 3.18, it is possible to observe the progress of two concentration experiments with different initial concentrations (1.60 and 1.76 g/L), both under the saturation value (27 and 22% undersaturation, respectively). The differences in the one-phase region (negative process recovery values) and the similarities in the two-phase region (positive process recovery values) can be explained in terms of the progress of the concentration factor (see Figure 3.6) and in terms of the formation of the second phase of ionic liquid by the nucleation and grow mechanism.

At the beginning of every concentration process, the concentration in the feed tank increases very slowly and a slight reduction of the permeate flux can be observed. From this point and until the saturation point, a pronounced decrease in the permeate flux is associated with pronounced changes in the concentration.

A possible explanation could consider that the viscosity of the mixture water-ionic liquid increases with increasing concentration of ionic liquid, leading to a higher resistance for the flow of permeate through the membrane. Unfortunately, there is no available data about the viscosity of the pure Pyr16 (CF₃SO₂)₂N ionic liquid [31,32] or the viscosity of its mixtures with water [32,33].

However, it was possible to estimate a viscosity value of 108±8 mPa.s for Pyr16 (CF₃SO₂)₂N at 25°C, using a group contribution method for viscosity estimation of ionic liquids recently published [34] and the density of the pure ionic liquid [35]. This value is in agreement with the values found in the literature for Pyr14 (CF₃SO₂)₂N and Pyr18 (CF₃SO₂)₂N at 25°C, which are 76 and 150 mPa.s, respectively [36-38]. With this information, it was possible to estimate either the viscosity for the binary mixture in the one-phase region (as solution) or in the two-phase region (as emulsion), using some predicting equations published in the literature [39-41]. These results are condensed in Table 3.3.

Although the concentration of ionic liquid can increase considerably during the concentration process (almost four times), the mixtures can be always considered as diluted, due to the elevated hydrophobicity of the ionic liquid. Then, the viscosity of the mixture, no matter how many phases are present in the system, remains similar to the viscosity of water at 25°C. At this point, it is possible to neglect viscosity effects as responsible for the reduction of the permeate flux.

Table 3.3: Estimation of the viscosity for a mixture water – ionic liquid at different concentrations.

Concentration of ionic liquid in feed		Viscosity of the mixture, μ (mPa.s)	
C_F (g/L)	x_F (mol/mol)	One-phase region	Two-phase region
0	0	0.900	---
1.60	6.42×10^{-5}	0.900 - 0.907	---
1.76	7.06×10^{-5}	0.900 - 0.908	---
2.20	8.83×10^{-5}	0.900 - 0.909	---
4.00	1.60×10^{-4}	---	0.907
6.00	2.41×10^{-4}	---	0.910

Nevertheless, it should be considered that the closer the feed concentration to the saturation limit, the higher the local formation of second phase. That means, that the drops of second phase formed locally at the membrane surface should provide a further resistance to the flow of permeate through the membrane. Additionally, under these conditions, their dissolution inside the module is more difficult, due to the reduced concentration gradient between the surface and the bulk stream, leading to the behaviour observed in the two-phase region.

In this region, both curves start at the same point due to the data treatment using the permeate flux at saturation but they show different trajectories, which are related to the previous formation of the second phase at the membrane surface. The drops locally formed in the case of the solution with higher initial concentration have fewer possibilities to dissolve immediately and to leave the module, due to the reduced concentration gradient and the high cross-flow velocity inside the module (0.5 m/s).

As consequence, the emulsion appears earlier than in the case in which the drops can be dissolved again. This previous drop-history show still influence even if the whole system has reached the solubility limit, and can be observed in Figure 3.18 for recovery rates between 0 and 20%. After that, the drops continues growing and new drops appear, but at the same time the volume of liquid in the system reduces continuously due to the removal of permeate.

For higher recovery rates (more than 20% in Figure 3.18, representing more than 50% in Figure 3.16) the level of liquid in the feed tank has descended considerably and the mixing effects inside the tank due to the returning streams (retentate and by-pass) become more and more important. In this case, no matter how the emulsion was previously formed, it is strongly mixed and the effects on permeate flux are almost the same, leading to a similar progress for both curves.

Even though the tendencies already shown have been represented using normalized parameters to make possible the comparison between different experiments, the heterogeneity of the membrane sheets used should play a role due to the small membrane surface employed (only 270 cm²). In Table 3.4 are summarized the absolute values of concentrations and permeate flux obtained for both concentration experiments.

Table 3.4: Performance parameters associated to the concentration experiments with Pyr16 (CF₃SO₂)₂N.

Percentage of undersaturation		27%	22%
Feed concentration C_F (g/L)	Initial, C_{F0}	1.60	1.76
	At saturation, C_F^{Sat}	2.20	2.24
Permeate Flux, J_P (L/m ² h)	Initial, J_{P0}	169	202
	At saturation, J_P^{Sat}	156	197
Mean Retention, R (%)	One-phase region	91.4	88.8
	Two-phase region	93.0	92.4

The saturation concentration for both experiments is practically the same, considering the errors associated with the preparation and analysis of the sample by chromatography. The permeate flux exhibit values between 150 and 200 L/m²h, which represents less than 50% of the permeate flux obtained with pure water at 25°C and a pressure difference of 35 bar [42-44], but exhibit the same order of magnitude that those observed during the membrane screening experiments.

A final point to be discussed in this section is the behaviour of the mean retention. The retention decreases with increasing feed concentration, and

the higher the initial feed concentration, the lower the retention obtained for the one-phase region. However, the retention values for the two-phase region are almost the same, indicating that in this case, the feed concentration remains constant and equal to the saturation value.

Owing to this high retention it was possible to concentrate the ionic liquid beyond its solubility value, thus promoting the formation of a second phase of hydrophobic ionic liquid in form of an unstable emulsion. However, an open question still remains: how much of this ionic liquid can be really recovered for practical purposes? A first approach to the answer will be presented in the next section.

3.5 RECOVERY OF PYR16 (CF₃SO₂)₂N

As it was already mentioned, during the concentration process an unstable emulsion is formed. Moreover, after removing the retentate stream and proceed to clean the equipment with about 4 L pure water, it was found that the rinsing water contained an elevated concentration of ionic liquid, around 1.40–1.50 g/L. This finding indicates that emulsified ionic liquid is coalescing and thus collecting inside the filtration equipment; especially at the pump, because it represents the deepest point of the system.

In order to reduce this undesired effect a coalescence filter (Figure 3.19), was installed between the outlet of the second filtration module and the feed tank. This should facilitate the coalescence of the drops as soon as they are formed inside the modules and to collect them at the feed tank, after decantation.

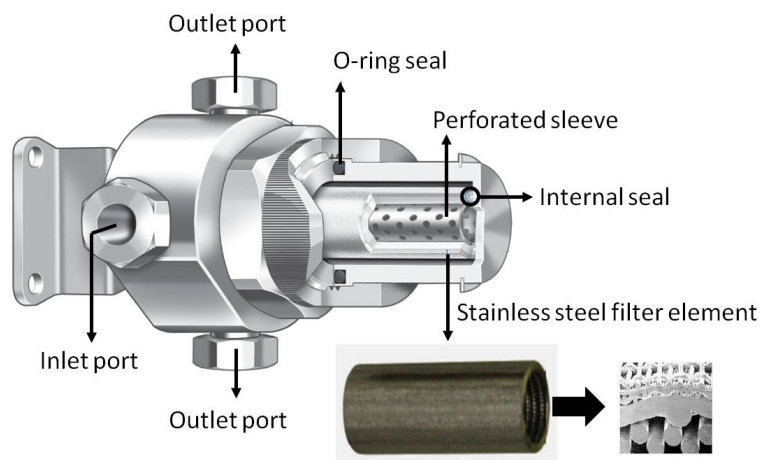


Figure 3.19: Coalescence filter employed.

First of all, a different behaviour inside the feed tank during the concentration experiment was observed, compared to the results obtained without using the coalescence filter. At the end of the experiment it was possible to observe a lot of drops, even some big drops, at the surface of the remaining liquid in the feed tank (Figure 3.20). Those drops could be collected with the retentate stream, leading to a higher recovery of ionic liquid.

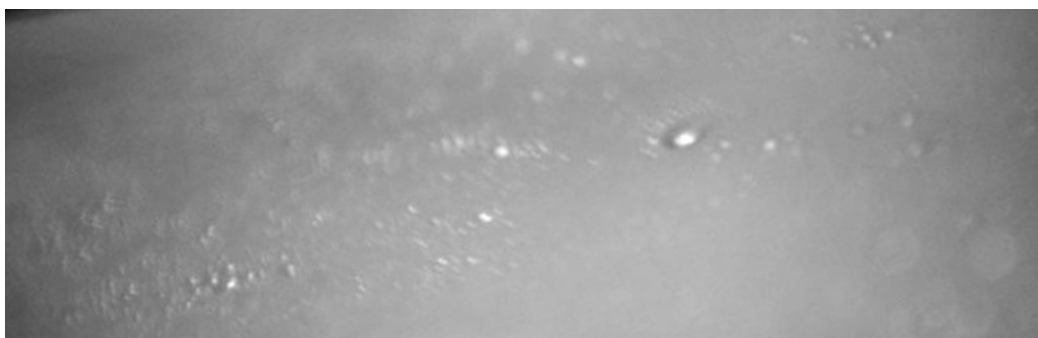


Figure 3.20: Second phase observed at the surface of the retentate at the end of the experiment.

However, more information about the formation of second phase can be collected if the recovery experiment is compared with one of the concentration experiments already shown. In Figure 3.21 both experiments are represented, starting at the saturation point.

When the coalescence filter was not used, no emulsion was observed at a recovery rate of 0%; while two different zones were appreciated with the coalescence filter (even so for negative recovery rates). The upper zone was cloudy and corresponds to the emulsion of ionic liquid, while the lower one was clear and corresponds to a saturated solution of ionic liquid. This result confirms the local formation of a second phase inside the filtration modules, and due to the presence of the coalescence filter, the drops are helped during their growing process.

This behaviour was observed until a recovery rate around 20%. After that the emulsion was occupying the whole tank in both cases, but it was cloudier as when the coalescence filter was used. Again, a cloudier emulsion can be associated with the presence of bigger drops, indicating that the coalescence filter is serving its purpose.

The installation of the coalescence filter had also an effect on the variation of the permeate flux, as can be observed in Figure 3.22.

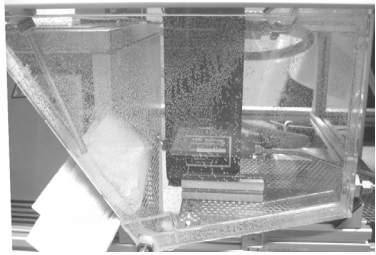
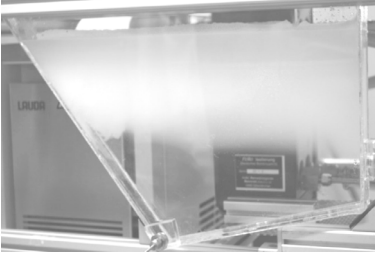
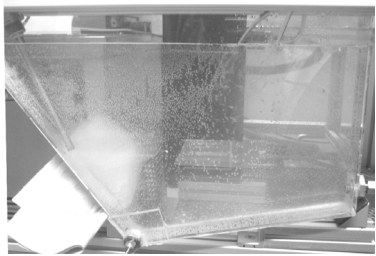
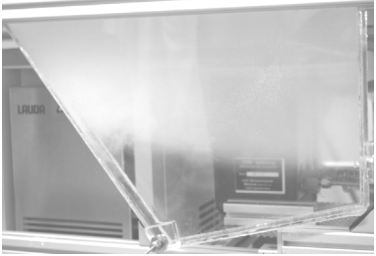
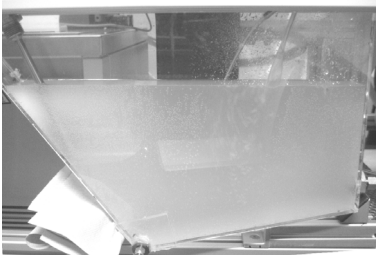


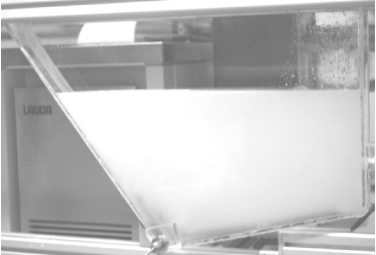




Process recovery, V_P/V_F (%)	Coalescence filter	
	Without	With
0		
10		
20		
30		
40		
50		

Figure 3.21: Comparison of the changes observed in the feed tank during the concentration process when a coalescence filter is used.

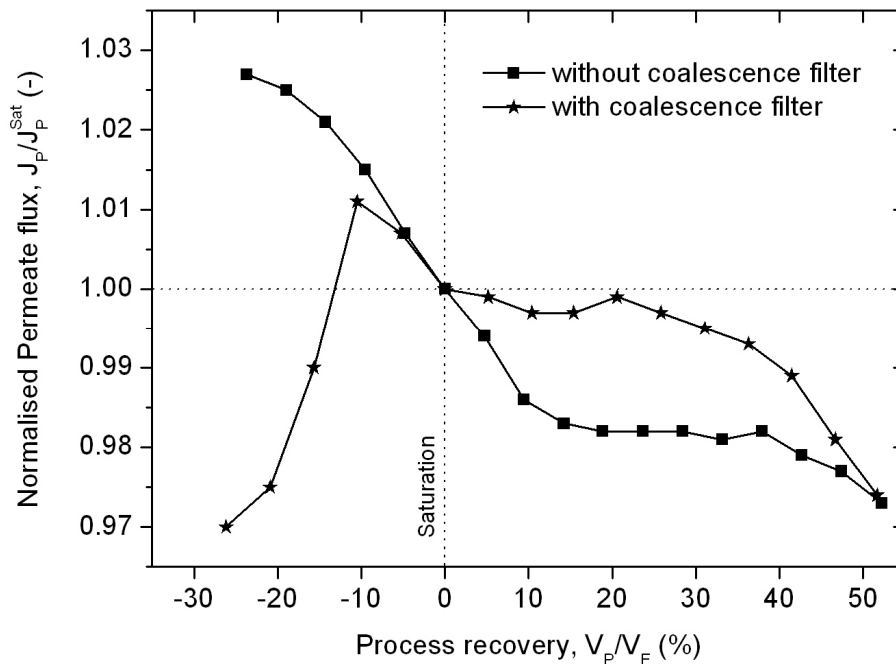


Figure 3.22: Comparison of the concentration process at 25°C for aqueous solutions of Pyr16 (CF₃SO₂)₂N when a coalescence filter is used.

In the one-phase region, the coalescence of the drops leads to an improvement of the permeate flux, which can be explained in terms of the two zones observed in Figure 3.21 (cloudy upper zone, clear lower zone). That means that the drops locally formed coalesce and remain on the top of the feed tank, while an undersaturated solution is fed again to the modules. Near the saturation point, this effect loses its importance, because the lower region is also reaching the saturation concentration.

In the two-phase region the effective coalescence of the drops as well as the presence of the two zones in the feed tank contribute to maintain the permeate flux similar than the permeate flux value at saturation, until a recovery rate of 20%. At this point, the emulsion occupies the whole tank at their effects in the permeate flux began to appear, but less pronounced than those observed when no coalescence filter is installed. Finally, for higher process recovery rates, the mixing effects due to low liquid level are similar for both cases.

The more effective drop size growing reduces not only the additional resistance to the permeating flow across the membrane, but also improves the retention values for the whole process (Table 3.5). In this case, the retention for the one-phase region is almost the same as the retention for

the two-phase region, indicating that the feed flowing across the modules exhibits similar characteristics in every moment.

Furthermore, the retention values are also higher than those obtained without using the coalescence filter. It can be explained in terms of a reduced accumulation of small drops on the membrane surface. They are forced to coalesce and stay at the feed tank before the solution is pumped again for a further filtration step.

Table 3.5: Performance parameters associated to the recovery experiments with Pyr16 (CF₃SO₂)₂N.

Coalescence filter		Without	With
Mean Retention, R (%)	One-phase region	88.8	93.8
	Two-phase region	92.4	94.8
Permeate Flux, J _P (L/m ² h)	Initial, J _{P0}	202	181
	At saturation, J _P ^{Sat}	197	186
Recovery, (%)	Total, Rec	66.4	68.6
	Effective at lab scale, Rec-eff-lab	15.1	33.4

The permeate fluxes are similar to those presented in Table 3.4, and the absolute differences between them are associated with the fact that different membrane sheets were employed. Such stochastic differences in permeate fluxes can be only minimized with large membrane surfaces, where membrane structure heterogeneity effects are reduced.

The last point in this section is related with the amount of ionic liquid which can be practically recovered as second phase. The mass balance, represented by Eq. 3.9, allows the determination of the amount of ionic liquid formed as second phase with respect to the ionic liquid original dissolved in feed. This recovery rate of ionic liquid is denominated total recovery. It exhibits values between 66 and 69% (Table 3.5), very similar to those obtained during the experiments in the dead-end filtration equipment (72%). Theoretically, once the membrane, the operational conditions and the extent of concentration (V_P/V_F) are selected, the total

recovery can be considered as a fixed value, and in consequence, it represents the maximal recovery rate possible.

However, as it was pointed out at the beginning of this section, after having rinsed the filtration equipment with water, large amounts of ionic liquid were determined in the rinsing water. That means, that the recovery of ionic liquid is not complete, and a new term should be introduced.

In this work, it was denominated effective recovery at lab scale. It represents the amount of ionic liquid as second phase formed that is not dissolved by the rinsing water and it can be recovered with the retentate stream. It can be also calculated using a material balance, similar to that shown in Eq. 3.9, but including the amount of ionic liquid from rinsing, as follows:

$$\text{Rec - eff - lab} = \frac{Q_F \cdot C_F - Q_P \cdot C_P - Q_R \cdot C_R - Q_{RW} \cdot C_{RW}}{Q_F \cdot C_F} \quad (\text{Eq. 3.11})$$

where:

Rec-eff-lab: Effective recovery of ionic liquid at lab scale (-)

Q_{RW} : Volume of rinsing water (L)

C_{RW} : Concentration of ionic liquid in rinsing water (g/L)

Comparing the values of effective recovery at lab scale for both experiments (Table 3.5), it is evident that the use of a coalescence filter improves the recovery of ionic liquid due to an effective coalescence of the drops after their formation.

3.6 APPROACHES TO IMPROVE IL-RECOVERY

It was already demonstrated that the recovery of hydrophobic ionic liquids by nanofiltration is possible. Additionally, if more understanding is first gained for the recovery of ionic liquids from aqueous solutions (the simplest binary system which can be studied), then it would be easier later to find properly solutions for the problems associated with the recovery of such ionic liquids from industrial wastewaters.

In this context, considering a total recovery rate of 70% as acceptable, the first challenge is in connection with the increase of the effective recovery rate in order to reach a value as close as possible to the total recovery rate. Once this aim is achieved, another challenge for further improvement deals with increasing the total recovery rate.

To increase the effective recovery rate, the following approaches might be useful:

- **Heterogeneous nucleation:** The formation of a new phase requires the formation of a nucleus from the old phase. Inhomogeneities in structure or composition play a role in catalyzing nucleation, which is then termed heterogeneous [20,45]. For example, seeding with pure ionic liquid could be an option, following the same principle of crystallization. On the other hand, any surface represents an important heterogeneity for nucleation as it was demonstrated by the use of a coalescence filter, which promotes both nucleation and growth of droplets of the new phase. Then, the supersaturated solution should be forced to nucleate and grow to a large extent before being collected and separated.
- **Second phase separation:** Methods for separation of liquid-liquid dispersions are well known: simple and enhanced gravity settling and coalescing [46]. The use of centrifugal force, electrocoalescence or membrane processes (MF, UF, NF or PV) can be also considered [47-52]. However, the choice should consider not only the effectiveness of the separation process itself, but also their incorporation into the actual equipment. That means it should not affect the actual operating concept or the equipment configuration. For instance, the use of a lamellar separator which also acts as a feed tank is in agreement with both conditions and could be used as a first test.
- **Equipment modifications:** Dead zones inside the equipment are ideal places for the second phase formed. Additionally, materials compatible with the ionic liquid should be used in order to reduce chemical attack of some of the equipment components, like seals. Due to these reasons, in the actual equipment the further use of a piston pump should be evaluated.

On the other hand, to increase the total recovery rate, some approaches would be considered:

- **Operation mode:** Contrary to the batch mode actually employed, in the modified batch an equal volume of fresh feed is added to the process tank to keep it at the same level as permeate is removed. In this case, the extent of concentration can be higher than those obtained in a simple batch mode of operation. Additionally, the mixing

effects due to low level can be completely avoided, but it requires working with larger amounts of feed.

- **Operational conditions:** It is believed that the profit by changing the operational conditions is marginal, but also possible. The pressure difference used (35 bar) is high enough to assure high permeate flux without risking to damage the membrane by exceeding the maximal pressure difference recommended (41 bar). Changes in temperature should be carefully considered, because it affects simultaneously retention and permeate flux, but also water solubility of the ionic liquid. An optimal cross-flow velocity could be found, for which the local formation of second phase is improved but without leading to settling of ionic liquid inside the modules. Finally, retention improvements by changing the feed pH should be avoided, due to potential ion exchange and lost of identity of the ionic liquid.
- **More selective membranes:** Theoretically, it would be possible to design a membrane which provide the best combination of retention and permeate flux for a given ionic liquid. Unfortunately, as it was pointed out in Chapter 2, the knowledge about membrane structure and membrane formation is limited and in most of the cases, manufacturer secrets are involved. Without closer cooperation between membrane producers and users, the traditional trial and error approach for membrane screening has to be used.

3.7 TWO CASE STUDIES WITH REAL WASTEWATERS

By recovering ionic liquids from wastewater, the water solubility of the ionic liquid plays an important role in the definition of the recovery scheme. Both ions have influence on the water solubility of the resulting ionic liquid and the choice of anion has been used to the greatest effect on controlling hydrophobicity. However, cations can be also used to increase the hydrophobicity of ionic liquids, especially when the head group is substituted with long alkyl side chains (>C8) [53]. Furthermore, water-ion interactions due to size and surface charge of both ions determine the solubility of ionic liquids in water [54].

In this section, first experiments to recover ionic liquids by nanofiltration have been carried out with wastewaters selected from applications which are expected to reach industrial scale in the upcoming years:

- Wastewater containing *hydrophobic ionic liquids*, like IM16 (CF₃SO₂)₂N, Pyr14 (CF₃SO₂)₂N and Pyr16 (CF₃SO₂)₂N; which are

used as second phase during the asymmetrical synthesis of chiral alcohols, and,

- Wastewater containing *hydrophilic ionic liquids*, like IM14 Cl and IM14 1COO; which are used for the dissolution and regeneration of cellulose.

3.7.1 Biocatalytic production of chiral alcohols

a) Description of the application:

The term biocatalysis or biotransformation is used for processes in which a starting material is converted into the desired product in just one step. This can be done by using either enzymes or whole cells [55].

The use of enzymes is advantageous because an undesirable by-product formation is avoided. However, extraction and purification of the enzyme is expensive and the stability could be lower than in crude preparation or when present in whole cells. On the other hand, despite whole cell biotransformations can manifest problems related to undesirable by-product formation due to the presence of other enzymes, these systems are especially advantageous when enzyme cofactors participate in the reaction and need to be regenerated [56].

In the case of low water solubility or high toxicity of substrate and/or product a biphasic process design is often applied, in which an additional organic solvent functions as a substrate reservoir, as well as an in situ-extractant [57]. Ionic liquids can be used to replace volatile organic solvents and their unconventional properties have extended the solvent range for biocatalysis: hydrophilic ionic liquids can be used as a co-solvent in aqueous systems, while hydrophobic ionic liquids can be used as pure solvents or in two-phase systems. Additionally, performing biocatalytic conversions in ionic liquids can be beneficial with regard to activity, selectivity and stability [58-60].

Optical active secondary alcohols are widely used as intermediates for the introduction of chiral information into products of the chemical and pharmaceutical industry. In particular, the number of industrial processes using alcohol dehydrogenases (ADHs) as isolated enzymes or whole cells is increasing. These biocatalysts catalyze the asymmetric reduction of prochiral ketones with remarkable chemo-, regio- and stereoselectivity and normally are dependent on the nicotinamide cofactors NADH oder NADPH [61].

Several studies have demonstrated that a biphasic ionic liquid – water system can improve the asymmetric reduction of prochiral ketones, either using isolated enzymes [62,63] or whole cells [64-67]. Ionic liquids like IM14 (CF₃SO₂)₂N, IM16 (CF₃SO₂)₂N, Pyr14 (CF₃SO₂)₂N, and Pyr16 (CF₃SO₂)₂N have been already proved, exhibiting better space-time and chemical yields and improving the enantiomeric excess in comparison to conventional aqueous systems. A schema for the biocatalytic reduction of ketones to produce chiral alcohols in a biphasic system using ionic liquids is shown in Figure 3.23.

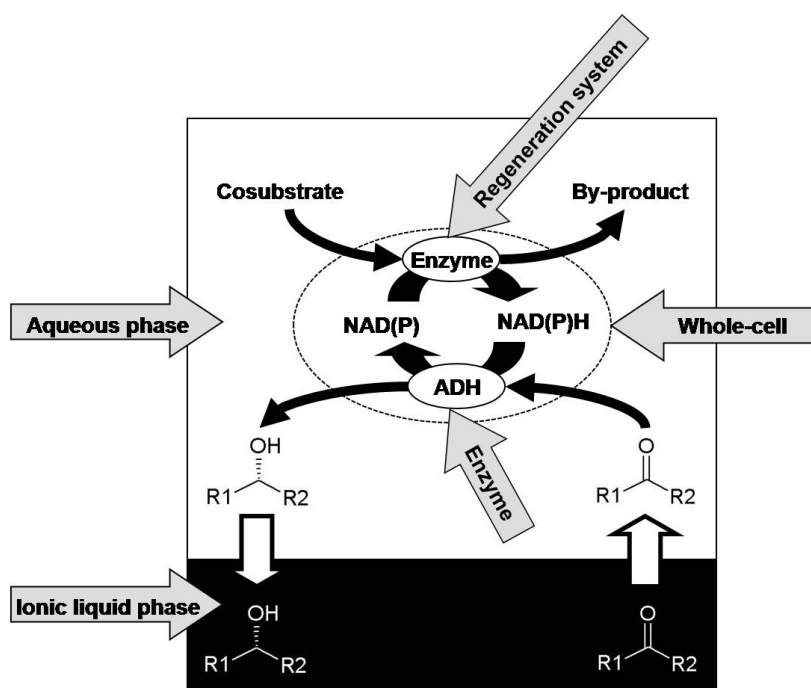


Figure 3.23: Reduction of ketone catalyzed by alcohol dehydrogenase with enzymatic cofactor regeneration. Adapted from [68].

The cofactor regeneration is carried out parallel to the conversion of substrate to product, and in the case of an enzymatic regeneration two different approaches are possible.

The enzyme-coupled approach uses an auxiliary cosubstrate that is converted by a second enzyme in the opposite redox direction. Some examples include the sodium formate oxidation by formate dehydrogenase (FDH) and the glucose oxidation by glucose dehydrogenase (GDH). The substrate-coupled approach applies only one enzyme for the production of the desired compound and the cofactor regeneration. For the production of chiral alcohols the auxiliary cosubstrate is in most cases 2-propanol, which is oxidized by the ADH to acetone as by-product. These regeneration

processes occur in the media if isolated enzymes are used, or inside the whole cells as a part of their metabolism [61,69].

For a given system of biocatalyst and substrate/product, the choice of the ionic liquid is crucial. The availability of the ionic liquid as well as its cost, stability, corrosive effects, biodegradability and eco(toxicological) data are important [65].

Furthermore, an important challenge is to use the unique solvent properties of ionic liquids to develop efficient methods for the separation of less volatile or non-volatile products and ionic liquid recycling, considering their stability over prolonged periods of time under reaction conditions [70,71].

b) Recovery of hydrophobic ionic liquids:

For such ionic liquids which are poor water soluble (< 5 g/L), the target is to concentrate the wastewater in order to promote the formation of a second phase of pure ionic liquid, as it is shown in Figure 3.24.

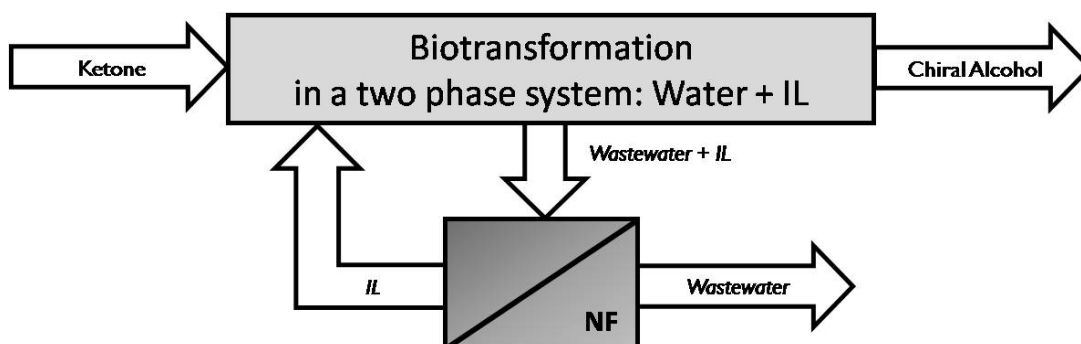


Figure 3.24: Recovery schema for hydrophobic ionic liquids.

Based on the results presented in Section 3.3, the membrane Desal DK was selected for the wastewaters from enzymatic biotransformations, while the membrane Filmtec NF-270 was selected for the wastewater from whole-cell biotransformation.

In all the cases, a pronounced reduction of the permeate flux during the concentration process was observed, as is reported in Figure 3.25.

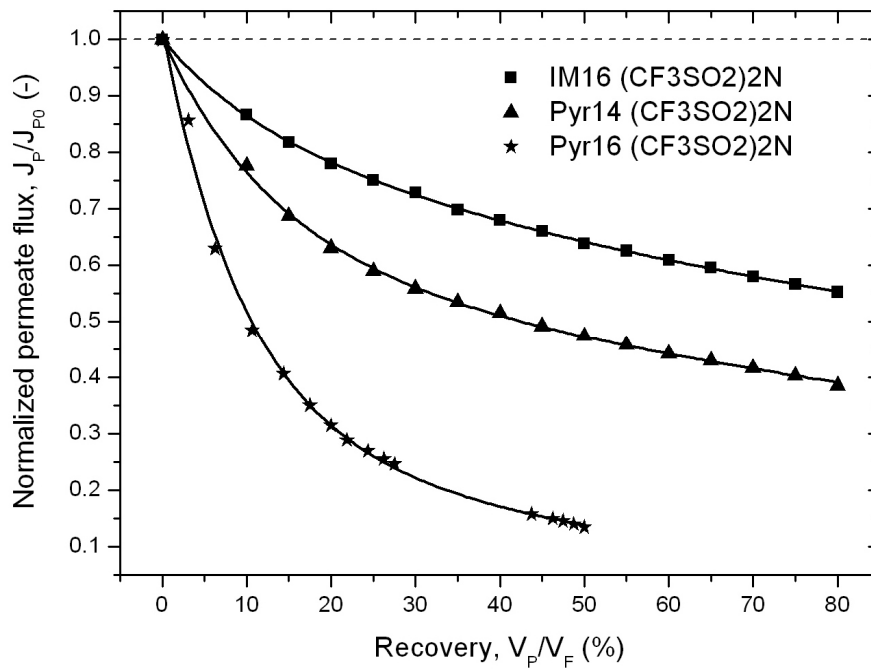


Figure 3.25: Variation of the normalized permeate flux with increasing recovery rate for several hydrophobic ionic liquids.

The more pronounced reduction of permeate flux was observed during the filtration of aqueous phase containing Pyr16 (CF_3SO_2)₂N, making the filtration process too slow: to obtain only 50% of the feed as permeate almost 28 hours were required. A less pronounced reduction of permeate flux was observed during the filtration of the aqueous phase from enzymatic biotransformations, which allowed to obtain 80% of the feed as permeate in a reasonable time (between 2 and 4 hours). The results obtained were summarized in Table 3.6.

Table 3.6: Performance of nanofiltration with hydrophobic ionic liquids in terms of permeate flux.

Ionic liquid		IM16 (CF_3SO_2) ₂ N	Pyr14 (CF_3SO_2) ₂ N	Pyr16 (CF_3SO_2) ₂ N
Recovery rate, V_P/V_F (%)		80	80	50
Permeate flux (L/m^2h)	Initial, J_{P0}	55	40	15
	Mean, J_{Pm}	30	16	2

It can be concluded that the presence of cellular material in wastewater from whole-cell biotransformations (although most of the cells were removed by centrifugation) contributes to the clogging of the membranes and should be removed before treatment. These materials reduce strongly both the permeate flux, compared to the wastewaters derived from enzymatic biotransformations. Despite these wastewaters could be considered cleaner than those derived from whole-cell biotransformations due to the absence of cellular material, the presence of other components in the mixture (2-octanol, 2-octanone, buffer and/or enzymes) has still an influence on the quantity of permeate obtained.

Theoretically, during the filtration process the concentration of ionic liquid in retentate goes beyond the solubility of the ionic liquid and the excess of ionic liquid must leave the solution as a second phase, leading to a more stable thermodynamically state. In the case of the wastewaters from enzymatic biotransformations, it was possible to observe in the retentate small drops of a second phase. However, in the case of Pyr16 (CF₃SO₂)₂N it was not possible to observe a second phase, presumably to the low process recovery rate achieved (only 50%).

To quantify the recovery of ionic liquid as second phase, the concentrations of ionic liquid in feed, retentate and permeate are required. The performance of the separation was determined for those wastewaters considered clean, as is presented in Table 3.7.

Table 3.7: Performance of nanofiltration with hydrophobic ionic liquids in terms of retention and recovery of ionic liquid.

Ionic liquid		IM16 (CF ₃ SO ₂) ₂ N	Pyr14 (CF ₃ SO ₂) ₂ N
Concentration (g/L)	Feed, C _F	1.82	4.74
	Retentate, C _R	1.82	9.64
	Permeate, C _P	0.67	2.50
Performance (%)	IL-Retention, R	63	50
	IL-Recovery, Rec	50	17

The best recovery was obtained for IM16 (CF₃SO₂)₂N, for which 50% of the ionic liquid originally dissolved in the wastewater can be forced to

produce a second phase. Though the retention is not high enough (63%), the concentration of retentate is the same than the concentration of feed. It means that the solubility level stayed inalterable during the concentration process and the formation of second phase was possible from the very beginning.

Other behaviour was observed for Pyr14 (CF₃SO₂)₂N, with a significantly lower recovery obtained of only 17%. This situation can be attributed to two different effects: the lost of ionic liquid in permeate (47% retention) and the apparent displacement of the solubility during concentration ($C_R/C_F = 2$). This last phenomenon can be imputable to the concentration of other components in solution, for example buffer phosphate salts.

On the other hand, an adsorption experiment was carried out with the industrial wastewater containing IM16 (CF₃SO₂)₂N at 23°C in order to compare the recovery of ionic liquid by nanofiltration with the removal with activated carbon, normally used as conventional treatment. The experimental data is presented in Figure 3.26, together with the corresponding Langmuir isotherm.

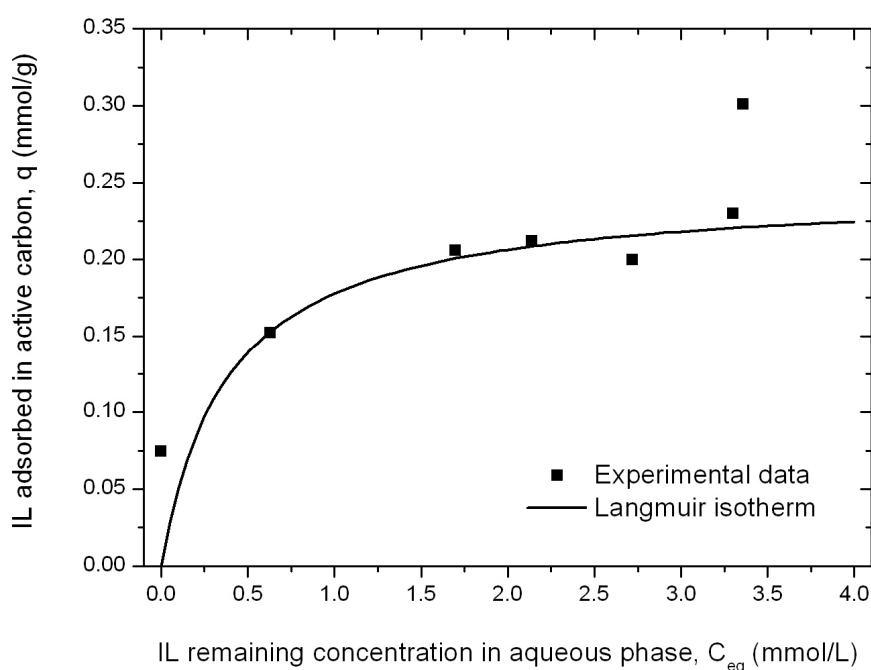


Figure 3.26: Adsorption of IM16 (CF₃SO₂)₂N from wastewater on active carbon.

The differences at higher concentrations are an indication of multilayer adsorption. This mechanism was already described for the adsorption of ionic liquids on natural soils [72], but not observed before on activated

carbon, despite similar results for concentrations below 3 mmol/L have been already published for other ionic liquids [73].

Treating the process wastewater to reach a final concentration of ionic liquid similar to that obtained in permeate by nanofiltration (0.67 g/L = 1.5 mmol/L), a concentration of activated carbon around 13 g/L is required, which could be consider too high. Furthermore, the possibilities to recover the ionic liquid from the activated carbon (desorption with acetone, for example) are not suitable for industrial application. However, adsorption with activated carbon can be used for a further reduction of the amount of ionic liquid in permeate and/or to treat the purge of the process before disposal.

Based on these results, a process for the recovery of hydrophobic ionic liquids is summarized in Figure 3.27. In order to improve the separation by nanofiltration, a previous filtration should be carried out. Microfiltration membranes are applied for the separation of whole cells, while ultrafiltration membranes have to be used to retain enzymes [74].

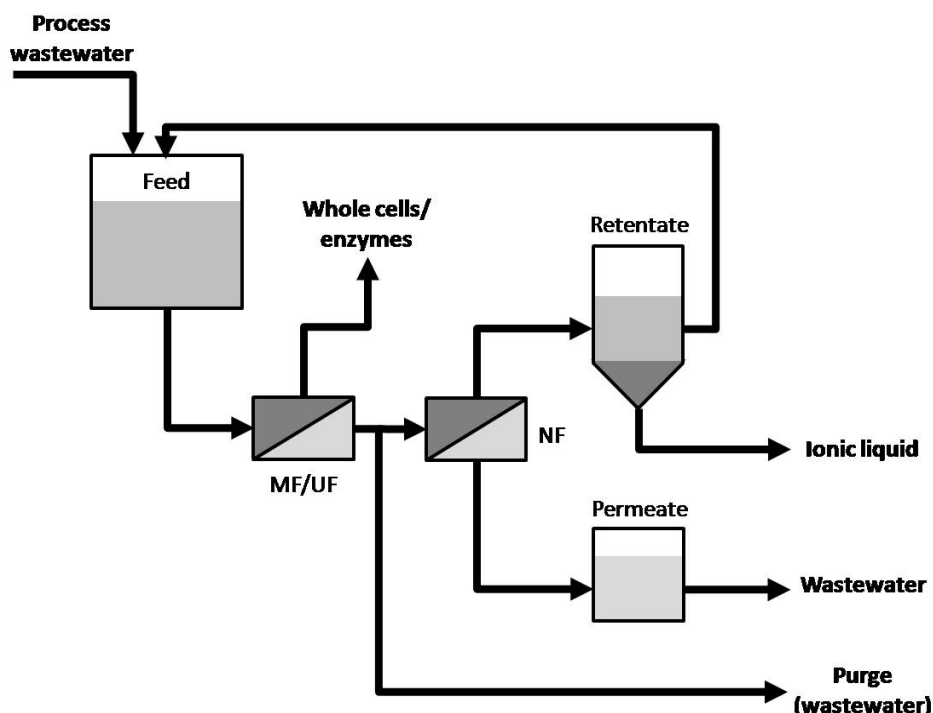


Figure 3.27: Process flow diagram for the recovery of IM16 (CF₃SO₂)₂N.

Due to the encouraging results obtained for IM16 (CF₃SO₂)₂N and the simplicity of the recovery operation, a cost-effectiveness analysis was performed. Considering a wastewater production around 25 L/kg 2-octanol

produced, a variety of scenarios for an alcohol production between 1 and 10 ton/year were studied.

The capital costs and operation and maintenance costs for the nanofiltration process were calculated using data recently published [75] and some other considerations (1€ = 1.2917\$, 5 years and 8%, 220 days/year), as follows:

$$C_{INV} = 14.32 \cdot Q^{0.774} \quad (\text{Eq. 3.12})$$

where:

C_{INV} : Nanofiltration capital cost (€/year)

Q : Amount of wastewater produced (L/day)

$$C_{O\&M} = 32.49 \cdot Q^{0.638} \quad (\text{Eq. 3.13})$$

where:

$C_{O\&M}$: Nanofiltration operation and maintenance cost (€/year)

$$C_{TOTAL} = C_{INV} + C_{O\&M} \quad (\text{Eq. 3.14})$$

where:

C_{TOTAL} : Nanofiltration total cost (€/year)

The total costs (Figure 3.28) were related with the amount of ionic liquid lost in wastewater (water solubility = 1.82 g/L), as follows:

$$W_{IL} = 0.04 \cdot Q \quad (\text{Eq. 3.15})$$

where:

W_{IL} : Amount of ionic liquid loss in wastewater (kg/year)

$$C_{NF-IL} = \frac{C_{TOTAL}}{W_{IL}} \quad (\text{Eq. 3.16})$$

where:

C_{NF-IL} : Nanofiltration recovery cost (€/kg)

According to Figure 3.28, the cost of the recovery by nanofiltration varies between 12 and 28 €/kg ionic liquid lost in wastewater, which compared with the actual high prices for ionic liquids, results very attractive for further research.

Furthermore, ionic liquids containing the (CF₃SO₂)₂N anion will be strongly restricted to only few applications, particularly those in which the ionic liquid is part of a closed loop. As consequence, nanofiltration appears to be not only an economical, also environmental, option for the recovery of ionic liquids.

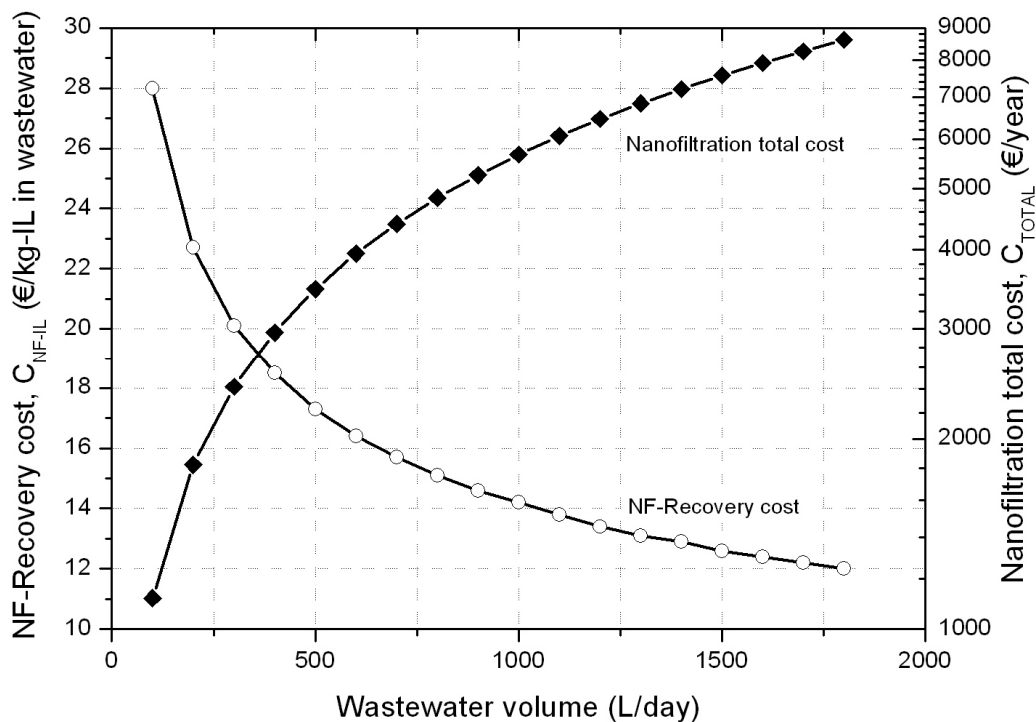


Figure 3.28: Cost-effectiveness analysis for the recovery of IM16 (CF₃SO₂)₂N from wastewater.

3.7.2 Dissolution and regeneration of cellulose

a) Description of the application:

Cellulose is a polysaccharide consisting of a linear chain of several hundred to over ten thousand $\beta(1\rightarrow4)$ linked D-glucose units. These polymer chains associate to each other through hydrogen bonds, resulting in the formation of microfibrils, which can interact to form fibres, as it is shown in Figure 3.29.

Dissolving a polymer like cellulose is a slow process that occurs in two stages. First, solvent molecules diffuse slowly into the polymer to produce a swollen gel. If the polymer-polymer intermolecular forces are high, the process may stop at this stage. However, if these forces can be overcome by strong polymer-solvent interactions, the second stage of solution can take place with a gradual disintegration of the gel into a true solution.

A useful classification of cellulose solvents identifies two types: derivatizing and non-derivatizing solvents. Derivatizing solvents refer to systems in which dissolution occurs in combination with the formation of

an unstable ester, ether or acetal derivative; one example is the carbon disulphide (CS₂)–aqueous sodium hydroxide system. Non-derivatizing solvents refer to systems dissolving cellulose only by intermolecular interaction, like in the case of the N-methylmorpholine-N-oxide (NMMO)–water system [77].

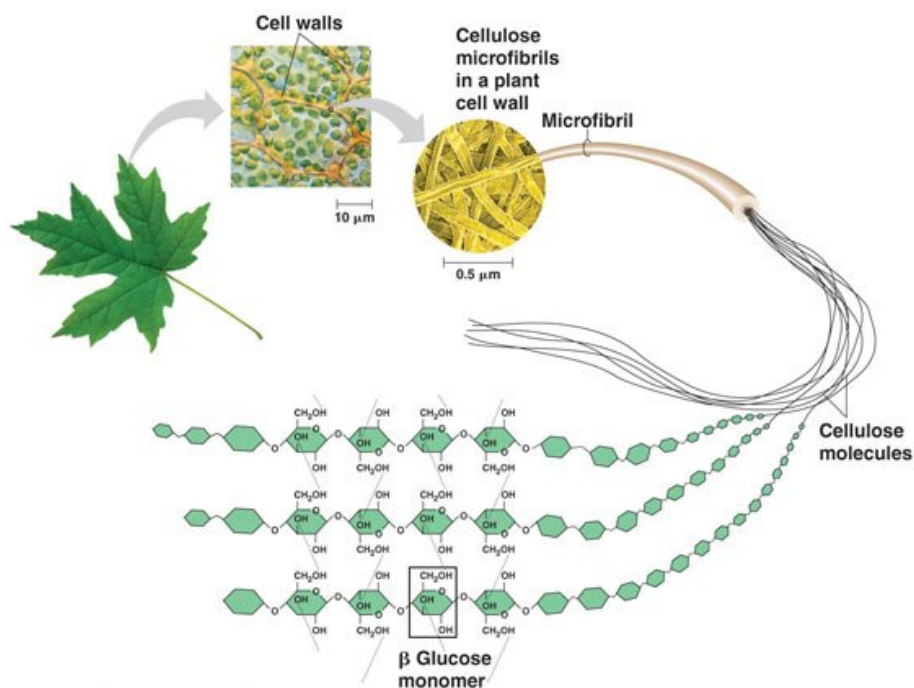


Figure 3.29: The arrangement of cellulose in plant cell walls [76].

Industrially, the CS₂–aqueous NaOH system has led to the viscose process. The proportion of the viscose process in the manufacture of cellulose products in relation to world production is still 95%, although this process has both ecological and economic drawbacks. One of the most important alternatives to the viscose process is the Lyocell process, commercialized at the beginning of the 90s and dealing with the NMMO–water system. Despite many advantages, the Lyocell process is not able to gain wide acceptance because it has problems in handling with the thermally unstable NMMO, but particularly with the fibre quality [78].

In 2002, Swatloski and co-workers showed that ionic liquids can be used as non-derivatizing solvents for cellulose. Cellulose can be dissolved in IM14 Cl and other hydrophilic ionic liquids, and can be regenerated from the solution by the addition of water, ethanol or acetone [79]. Recent studies have shown that cellulose dissolved in IM14 Cl is disordered, indicating that its hydrogen bonding network is disrupted. The proposed solvation mechanism involves the interaction of the chloride ions with the

hydroxyl protons of the carbohydrate, breaking the extensive hydrogen bonding network of the cellulose and promoting its dissolution [80,81].

These findings increased the interest in the regenerated cellulose industry in ionic liquids with respect to environmental issues and the single-component nature of the solvent system. A method for the production of cellulosic fibres and films from ionic liquids was described by the Thuringian Institute of Textile and Plastic Research (TITK) [82].

After cellulose dispersion in water, the moist cellulose is mixed with aqueous IM14 Cl solution. Stabilizers like sodium hydroxide and propyl gallate are added to prevent drastic degradation of the cellulose. Under shear strain, increased temperature and vacuum the suspension is transformed into a homogeneous, nearly water free solution. By passing through a spinneret and an air gap, the solution is shaped into fibres or foils. The cellulose is regenerated by precipitation in an aqueous spinning bath. To regenerate the solvent, the spinning bath is treated with alkaline hydrogen peroxide solution, metal ions are removed with the aid of an ion exchanger and the water is finally removed by evaporation.

Despite the interest of ionic liquids for cellulose fibre production is still growing, an industrial application of chloride ionic liquids for the production of man-made cellulosic fibres is not useful. Some drawbacks should be mentioned: no improvement of the fibre characteristics in comparison to already used technologies, corrosion caused by chloride containing ionic liquids, strong increase of viscosity with cellulose concentration, and degradation of the cellulose chain accompanying dissolution [77,83].

Some progresses have been achieved by the selection of the ionic liquids constituents [84]. The changing of the anion component from chloride to acetate results in a significant stronger difference in the solution state than the modification of the cation. Especially the ionic liquids IM14 Cl, IM12 Cl, IM14 1COO and IM12 1COO are suitable for the preparation of cellulose solutions in a concentration range exhibiting highly technical importance [85]. Additionally, ionic liquids containing the IM12 cation and alkylphosphate based anions have shown the potential to dissolve cellulose under mild conditions [86].

The fibres obtained by the dissolution of cellulose with ionic liquids are very similar to those fibres obtained by the Lyocell process, due to comparable dissolution step, the similar solution structure, and the same regeneration conditions. Actually, the regeneration of the ionic liquid is

more energy-consuming than in the Lyocell process, due to the required complete removal of water [83]. However, several methods can be used to recover the ionic liquid [87].

Additionally, it is expected that several side reactions that cause the formation of by-products in the system NMMO-celulose occurs with the use of ionic liquids too, especially those related with the formation of chromophores, degradation of cellulose and increased consumption of stabilizers [88,89]. As consequence, further research is necessary to optimize the recycling process and to keep track of by-product formation and accumulation of impurities during the process [78].

b) Recovery of hydrophilic ionic liquids:

Ionic liquids used for this application are highly water soluble (> 1000 g/L). Then, the target of the recovery scheme by nanofiltration is to obtain the ionic liquid solution free from dissolution stabilizers and by-products, and return it again into the process, as it is shown in Figure 3.30.

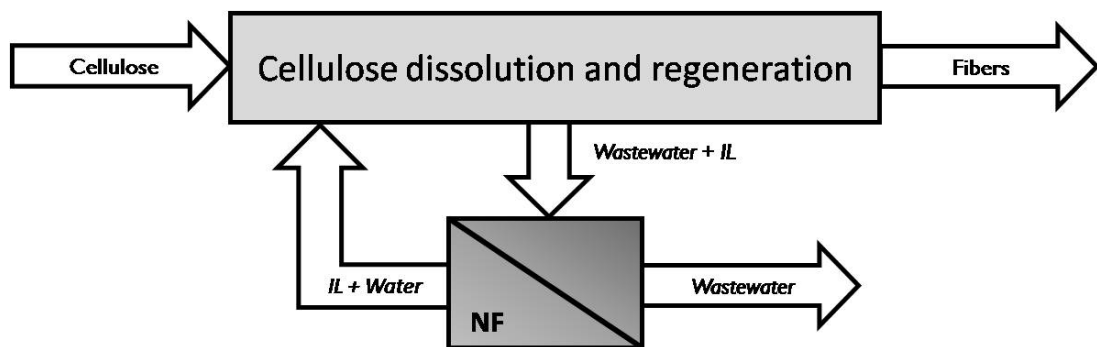


Figure 3.30: Recovery schema for hydrophilic ionic liquids.

In this case, a membrane with low retention for the ionic liquid but with a high retention for the undesirable (and unknown) compounds is required. According to the results from Chapter 2, the membrane FilmTec NF-270 was selected.

After recovering the 70% of the feed as permeate ($V_P/V_F = 0.70$) in a single stage process, it was possible to appreciate the magnitude of the separation by visual differences between the colours of the resulting streams: the retentate exhibited a caramel colour, while permeate was colourless. Those differences could be observed in Figure 3.31(a).

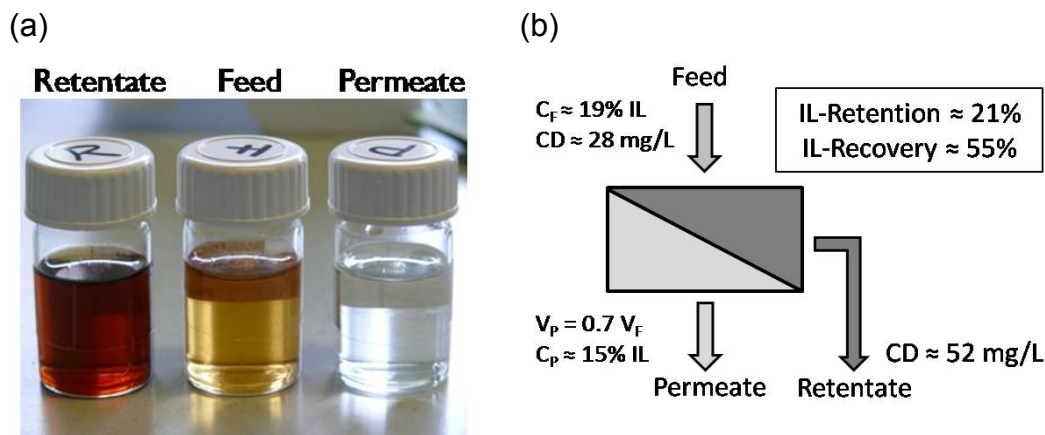


Figure 3.31: Recovery of IM14 Cl and IM14 1COO from wastewater in a single NF-stage: (a) Visual differences between feed and products, (b) Performance in terms of ionic liquid (IL) and cellulose degradation by-products (CD) separation.

Conductivity measurements were used to estimate the degree of separation of the ionic liquid, and the results were 49 mS/cm for retentate, 47 mS/cm for feed and 45 mS/cm for permeate. These results indicate that the ionic liquid distributes itself in all the samples, and the differences in colour are related to dissolution by-products and other compounds produced by side-reactions.

The ionic liquid content could be estimated by the provider (TITK) using its own refraction index-concentration calibration curves. It was found that 55% of the ionic liquid present in the wastewater can be recovered in the permeate stream, although the low retention, located around 21%, as it is shown in Figure 3.31(b).

The content of cellulose degradation by-products in feed and retentate were experimentally determined (28 and 52 mg/L, respectively) while the in permeate it was estimated in 18 mg/L, after applying material balances. Due to the presence of undesired compounds, the permeate stream can not be directly reused in the cellulose dissolution process without affecting its performance. For this reason, a multi-stage nanofiltration process was proposed with the idea to produce a permeate stream free of those undesired components.

The behaviour of the normalized permeate flux is represented in Figure 3.32 as a function of the recovery rate for each stage. During the first stage, the concentration of by-products (glucose dimmers and monomers) in retentate produces a pronounced decrease in the permeate flux. The

reduction of the permeate flux is less pronounced during the second stage, while during the third stage a constant permeate flux was reached.

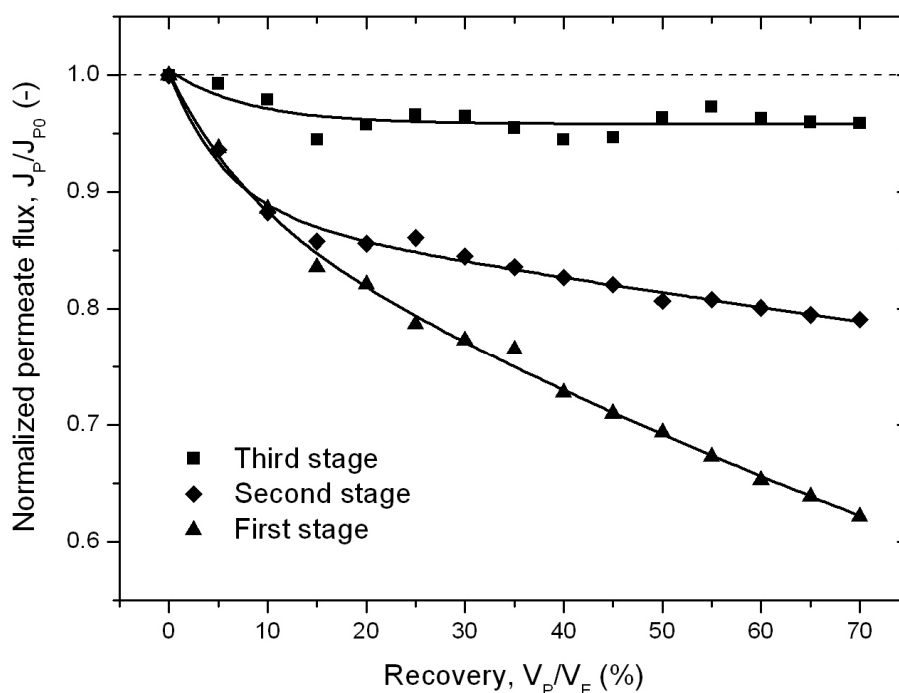


Figure 3.32: Variation of the normalized permeate flux with increasing recovery rate for a three-stage nanofiltration process.

According to the behaviour observed during the first stage, it can be concluded that after three stages it is possible to obtain a permeate stream almost free of dissolution by-products. An estimation of 15% of ionic liquid in permeate of the third stage indicates that the second and third stages are not selective for the ionic liquid, but for the undesired compounds.

As consequence, despite the ionic liquid retention remains around 21%, the recovery of ionic liquid decreases to 27% after three stages, as is represented in Figure 3.33.

Although the recovery rate of the ionic liquid could be considered low, it was possible to remove the undesired compounds and after evaporation of the water, a relative cleaner ionic liquid can be used for a further dissolution stage. Furthermore, the condensed water can be used to dilute again the retentate obtained, in order to processing it again by nanofiltration, as it is schematized in Figure 3.34.

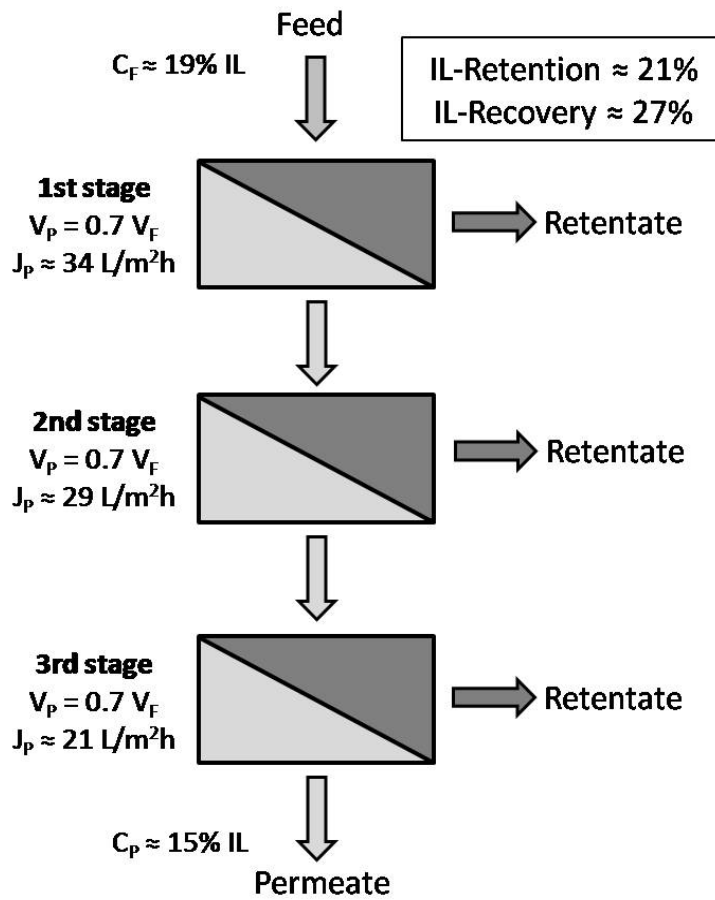


Figure 3.33: Recovery of IM14 Cl and IM14 1COO from wastewater in three NF-stages.

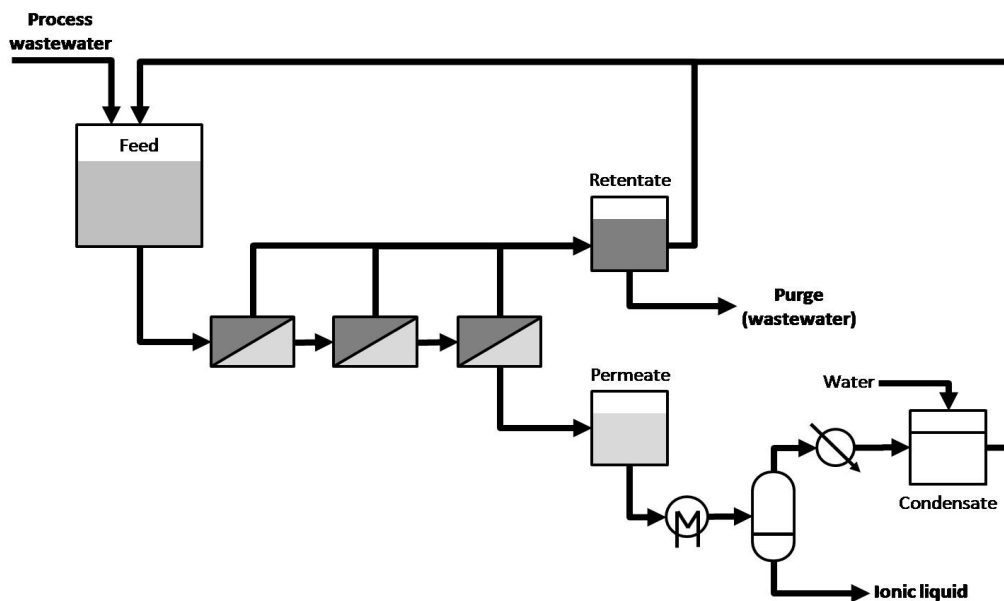


Figure 3.34: Process flow diagram for the recovery of IM14 Cl and IM14 1COO.

3.8 FACING PROBLEMS AND PROSPECT

Despite the already shown results can be considered promising, there is only the beginning of a long road. In order to improve the recovery of ionic liquids from wastewaters, not only by nanofiltration, a strategic approach was developed. The aim of this approach is to gain previously knowledge about some common issues related with wastewater characteristics, production and management; before to concentrate the attention in the recovery process itself. Acting this way, should be easier to recover ionic liquids from waste. The strategic approach is illustrated in Figure 3.35.

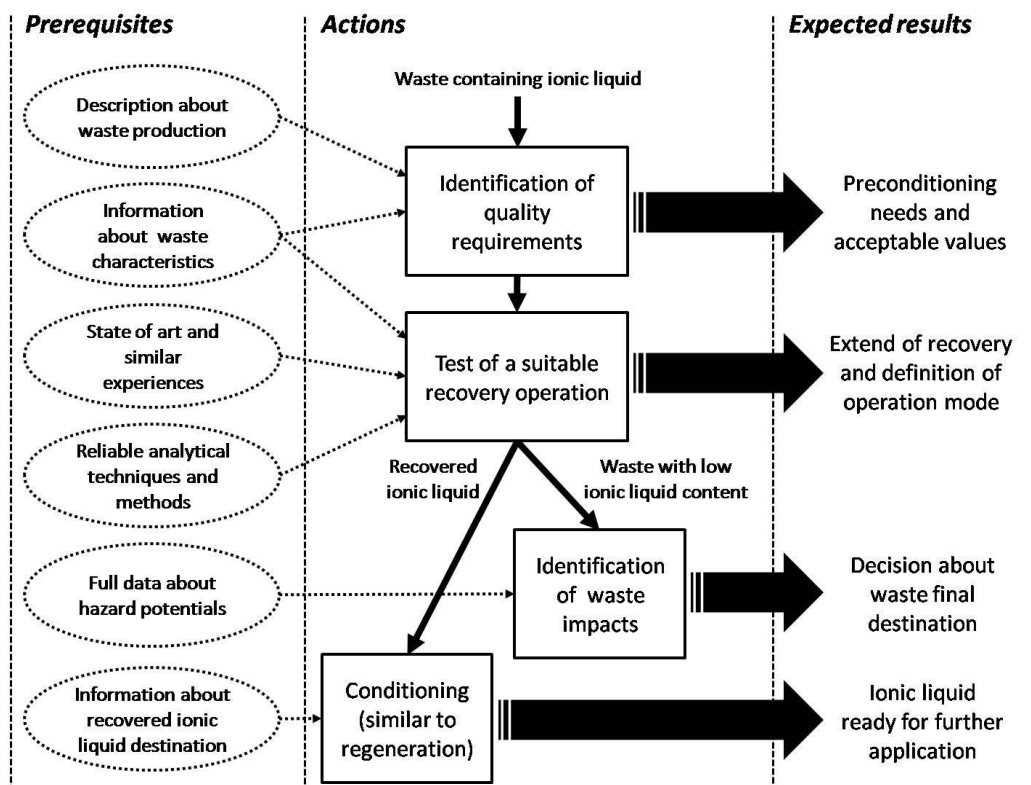


Figure 3.35: Strategic approach for the recovery of ionic liquids from waste.

The first action comprises the identification of quality requirements for the recovered ionic liquid. Previous knowledge about the way the waste is produced and information about the waste characteristics, mainly the information related with other waste constituents and their composition, are needed. In this study, the characteristics of the waste from cellulose dissolution and regeneration were completely unknown, and a trial-and-error procedure was required. Besides, the non-availability of physicochemical and thermodynamic data for ionic liquids and their

mixtures was missing. In the case of the wastewater from biotransformations, there is no information about the effects of a changing complexity of the mixture during recovery on the ionic liquid water solubility.

Such lack of information could complicate the recovery process extremely with the corresponding waste of time and resources. However, when these prerequisites are fulfilled as far as possible, acceptable values for the removal of other constituents, as well as preconditioning needs to reach these values after recovery, can be properly established.

As it should be expected, the characteristics of waste and collected information about similar experiences already published are useful to define the most suitable recovery option for the ionic liquid. Additionally, reliable analytical techniques and methods are required in order to quantify the extent of the recovery. Contrary to the case of regeneration of ionic liquids, where the ionic liquid is the principal constituent, the analytical challenges for a reliable characterisation of the recovered ionic liquid are considerably more complex, due to the heterogeneity of the waste and the inaccuracy generated by the presence of disturbing compounds.

For example, ionic liquids can be analyzed by chromatography [90,91], but a potential contamination of cellulose degradation by-products would suppress the surface quality of the HPLC/IC columns. On the other hand, size-exclusion chromatography (SEC) can be usually applied for the detection cellulose degradation by-products [92,93], but the ionic liquid would suppress the quality of the SEC columns. Furthermore, when other ions are present, like those from phosphate buffer in the wastewaters from biotransformations, simultaneous determination of the concentration of ionic liquid anion and cation is required to determine the extent of an eventual ion exchange (ionic liquid cation with strange anion, or ionic liquid anion with strange cation). A recent study in this direction was already published [94].

Once the recovery operation is selected and tested in order to establish the extent of the recovery, the definition of the operation mode should be achieved. Wastes are produced commonly in an unsteady form, thus a continuous recovery process can be difficult to carry out. For these cases, batch or semi-continuous recovery processes can be the solution.

After the recovery step, two streams are generated: the recovered ionic liquid and the waste stream with a reduced content of ionic liquid. In the case of the remaining waste, it is important to assess its environmental impact with help of reliable data about hazard potentials, like those published in the UFT / Merck Ionic Liquids Biological Effects Database [29], in order to decide its final destination. In this case, the waste stream could require special treatment to remove the remaining ionic liquid (by adsorption or advanced oxidation processes) or could be disposed directly in an industrial wastewater treatment plant.

For the recovered ionic liquid a further conditioning treatment (similar to those required to regenerate used ionic liquids) could be required, but the purification process and targets are dependent on the potential new application for the ionic liquid. Commonly it should be the same application that generates the wastewater, but not necessarily.

A last remark should be pointed out. The needs of recovery operations for ionic liquids should go down, if ionic liquids are rationally designed and the applications processes prevent the generation of wastes. Furthermore, the complexity of the recovery operation is related with deficiencies in the design procedures of processes and products.

REFERENCES

- [01] ERIKSON, P. Nanofiltration extends the range of membrane filtration. *Environmental Progress*, **1988**, 7, 58-62.
- [02] RAZDAN, U.; Shah, V.J. Nanofiltration membranes as suitable alternative to reverse osmosis / ultrafiltration membranes in separation processes. *Journal of Scientific and Industrial Research*, **2001**, 60, 560-563.
- [03] MELIN, T.; Rautenbach, R. *Membranverfahren*, 2nd ed.; Springer Verlag: Berlin (Germany), **2004**.
- [04] FANE, A.G. Module design and operation. In: *Nanofiltration: principles and applications*; Schäfer, A.I., Fane, A.G. and Walte, T.D., Ed.; Elsevier Ltd.: Oxford (UK), **2005**, pp. 67-88.
- [05] JUDD, S. Membrane Technology. In: *Membranes for Industrial Wastewater Recovery and Re-use*. Judd, S. and Jefferson, B., Ed.; Elsevier Science Ltd: Oxford (UK), **2003**, pp.13-74
- [06] WATSON, J.S. *Separation Methods for Waste and Environmental Applications*. Marcel Dekker, Inc.: New York (USA), **1999**.
- [07] STERLITECH CORPORATION. Sepa CF Systems Principles of Operation. <http://www.sterlitech.com/445430/products/Sepa-CF-II.html> (Accessed July 27, **2010**).
- [08] RAPAPORT, D. A membrane for all seasons. <http://www.eponline.com/articles/54103/> (Accessed July 27, **2010**).

- [09] VAN DER BRUGGEN, B.; Lejon, L.; Vandecasteele, C. Reuse, treatment and discharge of the concentrate of pressure-driven membrane processes. *Environmental Science and Technology*, **2003**, 37, 3733-3738.
- [10] NIELSEN, W.K. *Membranfiltration und verwandte molekulare Separationsverfahren*. APV-Verlag Th. Mann: Gelsenkirchen (Germany), **2004**.
- [11] MULDER, M. *Basic principles of membrane technology*. Kluwer Academic Publishers: Dordrecht (Netherlands), **1991**.
- [12] WAITE, T.D. Chemical speciation effects in nanofiltration separation. In: *Nanofiltration: principles and applications*; Schäfer, A.I., Fane, A.G. and Walte, T.D., Ed.; Elsevier Ltd.: Oxford (UK), **2005**, pp. 147-168.
- [13] FREIRE, M.G.; Santos, L.M.N.B.F.; Fernandes, A.M.; Coutinho, J.A.P.; Marrucho, I.M. An overview of the mutual solubilities of water-imidazolium-based ionic liquids systems. *Fluid Phase Equilibria*, **2007**, 261, 449-454.
- [14] WANG, S.; Jacquemin, J.; Husson, P.; Hardacre, C.; Costa Gomes, M.F. Liquid-liquid miscibility and volumetric properties of aqueous solutions of ionic liquids as a function of temperature. *Journal of Chemical Thermodynamics*, **2009**, 41, 1206-1214.
- [15] MAIA, F.M.; Rodríguez, O.; Macedo, E.A. LLE for (water+ionic liquid) binary systems using [C_xmim][BF₄] (x=6,8) ionic liquids. *Fluid Phase Equilibria*, **2010**, 296, 184-191.
- [16] JOHN, V.B. *Understanding phase diagrams*, 1st. ed; Macmillan Press Ltd.: London (UK), **1974**.
- [17] HILLERT, M. *Phase equilibria, phase diagrams and phase transformations*. Cambridge University Press: Cambridge (UK), **1998**.
- [18] COLOMBANI, J.; Bert, J. Toward a complete description of nucleation and growth in liquid-liquid phase separation. *Journal of Non-Equilibrium Thermodynamics*, **2004**, 29, 389-395.
- [19] FAVVAS, E.P.; Mitropoulos, A.Ch. What is spinodal decomposition? *Journal of Engineering Science and Technology Review*, **2008**, 1, 25-27.
- [20] KELTON, K.F.; Greer, A.L. *Nucleation in condensed matter. Applications in materials and biology*. Elsevier Ltd.: Amsterdam (Netherlands), **2010**.
- [21] KATZ, J.L. Three dimensional nucleation. In: *Interfacial aspects of phase transformations*; Mutaftschiev, B., Ed.; D. Reidel Publishing Company: Dordrecht (Netherlands), **1982**, pp. 261-286.
- [22] MIN, K.Y.; Stavans, J.; Piazza, R.; Goldberg, W.I. Steady-state nucleation in a binary mixture: the effect of stirring. *Physical Review Letters*, **1989**, 63, 1070-1073.
- [23] MIN, K.Y.; Goldberg, W.I. Nucleation of a binary liquid mixture under steady-state shear. *Physical Review Letters*, **1993**, 70, 469-472.
- [24] GOLDBURG, W.I.; Min, K.Y. Nucleation in the presence of shear. *Physica A: Statistical Mechanics and its Applications*, **1994**, 204, 246-260.
- [25] ONUKI, A. Spinodal decomposition and nucleation in the presence of flow. *International Journal of Thermophysics*, **1989**, 10, 293-308.
- [26] BRÄUTIGAM, S. Praktibiokat Projekt: Integrierte Prozesse mit ionischen Flüssigkeiten zur Gewinnung chiralen Alkohole. Präsentation vom 3. Zwischenbericht, **2008**.
- [27] TREVELYAN, W.E.; Forrest, R.S.; Harrison, J.S. Determination of yeast carbohydrates with the anthrone reagent. *Nature*, **1952**, 170, 626-627.
- [28] SESCOUSSE, R.; Gavillon, R.; Budtova, T. Aerocellulose from cellulose-ionic liquid solutions: Preparation, properties and comparison with cellulose-NaOH and cellulose-NMMO routes. *Carbohydrate Polymers*, **2011**, 83, 1766-1774.
- [29] UFT – Universität Bremen. The UFT / Merck Ionic Liquids Biological Effects Database. <http://www.il-eco.uft.uni-bremen.de> (Accessed August 23, **2010**).

- [30] FREIRE, M.G.; Neves, C.M.S.S.; Ventura, S.P.M.; Pratas, M.J.; Marrucho, I.M.; Oliveira, J.; Coutinho, J.A.P.; Fernandes, A.M. Solubility of non-aromatic ionic liquids in water and correlation using a QSPR approach. *Fluid Phase Equilibria*, **2010**, 294, 234-240.
- [31] ZHANG, S.; Sun, N.; He, X.; Lu, X.; Zhang, X. Physical properties of ionic liquids: Database and evaluation. *Journal of Physical and Chemical Reference Data*, **2006**, 35, 1475-1517.
- [32] IL THERMO. Ionic Liquids Database. NIST Standard Reference Database. <http://ilthermo.boulder.nist.gov/ILThermo/mainmenu.uix> (Accessed August 26, **2010**).
- [33] RODRÍGUEZ, H.; Brennecke, J.F. Temperature and composition dependence of the density and viscosity of binary mixtures of water + ionic liquid. *Journal of Chemical and Engineering Data*, **2006**, 51, 2145-2155.
- [34] GARDAS, R.L.; Coutinho, J.A.P. A group contribution method for viscosity estimation of ionic liquids. *Fluid Phase Equilibria*, **2008**, 266, 195-201.
- [35] NEBIG, S.; Liebert, V.; Gmehling, J. Measurement and prediction of activity coefficients at infinite dilution (γ^∞), vapour-liquid equilibria (VLE) and excess enthalpies (H^E) of binary systems with 1,1-dialkyl-pyrrolidinium bis(trifluoromethylsulfonyl)imide using mod. UNIFAC (Dortmund). *Fluid Phase Equilibria*, **2009**, 277, 61-67.
- [36] TOKUDA, H.; Tsuzuki, S.; Susan, M.A.B.H.; Hayamizu, K.; Watanabe, M. How ionic are room-temperature ionic liquids? An indicator of the physicochemical properties. *Journal of Physical Chemistry B*, **2006**, 110, 19593-19600.
- [37] SALMINEN, J.; Papaiconomou, N.; Kumar, R.A.; Lee, J.M.; Kerr, J.; Newman, J.; Prausnitz, J.M. Physicochemical properties and toxicities of hydrophobic piperidinium and pyrrolidinium ionic liquids. *Fluid Phase Equilibria*, **2007**, 261, 421-426.
- [38] PEREIRO, A.B.; Veiga, H.I.M.; Esperanca, J.M.S.S.; Rodriguez, A. Effect of temperature on the physical properties of two ionic liquids. *Journal of Chemical Thermodynamics*, **2009**, 41, 1419-1423.
- [39] BLOOMFIELD, V.A.; Dewan, R.K. Viscosity of liquid mixtures. *Journal of Physical Chemistry*, **1971**, 75, 3113-3119.
- [40] SAKSENA, M.P.; Harminder; Kumar, S. Viscosity of binary liquid mixtures. *Journal of Physics C*, **1975**, 8, 2376-2381.
- [41] VISWANATH, D.S.; Ghosh, T.K.; Prasad, D.H.L.; Dutt, N.V.K.; Rani, K.Y. *Viscosity of liquids: Theory, estimation, experiments, and data*. Springer: Dordrecht (Netherlands), **2007**.
- [42] NGHIEM, L.D.; Schäfer, A.I.; Elimelech, M. Nanofiltration of hormone mimicking trace organic contaminants. *Separation Science and Technology*, **2005**, 40, 2633-2649.
- [43] TANNINEN, J.; Mänttari, M.; Nyström, M. Effect of electrolyte strength on acid separation with NF membranes. *Journal of Membrane Science*, **2007**, 294, 207-212.
- [44] TANG, C.Y.; Kwon, Y.N.; Leckie, J.O. Effect of membrane chemistry and coating layer on physicochemical properties of thin film composite polyamide RO and NF membranes. II. Membrane physicochemical properties and their dependence on polyamide and coating layers. *Desalination*, **2009**, 242, 168-182.
- [45] BINDER, K. Spinodal decomposition versus nucleation and growth. In: *Kinetics of phase transitions*; Puri, S.; Wadhawan, V., Eds.; CRC Press: Boca Raton (USA), **2009**, pp. 63-99.
- [46] CUSAK, R. Rethink your liquid-liquid separations - A fresh look investigates general principles in designing process coalescers. *Hydrocarbon Processing*, **2009**, 6, 53-60.

- [47] BIRDWELL, J.F.; McFarlane, J.; Hunt, R.D.; Luo, H.; DePaoli, D.W. Separation of ionic liquid dispersions in centrifugal solvent extraction contactors. *Separation Science and Technology*, **2006**, 41, 2205-2223.
- [48] SHIN, W.; Yiacoymi, S.; Tsouris, C. Electric-field effects on interfaces: electrospray and electrocoalescence. *Current Opinion in Colloid and Interface Science*, **2004**, 9, 249-255.
- [49] MADAENI, S.S.; Yeganeh, M.K. Microfiltration of emulsified oil wastewater. *Journal of Porous Material*, **2003**, 10, 131-138.
- [50] LEIKNES, T.; Semmens, M.J. Membrane filtration for preferential removal of emulsified oil from water. *Water Science and Technology*, **2000**, 41, 101-108.
- [51] PARK, E.; Barnett, S.M. Oil/water separation using nanofiltration membrane technology. *Separation Science and Technology*, **2001**, 36, 1527-1542.
- [52] HADJ-ZIANE, A.Z.; Moulay, S. Microemulsion breakdown using the pervaporation technique: application to cutting oil models. *Desalination*, **2004**, 170, 91-97.
- [53] VISSER, A.E.; Reichert, W.M.; Swatloski, R.P.; Willauer, H.D.; Huddleston, J.G.; Rogers, R.D. Characterization of hydrophilic and hydrophobic ionic liquids: Alternatives to volatile organic compounds for liquid-liquid separations. In: *Ionic liquids: industrial applications for green chemistry*; R.D. Rogers and K.R. Seddon, Eds.; American Chemical Society: Washington DC (USA), **2002**; Vol. 818, pp. 289-308.
- [54] KLÄHN, M.; Stüber, C.; Seduraman, A.; Wu, P. What determines the miscibility of ionic liquids with water? Identification of the underlying factors to enable a straightforward prediction. *Journal of Physical Chemistry B*, **2010**, 114, 2856-2868.
- [55] KRAGL, U.; Eckstein, M.; Kaftzik, N. Biocatalytic reactions in ionic liquids. In: *Ionic liquids in synthesis*. Wasserscheid, P., Welton, T., Ed.; Wiley VCH: Weinheim (Germany), **2003**, 336-347.
- [56] NIKOLOVA, P.; Ward, O.P. Whole cell biocatalysis in nonconventional media. *Journal of Industrial Microbiology*, **1993**, 12, 76-86.
- [57] VERMUE, M.H.; Tramper, J. Biocatalysis in non-conventional media: medium engineering aspects. *Pure and Applied Chemistry*, **1995**, 67, 345-373.
- [58] SHELDON, R.A.; Madeira Lau, R.; Sorgedraeger, M.J.; van Rantwijk, F.; Seddon, R.K. Biocatalysis in ionic liquids. *Green Chemistry*, **2002**, 4, 147-151.
- [59] VAN RANTWIJK, F.; Sheldon, R.A. Biocatalysis in ionic liquids. *Chemical Reviews*, **2007**, 107, 2757-2785.
- [60] ROOSEN, C.; Müller, P.; Greiner, L. Ionic liquids in biotechnology: applications and perspectives for biotransformations. *Applied Microbiology and Technology*, **2008**, 81, 607-614.
- [61] GOLDBERG, K.; Schroer, K.; Lütz, S.; Liese, A. Biocatalytic ketone reduction - a powerful tool for the production of chiral alcohols – part I: processes with isolated enzymes. *Applied Microbiology and Technology*, **2007**, 76, 237-248.
- [62] ECKSTEIN, M.; Villela Filho, M.; Liese, A.; Kragl, U. Use of an ionic liquid in a two-phase system to improve an alcohol dehydrogenase catalysed reduction. *Chemical Communications*, **2004**, 9, 1084-1085.
- [63] HUSSAIN, W.; Pollard, D.J.; Truppo, M.; Lye, G.J. Enzymatic ketone reductions with co-factor recycling: Improved reactions with ionic liquid co-solvents. *Journal of Molecular Catalysis B: Enzymatic*, **2008**, 55, 19-29.
- [64] PFRUENDER, H.; Amidjojo, M.; Kragl, U.; Weuster-Botz, D. Efficient whole-cell biotransformation in a biphasic ionic liquid/water system. *Angewandte Chemie, International Edition*, **2004**, 43, 4529-4531.

- [65] PFRUENDER, H.; Jones, R.; Weuster-Botz, D. Water immiscible ionic liquids as solvents for whole cell biocatalysis. *Journal of Biotechnology*, **2006**, 124, 182-190.
- [66] BRÄUTIGAM, S.; Bringer-Meyer, S.; Weuster-Botz, D. Asymmetric whole cell biotransformations in biphasic ionic liquid/water systems by use of recombinant *Escherichia coli* with intracellular cofactor regeneration. *Tetrahedron: Asymmetry*, **2007**, 18, 1883-1887.
- [67] BRÄUTIGAM, S.; Dennewald, D.; Schürmann, M.; Lutje-Spelberg, J.; Pitner, W.R.; Weuster-Botz, D. Whole-cell biocatalysis: Evaluation of new hydrophobic ionic liquids for efficient asymmetric reduction of prochiral ketones. *Enzyme and Microbial Technology*, **2009**, 45, 310-316.
- [68] WEUSTER-BOTZ, D. Process intensification of whole-cell biocatalysis with ionic liquids. *The Chemical Record*, **2007**, 7, 334-340.
- [69] GOLDBERG, K.; Schroer, K.; Lütz, S.; Liese, A. Biocatalytic ketone reduction - a powerful tool for the production of chiral alcohols – part II: whole-cell reductions. *Applied Microbiology and Technology*, **2007**, 76, 249-255.
- [70] VAN RANTWIJK, F.; Madeira Lau, R.; Sheldon, R.A. Biocatalytic transformations in ionic liquids. *Trends in Biotechnology*, **2003**, 21, 131-138.
- [71] LOU, W.; Zong, M.; Wu, H.; Xu, R. Recent progress on biocatalysis and biotransformations in ionic liquids. *Chinese Journal of Chemical Engineering*, **2004**, 12, 543-549.
- [72] STEPNOWSKI, P.; Wojciech, M.; Nichthäuser, J. Adsorption of Alkylimidazolium and Alkylpyridinium Ionic Liquids onto Natural Soils. *Environmental Science and Technology*, **2007**, 41, 511-516.
- [73] PALOMAR, J.; Lemus, J.; Gilarranz, M.A.; Rodríguez, J.J. Adsorption of ionic liquids from aqueous effluents by activated carbon. *Carbon*, **2009**, 47, 1846-1856.
- [74] RAO, N.N.; Lütz, S.; Seelbach, K.; Liese, A. In: *Industrial Biotransformations*; A. Liese, K. Seelbach and C. Wandrey, Eds.; Wiley VCH: Weinheim (Germany), **2006**, 115-145.
- [75] MCGIVNEY, W.; Kawamura, S. *Cost estimating manual for water treatment facilities*, John Wiley & Sons: New Jersey (USA), **2008**.
- [76] CAMPBELL, N.A.; Reece, J.B. *Biology*, 7th ed.; Benjamin Cummings Publishing Company: Reading (USA), **2005**.
- [77] WERTZ, J.L.; Bédué, O.; Mercier, J.P. *Cellulose Science and Technology*, 1st ed.; EPFL Press: Lausanne (Switzerland), **2010**.
- [78] HERMANUTZ, F.; Meister, F.; Uerdingen, E. New developments in the manufacture of cellulose fibers with ionic liquids. *Chemical Fibers International*, **2006**, 6, 342-343.
- [79] SWATLOSKI, R.P.; Spear, S.K.; Holbrey, J.D.; Rogers, R.D. Dissolution of cellulose with ionic liquids. *Journal of the American Chemistry Society*, **2002**, 124, 4974-4975.
- [80] MICHELS, C.; Kosan, B. Contribution to the dissolution state of cellulose and cellulose derivatives. *Lenzinger Berichte*, **2005**, 84, 62-70.
- [81] REMSING, R.C.; Swatloski, R.P.; Rogers, R.D.; Moyna, G. Mechanism of cellulose dissolution in the ionic liquid 1-n-butyl-3-methylimidazolium chloride: a ¹³C and ^{35/37}Cl NMR relaxation study on model system. *Chemical Communications*, **2006**, 12, 1271-1273.
- [82] MICHELS, C.; Kosan, B.; Meister, F. Verfahren und Vorrichtung zur Herstellung von Formkörpern aus Cellulose. DE Patent 10 2004 031 025 B3, December 29, **2005**.
- [83] BENTIVOGLIO, G.; Röder, T.; Fasching, M.; Buchberger, M.; Schottenberger, H.; Sixta, H. Cellulose processing with chloride-based ionic liquids. *Lenzinger Berichte*, **2006**, 86, 154-161.

- [84] OHNO, H.; Fukaya, Y. Task specific ionic liquids for cellulose technology. *Chemistry Letters*, **2009**, 38(1), 2-7.
- [85] KOSAN, B.; Michels, C.; Meister, F. Dissolution and forming of cellulose with ionic liquids. *Cellulose*, **2008**, 15, 59-66.
- [86] FUKAYA, Y.; Hayashi, K.; Wada, M.; Ohno, H. Cellulose dissolution with polar ionic liquids under mild conditions: required factors for anions. *Green Chemistry*, **2008**, 10, 44-46.
- [87] ZHU, S.; Wu, Y.; Chen, Q.; Yu, Z.; Wang, C.; Jin, S.; Ding, Y.; Wu, G. Dissolution of cellulose with ionic liquids and its application: a mini-review. *Green Chemistry*, **2006**, 8, 325-327.
- [88] ROSENAU, T.; Potthast, A.; Milacher, W.; Hofinger, A.; Kosma, P. Isolation and identification of residual chromophores in cellulosic materials. *Polymer*, **2004**, 45, 6437-6443.
- [89] ROSENAU, T.; Potthast, A.; Sixta, H.; Kosma, P. The chemistry of side reactions and byproduct formation in the system NMMO/cellulose (Lyocell process). *Progress in Polymer Science*, **2001**, 26, 1763-1837.
- [90] STEPNOWSKI, P. Application of chromatographic and electrophoretic methods for the analysis of imidazolium and pyridinium cations as used in ionic liquids. *International Journal of Molecular Sciences*, **2006**, 7, 497-509.
- [91] BUTT, S.B.; Riaz, M. Determination of cations and anions in environmental samples by HPLC: Review. *Journal of Liquid Chromatography and related technologies*, **2009**, 8, 1045-1064.
- [92] EMSLEY, A.M.; Ali, M.; Heywood, R.J. A size exclusion chromatography study of cellulose degradation. *Polymer*, **2000**, 41, 8513-8521.
- [93] ROSENAU, T.; Potthast, A.; Kosma, P. Trapping of reactive intermediates to study reaction mechanisms in cellulose chemistry. *Advances in Polymer Science*, **2006**, 205, 153-197.
- [94] MARKOWSKA, A.; Stepnowski, P. Simultaneous determination of ionic liquid cations and anions using Ion Chromatography with tandem ion exchange columns: a preliminary assessment. *Analytical Sciences*, **2008**, 24, 1359-1361.

4 CONCLUSIONS & OUTLOOK

4.1 CONCLUSIONS

Based on the novel methodology to understand the chemical functionality of active membrane layers that derived from the T-SAR approach, it can be now qualitatively predicted both related properties and separation performance for several different solute classes, not only ionic liquids.

At first sight, this qualitative analysis provides a tangible picture of a nanofiltration membrane which shakes off the black-box concept so far used for such membranes. Admittedly, this new picture is only a small contribution possessing its own limitations. But it can be assumed to provide a new avenue to systematically design task-specific nanofiltration membranes.

Additionally and mainly due to its simplicity, the proposed picture could also serve as a meeting point for engineers, chemists, scientists and technicians working in the field of membrane technology. It can also encourage further developments by interdisciplinary work, especially in the fields of membrane synthesis and membrane characterization.

The few studies already published about the use of nanofiltration for separation of ionic liquids from aqueous solutions only paid attention to hydrophilic ionic liquids. But as demonstrated in this study also the separation of hydrophobic ionic liquids from aqueous solutions is both necessary and possible. Furthermore, these compounds can be separated efficiently in terms of associated costs, and even a phase separation for a direct recovery can be performed successfully.

Considering that most of the hydrophobic ionic liquids known up to date are either toxic or not easily biodegradable, their recovery from wastewater will allow the establishment of those potential applications of ionic liquids which are till now threatened, once the associated risks of environmental damages and economical losses are successfully overcome.

However, despite the use of nanofiltration for such purposes exhibits an encouraging future, when dealing with the quest of applications for ionic liquids (or even for other novel and trendy chemicals) the “keep it simple and straightforward” principle must be always considered. This means that all endeavours should be focused on the development of processes with zero waste production, while recovery operations like the one developed in this study should remain always as a last option.

4.2 SUGGESTIONS FOR FURTHER RESEARCH

As it is shown in Figure 4.1, the lifetime of ionic liquids in solution can be extended by means of regeneration and recovery processes, in order to reuse them as long as possible and to avoid the use of new ionic liquids to compensate the losses during application. Only when these processes are not feasible or cost-efficient, a removal process has to be considered to prevent the entrance of ionic liquids into the environment.

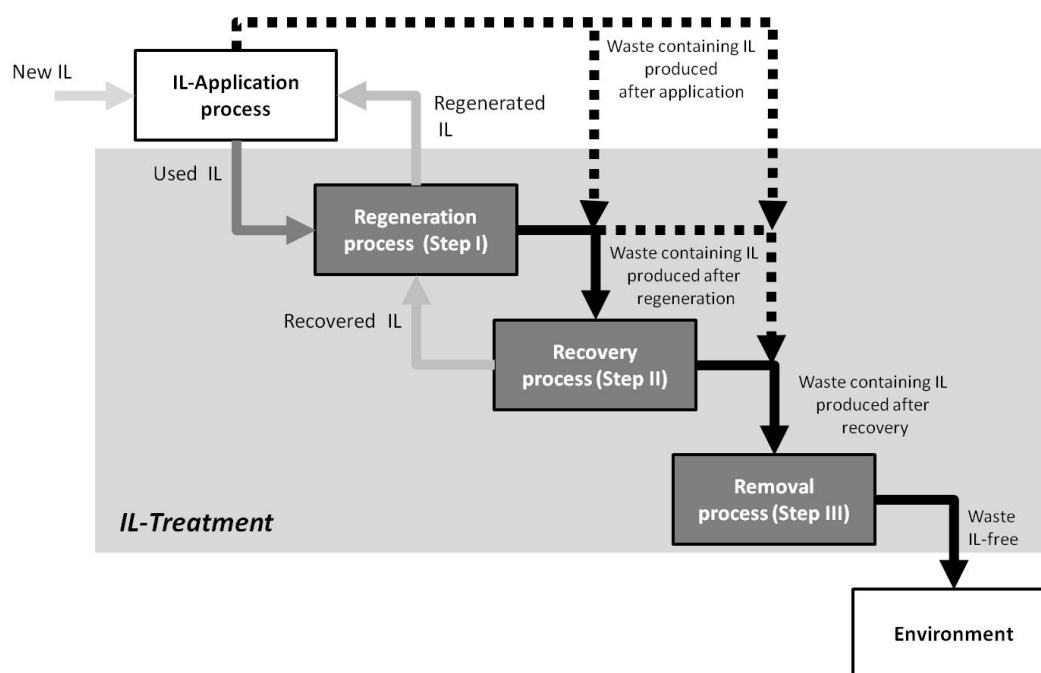


Figure 4.1: Approaches used to extend the lifetime of ionic liquids.

Due to the enormous diversity of ionic liquids, every possible application of ionic liquids represents a specific problem with its own challenges. Similar to the systematic approach presented in this work for the recovery of ionic liquids, a strategic approach for the properly selection of regeneration operations was recently published [1].

Although this work was focused on the use of nanofiltration for the recovery of ionic liquids from wastewater (Step II in Figure 4.1), nanofiltration might also have high potential as operation for the regeneration of ionic liquids (Step I in Figure 4.1). Indeed, some experiences have been already published in the field of organo-metallic catalysis for the regeneration of both, ionic liquid and catalyst, by organic solvent nanofiltration [2-4].

In the case of the applications of ionic liquids already described (dissolution and regeneration of cellulose, and biotransformations in biphasic systems), further studies should be carried out in order to materialize the recovery of such ionic liquids in bigger scales, and thus contributing to the establishment of these ionic liquids applications as new chemical processes. Furthermore, the use of nanofiltration as recovery operation of ionic liquids used in aluminium deposition is now being considered [5], and the knowledge gained in this work could be used for further research in this direction.

According to this, suggestions for further applied research in the use of nanofiltration together with ionic liquids appear to be application-dependent. However, other aspects are suggested for systematically study, as follows.

In order to gain more understanding about the formation of an ionic liquid phase from an aqueous solution, oriented research to the principles of drop formation, growth and separation is highly recommended. For example, the phase equilibrium diagrams for ionic liquids in water should be produced and/or completed. Also the effect of pressure should be considered, as it was found that pressure determines the local formation of second phase. Some work in this direction is already done at the University of Bremen with hydrophobic liquids containing the $(CF_3SO_2)_2N$ anion, but in non polar solvents and n-alkyl alcohols [6-8]. Furthermore, ternary systems (ionic liquid + water + electrolyte) should be considered, as their possible salting-out effects might dominate the process [9,10].

Moreover, the formation of drops at the membrane surface and the following growth can be followed by optical methods, like microscopy and light scattering [11-13]. Once the structure of the formed emulsion is well understood, it should be easy to select the proper way for the coalescence and further separation of second phase.

Another interesting field for further research is the behaviour of ionic liquids exhibiting aggregation during the concentration process by nanofiltration. It is well known that some ionic liquids behave like amphiphilic compounds [14] and that the anion (the cation to a less extent), but also the presence of electrolytes decide, if an ionic liquid aggregates or not [15]. Nucleation (formation of a new phase within a metastable ambient phase) and micellization (formation of micelles in surfactant solutions) have the common feature to proceed through spontaneous aggregation of molecules or ions [16]. As a consequence, the changes in the organization of the ionic liquid in aqueous solution (from ion pairs to micelles and more complex aggregates) should lead to variations in the behaviour of permeate flux and retention, as it was already reported for an anionic surfactant [17].

Finally, in order to improve the membrane model developed, further research can be done to study systematically the structure-activity-relationships of ionic liquids and nanofiltration membranes, but also to extent the model developed in this work to fulfil its limitations.

The development of an ionic liquid test-kit, based on the concept created and successfully tested by Jastorff and co-workers [18], is suggested. Then it would be possible to predict the interactions between ionic liquids and the membrane and confirming then after obtaining the required experimental data. An appropriate selection of key ionic liquids will conduce to more knowledge about the interactions that take place between the membrane structure and the ionic liquids. Moreover, the diversity of ionic liquids would make possible to investigate separately the acting mechanisms in a nanofiltration membrane: steric hindrance, solution-diffusion, and charge exclusion (for those ionic liquids containing divalent anions like sulphate or functionalized side chains with groups able to acquire electrical charge in aqueous solutions, for example, carboxyl group). Some suggestions for such a test-kit were considered during the realization of this study [19].

By using the methodology developed in this work and combining results of XPS measurements at different thickness of the top layer, it can be possible to gain more information about the constitution of the different membrane sheets and thus, about the morphology of the nanopores. Furthermore, the information derived from this analysis can be used to simulate the formation of the top layer, improving the actual approach that represents both monomers like soft spheres [20,21]. However, there is a challenge related to the calculation capacity of the software used for such

purposes. In this study, the work with chemical structures containing more than 600 atoms proved to be complex and geometric optimizations cannot proceed successfully in all cases.

REFERENCES

- [01] FERNÁNDEZ, J.F.; Neumann, J.; Thöming, J. Regeneration, recovery and removal of ionic liquids. *Current Organic Chemistry*, **2011**, 15, 1992-2014.
- [02] HAN, S.; Wong, H.T.; Livingston, A.G. Application of organic solvent nanofiltration to separation of ionic liquids and products from ionic liquid mediated reactions. *Chemical Engineering Research and Design*, **2005**, 83, 309-316.
- [03] WONG, H.; Pink, C.J.; Castelo Ferreira, F.; Livingston, A.G. Recovery and reuse of ionic liquids and palladium catalyst for Suzuki reactions using organic solvent nanofiltration. *Green Chemistry*, **2006**, 8, 373-379.
- [04] WONG, H.; See-Toh, Y.H., Castelo Ferreira, F.; Crook, R.; Livingston, A.G. Organic solvent nanofiltration in asymmetric hydrogenation: enhancement of enantioselectivity and catalyst stability by ionic liquids. *Chemical Communications*, **2006**, 19, 2063-2065.
- [05] SOLÁ CERVERA, J.L.; König, A. Recycling concept for aluminium electrodeposition from the ionic liquid system EMIM[Tf₂N]-AlCl₃. *Chemical Engineering and Technology*, **2010**, 33, 1979-1988.
- [06] SCHRÖER, W.; Vale, V.R. Liquid-liquid phase separation in solutions of ionic liquids: phase diagrams, corresponding state analysis and comparison with simulations of the primitive model. *Journal of Physics: Condensed Matter*, **2009**, 21, 424119.
- [07] VALE, V.R.; Rathke, B.; Will, S.; Schröer, W. Liquid-liquid phase behavior of solutions of 1-octyl- and 1-decyl-3-methylimidazolium bis(trifluoromethylsulfonyl)imide (C_{8,10}mimNTF₂) in n-alkyl alcohols. *Journal of Chemical and Engineering Data*, **2010**, 55, 2030-2038.
- [08] VALE, V.R.; Rathke, B.; Will, S.; Schröer, W. Liquid-liquid phase behavior of solutions of 1-dodecyl-3-methylimidazolium bis(trifluoromethylsulfonyl)amide (C₁₂mimNTF₂) in n-alkyl alcohols. *Journal of Chemical and Engineering Data*, 10.1021/je100359x.
- [09] NAJDANOVIC-VISAK, V.; Canongia Lopes, J.N.; Visak, Z.P.; Trindade, J.; Rebelo, L.P.N. Salting-out in aqueous solutions of ionic liquids and K₃PO₄: aqueous biphasic systems and salt precipitation. *International Journal of Molecular Sciences*, **2007**, 8, 736-748.
- [10] ZAFARANI-MOATTAR, M.T.; Hamzehzadeh, S. Phase diagrams for the aqueous two-phase ternary system containing the ionic liquid 1-butyl-3-methylimidazolium bromide and tri-potassium citrate at T = (278.15, 298.15 and 318.15) K. *Journal of Chemical and Engineering Data*, **2009**, 54, 833-841.
- [11] DÖRFLER, H.D. *Grenzflächen- und Kolloidchemie*, VCH Verlagsgesellschaft mbH: Weinheim (Germany), **1994**.
- [12] ARORA, A.K.; Tata, B.V.R. Interactions, structural ordering and phase transitions in colloidal dispersions. *Advances in Colloid and Interface Science*, **1998**, 78, 49-97.
- [13] BIBETTE, J.; Leal Calderon, F.; Poulin, P. Emulsions: basic principles. *Reports on Progress in Physics*, **1999**, 62, 969-1033.
- [14] LUCZAK, J.; Hupka, J.; Thöming, J.; Jungnickel, C. Self-organization of imidazolium ionic liquids in aqueous solution. *Colloids and Surfaces A: Physicochemical and Engineering Aspects*, **2008**, 329, 125-133.

- [15] GUZMÁN, N.M., Fernández, J.F., Parada, M.; Orbegozo, C.; Rodríguez, M.A.; Padrón A.; Thöming, J. Efecto del catión, del anión y del co-ión sobre la agregación de líquidos iónicos en solución acuosa, *Química Nova*, **2010**, 33, 1703-1708.
- [16] SHCHEKIN, A.K.; Kuni, F.M.; Grinin, A.P.; Rusanov, A.I. Nucleation in micellization processes. In: *Nucleation theory and applications*. Schmelzer, J.W.P., Ed.; Wiley-VCH Verlag: Weinheim (Germany), **2005**, pp.312-374
- [17] ARCHER, A.C.; Mendes, A.M.; Boaventura, R.A.R. Separation of an anionic surfactant by nanofiltration. *Environmental Science and Technology*, **1999**, 33, 2758-2764.
- [18] JASTORFF, B.; García Abbad, E.; Petridis, G.; Tegge, W.; de Wit, R.; Erneux, C.; Stec, W.J.; Morr, M. Systematic use of cyclic nucleotide analogues – mapping of essential interactions between nucleotides and proteins. *Nucleic Acids Research*, **1981**, 9, 219-223.
- [19] FERNÁNDEZ, J.F., Bartel, R.; Thöming, J. Understanding the recovery of ionic liquids by nanofiltration: Combining classical characterization methods with T-SAR approach. *EUROMEMBRANE 2009 (Montpellier, France)*, September 6-10, **2009**.
- [20] NADLER, R.; Srebnik, S. Molecular simulation of polyamide synthesis by interfacial polymerization. *Journal of Membrane Science*, **2008**, 315, 100-105.
- [21] OIZEROVICH-HONIG, R.; Raim, V.; Srebnik, S. Simulation of thin film membranes formed by interfacial polymerization. *Langmuir*, **2010**, 26, 299-306.

APPENDIXES

APPENDIX A. DEAD-END MODULE

The HP4750 Stirred Cell (Corporation Sterlitech) is a high-pressure chemical resistant stirred cell in which is possible to perform several membrane separations with a maximal operational pressure of 69 bar (1000 psig). The cell is made of stainless steel 316L and internal components are chemical resistant (nitrile rubber o-rings and gaskets and teflon-coated magnet). Figure A.1 shows the schematic diagram taken for the instruction manual of the HP4750 Stirred Cell.

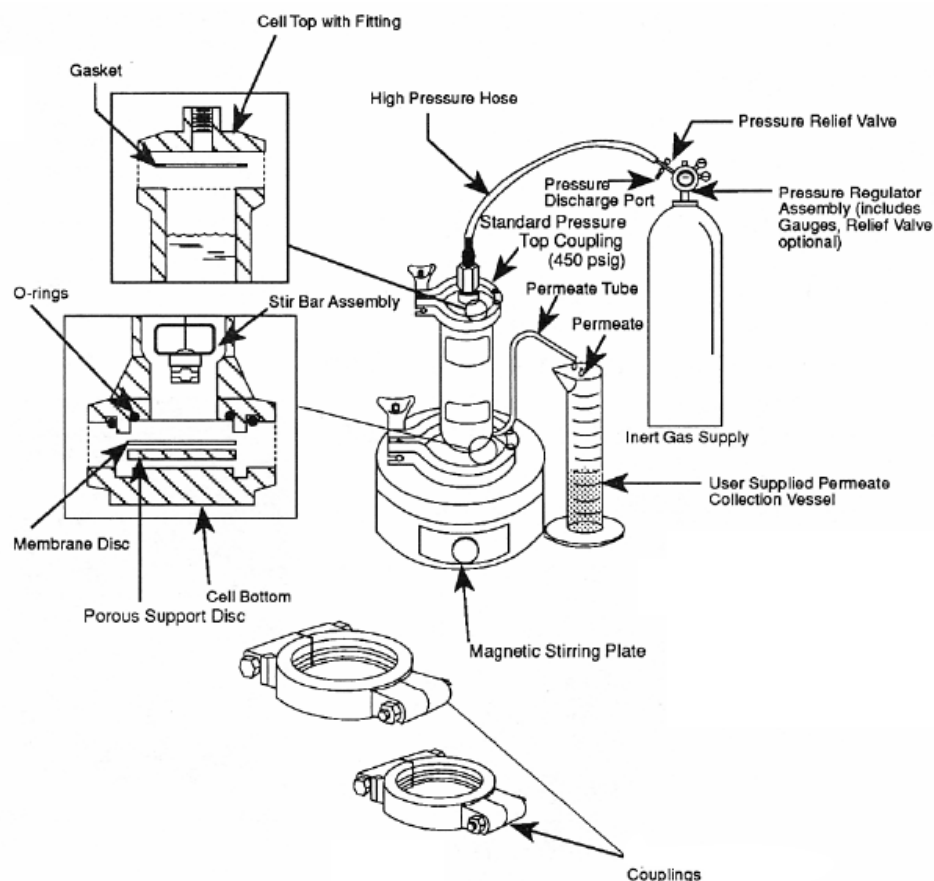


Figure A.1: Schematic diagram of the dead-end module used in this work.

The cell consists in three major components: the cell body with removable top and bottom parts, the stir bar assembly and standard couplings. In

addition, a magnetic stirrer (230 VAC, 50 Hz) and a source of gas pressure (nitrogen, purity 5.0, Linde AG) to pressurize the cell are required. The top part of the cell can be removed to fill the vessel with up to 300 mL of feed solution with a hold-up volume around 1 mL. The bottom part is removable to change out the membrane. The top and bottom parts are secured to the cell body with mechanical couplings. All the cell components are shown in Figure A.2.

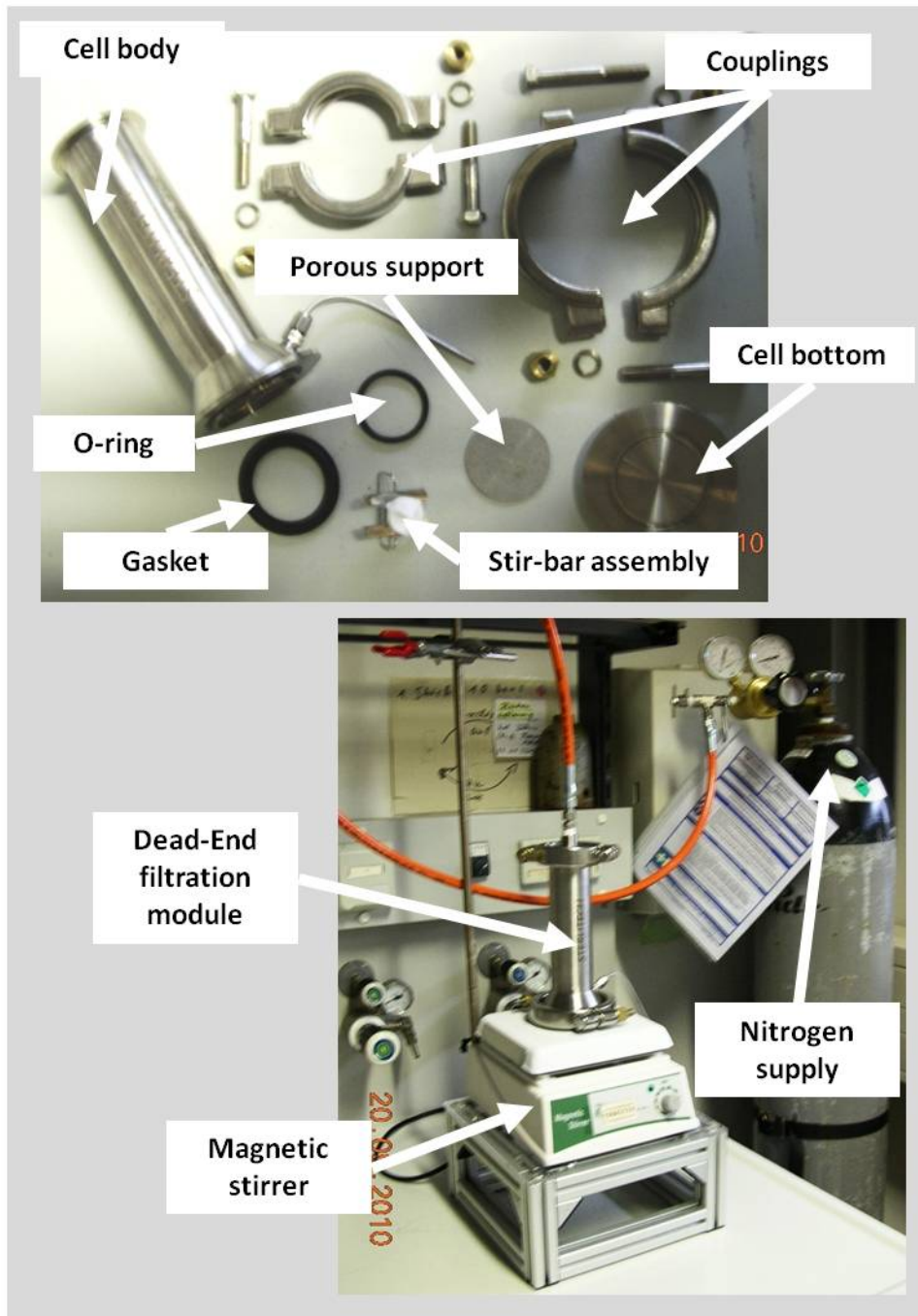


Figure A.2: Components of the dead-end module used in this work.

LIST OF PUBLICATIONS

The publications and contributions listed were authored during the work for this thesis:

Scientific Articles:

Fernández, J.F., Sojo, E.; Ferreira, J.; Rodríguez, M.A.; Guzmán, N.M., Padrón A.; Thöming, J. Agregación de líquidos iónicos en solución acuosa: Efecto del método empleado para determinar la concentración micelar crítica. *Ingeniería Química*, submitted.

Fernández, J.F.; Bartel, R.; Bottin-Weber, U.; Stolte, S.; Thöming, J. Recovery of ionic liquids by nanofiltration. *Journal of Membrane Science and Technology*, **2011**, 4, 1-8. Open Access: <http://www.omicsonline.org/2155-9589/2155-9589-S4-001.pdf>

Fernández, J.F.; Jastorff, B.; Störmann, R.; Stolte, S.; Thöming, J. Thinking in terms of Structure-Activity-Relationships (T-SAR): A tool to better understand nanofiltration membranes. *Membranes*, **2011**, 1, 162-183. Open Access: <http://www.mdpi.com/2077-0375/1/3/162/pdf>

Fernández, J.F.; Neumann, J.; Thöming, J. Regeneration, recovery and removal of ionic liquids. *Current Organic Chemistry*, **2011**, 15, 1992-2014.

Guzmán, N.M., Fernández, J.F., Parada, M.; Orbegozo, C.; Rodríguez, M.A.; Padrón A.; Thöming, J. Efecto del catión, del anión y del co-ión sobre la agregación de líquidos iónicos en solución acuosa, *Química Nova*, **2010**, 33, 1703-1708.

Jungnickel, C.; Łuczak, J.; Ranke, J.; Fernández, J.F.; Müller, A.; Thöming, J. Micelle formation of imidazolium ionic liquids in aqueous solution. *Colloids and Surfaces A: Physicochemical and Engineering Aspects*, **2008**, 316, 278-284.

Fernández, J.F., Waterkamp, D.; Thöming, J. Recovery of Ionic Liquids from Wastewater: Aggregation Control for Intensified Membrane Filtration. *Desalination*, **2008**, 224, 52-56.

Conference Proceedings:

Fernández, J.F.; Chilyumova, E.; Waterkamp, D.; Thöming, J. Ionic liquid recovery from aqueous solutions by cross-flow nanofiltration. *10th World Filtration Congress (Leipzig, Germany)*, **2008**, Volume II, 528-532.

Jungnickel, C.; Łuczak, J.; Ranke, J.; Fernández, J.F.; Müller, A.; Thöming, J. Aggregate formation of imidazolium ionic liquids in aqueous solution. *SURUZ 2007: Surfactants and Dispersed Systems in Theory and Practice (Wałbrzych, Poland)*, **2007**, 153-156.

Fernández, J.F.; Waterkamp, D.; Thöming, J. Recovery of Ionic Liquids from Wastewater: Aggregation Control for Intensified Membrane Filtration. *11th Aachener Membran Kolloquium (Aachen, Germany)*, **2007**, 391-396.

Poster Presentations:

Fernández, J.F., Bartel, R.; Thöming, J. Understanding the recovery of ionic liquids by nanofiltration: Combining classical characterization methods with T-SAR approach. *EUROMEMBRANE 2009 (Montpellier, France)*, September 6-10, **2009**.

Dennewald, D.; Bräutigam, S.; Weuster-Botz, D.; Fernández, J.F.; Waterkamp, D.; Ranke, J.; Thöming, J.; Schürmann, M.; Lutje Spelberg, J.; Dünkemann, P.; Pitner, W.; Ambrosius, K. Praktikable assymetrische Reaktionen durch Biokatalyse: Integrierte Prozesse mit ionischen Flüssigkeiten zur Gewinnung chiraler Alkohole. *42. Jahrestreffen Deutscher Katalytiker (Weimar, Germany)*, March 11-13, **2009**.

Fernández, J.F.; Sojo, E.; Orbegozo, C.; Ferreira, J.; Rodríguez, M.A.; Thöming, J. Aggregation behaviour in aqueous solution of 1-alkyl-3-methylimidazolium chloride ionic liquids. *EUCHEM 2008 – Conference on molten salts and ionic liquids (Copenhagen, Denmark)*. August 24-29, **2008**.

Book chapter:

Siedlecka, E.M.; Czerwicka, M.; Neumann, J.; Fernández, J.F.; Stepnowski, P.; Thöming, J. Ionic liquids: methods of degradation and recovery. *Submitted*.

CURRICULUM VITAE

May 7th 1976 Born in Caracas, Venezuela.

Studies and degrees:

1982 – 1993 Primary, secondary and high school (Caracas, Venezuela). High school graduation (Jul 1993)

1993 – 1999 Chemical Engineering studies at the Central University of Venezuela (Caracas, Venezuela). Chemical Engineer degree (Jul 1999)

2000 – 2005 Master studies at the Central University of Venezuela. Magister Scientiarum in Chemical Engineering (Dec 2005)

2005 – 2006 Research stay in the working group of Prof. Dr.-Ing. Jorg Thöming at the Centre for Environmental Research and Sustainable Technologies (UFT), University of Bremen

2007 – 2011 PhD student in the working group of Prof. Dr.-Ing. Jorg Thöming at the Centre for Environmental Research and Sustainable Technologies (UFT), University of Bremen

Professional experience:

2000 – 2005 Instructor Professor at the Central University of Venezuela (Caracas, Venezuela)

2005 – 2008 Assistant Professor at the Central University of Venezuela (Caracas, Venezuela)

2008 – 2011 Aggregate Professor at the Central University of Venezuela (Caracas, Venezuela)

Since 2009 Research assistant with a part-time job in the working group of Prof. Dr.-Ing. Jorg Thöming at the Centre for Environmental Research and Sustainable Technologies (UFT), University of Bremen

ERKLÄRUNG

Hiermit erkläre ich, *José Francisco Fernández Dámaso*, geboren am *07.05.1976* in *Caracas (Venezuela)*, dass ich

- die Arbeit ohne unerlaubte fremde Hilfe angefertigt habe,
- keine anderen als die von mir angegebenen Quellen und Hilfsmittel benutzt habe und
- die den benutzten Werken wörtlich oder inhaltlich entnommenen Stellen als solche kenntlich gemacht habe.

Bremen, 15. März 2011

José F. Fernández D.